

https://dspace.org/

Histo-morphological perturbations in the hippocampus of the diabetic male Sprague Dawley rat following Atripla® and alcohol administration

Asouzu Johnson, Jaclyn

2022
https://hdl.handle.net/10539/35650

Downloaded from a DSpace repository. https://dspace.org/

UNIVERSITY OF THE WITWATERSRAND, JOHANNESBURG

Histo-morphological perturbations in the hippocampus of the diabetic male Sprague Dawley rat following Atripla® and alcohol administration

Name: Jaclyn Asouzu Johnson

Student number: 1312779

This thesis is submitted in fulfillment of the requirements for the degree of Doctor of Philosophy (Ph.D.) in Anatomy

Faculty of Health Sciences, University of the Witwatersrand, Johannesburg

October 2022

Supervisor 1

Prof. Ejikeme Felix Mbajiorgu (PhD)

Supervisor 2

Prof. Robert Ndou (Ph.D.)

Declaration

I Jaclyn Asouzu Johnson declare that this thesis is my own, original work. It is being submitted for the degree of Doctor of Philosophy in the School of Anatomical Sciences, Faculty of Health Sciences, University of the Witwatersrand, Johannesburg, and has never been submitted before for any degree or examination in this University or any other university.



_____

Jaclyn Asouzu Johnson

October 2022

DEDICATION

This work is dedicated to my Saviour and Lord, Jesus Christ

My husband, **Stanley Brian Johnson.** Thank you for working with God to help me achieve impossible milestones. Thank you for believing in me and loving me unconditionally.

My children, **Obianuju, Amarachi, Glory, and Ifeanyi Johnson.** I am beyond blessed to have you, thank you for continually changing my life, inspiring me, and caring for me.

My father, **Christian Ifeanyi Asouzu**. Thank you for all the motivation and unwavering support.

(1950-2020)

Acknowledgments

The completion of this thesis would have not been possible without the support of many people.

I would like to express my very profound gratitude to my mother, Dr. Ann Asouzu, and sister Mrs. Valentina Utoh, thank you for providing me with unfailing love and support, and continuous encouragement throughout the years of my Ph.D.

I would also like to express my deep and sincere gratitude to my supervisor, Prof Felix Mbajiorgu for his constant encouragement, mentoring, teaching, and coaching and for providing invaluable guidance throughout the research, publication, and write-up. I am extremely grateful for his patience, contributions, and effort. It is a great privilege to work under his guidance, and leadership, and strive for excellence which has always inspired me.

My thanks also go to my co-supervisor Prof Robert Ndou for his valuable feedback and expertise; and my co-workers Dr. Eguavoen Idemudia and Vaughan Perry for their collaborative work. Also, I would like to express my heartfelt thanks to Mrs. Hasiena Ali for her technical assistance in all the laboratory experiments utilized in this thesis. Furthermore, I would like to thank her for her friendship, empathy, and availability all of which are greatly appreciated.

A thank you goes out to Lorraine, Nico, Emelia, Mushudu, and all staff members in the Wits Research Animal Facility (WRAF) who were involved, thank you for your assistance with the animal husbandry and termination of the animal study.

Finally, I also appreciate the support of Dr. Pilani Nkomozepi of the University of Johannesburg for his statistical, software, and technical contributions to this project and the use of their microscopes and facilities.

Presentations arising from this study

Asouzu Johnson, J., Ndou, R., & Mbajiorgu, E.F. (October 2021). Neuroinflammatory and neurogenesis perturbations in the hippocampus of male Sprague Dawley rats treated with alcohol and combined antiretroviral therapy (cART).15th SONA/4th GNS Hybrid Conference 2021 Accra, Ghana.

Asouzu Johnson, J., Ndou, R., & Mbajiorgu, E.F. (November 2021). Hippocampal neuroinflammatory and neurogenesis perturbations in diabetic male rats treated with combined antiretroviral therapy (cART). Virtual 50th Annual meeting of SFN "Neuroscience 2021".

Publications arising from this study

Asouzu Johnson, J., Ndou, R., & Mbajiorgu, E. F. (2022). Combination Antiretroviral Therapy (cART) in Diabetes Exacerbates Diabetogenic Effects on Hippocampal Microstructure, Neurogenesis and Cytokine Perturbation in Male Sprague Dawley Rats. *Diagnostics*, *12*(4), 905.

Asouzu Johnson, J., Ndou, R., & Mbajiorgu, E.F. (2022). **Immunohistochemical and Molecular toxicity Evaluation of Alcohol use in Diabetic male Sprague Dawley Rat Hippocampus**. *Diagnostics.* (Manuscript submitted)

Asouzu Johnson, J., Ndou, R., & Mbajiorgu, E.F. (2022). **Interactions of Alcohol and Combination Antiretroviral drug in diabetic Male Sprague Dawley Rats: Hippocampal Perturbations and Toxicosis.** *The Journal of Neuroscience.* (Invited to submit to the Journal's call for papers on Metabolic Mechanisms in Neurodegeneration, manuscript submitted)

ABSTRACT

Multimorbidity of type 2 diabetes, excessive alcohol consumption and HIV infection, and the ultimate antiretroviral therapy are commonplace in our society due to lifestyle choices. Reports indicate that high carbohydrate intake, linked to type 2 diabetes is concurrent with excessive alcohol consumption. The latter is associated with risky sexual behavior that leads to HIV infection and immediate enrollment into combined antiretroviral therapy (cART) programs. The three conditions, diabetes, cART therapy, and alcohol abuse therefore may occur in an individual combinatorial. Additionally, each of these conditions (diabetes, cART therapy, and alcohol abuse), affects cognitive functions. The structure and quantity of hippocampal neurons and their regenerative abilities are crucial for optimal cognitive functions due to their connections to other brain regions. The level of inflammatory cytokines and apoptosis in the hippocampus is equally fundamental. To our knowledge, the impact of this multimorbidity on hippocampal histomorphology and consequent possible functional implications is absent in scientific literature.

Therefore, this study investigated the combined toxicity, effects, or otherwise of alcohol, diabetes, and cART plus their combinations on neurohistological, molecular gene expression of junctional proteins, and neurogenesis parameters of the hippocampus. A total of one hundred and eight HIV naive male adult rats (108) divided into two main groups, diabetic and non-diabetic were used. The diabetic group was further divided into 4 subgroups as follows: (A) diabetic with no treatment (DB), (B) diabetic and cART (DAV), (C) diabetic alcohol (DAL), and (D) diabetic, treated with both alcohol & cART (DAA). The non-diabetic group was further divided into 7 subgroups viz: (E) alcohol and cART treated (AA); (F) received antiretroviral (cART) medication (efavirenz 600mg+ emtricitabine 200mg+ tenofovir 245mg) in gelatine cubes (AV); (G) received 10% alcohol in distilled water v/v *ad libitum* (AL); (H) received plain gelatine cubes (PG); (I) received 20% fructose feed for two weeks and after remained untreated (2FT); (J), received a once off IP injection of citrate buffer (SNC); and (K), untreated controls (NC). The rats were terminated after 90 days, and following perfusion, the brains were harvested, one hemisphere stored at -80°C for immunoassay and PCR while the other hemisphere was fixed in 4% paraformaldehyde for histology and immunohistochemistry analysis.

The diabetic groups (DB, DAV, DAL, and DAA) were observed to be hyperglycaemic, with low glucose tolerance and polydipsia throughout the experiment but these were not observed

in the other groups. The pro-inflammatory cytokines were significantly elevated in AL (IL1α, IL6, and TNFα), AV (IL6 and TNFα), and DAA (IL1α, and TNFα) groups but reduced in the DB and DAV (IL1α, IL6, and TNFα) groups. On the other hand, diabetes, cART, and alcohol independently and or in combination significantly reduced antioxidant GPX. An upregulation of antiapoptotic Bcl_2 (DAL, and DAA), pro-apoptotic genes BAX (DB, DAL, DAV, and DAA), and Caspase-3 (DB, DAV, DAL, and DAA) were observed, indicating a central role of Caspase-3 and BAX in diabetes associated hippocampal apoptosis. Additionally, the downregulation of junctional proteins (claudin-5 and occludin) was observed in AV and DB groups only, while hippocampal insulin receptors (INSR and IRS1) were downregulated in AA, and DB-treated groups, but IRS1 was upregulated in the DAL group. Furthermore, a reduction in neuronal number was observed in the CA1 (AL, DB, DAV, DAL, and DAA), CA3 (DAV, DAL, and DAA), and DG (AL, AV, AA, DB, DAV, DAL, DAA) regions of the hippocampus, while the neuronal nuclei size significantly increased in the CA1 and DG hippocampal regions of the AL and DB groups. These histomorphology effects are corroborated by the significant reduction in hippocampal DCX (AL, DB, DAV, DAL, DAA) and Ki67 (AL, AA, DB, DAV, DAL, DAA) expressions in maturing and proliferating neurons. On the other hand, our results highlight the antagonistic interaction of cART and alcohol (AA), on Bcl_2, BAX, Caspase-3 expression, cytokine concentration, neuronal number, and neurogenesis. Additionally, the AA group reveals significant downregulation of junctional proteins and insulin receptors which may induce hippocampal insulin resistance through impaired insulin receptor function. Finally, alcohol and/or cART in diabetes may result in several histological, biochemical, and molecular adverse effects. Furthermore, the significant loss of neurons in the CA3 hippocampal is observed in the DAV, DAL, and DAA, unlike other treated groups. The clinical implication of these findings hinges on possible neural toxicity following a chronic cART regimen amongst diabetic patients who regularly consume alcohol.

TABLE OF CONTENTS

Declaration ..... **i**
DEDICATION ..... **ii**
Acknowledgments ..... **iii**
Presentations arising from this study ..... **iv**
Publications arising from this study ..... **iv**
ABSTRACT ..... **v**
TABLE OF CONTENTS ..... **vii**
LIST OF FIGURES ..... **xiii**
LIST OF TABLES ..... **xv**
LIST OF ABBREVIATIONS ..... **xvi**
CHAPTER 1 Introduction and chapter outline **1**
1.0 Background of the study 1
1.1 Rationale of the study 5
1.2 Aim 5
1.3 Objectives 6
1.4 Hypothesis 6
1.5 Chapter outline 7
CHAPTER 2 LITERATURE REVIEW **9**
2.1 Diabetes Mellitus 9
2.1.1 Prevalence of diabetes mellitus 9
2.1.2 Diabetes classification 11
2.2 Drug and chemically induced diabetes 12
2.2.1 Epidemiology of HIV 12
2.2.2 Combined antiretroviral therapy 15
2.2.3 Alcohol use 16
2.3 Neuronal disease burden: diabetes, alcohol, and cART 16
2.3.1 Type 2 diabetes-associated dementia 16
2.3.2 HIV-associated neurological pathologies (HAND) 17
2.3.3 Alcohol-induced neuronal pathologies 18
2.4 The hippocampus 18
2.4.1 Anatomy and function of the brain 18
2.4.2 Morphology of the hippocampus 19
2.4.3 Cells and circuitry of the hippocampus 20
2.4.4 Function of the hippocampus 23

2.5 Hippocampal pathology in diabetes, alcohol, and cART 23
2.5.1 Hyperglycaemia with the progression of diabetes 23
2.5.2 Insulin resistance 24
2.5.2.1 Insulin receptor (INSR) and insulin receptor substrate (IRS1) 25
2.5.3 Blood-brain barrier and junctional proteins 26
2.5.4 Neuronal inflammation 27
2.5.4.1 Cytokines 28
2.5.4.2 Pro-inflammatory cytokines 28
2.5.4.2.1 Interleukin six (IL6) 29
2.5.4.2.2 Tumour necrosis factor alpha (TNF-α) 30
2.5.4.2.3 Interleukin one alpha (IL1-α) 30
2.5.5 Oxidative stress 31
2.5.6 Cell death in the hippocampus 32
2.5.6.1 Apoptosis 32
2.5.6.2 Necrosis 33
2.5.7 Proliferation and maturation of neurons in the hippocampus 34
2.5.7.1 Ki67 35
2.5.7.2 Double courtin (DCX) 36
2.6 The experimental model 37
2.6.1 The male diabetes rat model 37
2.6.2 HIV naïve model 38
CHAPTER 3. MATERIALS AND METHODS 40
3.1 Sprague Dawley rat diabetic model 40
3.1.1 Diabetes induction 40
3.1.2 Routine tests for diabetes model 40
3.2 Dosage and preparation of treatments ARV and alcohol treatments 41
3.3 Animal experiments 42
3.3.1 Animal husbandry 42
3.3.2 Experimental design 42
3.3.3 Termination 43
3.4 Laboratory analysis 45
3.4.1 Enzyme-linked immunoassay of proinflammatory cytokines (IL-1α, IL-6, TNFα) and oxidative stress markers (GPX, and MDA) 45
3.4.2 Quantitative qPCR for junctional proteins and apoptotic markers 46
3.4.2.1 RNA extraction 46

3.4.2.2 cDNA synthesis 46
3.4.2.3 qPCR experiment 47
3.5 Brain tissue preparation for histology 48
3.6 Routine Histology using Cresyl violet for Nissl stain 49
3.7 Histomorphometry 49
3.7.1 Volume of the dentate gyrus 49
3.7.2 Neuronal number and nuclei area 50
3.8 Immunohistochemistry for neurogenesis 50
3.9 Statistical analysis 51
3.10 Ethical clearance 51
CHAPTER 4 A Diabetic Model Suitable for Investigating Multidrug Therapy 52
4.0 Abstract 52
4.1 Introduction 53
4.2 Methods and materials 55
4.2.1 Formulation of fructose feed 55
4.2.2 Induction of diabetes 55
4.2.3 Routine tests 56
4.2.4. Experimental design 56
4.3 Results 56
4.3.1 Diabetic parameters: Experimental vehicle groups 57
4.3.1.1 Mortality in experimental vehicles groups 57
4.3.1.2 Mean body weight of experimental vehicle groups 57
4.2.1.3 Mean fasting and non-fasting blood glucose of experimental vehicle groups 58
4.3.1.4 Food and fluid intake of experimental vehicles 60
4.3.1.5 Oral glucose tolerance test of experimental vehicles groups 61
4.3.1.6 Discussion 63
4.3.2 Diabetic parameters: Treatment groups 63
4.3.2.1 Mortality in treated groups 63
4.3.2.2 Mean body weight of treated groups 64
4.3.2.3 Random non-fasting and fasting glucose of treated groups 67
4.3.2.4 Food and fluid intake of treated groups 68
4.3.2.5 Oral glucose tolerance test and AUC of treated groups 69
4.3.2.6 Discussion 71

CHAPTER 5 Combination Antiretroviral Therapy (cART) in Diabetes Exacerbates Diabetogenic Effects on Hippocampal Microstructure, Neurogenesis, and Cytokine Perturbation in Male Sprague Dawley Rats....73
5.0 Abstract....73
5.1 Introduction....74
5.2. Materials and Methods....76
5.2.1 Chemical and reagents....76
5.2.2 Ethical clearance....76
5.2.3 Animal husbandry....76
5.2.4 Experimental design....77
5.2.5 Enzyme-linked immunoassay of proinflammatory cytokines and malondialdehyde (MDA)....77
5.2.6 Brain tissue preparation for histology....77
5.2.7 Histology and histomorphometry....77
5.2.8 Immunohistochemistry for neurogenesis....77
5.2.9 Statistical analysis....78
5.3. Results....78
5.3.1 Mortality....78
5.3.2 Body weight....78
5.3.3 Blood glucose levels....78
5.3.4. Oral Glucose Tolerance Test....80
5.3.5. Inflammatory Cytokines and MDA....81
5.3.6. Histopathology of the Hippocampus....83
5.3.6.1. Number of Neurons in Hippocampal Regions....83
5.3.6.2. Neuronal Nuclei Area in Hippocampal Regions....83
5.3.7. Immunohistochemistry for Neurogenesis in the Hippocampus Double Cortin and Ki67....87
5.3.8. Correlation of Histomorphology and Neurogenic Parameters....89
5.4 Discussion....91
CHAPTER 6 Immunohistochemical and Molecular Evaluation of Alcohol toxicity on Diabetic Sprague Dawley Rat Hippocampus....95
6.0 Abstract....95
6.1 Introduction....96
6.2. Materials and methods....98
6.2.1 Chemicals....98
6.2.2 Animals & housing....98

6.2.3 Experimental design 98
6.2.4 Enzyme-linked immunoassay of oxidative stress markers (GPx, and MDA) 99
6.2.5 Quantitative qPCR for junctional proteins, insulin receptors, and apoptosis gene expression 99
6.2.6 Histology and immunohistochemistry 99
6.2.7 Statistical analysis 100
6.3 Results 100
6.3.1 Food and fluid consumption 100
6.3.2 Mean blood glucose levels 101
6.3.3 Mean oral glucose tolerance levels 101
6.3.4 Oxidative stress markers 103
6.3.5 Expression of apoptotic markers RT qPCR 104
6.3.6 Expression of BBB junctional proteins (claudin-5 and occludin) 105
6.3.7 Expression of insulin receptors and insulin receptor substrate (INSR and IRS1) 106
6.3.8 Mean number of neurons in hippocampal regions 107
6.3.9 Immunohistochemistry for neurogenesis in the hippocampus Double Cortin and Ki67 110
6.3.10 Pearson's correlation analysis: relationships between parameters 112
6.4 Discussion 113
CHAPTER 7 Interactions of Alcohol and Combination Antiretroviral drug in diabetic Male Sprague Dawley Rats: Hippocampal Perturbations and Toxicosis 118
7.0 Abstract 118
7.1 Introduction 119
7.2 Materials and methods 121
7.2.1 Experimental groups 121
7.2.2 Enzyme-linked immunoassay of proinflammatory cytokines (IL-1α, IL-6, TNFα) and oxidative stress markers (GPX, and MDA) 121
7.2.3 Quantitative qPCR for junctional proteins, insulin receptors, and apoptotic markers 121
7.2.4 Histomorphometry using Cresyl violet stain and Immunohistochemistry for neurogenesis 122
7.3 Results 122
7.3.1Oral glucose tolerance test and AUC of treated groups 122
7.3.2 Proinflammatory cytokines 123
7.3.3 Oxidative stress markers 126
7.3.4 Mean apoptotic genes expression in hippocampal tissue 127

7.3.5 Mean membrane junctional genes expression in hippocampal tissue 129
7.3.6 Mean insulin receptor genes expression in hippocampal tissue 131
7.3.7 Histomorphology of hippocampus 133
7.3.7.1 Mean volume of granular and molecular layer in the dentate gyrus..... 133
7.3.7.2 Mean number of neurons in different hippocampal regions 136
7.3.7.3 Mean neuronal nuclei in different hippocampal regions 144
7.3.8 Immunohistochemical expression of hippocampal Double Cortin 144
7.3.9 Immunohistochemical expression of hippocampal Ki67 149
7.3.10 Relationship between parameters 153
7.4 Discussion 156
Chapter 8 Concluding discussion 160
8.0 Independent effects of alcohol, cART, and diabetes on hippocampal histopathology 160
8.1 The hippocampal impact of diabetes and cART interaction 161
8.2 Hippocampal pathology with alcohol use in diabetes 162
8.3 The hippocampal impact of alcohol and cART interaction 162
8.4 Hippocampal histopathology of diabetes, alcohol, and cART 163
8.5 Focal hippocampal effects of diabetes, alcohol, cART, and their combinations 163
8.6 Limitations of the study 164
8.7 Recommendation for future studies 164
REFERENCE LIST 165

LIST OF FIGURES

Figure 2. 1. Coronal slice through the transverse axis of the dorsal hippocampus showing circuitry interconnection between regions adopted from histological images in this thesis (By Jaclyn Asouzu Johnson).....22
Figure 2. 2. Schematic diagram illustrating the different phases of neurogenesis in the dentate gyrus.. 35
Figure 2. 3. A schematic representation of different stages of the cell cycle and the Ki-67 expression observed in a study reported by (Scholzen and Gerdes, 2000) (animation by Jaclyn Asouzu Johnson).....36
Figure 2. 4. Pictorial representation of the rodent, primate, and human brain and hippocampus showing the long axis model of the hippocampus in each model. 38
Figure 2. 5. Schematic representation of summarized independent effects of diabetes, alcohol and cART and other potential hippocampal effects reported in literature.....39
Figure 3. 1 Flow diagram of experimental design 44
Figure 4.1. 1. Mean weekly body weight in experimental vehicle groups 58
Figure 4.1. 2. Mean fasting and non-fasting blood glucose across experimental vehicle groups. 59
Figure 4.1. 3. Mean food and water intake across experimental vehicle groups. 60
Figure 4.1. 4. Mean initial and final OGTT across experimental vehicle groups.....**Error! Bookmark not defined.**
Figure 4.2. 1. Percentage mortality of animals in treated groups. No mortality occurred in the control and non-diabetic groups.....64
Figure 4.2. 2. Mean Weekly Body Weight in treated groups. 66
Figure 4.2. 3. Mean non-fasting and fasting blood glucose across treated groups. 67
Figure 4.2. 4. Mean food and fluid intake across treated groups. 68
Figure 4.2. 5. Mean terminal AUC and OGTT of treated groups. 70
Figure 5. 1. Mean mortality, terminal body weight, and fasting and non-fasting blood glucose levels. 79
Figure 5. 2. Mean oral glucose tolerance test and area under the curve. 80
Figure 5. 3. Mean terminal concentrations of IL-1α, IL-6, TNFα, and MDA in hippocampal tissue homogenate.. 82
Figure 5. 4. Mean nuclei area and number of neurons in the CA1 region of the dorsal hippocampus. 84
Figure 5. 5. Mean nuclei area and number of neurons in the CA3 region of the dorsal hippocampus. 85
Figure 5. 6. Mean nuclei area and number of neurons in the dentate gyrus region of the dorsal hippocampus. 86
Figure 5. 7. Photomicrograph of the hippocampus showing the expression of DCX in the sub-granular zone of the dentate gyrus region. 89
Figure 6. 1. Mean food intake, fluid consumption, fasting, and non-fasting blood glucose levels. 101
Figure 6. 2. Mean monthly oral glucose tolerance test (OGTT) and area under the curve (AUC). 103
Figure 6. 3. Mean concentrations of MDA and GPX in hippocampal tissue homogenate.. .104
Figure 6. 4. Mean relative expression of apoptotic genes in the hippocampal homogenate.. 105

Figure 6. 5. Mean relative expression levels of membrane junctional proteins in the hippocampal homogenate.. 106
Figure 6. 6. Mean levels of insulin receptors (INSR and IRS) in the hippocampal homogenate. 107
Figure 6. 7. Mean number of neurons in the CA1, CA3, and DG regions of the dorsal hippocampus. 108
Figure 6. 8. Histomorphology in the CA1, CA3, and DG regions of the dorsal hippocampus. 109
Figure 6. 9. Photomicrograph of the hippocampus showing DCX and Ki67 expression in the sub-granular zone of the dentate gyrus region. 111
Figure 6. 10. Correlation analysis with significant Pearson correlation of hippocampal parameters affected in diabetes and alcohol experimental groups. 113
Figure 7. 1. Mean terminal AUC and OGTT of treated groups.. 123
Figure 7. 2. Mean expression of apoptotic associated genes Bcl_2, BAX, and Caspase-3 in hippocampal tissue. 128
Figure 7. 3. Mean expression of junctional membrane-associated genes claudin-5 and occludin in hippocampal tissue. 130
Figure 7. 4. Mean expression of insulin receptor and insulin receptor substrate in hippocampal tissue. 132
Figure 7. 5. Photomicrographs of the dorsal hippocampus across different experimental groups. 134
Figure 7. 6. Mean volume of granular and molecular layers in the dentate gyrus of dorsal hippocampal sections. 135
Figure 7. 7 Photomicrographs of the CA1 region in the dorsal hippocampus across different experimental groups. 138
Figure 7. 8. Photomicrographs of the CA3 region in the dorsal hippocampus across different experimental groups. 139
Figure 7. 9. Photomicrographs of the CA1 region in the dorsal hippocampus across different experimental groups. 140
Figure 7. 10. Mean neuronal number and mean nuclei area in CA1 region of the dorsal hippocampus. 141
Figure 7. 11. Mean neuronal number and mean nuclei area in the CA3 region of the dorsal hippocampus. 142
Figure 7. 12. Mean neuronal number and mean nuclei area in the dentate gyrus region of the dorsal hippocampus. 143
Figure 7. 13. Mean number of neurons expressing DCX in the dentate gyrus region of the dorsal hippocampus.. 146
Figure 7. 14. Representative photomicrographs illustrating expression of DCX in the dentate gyrus region of the dorsal hippocampus.. 147
Figure 7. 15 Representative photomicrographs illustrating expression of DCX in the dentate gyrus region of the dorsal hippocampus.. 148
Figure 7. 16. Mean number of neurons expressing Ki67 in the dentate gyrus region of the dorsal hippocampus. 150
Figure 7. 17. Representative photomicrographs illustrating expression of Ki67 in the dentate gyrus region of the dorsal hippocampus. 151

Figure 7. 18. Representative photomicrographs illustrating expression of Ki67 in the dentate gyrus region of the dorsal hippocampus.. 152

LIST OF TABLES

Table 2. 1 Global prevalence and projection and death caused by diabetes mellitus 10
Table 2. 2. Prevalence, projection, and death caused by diabetes mellitus in Africa 11
Table 2. 3. Regional data on HIV/AIDS and antiretroviral therapy 13
Table 2. 4. Regional data on HIV/AIDS and antiretroviral therapy 14

Table 3. 1. Primer sequence for the gene of interest and housekeeping genes 48

Table 5. 1. Spearman's rho nonparametric correlation of diabetes parameters with the neuronal number and neurogenic parameters. 90
Table 5. 2. Spearman's rho nonparametric correlation of diabetes parameters with neuronal nuclei area and neurogenic parameters. 91

Table 7. 1. Mean concentration of cytokines IL-1α, IL-6, and TNFα in hippocampal tissue homogenate. 125
Table 7. 2. Mean concentration of oxidative stress markers MDA and GPX in hippocampal tissue homogenate. 126
Table 7. 3. Spearman's rho correlation of diabetes parameters with proinflammatory cytokines, BBB genes, and insulin receptor genes. 154
Table 7. 4. Spearman's rho nonparametric correlation of diabetes parameters, oxidative stress, neuronal histomorphology, neurogenesis, apoptotic genes, BBB genes, and insulin receptor genes. 155

LIST OF ABBREVIATIONS

α	Alpha
β	Beta
%	Percentage
^{o}C	Degrees Celsius
g	Gram
kg	Kilogram
L	Litre
M	Molar
mg	Milligram
mL	Millilitre
mmol	Millimoles
pg	Picogram
µg	Microgram
µL	Microlitre
µm	Micrometre
µmol	Micromole
ANOVA	Analysis of variance
ART	Antiretroviral therapy
ARV	Antiretrovirals
BBB	Blood-brain barrier
CA1A	Area of neuronal nuclei at CA1
CA1N	Number of neurons at CA1
CA3A	Area of neuronal nuclei at CA3
CA3N	Number of neurons at CA3

CNS	Central nervous system
DCX	Doublecortin
DG	Dentate gyrus
DGA	Area of neuronal nuclei at DG
DGGL	Volume of the granular layer of the dentate gyrus
DGML	Volume of the molecular layer of the dentate gyrus
DGN	Number of neurons at DG
GPx	Glutathione peroxidase
HIV	Human immunodeficiency syndrome
H_2O_2	Hydrogen peroxide
INSR	Insulin receptor
IRS1	Insulin receptor substrate 1
i.p.	Intra-peritoneal
IHC	Immunohistochemistry
MDA	Malondialdehyde
mRNA	Messenger ribonucleic acid
NA	Neuronal nuclei area
NN	Number of neurons
PB	Phosphate buffer
PCR	Polymerase chain reaction
PLWHAs	People living with HIV/AIDS
SD	Sprague-Dawley
SEM	Standard error of the mean
WHO	World Health Organisation

CHAPTER 1 Introduction and chapter outline

1.0 Background of the study

Lifestyle factors such as high carbohydrate intake and excessive alcohol consumption are increasingly becoming the leading cause of several diseases worldwide (Barve et al., 2017; Li and Sun, 2022). Excessive alcohol consumption is associated with risky behaviours such as multiple concurrent sex partners and unprotected sex with a high risk of HIV infection and consequent admission into an antiretroviral (ARV) program (Johnson et al., 2017; Duko et al., 2019). Additionally, excessive alcohol consumption (Kim and Kim, 2012), high carbohydrate consumption (Kodama et al., 2009; Feng et al., 2015) in combination with obesity amongst South Africans (Schulze et al., 2008; Cois and Day, 2015) may underline the rise in type 2 Diabetes Mellitus (T2DM).

Type 2 diabetes is a metabolic disorder, characterized by hyperglycaemia, insulin resistance, or lack of insulin secretion (Association, 2015; Goyal and Jialal, 2022). This disease is associated with cognitive anomalies (Kodl and Seaquist, 2008; van Bussel et al., 2017), dementia (McNay and Recknagel, 2011; Beeri and Bendlin, 2020), hippocampal apoptosis, and deficiencies in synaptic plasticity (Sadeghi et al., 2016; Milne et al., 2017). Organ pathologies resulting from type 2 diabetes such as retinopathy (Nentwich and Ulbig, 2015; Lynch and Abràmoff, 2017) and nephropathy (Lim, 2014; Alaofi, 2020), and their association with vascular injury (Chawla et al., 2016; Wang and Zhang, 2021) have been well researched. However, more neuropathology studies are required in diabetes, considering the susceptibility of the central nervous system (CNS) to metabolic perturbations. Additionally, diabetes hardly occurs independently but is often found as a co-morbidity in chronic chemical/ drug therapy such as combination antiretroviral drug (cART) and alcohol use (Engler et al., 2013; Iglay et al., 2016; Karamchand et al., 2016) with attendant adverse health implications and therefore,

imperative to evaluate brain pathologies associated with diabetes concurrent with cART and alcohol.

Metabolic syndrome in diabetes generally ensued by hyperglycaemia and/or hypoglycaemia, insulin disorder, and dyslipidaemia, all with attendant cognitive dysfunction (Manschot et al., 2006; Yates et al., 2012). Disrupted insulin regulation and glucose metabolism in diabetes have also been implicated in brain atrophy (Moran et al., 2013; Milne et al., 2017), altered plasticity, and hippocampal memory functions of the brain (Gispen and Biessels, 2000; McNay et al., 2010). While the endocrinology aspects of diabetes are well known, the long-term effect of diabetes on neurons of the hippocampus requires more studies considering the associated memory loss and learning difficulties. The potential for type 2 diabetes to impair cognitive function (Kodl and Seaquist, 2008; Kawamura et al., 2012) is associated with a disruption in the blood-brain-barrier and neurovascular damage (Hawkins et al., 2007; Salameh et al., 2016) which impairs hippocampal synaptic plasticity and impedes or hinders memory and learning (Gispen and Biessels, 2000; Braganza et al., 2021). The perturbation of pro-inflammatory cytokines (Muriach et al., 2014) and reactive oxygen species (ROS) (Sasaki and Inoguchi, 2012) in type 2 diabetes activates a cascade of intracellular events that leads to autophagy in hippocampal neurons (Gonzalez et al., 2011; Sadeghi et al., 2016). At elevated levels, pro-inflammatory cytokines and ROS have been shown to independently increase the permeability of the blood-brain barrier (BBB) in type 2 diabetes (Huber et al., 2006; Salameh et al., 2016). Pro-inflammatory cytokines may also decrease cell proliferation within the hippocampus leading to hippocampal dysfunction and attendant learning and memory deficits (Seguin et al., 2009; Russo et al., 2011). Therefore, brain pathologies associated with type 2 diabetes require more research, particularly in the light of alcohol abuse and antiretroviral treatment. We postulate that diabetes-induced neuronal inflammation, histopathology, and oxidative stress

effects may be negatively impacted or otherwise by such lifestyle factors as excessive alcohol use and cART regime.

Atripla®, a combination antiretroviral drug (cART) is one of the most effective and readily available antiretroviral medications (Julg and Bogner, 2008; Horberg and Klein, 2010). However, the efficacy of some of the drug components such as efavirenz may be counteracted by its role in blood-brain-barrier (BBB) permeability (Bertrand et al., 2016), elevating pro-inflammatory cytokines (O'Mahony et al., 2005) which in-turn induces oxidative stress (Möller et al., 2018) and insulin resistance (Honnapurmath and Patil, 2017), thereby enhancing the development of type 2 diabetes. Since type 2 diabetes and cART can each increase the permeability of the blood-brain barrier, their combined presence may further exacerbate the permeability to toxins (such as alcohol) and probably result in an increased toxicity effect. Within the cART (Atripla®) combination formulation, efavirenz (NNRTI) has received the most attention due to its impact on the central nervous system. Efavirenz penetrates the CNS effectively reducing the CNS viral load by binding to HIV-1 reverse transcriptase and preventing viral replication by blocking access to substrates (Dellamonica et al., 2012). However, the presence of efavirenz in the CNS may induce neuropsychiatric and neurocognitive disorders (Gutiérrez et al., 2005; Romao et al., 2011; Apostolova et al., 2017). Efavirenz and its metabolites increase neuronal dendritic beading and pruning, simplification of dendritic processes and neuronal shrinkage in vivo (Robertson et al., 2012), and induce a reduction in cerebral claudin-5; which are transmembrane junctional proteins that are regulated in the CNS during homeostatic and pathological conditions (Avison et al., 2004; Greene et al., 2019). Similarly, other NNRTIs increase the levels of hippocampal pro-inflammatory cytokines (Zulu, 2014) and induce oxidative stress (Möller et al., 2018), with correlated effects on the BBB (Varatharaj and Galea, 2017) and neuronal loss, suggesting possible means through which cART may induce neuronal toxicity.

Alcohol use is common among several age groups in South Africa and globally. The effects of alcohol abuse involve the alteration of structural, physiological, and regenerative aspects of the nervous system. In the hippocampus, a reduction in volume, and size of the dentate gyrus, and decreased number and size of pyramidal cell spines (Dhanabalan et al., 2018; Zahr et al., 2019) with diminished neurogenesis as shown by diminished DCX and Ki67 expression (Taffe et al., 2010) has been reported. Alcohol readily crosses the BBB and induces oxidative stress and cognitive deficits (Barnham et al., 2004; Wei et al., 2021). Alcohol-induced oxidative stress may increase pro-inflammatory cytokines (Kalejaiye et al., 2017) and impair the BBB (Haorah et al., 2007). Chronic alcohol consumption and alcohol use disorder (AUD) increases pro-inflammatory cytokine levels which, consequently, alters the integrity of BBB proteins (Rubio-Araiz et al., 2017), inducing hippocampal atrophy with attendant disruption in executive function (Wilcox et al., 2014). Therefore, cART, alcohol, and type 2 diabetes are all independently implicated in oxidative stress induction, cytokine perturbation, and disruption of BBB structural integrity relative to hippocampal-associated pathologies.

This study investigated the effect of alcohol intake and sub-chronic cART therapy in type 2 diabetic disease on the hippocampus of the HIV naïve Sprague Dawley rat model. The proposed study, therefore, evaluated the combined effect of diabetes, alcohol, and cART on the number of hippocampal neurons and their nuclei morphology in the hippocampus using several techniques such as Nissl stain as well as the immunohistochemical techniques for the expression of DCX and Ki67 for neuronal cell maturation and proliferation respectively. Additionally, the relative expression of apoptotic genes (Bcl_2, BAX, and Caspase-3) and junctional proteins of BBB (claudin-5 and occludin) were investigated using real-time quantitative PCR, and the assessment of the level of pro-inflammatory cytokines and oxidative stress markers in the hippocampus were evaluated using immunoassay. The above techniques were applied in all the treated groups.

1.1 Rationale of the study

Lifestyle factors involving high-calorie diet and alcohol abuse are implicated in the pathogenesis of type 2 diabetes (Carlsson et al., 2003; Schulze et al., 2008). Alcohol abuse has been associated with reckless behaviour resulting in a high rate of HIV infection and the consequent anti-retroviral drug therapy which is implicated in the pathogenesis of type 2 diabetes. The consequence of the above scenario is the multiple morbidity of diabetes, alcohol, and anti-retroviral drug presence in one individual, a prevalent condition in our societies. These three conditions; diabetes, alcohol abuse, and anti-retroviral drug intake especially in non-infected people (due to occupational exposure to HIV infection) have each been associated with adverse effects on the hippocampus with resultant dementia, cognitive dysfunction, impaired working memory, and cerebrovascular diseases amongst others. The combined effects of these three co-morbidities relative to neurovascular morphology, hippocampal anatomy, apoptosis, and neurogenesis have not been studied. The present study, therefore, evaluated the neurotoxicity of the concomitant presence of alcohol and antiretroviral drug in a diabetic condition. The results are expected to help clinicians with the better management of possible neuropathological conditions that may be experienced by diabetic patients on cART therapy and alcohol abuse.

1.2 Aim

To delineate the effects of alcohol and cART concurrent exposure on neuro-morphology and neurogenesis, neuroinflammation and toxicity in the hippocampus of male diabetic Sprague Dawley rats.

1.3 Objectives

To investigate the combined effects of alcohol intake and antiretroviral therapy in type 2 diabetes.

- On the concentration of oxidative stress markers (MDA and GPX) in the hippocampus using ELISA immunoassay techniques.
- On the levels of pro-inflammatory cytokines (IL-1 α, IL-6, TNF-α) in the hippocampus using ELISA immunoassay techniques.
- On hippocampal insulin resistance using reverse transcription coupled with real-time quantitative PCR to quantify the gene expression of insulin receptor and insulin receptor substrate (INSR and IRS1).
- On hippocampal apoptosis using real-time quantitative PCR to quantify the expression of apoptotic genes (BCL, BAX, and Caspase-3).
- On the mRNA gene expression of membrane junctions (claudin-5 and occludin) in the hippocampus, using reverse-transcription coupled with real-time quantitative PCR.
- On hippocampal histoarchitecture (neuronal number, nuclei area, and dentate gyrus volume) using Nissl stain.
- On hippocampal neurogenesis by assessing the expression of hippocampal cell migration and proliferation of DCX and Ki67 labelled neurons respectively using immunohistochemistry techniques.

1.4 Hypothesis

It is hypothesized that the interactive effects of alcohol and cART therapy in the diabetic condition will adversely affect and alter the hippocampal histomorphology, which may potentially affect the gene expression and microstructure of functional neurogenesis and BBB junctional proteins.

1.5 Chapter outline

The thesis is organized into several chapters, with four main chapters (chapters 4 to 7 plus the concluding discussion) examining diabetes comorbidities with alcohol /and or cART for specifically induced mechanisms that affect the hippocampus.

Chapter 1 Describes the background of diabetes, alcohol, and cART and identifies several associated mechanisms, and highlights the research questions relative to the hippocampus, cognitive, and neuropathological conditions.

Chapter 2 This chapter presents a concise literature review of the relationships between diabetes, alcohol, and cART, in addition, the synthesis of information concerning known hippocampal effects by each of these independent factors is unpacked. This chapter further describes the role of oxidative stress, neuro-inflammation, BBB permeability, apoptosis, and hippocampal insulin receptor relative to diabetes, alcohol, and cART hippocampal histopathology.

Chapter 3 This chapter describes in detail the experimental design, routine test observations, and laboratory techniques used to investigate several parameters.

Chapter 4 This chapter investigated the diabetic model in combination with different therapies using a fructose-enriched diet in combination with a single low-dose STZ administration. Diabetic parameters were periodically observed and recorded in the experimental vehicles and treated groups. The experimental vehicles were completely void of any diabetogenic effect, while elevated diabetogenic parameters were consistently observed in all the diabetic groups.

Chapter 5 This chapter investigated the dual effect of cART and diabetes on the hippocampus. Elevated neuroinflammation, oxidative stress, and loss of dentate gyrus neurons were induced by cART while diabetes and cART exacerbated diabetogenic effects, hippocampal neuronal loss and neurogenesis and maintained the diabetogenic effect of impaired neuro-inflammation.

Chapter 6 This chapter investigated the hippocampal effect of alcohol use in the diabetic condition by assessing hippocampal apoptosis, insulin resistance, and blood-brain permeability. The presence of alcohol in diabetes ameliorated diabetic effects on blood glucose and glucose tolerance and alleviated insulin resistance, however, this comorbidity also exacerbated hippocampal apoptosis and impaired neurogenesis beyond levels observed independently in diabetes or alcohol.

Chapter 7 This chapter investigated the dual effect of cART and alcohol interaction in the diabetic condition (DAA) for neuro-inflammatory, oxidative stress, apoptosis, insulin resistance, blood-brain barrier (BBB), and neurogenesis effects. These results indicated that concomitant use of alcohol with cART administration depleted proliferating neurons and induced heightened BBB permeability and insulin resistance, which may lead to the development of diabetes with chronic exposure. Consequently, continued alcohol use and cART regime (AA) within a diabetic individual may maintain and exacerbate diabetogenic effects by elevating hippocampal oxidative stress, apoptosis, and impairing neurogenesis with induction of neuroinflammation which finding is peculiar to DAA-treated group.

Chapter 8 This chapter gives a general concluding discussion of the key findings in the different treatment groups. A central hippocampal effect that underpins all treated groups is the reduction of DG neuronal number and antioxidant (GPx). Furthermore, the diabetic comorbidity groups (DAV, DAL, and DAA) all share a central effect of reduced CA3 neuronal number and nuclei area, DG granular, and molecular layer volume, implicating the negative impact of these comorbidity treatments on the unique functional neuronal network/interconnectivity provided by hippocampal CA3 neurons and DG volume.

CHAPTER 2 LITERATURE REVIEW

2.1 Diabetes Mellitus

Lifestyle factors like unhealthy diet and physical inactivity commonly lead to the development of non-communicable diseases, such as heart disease, stroke, obesity, metabolic syndrome, and diabetes (Budreviciute et al., 2020; Li and Sun, 2022) amongst others. Diseases such as diabetes often occur without proper diagnosis or treatment which can result in loss of independence, disability, or death, and as such impose a substantial economic burden on health services (Kirigia et al., 2009; Rushforth et al., 2016).

2.1.1 Prevalence of diabetes mellitus

Type 2 diabetes mellitus (T2DM) is a non-communicable disease with a 54% increasing prevalence globally according to the International Diabetes Federation (IDF) in 2016. Amongst the South African population, it is estimated that 2.286 million adults (aged 20-79 years) are diabetic (IDF 2016), with a 3-28% prevalence of type 2 diabetes mellitus (T2DM) globally (2013) and 5.4 % in South Africa (Guariguata et al., 2014; Pheiffer et al., 2018). This prevalence of T2DM stems from high carbohydrate consumption and obesity (29% men, 56.6% women) among South Africans (Rheeder, 2006). In sub-Saharan Africa, 14.2 million people were diabetic in 2015 (Pastakia et al., 2017), while a projected estimate of 25.5 million in South Africa, 65.8 million in Africa, and 5587 million globally will be diabetic by 2030 (Whiting et al., 2011). According to the IDF, a steady increase in diabetes has been maintained globally, especially in the west pacific, South-East Asia, Middle East, and North Africa. Although Africa is the least affected globally, the most affected countries in Africa in the year 2021 include Egypt, with > 8 million people, 4.2 million people in South Africa, 3.6 million in Nigeria, 3.5 million in Sudan, 2.9 million in Tanzania, 2.3 million in Morocco while 1.9 million people in

Democratic Republic of Congo and Ethiopia are currently affected with DM (IDF, 2021) (Table 2.1 and 2.2).

Table 2. 1 Global prevalence and projection and death caused by diabetes mellitus

Regions/ Diabetes parameters	**2000**	**2011**	**2021**	**2030**	**2045**	**Death caused by diabetes in 2021**
Africa	2.5 million	14.7 million	24 million	33.4 million	55.2 million	416,000
North America and the Caribbean	21.4 million	37.7 million	51 million	57 million	63 million	931,000
The Middle East and North Africa	17 million	32.6 million	73 million	95 million	135.7 million	796,000
South and Central America	8.5 million	25.1 million	32 million	40 million	49 million	410,000
South-East Asia	34.8 million	71.4 million	90 million	113.3 million	151.5 million	747,000
Western Pacific	44 million	131.9 million	206 million	238.3 million	260.2 million	2.3 million
Europe	22.4 million	52.7 million	61 million	67 million	69 million	1.1 million

Source: International Diabetes Federation Diabetes Atlas 10th edition, 2021,. (IDF, 2021).

Table 2. 2. Prevalence, projection and death caused by diabetes mellitus in Africa

Country/Year	2011/people	2021/people	2030/people	2045/people
Algeria	1.4 million	2 million	2.5 million	3.4 million
Democratic Republic of Congo	730,000	1.9 million	2.7 million	4.8 million
Egypt	7.3 million	> 8 million	13.7 million	19.9 million
Ethiopia	1.3 million	1.9 million	2.7 million	4.7 million
Morocco	1.2 million	2.3 million	2.8 million	3.5 million
Nigeria	3 million	3.6 million	4.9 million	7.9 million
South Africa	1.9 million	4.2 million	5.4 million	7.4 million
Sudan	1.6 million	3.5 million	4.7 million	7.4 million
Uganda	307,000	716,000	1 million	1.9 million
Tanzania	472,000	2.9 million	4.2 million	7.3 million

Source: International Diabetes Federation Diabetes Atlas 10th edition, 2021. (IDF, 2021).

2.1.2 Diabetes classification

According to the American diabetic association (Association, 2015), there are four general categories of diabetes: 1) type 1 diabetes is caused by autoimmune pancreatic β-cells destruction inducing insulin deficiency, 2) type 2 diabetes is caused by progressive insulin resistance and defective insulin secretion, 3) gestational diabetes which is diagnosed in the second half of pregnancy, and 4) a specific type of diabetes with several causes such as diseases, drug or chemically induced. This suggests that despite the lifestyle and genetic predisposition to diabetes, factors such as combined antiretroviral (cART) and alcohol use can induce diabetes with chronic exposure.

2.2 Drug and chemically induced diabetes

2.2.1 Epidemiology of HIV

Globally in 2020 HIV infections is reported in approximately 37.7 million individuals comprising of 36 million adults and 1.7 million children aged 14 and below (UNAIDS, 2021; WHO, 2021). According to UNAIDS (Table 2.3 and 2.4), the highest burden of HIV/AIDS is observed in Eastern and Southern Africa (Sub-Saharan Africa), with peak infections in Botswana, Swaziland, Zimbabwe, Namibia, South Africa, Zimbabwe, Lesotho, Zambia, Malawi, and Mozambique accounting for 54.6% of infections (Jahagirdar et al., 2021; UNAIDS, 2021), especially in South Africa with 8.3 million individuals living with HIV/AIDs (Akullian et al., 2021; SSA, 2021; UNAIDS, 2021). Following Eastern and Southern Africa, the rate of HIV infection is prevalent in Asia, the Pacific, Western and Central Africa, Western and Central Europe, North America while the least prevalence is reported in Latin America (Table 2.3 and 2.4). Additionally, as a greater number of people with HIV infection are increasingly accessing ART, HIV-associated deaths are on the decline (Table 2.4).

Table 2. 3. Regional data on HIV/AIDS and antiretroviral therapy

HIV indices/Year	2000	2005	2010	2015	2016	2017	2018	2019	2020/June 2021
People living with HIV	25.5 million	28.6 million	31.1 million	34.6 million	35.3 million	35.9 million	36.6 million	37.2 million	37.7 million
New HIV infections (Adults and children)	2.9 million	2.4 million	2.1 million	1.8 million	1.7 million	1.7 million	1.6 million	1.5 million	1.5 million
AIDS-related deaths	1.5 million	1.9 million	1.3 million	900 000	850 000	800 000	750 000	720 000	680 000
People accessing antiretroviral therapy	560 000	2.0 million	7.8 million	17.1 million	19.3 million	21.5 million	23.1 million	25.5 million	27.5 million

Source: https://www.unaids.org/sites/default/files/media_asset/UNAIDS_FactSheet_en.pdf.

Table 2. 4. Regional data on HIV/AIDS and antiretroviral therapy

Regions/HIV data	People living with HIV in 2020	New HIV infections (Adults and children in 2020)	AIDS-related deaths as of 2020	People accessing antiretroviral therapy as of 2020
Eastern and southern Africa	20.6 million	670 000	310 000	16.0 million
Asia and the Pacific	5.8 million	240 000	130 000	3.7 million
Western and Central Africa	4.7 million	200 000	150 000	3.5 million
Latin America	2.1 million	100 000	31 000	1.4 million
The Caribbean	330 000	13 000	6000	220 000
Middle East and North Africa	230 000	16 000	7900	96 000
Eastern Europe and Central Asia	1.6 million	140 000	35 000	870 000
Western and Central Europe and North America	2.2 million	67 000	13 000	1.9 million
Global totals	37.7 million	1.5 million	680 000	27.5 million

Source: https://www.unaids.org/sites/default/files/media_asset/UNAIDS_FactSheet_en.pdf.

2.2.2 Combined antiretroviral therapy

A combination antiretroviral drug (cART; Atripla®) is an antiretroviral medication with three drugs combined into a single, once-daily pill. It consists of a combination of one non-nucleoside reverse transcriptase inhibitor (NNRTI), efavirenz, and two nucleoside reverse transcriptase inhibitors (NRTI), tenofovir disoproxil fumarate (DF) and emtricitabine (Julg and Bogner, 2008). South Africa is one of the countries with the highest prevalence of HIV in the world and has one of the largest antiretroviral treatment programs in the world (Shisana et al., 2014; Johnson et al., 2017). In recent decades, the cART has been reportedly efficient in suppressing viral load in the blood and major organs of HIV-infected individuals (Tseng et al., 2015), cost-effective and easily available (Harris et al., 2012), and reduces the rate of HIV reinfection with early treatment (Chéret et al., 2017). However, the success of cART in combating the effects of HIV has been marred by its contribution to the development of metabolic syndrome (Paula et al., 2013). Recent studies report a four-fold prevalence of T2D amongst patients on cART compared to non-treated HIV patients (Brown et al., 2005; NigatuHaregu et al., 2012). Additionally, efavirenz is associated with a higher risk of diabetes induction (Karamchand et al., 2016), NRTI inhibits pancreatic β-cell activity, protease inhibitors (PI) may increase insulin resistance and decrease insulin secretion (Monroe et al., 2014), while highly active antiretroviral therapy (HAART) induces metabolic dysfunction such as lipodystrophy and diabetes dyslipidemia (Kalejaiye et al., 2017). All these effects consequently induce type 2 diabetes and have led to an alarming prevalence of diabetes and its co-morbidity among people living with HIV and AIDs (PLWHA) (Karamchand et al., 2016; Kousignian et al., 2021).

2.2.3 Alcohol use

Alcohol abuse is a prevalent lifestyle factor that may lead to impaired glycaemic control or diabetes (Carlsson et al., 2003; Ahmed et al., 2008). South Africa is among the countries with the riskiest pattern of alcohol abuse and binge drinking (World Health Organization and World Health Organization, Management of Substance Abuse Unit, 2014; Vellios and Van Walbeek, 2018). The excess calories obtained through sustained alcohol abuse lead to obesity, insulin resistance, and consequently impaired insulin secretion (Kao et al., 2001; Kim and Kim, 2012). Beyond the induction of diabetes, alcohol abuse contributes immensely to health risk behaviours and as such has been implicated in the increased rate of HIV infection through multiple sex partners and unprotected sex engagement with subsequent enrolment in the cART treatment program (Du et al., 2015). In addition, alcohol abuse has been reported to interfere with the absorption and metabolism (responsiveness) of cART (Molina et al., 2014) with a consequent reduction in cART efficacy. It is not known how alcohol and cART interaction (Schneider et al., 2014; Williams et al., 2016) would impact associated neurological parameters in the diabetic condition, and herein lies the import of this study as an increasing population of South Africans and probably other population groups, that regularly use alcohol, are on cART therapy and may develop diabetes.

2.3 Neuronal disease burden: diabetes, alcohol, and cART

2.3.1 Type 2 diabetes-associated dementia

Cognitive impairment is commonly found at different stages of T2D, especially in aging adults (Cholerton et al., 2016; Mallorquí-Bagué et al., 2018). T2D is associated with the risk of developing mild cognitive impairment and dementias such as Alzheimer's and vascular dementia (Beeri and Bendlin, 2020; Reinke et al., 2022). These deficits can be categorized by severity into three stages; diabetes-associated cognitive decrements, mild cognitive impairment

(MCI), and dementia being the most severe (Koekkoek et al., 2015). Perturbation in insulin signalling, cerebral insulin resistance, vascular brain injury, hyperglycaemia, and hippocampal atrophy have been implicated in T2D dementia (Biessels and Reijmer, 2014; Biessels and Reagan, 2015). The early onset of diabetes is also associated with a higher risk of subsequent dementia (Barbiellini Amidei et al., 2021) while the duration of diabetes is closely associated with dementia and cognitive decline (Biessels and Despa, 2018; Reinke et al., 2022). All these conditions require critical clinical and physiological management to optimize the patient's quality of life (Trikkalinou et al., 2017). Furthermore, diabetes significantly impacts HIV-associated dementia (HAD) and white matter volume in HIV-infected patients (Valcour et al., 2005; Wu et al., 2018)

2.3.2 HIV-associated neurological pathologies (HAND)

HIV-associated neurocognitive disorder (HAND) describes an array of neurocognitive disorders associated with HIV and includes asymptomatic neurocognitive impairment (ANI), mild neurocognitive disorder (MND), and HIV-associated dementia (HAD) (Clifford and Ances, 2013; Saylor et al., 2016). HIV can infiltrate the CNS in the early stages of disease progression and serve as a reservoir for HIV multiplication even while the viral load is controlled in other peripheral organs (Wallet et al., 2019). The introduction of cART has efficiently reduced the effects of HIV in several organs and facilitated the reduction of HAD, but HAND has persisted even with the cART regime (Saylor et al., 2016). However, several in vitro studies have reported neurotoxic effects of the cART and some of its components in neuronal damage and neurocognitive deficits (Robertson et al., 2012; Tovar-y-Romo et al., 2012; Ma et al., 2016). These neurotoxic effects of cART require further elucidation in an in vivo HIV naïve model to delineate the neurotoxic effects of cART from the effects of HIV.

2.3.3 Alcohol-induced neuronal pathologies

Alcohol is an addictive toxin and its persistent and excessive consumption results in several diagnosable neurological concomitants such as hepatic encephalopathy, Wernicke encephalopathy (WE), Korsakoff syndrome (KS), Marchiafava–Bignami disease (MBD), and central pontine myelinolysis (CPM)(Zahr and Pfefferbaum, 2017). Additionally, alcohol has been identified as a risk factor for dementia and mild cognitive impairment even with self-reported alcohol consumption in adults (Koch et al., 2019). Furthermore, alcohol use can also induce anatomical and physiological effects termed alcohol-related brain damage (ARBD) and impair cognitive and executive function (Zahr et al., 2011). Though some of the effects of alcohol have been proposed to be age or dose-dependent and reversible with sobriety, the persistent use of alcohol is reported in hippocampal atrophy, loss of neurons, and decline of white matter in cognitive associated regions of the brain (Dhanabalan et al., 2018; Meda et al., 2018; Zahr et al., 2019). Considering that diabetes, alcohol, and cART are independently related to cognitive and memory pathologies, this study has focused on the molecular and histopathological investigations of alcohol and cART in diabetes in the hippocampus.

2.4 The hippocampus

2.4.1 Anatomy and function of the brain

The brain is a large organ made up of nervous tissue which regulates many body functions, morphologically it is divided into the: cerebrum, cerebellum, and brain stem (Dekeyzer et al., 2017; Maldonado and Alsayouri, 2022). The cerebrum consists of an outer grey matter cortex composed of four lobes (frontal, parietal, temporal, and occipital) and an inner white matter comprised of primarily myelinated axons and glial cells (Scatliff and Clark, 1992; Jawabri and Sharma, 2022). The cerebellum is divided into three lobes (anterior, middle, and flocculonodular), while the brain stem is divided into three sections (midbrain, pons, and

metencephalon) (Singh, 2020; Basinger and Hogg, 2022). Physiologically, the cerebellum coordinates voluntary movement, the brainstem connects the cerebellum and cerebrum to the spinal cord, while the cerebrum controls the motor and sensory information, behaviour, feeling, intelligence, and memory (Baizer, 2014; Maldonado and Alsayouri, 2022). The brain cortex consists of support cells (oligodendrocytes, microglia, and astrocytes) which myelinate, form part of BBB, and stimulate immune response; and neurons that communicate with other neurons via neurotransmitters (Lovinger, 2008; Xu et al., 2020). Neuronal activity and function are dependent on glucose and oxygen delivery from the blood and therefore require adequately regulated energy homeostasis (Shetty et al., 2012; Watts et al., 2018). Although the brain is isolated from the blood by the BBB, glucose uptake from the blood is facilitated by neurons and support cells to augment the limited glycogen reserves in astrocytes and neurons (Brown and Ransom, 2007; Saez et al., 2014). Additionally, brain regions such as the hippocampus are sensitive to insulin which regulates glucose uptake into the neuron to meet the energy requirements for its cognitive and memory functions (Bryant et al., 2002; S et al., 2002; McNay and Pearson-Leary, 2020).

2.4.2 Morphology of the hippocampus

The hippocampus is part of the limbic system (primitive brain) that lies along the medial longitudinal axis of the temporal lobe (Andersen et al., 2007; Anand and Dhikav, 2012). It consists of 3 regions, the hippocampus proper which interlocks with the dentate gyrus, the subiculum positioned intermediately, and the entorhinal cortex (EC). The hippocampus proper consists of the dentate gyrus (DG) and the Cornu Ammonis (CA) which is a seahorse-like or ram's horn-like structure that describes the different regions of the hippocampus (Amaral and Witter, 1989; Fogwe et al., 2022). The CA is histologically divided into four major hippocampal regions (subfields) CA1, CA2, CA3, and CA4 according to the size, location, and

shape of neuronal cell bodies (Fig. 1). The hippocampus is structurally and functionally different from the cerebral cortex and is arranged into layers with several cells and connects several parts of the brain.

2.4.3 Cells and circuitry of the hippocampus

The hippocampus proper mainly consists of pyramidal cells and their associated interneurons which are clustered into one layer out of the three layers (El Falougy et al., 2008). Pyramidal cells have basal and apical dendrites with dendritic spines for excitatory synaptic transmission. The axons of pyramidal are efferent processes that take information received by the hippocampus to other brain structures through the entorhinal cortex (EC)(Spruston, 2008). In the dentate gyrus, the granule cells are the main constituents with a deeper layer (polymorphic) of pyramidal cells and an outer molecular layer of axonal afferent fibres, while the granule cells' axons are mossy fibres (Oliva et al., 2016). Hippocampal circuitry involves the tri-synaptic circuitry loop, starting with projections from entorhinal cells to the dentate gyrus and CA3 via the perforant path collateral, then mossy fibres send projections from the DG to CA3, and the Schaefer collaterals send projections from CA3 to CA1 subfields. Other circuits project from CA1 back to the entorhinal cortex through the subiculum and from the EC directly to the CA1, CA2, and CA3 (Schultz et al., 1997; Knierim, 2015) (Fig. 2.1).

CA3 is a pivotal crossroad between synaptic convergence and integration (Migliore et al., 2010). In addition to the trisynaptic pathway, the CA3 cells provide feedback to the dentate gyrus cells and recurrent collaterals from other CA3 pyramidal cells (Scharfman, 2007; Scharfman and Myers, 2016; Fogwe et al., 2022) (Fig 2.1). CA3 is the largest region in the hippocampus with recurrent axon collateral of CA3 pyramidal cells ramifying extensively, making excitatory contacts with neighbouring excitatory and inhibiting neurons, and so creating rich internal connectivity (Miles et al., 2014). CA3 has a specific role in memory

processes with susceptibility to seizures and neurodegeneration (Cherubini and Miles, 2015). CA3 neurons also have an inconspicuous role in the regulation of neurogenesis in the dentate gyrus (Liu et al., 2011) as loss of this terminal area reduces the ability to make connections with other hippocampal regions which impairs the survival of newly born neurons in the DG and additionally, are centrally involved in spatial memory acquisition and recall (Nakazawa et al., 2002, 2003).

The flow of impulses between the complex circuitry of the hippocampus and other cortical areas is necessary for the optimal functioning of the hippocampus and is susceptible to atrophy in response to drug and chemical injuries (Dhikav and Anand, 2007; Anand and Dhikav, 2012).

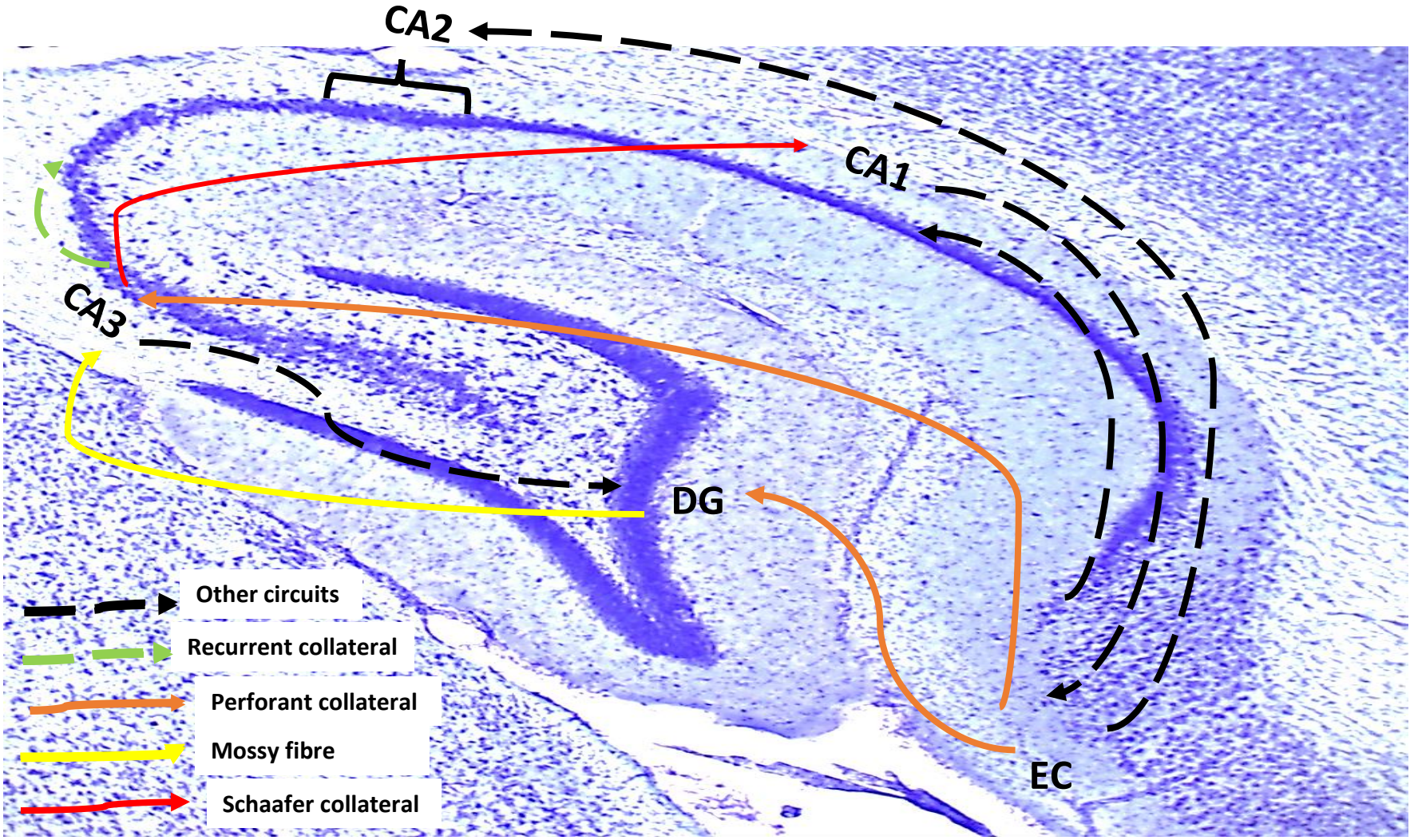

Figure 2. 1. Coronal slice through the transverse axis of the dorsal hippocampus showing circuitry interconnection between regions adopted from histological images in this thesis (By Jaclyn Asouzu Johnson)

2.4.4 Function of the hippocampus

The hippocampus is widely known for its role in learning and memory which has three phases including registration, storage, and retrieval of information. The hippocampus is also involved in spatial memory, regulating emotion, learning, and forming relationships between learned materials (Lautin, 2001; Rubin et al., 2014; Yang and Wang, 2017). Recently, the hippocampus is associated with emotional behaviour, regulation of hypothalamic function, consolidation, and decision making (Anand and Dhikav, 2012; Rubin et al., 2014). This is achieved by its close association with the amygdala, hypothalamus, septum, and mammillary bodies, these brain regions may also slightly stimulate the hippocampus (Rajmohan and Mohandas, 2007; Fogwe et al., 2022). Additionally, the dentate gyrus is one of the few places where neurons are generated and incorporated into hippocampal circuitry in adulthood (Eriksson et al., 1998; van Praag et al., 2002; Leuner and Gould, 2010). Furthermore, the hippocampus has been widely studied for its implications for neuropsychological conditions adversely affecting the quality of life (Wicking et al., 2014; Vogel and Schwabe, 2016). Considering that most hippocampal functional deficits are associated with toxicological and biochemical agents, as well as metabolic stress (Cannon and Greenamyre, 2011; Bartsch, 2012), it is important to focus this study on the possible hippocampal structural and functional implications related to cART and alcohol treatment in a diabetic disease condition.

2.5 Hippocampal pathology in diabetes, alcohol, and cART

2.5.1 Hyperglycaemia with the progression of diabetes

Diabetes condition is heterogeneous and develops through several dynamic phases (Boles et al., 2017; Galicia-Garcia et al., 2020). The five stages of diabetes were profiled by Weir and Bonner-Weir profiled according to beta cell dysfunction and fasting blood glucose (Weir and Bonner-Weir, 2004). The first stage (compensation); is highlighted by insulin resistance due to obesity, and physical and genetic factors which are compensated by hyper insulin secretion to

maintain normal fasting glucose levels. In stage 2 (stable adaptation); fasting glucose levels increase (5-7.3mmol/L) and glucose-stimulated insulin secretion (GCIS) is lost. Stage 3 (early unstable decompensation) is an unstable transient stage with relatively high fasting glucose ranging between 7.3 mmol/L (stage 2) to -16 mmol/L (stage 4), polydipsia, and weight loss may occur in this stage. In stages 4 and 5 (stable and severe decomposition); fasting glucose levels range from 16-20 and above 21 mmol/L respectively, whereby beta cell survival progresses to ketoacidosis in stage 5. Several non-genetic animal models of T2D employ protocols such as streptozotocin and pancreatectomy to reduce beta cells, suggesting that animals in these diabetes models may be at stages 3 to 4 of diabetes. However, at any of these stages mentioned above, hyperglycaemia may induce hippocampal pathologies when associated with other factors such as insulin resistance, oxidative stress, inflammation, and apoptosis.

2.5.2 Insulin resistance

Diabetes is a metabolic disease that impairs lipid and glucose homeostasis, and this dysfunction is associated with insulin resistance in T2D. The adipose tissue (an endocrine organ and energy repository) and other tissues such as the liver and muscle secrete hormones and cytokines that regulate insulin sensitivity, lipotoxicity, glucose metabolism, and inter-organ communication (Galic et al., 2012; Mastrototaro and Roden, 2021). In adipocytes and other cells (such as hepatocytes and myocytes), insulin-responsive glucose transporter GLUT 4 facilitates glucose uptake as the convergent step of the insulin signalling pathway (Chang et al., 2004; Stöckli et al., 2011). Likewise, hippocampal neurons have abundant insulin receptors and insulin-sensitive GLUT 4 glucose transporters associated with hippocampus-dependent memory, plasticity, and neurogenesis (Stranahan et al., 2008).

2.5.2.1 Insulin receptor (INSR) and insulin receptor substrate (IRS1)

Hippocampal and peripheral tissue (muscle and liver) cells possess pairs of insulin receptor (INSR) membrane proteins with two extracellular α- subunit ligand binding sites for insulin molecules and two transmembrane β subunits with tyrosine kinase domains. With insulin binding on the extracellular α- subunit, INSR undergoes conformational changes with the activation and transphosphorylation of the intracellular β subunit, which recruits the insulin receptor substrate (IRS1) to the membrane. Intracellular IRS proteins bind to the phosphorylated tyrosine residues, and the tyrosine phosphorylation of IRS1 leads to downstream activation of several intracellular molecules (P1-3-Kinase, PIP3, PDK1, AKT, and others) which ultimately leads to the recruitment of glucose transporters (GLUT) from storage. Translocation of GLUT 4 to the cell membrane facilitates glucose transport into the cells. Therefore, impaired insulin signalling (insulin resistance) is not only induced by reduced insulin availability but also by compromised INSR and IRS1 activation and signalling downstream. This CNS insulin resistance has been broadly linked to obesity, diabetes, neurotoxicity, neurodegenerative, and neurophysiological conditions (Pomytkin et al., 2018). Additionally, components of cART have an affinity and bind to GLUT 4, and consequently, interrupt and inhibit glucose transport into adipocytes and subsequently induce insulin resistance with its (cART) prolonged therapy (Hertel et al., 2004; Hruz, 2006; Masuku, 2019). On the other hand, the amount of alcohol consumed (moderate, binge, or chronic) may improve, suppress, or inhibit insulin action respectively (Lindtner et al., 2013; Jang et al., 2019) and thereby alleviate or induce the diabetic condition accordingly. Similarly, insulin resistance has been identified at the intersection between impaired glucose homeostasis and hippocampal pathologies such as impaired cognition, plasticity, and neurogenesis (Soto et al., 2019; Spinelli et al., 2019). Furthermore, cognitive, and neurodegenerative perturbations characterized by hyperglycaemia and impaired insulin sensitivity are closely associated with BBB dysfunction

(Takechi et al., 2017; Salameh et al., 2019). Therefore, it is important to investigate if and how diabetes-induced BBB disruption (Starr et al., 2003; Salameh et al., 2016) may be affected by sub-chronic exposure to chemical agents such as alcohol and cART which can penetrate the CNS.

2.5.3 Blood-brain barrier and junctional proteins

Type 2 diabetes factors (Salameh et al., 2016), alcohol abuse (Haorah et al., 2007) and cART medication (Bertrand et al., 2016) have all been shown to independently penetrate the CNS and affect the hippocampus. The blood-brain barrier (BBB) is a multi-layered unit, consisting of a single layer of densely packed specialized endothelial cells, linked by tight and adherent junctions, surrounded by vascular basement membranes (endothelial basement membrane and pericytes) and astrocytic end feet projections and microglia (Abbott et al., 2010; Luissint et al., 2012). Tight junctions are found at the apex of the endothelial cells, with their main components consisting of claudin -1, -3, -5, -12, and occludin which act together to maintain the BBB integrity and prevent para-cellular diffusion of substances (Greene et al., 2019; Yuan et al., 2020). Claudin-5 is highly expressed in the brain, up to about 600 times above that of claudin -1, -3, and -12 (Daneman and Prat, 2015), and is therefore of utmost interest in pathological and toxicology studies. Claudins are linked to adaptor proteins, zona occludens (ZO1) (Keaney and Campbell, 2015); and both proteins (Claudins and ZO1) together with occludins form a tight restriction between brain microvascular endothelial cells (Daneman and Prat, 2015). This junctional restriction regulates CNS homeostasis and protects the CNS from toxins, inflammation, and pathogens (Keaney and Campbell, 2015). However, endothelial cells may be activated with danger signals and facilitate leukocyte entry into the CNS through para-cellular channels, a process referred to as trans-endothelial migration. Pathogens such as the human immunodeficiency virus (HIV) utilize these para-cellular pathways to infiltrate the CNS and may compromise the BBB (Avison et al., 2004; Persidsky et al., 2006; Greene et al., 2019).

Efavirenz reportedly disrupts the BBB by altering claudin-5 expression (Bertrand et al., 2016), however, the therapeutic effect of the cART regime on the BBB remains unclear. Previous STZ diabetic studies have reported decreased cerebral occludin protein without change in its mRNA levels and non-significant loss in claudin-5 (Chehade et al., 2002; Hawkins et al., 2007) yet another study reported decreased claudin-5 and occludin in chronic diabetes (Yoo et al., 2016). In all, these reports indicate that diabetes is implicated in the alteration of the levels of these junctional proteins. Furthermore, binge alcohol intake has been reported to decrease cerebral claudin-5 expression (Rubio-Araiz et al., 2017). However, these reported increased disruptions in BBB structure and consequent increases in BBB permeability may facilitate the entry of neuroinflammatory mediators into the CNS which in turn will further decrease the para-cellular regulation of tight junction by reducing the expression of CLDN5 and occludin (Camire et al., 2015). These points highlight the fact that mechanisms that impair the BBB are multifactorial, but it is not known how the combined chemo-toxic effect that may exist in cART and alcohol therapy in a diabetic condition will affect the BBB structure.

2.5.4 Neuronal inflammation

In insulin-sensitive metabolic organs such as the brain (Milstein and Ferris 2021), immune cells highlight crosstalk between the metabolism and immune systems termed ‘immunometabolism”. Diabetes is characterized as an inflammatory condition (Donath and Shoelson, 2011) with elevated levels of systemic pro-inflammatory cytokines often reported in the serum and tissue of T2D patients and animals (Herrero et al., 2010; Tsalamandris et al., 2019). Similarly, cART components (PI’s, NNR1’s, and NRTI) induce insulin resistance and thereby stimulate inflammatory response (Zhou et al., 2007; Wu et al., 2017; Osuji et al., 2018), while alcohol at different doses has mixed reports of elevated plasma, liver, and brain TNFα and IL1β (Qin et al., 2008), absence of significant changes in IL4 and IL6 (Al-Humadi et al.,

2018), and lower plasma levels of tumour necrosis factor receptor-2 (sTNF-R2) (Shai et al., 2004).

2.5.4.1 Cytokines

Cytokines are a large group of proteins (interleukins, chemokines, interferons, stimulating factors, and tumour necrosis factors) produced by a vast group of immune and body cells (lymphocytes, monocytes, adipocytes, hepatocytes), whose action may be autocrine, paracrine or endocrine (Zhang and An, 2007; Shi et al., 2019). Cytokines mediate several CNS functions including immune, inflammatory, and physiologic responses to infection and injury (Benveniste, 1992; Rothwell and Luheshi, 1994). However, considering the inflammatory state of diabetes, alcohol use, and possible insulin resistance induced by cART (Al-Humadi et al., 2018; Osuji et al., 2018; Tsalamandris et al., 2019), our investigation is focused mainly on pro-inflammatory cytokines (interleukins and tumour necrosis factor).

2.5.4.2 Pro-inflammatory cytokines

These cytokines (IL-1, IL-6, and TNF-α) are produced by hippocampal microglia and are not directly neurotoxic, inherently beneficial, or detrimental, but must be produced at the right time and amount for proper immune function (Rothwell, 1999; Ferlita et al., 2019). A previous report has associated deficient immune response and cytokine production due to hyperglyceamia with failure to control the spread of pathogens in diabetic subjects and hence their susceptibility to infections (Berbudi et al., 2020). However, elevated levels of pro-inflammatory cytokines may mediate insulin resistance, stimulate lipolysis, decrease cell proliferation in the hippocampus and activate pathways for neuronal injury and apoptosis (Harry and Kraft, 2008; Seguin et al., 2009; Zhou et al., 2021). Collectively, astrocytes are reported to modulate intricate inflammatory signalling that dynamically regulates several cytokines required for normal synaptic functions such as the creation and transmission that

occurs at the synapses in response to neuroinflammatory and neuroprotective signals (Muhammad, 2019; Salmeron et al., 2019).

2.5.4.2.1 Interleukin six (IL6)

Neural inflammatory markers such as IL6 plays are small signalling glycoproteins that induce an immune response in the CNS, they are mainly produced by astrocytes and in some cases by neurons and microglial (Choi et al., 2014). IL6 is reported to occur in the cerebellum and hippocampus under normal physiological conditions (Gadient and Otten, 1994; Erta et al., 2012) and is believed to play a role in both anti-inflammatory and pro-inflammatory activities (Gabay, 2006; Borsini et al., 2020). Additionally, in an inflammatory state IL6 is reportedly elevated in astrocytes and systemic circulation of HIV and cART-treated HIV patients, with impaired learning and memory functions (Neuhaus et al., 2010; Liu and Kumar, 2015; Valdez et al., 2016). In diabetes, IL6 is complex and multifunctional, acting as both stimulator and inhibitor of insulin action (LaPensee et al., 2008; Rehman et al., 2017), inducing long-term inhibitory effects on insulin receptor substrate (IRS), GLUT 4, insulin signalling and action at elevated levels (Shi et al., 2019). Furthermore, IL6 plays a modulatory role in memory and cognition with reports of elevated IL-6 after learning, impaired neuronal circuitry, cognition, and learning with IL-6 elevation, but improved long-term memory and cognitive function with IL6 blockage; suggesting a plasticity limiting role of IL-6 in learning and memory functions (Balschun et al., 2004; Braida et al., 2004; Wei et al., 2012; Bourgognon and Cavanagh, 2020). Therefore, the absence of IL6 may not disrupt learning and memory, but overexpression of IL6 may cause memory impairments, and as such these perturbations need to be profiled in response to diabetes, alcohol, and cART.

2.5.4.2.2 Tumour necrosis factor alpha (TNF-α)

Tumour necrosis factor alpha (TNF-α) (a pro-inflammatory cytokine) is a mediator of insulin resistance, induces free fatty acids by stimulating lipolysis, and therefore TNF-α systemic concentration is elevated in T2D (Qi and Pekala, 2000; Cawthorn and Sethi, 2008; Shi et al., 2019). In the CNS, TNF-α is produced by glia and neurons, mostly microglia and astrocytes (Santello and Volterra, 2012; Neniskyte et al., 2014), and plays an important role in CNS physiology and pathology as it is required for developmental and normal hippocampal memory, learning and plasticity processes (Prieto et al., 2019; Mygind et al., 2021). Additionally, in neuroinflammatory states such as ischemia TNF -α can be produced by blood-borne macrophages (Gregersen et al., 2000; Muhammad, 2019). TNF-α also promotes the extravasation of white blood cells across the endothelium from the blood into the CNS parenchyma (D'Mello et al., 2009; Galic et al., 2012). However, overexpression of TNF-α in neurons and glial cells is implicated in memory (retrieval and reconsolidation of hippocampus-dependent memory), learning, plasticity, and neurodegenerative deficits (Donzis and Tronson, 2014; Kempuraj et al., 2016; Takahashi et al., 2021), as such the need to study and document the role of TNF-α in diabetes, alcohol, and cART toxicities relative to hippocampal pathologies is crucial.

2.5.4.2.3 Interleukin one alpha (IL1-α)

IL1-α is one of the receptor agonists in the 11 members family of IL-1, which have active precursors, are found in healthy tissues, and can induce the production of other cytokines (IL-6, and TNF-α) in vitro in human blood cells, suggesting it plays a role in non-pathogen induced inflammation (Kim et al., 2013; Kaneko et al., 2019). IL1-α has a dual intracellular location and function, translocating between the nucleus as a chromatin-associated nuclear factor and the extracellular receptor-mediated cytokine activity (Cohen et al., 2010; Dinarello, 2018). Although, most reports on inflammation have focused primarily on IL1β, in stroke brain IL-1α

is predominantly produced by microglia in the areas of ischaemic neuronal injury with BBB disruption compared to IL1β (Luheshi et al., 2011; Hewett et al., 2012). Additionally, IL-1α treatment showed neuroprotection in ischemic stroke with overall improved angiogenesis and neurogenesis in mice (in vivo) and brain endothelial cells (in vitro) (Salmeron et al., 2019). Perturbations in these pro-inflammatory cytokines may induce oxidative stress or occur with it, which may lead to a cascade of events resulting in apoptosis of neuronal cells (Yang et al., 2007; Prasad, 2017).

2.5.5 Oxidative stress

Oxidative stress is characterized by an imbalance in the generation, accumulation, production, and ability to detoxify biological by-products such as superoxide radicals ($O_2^{\bullet-}$), hydrogen peroxide (H_2O_2), hydroxyl radicals (OH), and singlet oxygen ($1O_2$), which are generally referred to as reactive oxygen species (ROS) (Chen et al., 2012; Pizzino et al., 2017). These oxidants when produced at elevated levels, may induce lipid peroxidation with attendant malondialdehyde (MDA) production. Lipid peroxidation rapidly affects lipids, proteins, and DNA by inducing modifications, loss, or impairment of their enzymatic activity. Oxidative stress-induced lipid peroxidation damages cell membranes and lipoproteins and induces DNA modifications (Cejas et al., 2004; Gaschler and Stockwell, 2017). On the other hand, cells utilize antioxidant enzymes such as superoxide dismutase (SOD), catalase (CAT), and glutathione peroxidase (GPx) as a protective mechanism against oxidants (Jeeva et al., 2015; Ighodaro and Akinloye, 2018). Since MDA is an ideal marker for oxidative stress (Meagher and FitzGerald, 2000) and GPx is a vital antioxidant enzyme involved in the enzymatic catabolism of ROS and reduces the accumulation of hydrogen peroxide (Lubos et al., 2011), this research concentrated on these two factors (MDA and GPx) for the oxidative stress profile.

Components of cART (NRTIs) induce oxidative stress by inhibiting important mitochondrial replication enzymes (DNA poly), mitochondrial DNA depletion, and inducing synaptic

damage and neuronal loss in vivo and in vitro (Nolan and Mallal, 2004; Akay et al., 2014). The metabolism of alcohol is associated with acetaldehyde production which elevates MDA and depletes antioxidants such as GPx, cumulating in impaired neuronal viability and neurofilament expressions (Das and Vasudevan, 2007; Haorah et al., 2008; Han et al., 2015). Similarly, T2D induces oxidative stress (Muriach et al., 2014; Zhang et al., 2020) which activates a cascade of intracellular events that leads to autophagy, apoptosis, and disturbances of synaptic plasticity in hippocampal neurons (Gonzalez et al., 2011; Sadeghi et al., 2016). Furthermore, elevated serum and hippocampal MDA and reduced antioxidants are reported with hyperglycaemia and dyslipidaemia associated with lipid peroxidation in T2D and alcohol use (Pan et al., 2010; Almansa et al., 2013; Manohar et al., 2013). Therefore, their consideration in this study for their attendant role in neuronal cell death.

2.5.6 Cell death in the hippocampus

Cell death is generally classified by mechanisms of apoptosis or necrosis characterized by different biochemical and morphological stimuli.

2.5.6.1 Apoptosis

Apoptosis (programmed cell death) is a normal homeostatic mechanism in development for maintaining cell population and preventing the accumulation of damaged cells within tissue and organs including neurons (Elmore, 2007; Cavallaro, 2015). Dysfunction in neuronal apoptotic regulation is implicated in the development of neurodegenerative diseases (Sajan et al., 2007; Ghavami et al., 2014). The intrinsic apoptotic pathway is regulated by Bcl_2 family proteins (Bcl_2; anti-apoptotic and BAX; pro-apoptotic), and mediated by the mitochondria where BAX insertion alters the structure and permeability of the mitochondrial outer membrane and produces apoptotic enzymes and proteins such as cytochrome *c*, apoptosis-inducing factor, endonuclease G, Smac/DIABLO and Omi/HtrA2 (Wang, 2001; Uren et al.,

2005; Hardwick and Soane, 2013; Kilbride and Prehn, 2013). Apoptosis is also facilitated by the extrinsic pathway involving extracellular ligands such as TNFα (Guicciardi and Gores, 2009). The extrinsic and intrinsic pathways at the final apoptotic step with the execution phase involving Caspase-3, 6, and 7 proteins of which Caspase-3 is the most important, indicate irreversible apoptosis (Sankari et al., 2012; Jan and Chaudhry, 2019). Therefore, levels of Bcl-2, BAX, and Caspase-3 determine the occurrence and rate of apoptosis (Elmore, 2007; Yu et al., 2014). Considering the reports of increased hippocampal atrophy in type 2 diabetes (Sadeghi et al., 2016b), alcohol abuse (Broadwater et al., 2014; Zahr et al., 2019), and cART medication (Tovar-y-Romo et al., 2012), it is vital to document the combined impact of these conditions on apoptotic mRNA levels (BAX, Bcl_2, and Caspase-3) in the hippocampus.

2.5.6.2 Necrosis

Necrosis is an unprogrammed accidental cell death that entails the degenerative processes that occur after cell death, some morphological changes include cell or nuclei swelling and membrane disruption (Fink and Cookson, 2005; Elmore, 2007). This has led to the postulation that necrosis regulates nucleus morphology (Kwon et al., 2015). The size of a nucleus could be directly proportional to the amount of DNA or the extent of DNA compaction (Webster et al., 2009). Post mitotic nuclear assembly can impact nuclear size, and is associated with cell differentiation, development, and disease (Jevtić et al., 2014). Similarly, nuclei and cell body size are increased in cases of vascular dementia and Alzheimer's (Ishunina et al., 2019). Furthermore, the selective and persistent loss of hippocampal neurons and increased Caspase-3 immunoreactivity in adolescent rats have been suggested to not only be induced by neuronal cell death but also by decreased hippocampal neurogenesis (Broadwater et al., 2014). Therefore, investigations of neuronal loss in the hippocampus should be accompanied by reports on neurogenesis impact.

2.5.7 Proliferation and maturation of neurons in the hippocampus

In recent decades, the adult brain is reported to have neural stem cells that continue during post-natal proliferation to form new neurons (neurogenesis) beyond adolescence (Doetsch et al., 1999; Lepousez et al., 2015). Neural stem cells are localized in the cerebellum, cortex, hypothalamus, striatum, and substantia nigra (Reynolds and Weiss, 1992; Chipperfield et al., 2005), but they are generally accepted to only differentiate in the lateral ventricle (sub-ventricular zone) and the dentate gyrus of the hippocampus (sub-granular zone)(Landgren and Curtis, 2011; Martínez-Cerdeño and Noctor, 2018). Adult neurogenesis is divided into four phases: originating as radial-glial-like precursor cell phase, intermediate progenitor glial in the early survival phase, migratory neuroblast in a postmitotic maturation phase, and a late survival phase with mature neuronal type cells (Steiner et al., 2006; Kempermann et al., 2015)(Fig 2.2). Newly created neurons in the adult hippocampus are modified structurally by sending axonal projections to the CA3 region of the hippocampus and contain functional synaptic inputs that ensure their full integration as granule cells (Markakis and Gage, 1999; van Praag et al., 2002). This neurogenesis and incorporation of new granule cells into the hippocampus increases plasticity and is associated with learning, memory, and alcohol-related pathologies (Deng et al., 2010; Nixon et al., 2010; Lodge and Bischofberger, 2019). Similarly, type 2 diabetes (Ho et al., 2013; Ramos-Rodriguez et al., 2014), cART therapy (Jin et al., 2016; Xu et al., 2017), and alcohol abuse (Taffe et al., 2010; Geil et al., 2014) have been shown to independently impair hippocampal neurogenesis. However, it is not known if the concurrent presence of alcohol and cART administration in diabetes will exacerbate neurogenesis disruption or induce compensatory mechanisms on neurogenesis. This possible dual effect on neurogenesis requires further investigation using common neurogenesis markers DCX and Ki67.

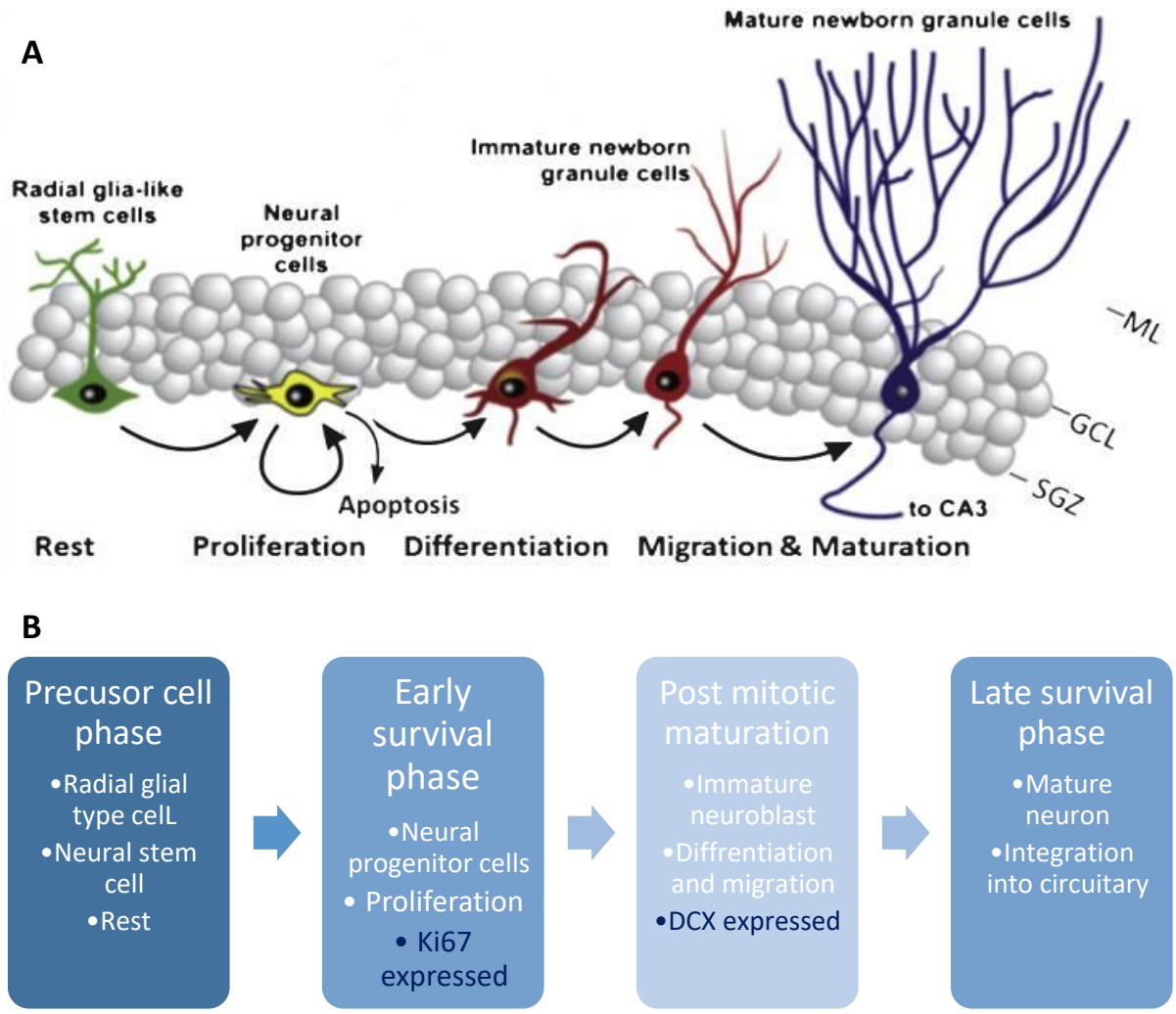

Figure 2. 2. Schematic diagram illustrating the different phases of neurogenesis in the dentate gyrus. **A)** Animated representation of morphological changes in stem cells until they become mature neurons in the dentate gyrus adapted from (Bolijn and Lucassen, 2015). **B)** Flow chart diagram illustrating the major phases of neurogenesis as described by (Kempermann et al., 2015), illustrated by Jaclyn Asouzu Johnson. ML-molecular layer, GL-granular cell layer, SGZ- sub granular zone.

2.5.7.1 Ki67

The process of division in the cell cycle of a proliferating cell starts with interphase which is divided into G1 when proteins are synthesized for DNA replication, S, in DNA replication, and G2, when proteins are synthesized for cell division; after which is M stage, when mitosis occurs with cytokinesis (Cooper, 2000; Bertoli et al., 2013). Cells are at G0 when they are withdrawn from the cell cycle such as undifferentiated cells (Fig 2.3). KI67 is an endogenous marker of cell proliferation that is expressed throughout the active phases of cell division except for G0

(Endl and Gerdes, 2000; Scholzen and Gerdes, 2000). Ki67 is reported to be significantly reduced in T2D and alcohol binge drinking (Stranahan et al., 2008; Taffe et al., 2010). Though Ki67 expression is reported to be increased in T lymphocytes and decreased in the hippocampus of HIV rat models (Sachsenberg et al., 1998; Nemeth et al., 2014), there is a dearth of information on the effects of cART on the Ki67 expression, especially in the light of alcohol use and diabetes.

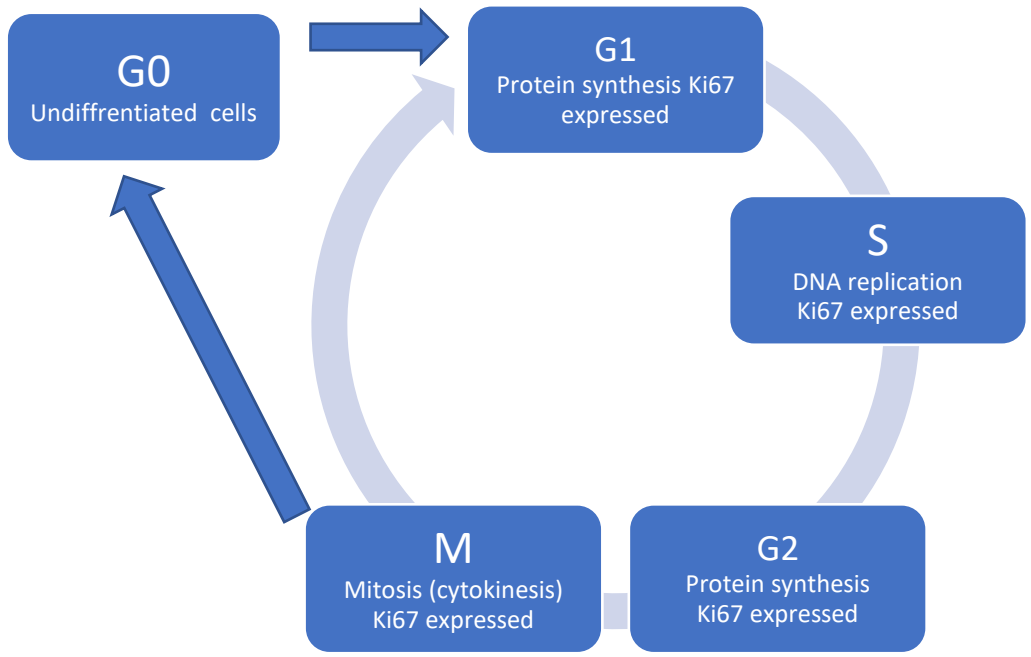

Figure 2. 3. A schematic representation of different stages of the cell cycle and the Ki-67 expression observed in a study reported by (Scholzen and Gerdes, 2000) (animation by Jaclyn Asouzu Johnson).

2.5.7.2 Double courtin (DCX)

Newly divided neural stem cells modify structurally and functionally to adopt mostly neuronal (90%) or glial (10%) fates in adolescents, after which these cells begin to migrate (Kempermann et al., 2003; Morris et al., 2010). DCX is a microtubule-associated protein (MAP), used as a marker in the adult CNS and peripheral nervous system (PNS) for migrating neuroblast or immature neurons (Cayre et al., 2009; Mauffrey et al., 2019; Sorrells et al., 2019).

An earlier study reported that DCX is initially expressed in proliferating neuronal progenitor cells (NPCs) and new neuroblasts, but this expression declines as new cells start expressing mature neuronal markers (Brown et al., 2003; Nkomozepi et al., 2019), while recent studies indicate that DCX is not required for survival and maturation of adult hippocampal neurons and is not expressed by newly formed neurons (Dhaliwal et al., 2016; Sorrells et al., 2021). Although DCX does not alter hippocampal neurogenesis and can be expressed in the absence of adult hippocampal neurogenesis (AHN), DCX is necessary for microtubule stabilization during the migration of immature neurons (Gleeson et al., 1999; Ayanlaja et al., 2017), which is required for the integration of newly proliferated neurons (Ghashghaei et al., 2007; Deng et al., 2010). Furthermore, hippocampal DCX expression is depleted in T2D (Nam et al., 2016; Bonds et al., 2020), chronic alcohol intake (He et al., 2005; Geil et al., 2014), and Efavirenz in cART decreased sub-ventricular DCX in vivo and in vitro (Jin et al., 2016) and therefore its consideration in this study.

2.6 The experimental model

2.6.1 The male diabetes rat model

The induction of type 2 diabetes in a non-genetic animal model has been severally researched and reported. These models include single high dose streptozotocin (STZ) (Ito et al., 1999), multiple-dose STZ (Wu and Huan, 2007), high-fat diet with STZ (Reed et al., 2000), nicotinamide with STZ (Masiello et al., 1998; Ghasemi et al., 2014), prolonged fructose feeding (Lozano et al., 2016), and fructose enriched diet (Wilson and Islam, 2012). According to available literature, the most common model reported is the use of STZ (Furman, 2015) due to its ability to swiftly impair insulin secretion preceded by fructose-enriched diets which is an effective dietary means of inducing obesity, insulin resistance, and hyperglycaemia in laboratory rats and mimics symptoms of type 2 diabetes mellitus in humans (Bell and Polonsky, 2001; Chao et al., 2018; Fang et al., 2019). Additionally, a male rat model was chosen in order

to eliminate the conflicting factor of oestrogen in female rats which is reportedly implicated in regulating glucose metabolism(Alemany, 2021). Thus, a male model will be exempt from this conflicting factor in the diabetic rats. Furthermore, the hippocampus in the rat extends on a longitudinal axis that provides a potential framework to explain and test several effects associated with the hippocampus (Fig 4).

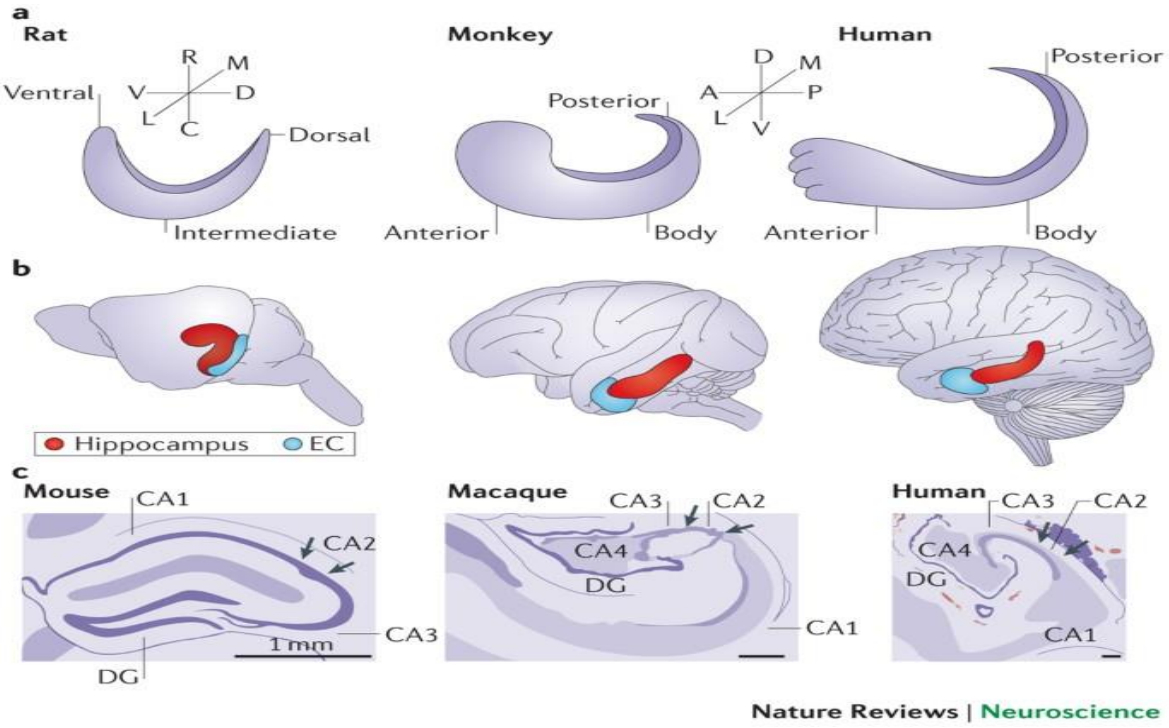

Figure 2. 4. Pictorial representation of the rodent, primate, and human brain and hippocampus showing the long axis model of the hippocampus in each model. A-anterior, P-posterior, M-medial, L-lateral, D-dorsal, V-ventral, R-rostral, C-caudal, EC-entorhinal cortex, adopted from (Strange et al., 2014).

2.6.2 HIV naïve model

Reservoirs of HIV created during primary HIV infection in the semen, blood, and genital secretions may be purged by early cART administration thereby reducing HIV transmission (Chéret et al., 2017). This preventive potential of the cART has led to the encouragement of cART administration as chemical prophylaxis to patients at risk of contracting HIV, especially sex workers who are recently being targeted for preventing sexual transmission of HIV (Cu-Uvin et al., 2000; Cohen et al., 2007). Additionally, the administration of cART goes beyond

treatment and is recently being targeted toward the prevention of HIV infection as pre or post-exposure prophylaxis in uninfected people, especially health workers with occupational exposure to HIV (Panlilio et al., 2005; Mayer and Venkatesh, 2010; Ajibola et al., 2014). Therefore, there is a growing need for the neurotoxic effects of cARTs to be studied in an HIV naïve model, as most clinical and patient information on HIV and cART-associated neuropathology has been on HIV-infected patients.

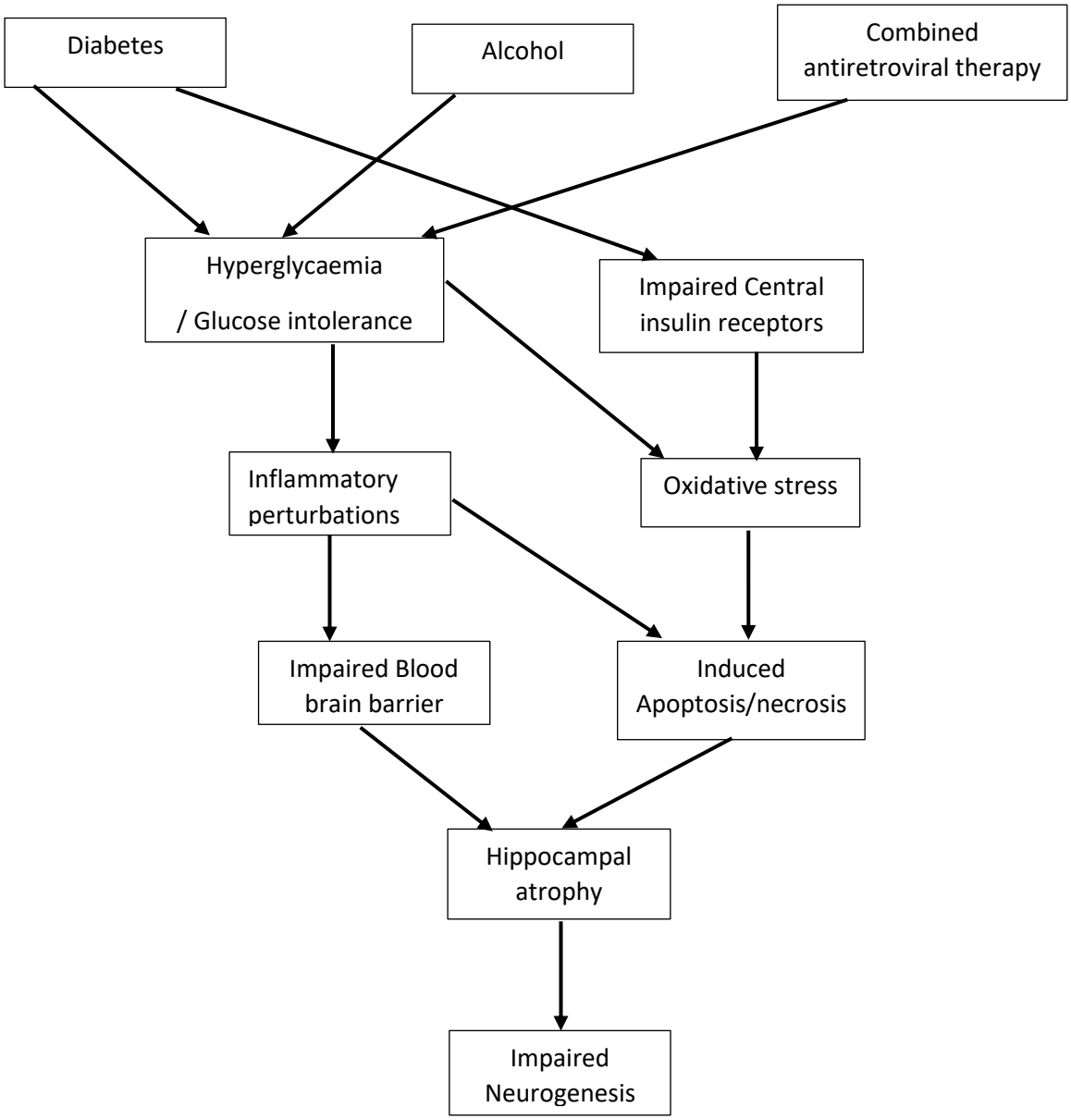

Figure 2. 5. Schematic representation of summarized independent effects of diabetes, alcohol and cART and other potential hippocampal effects reported in literature

CHAPTER 3. MATERIALS AND METHODS

3.1 Sprague Dawley rat diabetic model

3.1.1 Diabetes induction

A diabetic model modified from (Wilson and Islam, 2012), which incorporated a fructose diet (to induce peripheral insulin resistance) followed by Streptozotocin (STZ) administration was used in the study. The adult male rats in both treated and control groups were tested for baseline fasting blood glucose levels (FBG) to establish that no previous diabetic conditions existed before diabetes induction. To prevent the possible interaction of fructose and ethanol in water, the use of a 20% fructose diet was therefore chosen. The rats in the diabetic groups received reconstituted chow pellets with 20% formulated fructose for two weeks (Appendix B1). The rats then received a once-off intraperitoneal (I.P) injection of freshly prepared 40mg/kg body weight (BW) STZ (Sigma; S0130) prepared in 0.05M citrate buffer at a concentration of 4mg/ml (pH 4.5; Appendix B2) after 5 hours fasting to induce degeneration of some pancreatic Langerhans islets β-cell and therefore diabetes. The rats were expected to develop diabetes within 3-7 days after the injection of STZ (Akbarzadeh et al., 2007). Therefore, seventy-two hours following the STZ administration, non-fasting blood glucose levels were measured and values above 250mg/dl (13.8mmol/L) were considered diabetic (Deeds et al., 2011). After confirmation of diabetes, the diabetic-induced rats were withdrawn from the 20% fructose enriched diet and placed on a normal rat chow diet.

3.1.2 Routine tests for diabetes model

The rats were weighed weekly, and in addition, bi-weekly fasting blood glucose tests (FBG), weekly random non-fasting blood glucose tests (NFBG), and monthly oral glucose tolerance tests were carried out. All non-fasting blood glucose measurements were taken at night, during the 12hrs dark period (20h00 and 08h00) when most feeding intake occurs in conformity with

their nocturnal nature (Jensen et al., 2013). The biweekly screening of fasting blood glucose levels ≥ 250 mg/dl was conducted using AccuChek Compact glucometer (Roche Diagnostics, Indianapolis, IN) via tail vein puncture to establish that the induction of diabetes (hyperglycaemia) was successfully and remained/maintained throughout the experiment. Monthly oral glucose tolerance tests (OGTT) were also documented as additional diagnostics to monitor glucose tolerance and the diabetic condition of the animals throughout the experiment (Furman, 2015). In this procedure, the diabetic rats were fasted for 12 hours overnight before the oral gavage of 2g/kg body weight of glucose solution 0.5g/ml (50g glucose in 100ml distilled water), and blood glucose was recorded periodically at time intervals of 0, 15, 30, 60, 120 minutes. The OGTT data was further analysed using the trapezoid method in GraphPad prism 5 statistical package to calculate the area under the curve for each set of OGTT data.

3.2 Dosage and preparation of treatments ARV and alcohol treatments

A combination antiretroviral drug (Atripla) made by Bristol-Myers Squibb and Gilead Sciences, California, USA was administered at a daily dose of 23mg active ingredients/kg body weight of the animal. This dosage of cART is a direct extrapolation from the human equivalent (Frampton and Croom, 2006). Based on an average adolescent body weight of 45 kg receiving a total of 1045mg active ingredient of cART treatment (consisting of efavirenz 600mg+ emtricitabine 200mg+ tenofovir 245mg). The equivalent dose of cART tablet per gram per body weight was calculated and then formulated into (added to gelatine) 5ml gelatine cubes for daily treatments (Appendix B3 and B4). The recipe for ingredients used in preparing the gelatine cubes is adapted from (Zhang and Zhang, 2011) but minimizing the entire content of each gelatine cube to one calorie to ensure that the gel administration does not contribute to or influence the diabetic condition. Alcohol was diluted in distilled water in the ratio of 1 to 10 and administered as drinking water in the water bottles of rats treated with alcohol. Throughout

the experiment, total alcohol and water consumption for treated, and untreated animals were recorded.

3.3 Animal experiments

3.3.1 Animal husbandry

One hundred and eight (108) adult male Sprague Dawley rats (10 weeks old) were housed separately under clean conditions in cages (Length 430mm, W220mm wide, and H200mm height) with beddings of pinewood shaving and a maintained temperature of 21-23ºC and 12 hours light-dark cycle. For the duration of the experiment, the rats had free access to drinking water or alcohol and normal rat chow or 20% fructose according to their allocated group treatment. The rats were acclimatized for 7 days to their environment, handling, and retainers for the blood glucose test to ensure their familiarity with it before glucose readings. Weekly, monthly, and total normal rat chow consumed in treated and untreated animals were recorded

3.3.2 Experimental design

The animals were casually divided into two main groups diabetic and non-diabetic groups, these two main groups were further divided into a total of eleven groups (A-K). The diabetic group was further divided into 4 subgroups *(n=13* in each group to accommodate for possible mortality) as follows: (A) diabetic with no treatment (DB), (B) diabetic and ARV treated (DAV), (C) diabetic alcohol treated (DAL), and (D) diabetic, treated with both alcohol & cART (DAA). The non-diabetic group was further divided into 7 subgroups with 8 animals in each group viz: (E) received the same dose of alcohol and cART (AA); (F) received only antiretroviral (cART) medication (efavirenz 600mg+ emtricitabine 200mg+ tenofovir 245mg) in gelatine cubes (AV); (G) received 10% alcohol in distilled water v/v *ad libitum* (AL); (H) received plain gelatine cubes (PG); (I) received 20% fructose feed for two weeks and after remained untreated (2FT); (J), received a once off IP injection of citrate buffer (SNC); and (K),

untreated controls (NC). Groups I and J served as a control for the diabetic model while group H is a control for the cART treatment. Immediately following the confirmation of diabetes (end of the third week following two weeks commencement of fructose feeding), the daily cART and alcohol treatments commenced and continued for ninety days after which the rats were terminated (Fig 5).

3.3.3 Termination

At the end of the 90 days treatment, the rats were anaesthetized with an overdose of sodium pentobarbitone. The hearts were perfused with 2ml/min 0.1M phosphate buffer (PB) in 0.9% saline to flush out the blood from the blood vessels. The cranium was excised, and the whole brain was immediately harvested, dried on filter paper, and separated into hemispheres. One hemisphere was fixed in 0.4 paraformaldehyde for histology and the other hemisphere was stored at -80°C for immunoassay and molecular analysis.

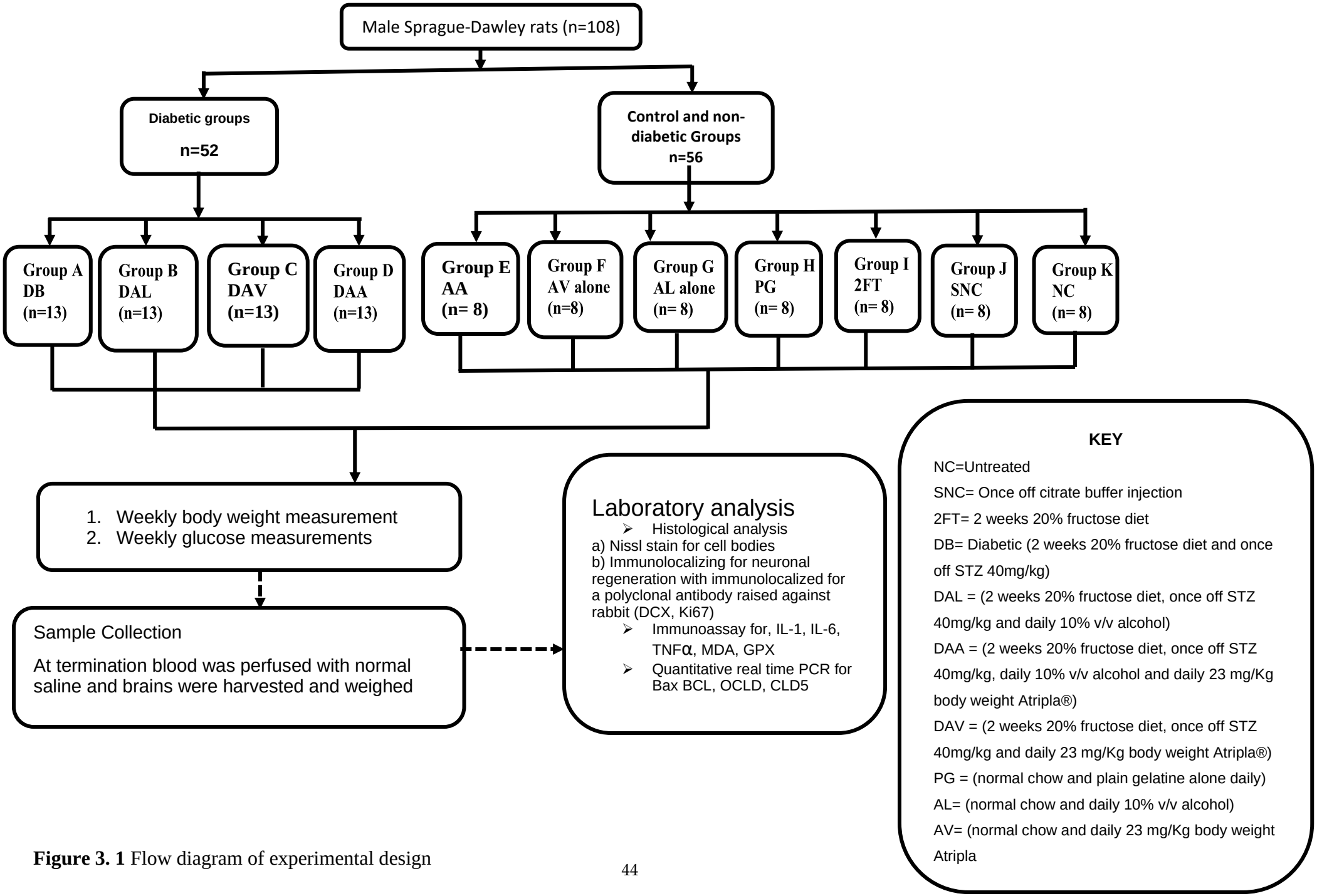

Figure 3. 1 Flow diagram of experimental design

3.4 Laboratory analysis

3.4.1 Enzyme-linked immunoassay of proinflammatory cytokines (IL-1α, IL-6, TNFα) and oxidative stress markers (GPX, and MDA)

Dissected brain samples from each hemisphere per animal were homogenized using a handheld tissue grinder G-50 (Coyote Bioscience, Jiangsu China) in 1:9 volume of 0.01MPBS (pH 7.4), centrifuged at 1000g for 10 minutes and the supernatant collected. The samples were used to run an enzyme-linked immunosorbent assay for proinflammatory cytokines (Rat IL-1α, Rat IL-6, Rat TNFα) according to the manufacturer's protocol (Elabscience, USA; E-EL-R0011, E-EL-R0015, E-EL-R0019 respectively). Oxidative stress markers were assessed using malondialdehyde (MDA) Colorimetric assay kit: TBA method (Elabscience, Houston, Texas USA; E-BC-K025-M), and Glutathione Peroxidase (GSH-Px) Activity Assay Kit (Elabscience, Houston, Texas USA; E-BC-K096-M WST-1 Method). All samples were diluted 1:2, all standards, and run-in duplicates. Diluted samples and standards were transferred to manufacturer-coated 96 well plates and incubated for 90 minutes. After decanting, the biotinylated detection antibody was incubated in the wells for 60 minutes. The wells were incubated in HRP conjugate for 30 min following aspiration and washes. Thereafter, the wells were washed and incubated in substrate reagent for 15 minutes and finally in stop solution.; all incubations were at 37 °C. The optical density (OD) values were read at 450nm. The analysis for MDA was according to the TBA colorimetric method following the manufacturer's protocol, the concentration was calculated in μmol/g protein. The OD was read at 620nm using an Anthos 2010, 96 well plate reader coupled to an ADAP software. OriginPro software was used to calculate the concentration of cytokines in the samples from obtained OD values according to the manufacturer's directions in pg/ml. Total protein concentration for each sample of brain homogenate was tested using the Bradford reagent. The standards were made

in bovine serum albumin (BSA), and the calculated concentration of protein in each sample was applied in calculating the final concentration of cytokines (pg/mg of protein).

3.4.2 Quantitative qPCR for junctional proteins and apoptotic markers

3.4.2.1 RNA extraction

From each brain sample, total RNA was extracted by homogenizing samples in TRIzol reagent (Merck; T9424) at a ratio of 30mg tissue to 1000µl Tri-reagent using a handheld tissue grinder G-50 (Coyote Bioscience, Jiangsu, China). The homogenates were vortexed for 15 seconds, followed by 200 µl of chloroform vortexed again and allowed to stand for 3 minutes at room temperature. The samples were centrifuged at 14000rpm for 15 minutes, supernatant collected, 500 µl iso-propanol (Merck; B6916) added, and centrifuged at 14000rpm for 15 minutes. The supernatant was decanted and 1000 µl of 75% alcohol was added to the pellet and centrifuged at 8000rpm for 5 minutes. Alcohol was poured off and pellets were resuspended in RNAase-free water, heated at 60°C, cooled then stored at -80°C for further analysis. Subsequently, the RNA samples were analyzed using a Nano-Drop® spectrophotometer, Series ND-100 to determine the RNA concentration and purity, thereafter RNA samples were stored at 80°C.

3.4.2.2 cDNA synthesis

RNA samples were diluted according to their concentrations to a final concentration of 50µg/µl. Total RNA was used in a reverse transcriptase reaction to synthesize cDNA using a high-capacity cDNA RT kit (Applied Biosystems; 4368814). Ten microlitres of 2x RT master mix and 10µl of RNA samples were pipetted into each well of a 96 well plate, which were centrifuged at 2500rpm for 2 minutes. The thermocycler for a reaction volume of 20µl was set at 25°C for 10 minutes, 37°C for 60 minutes x2, 85°C for 1 minute, and 4°C for infinity.

3.4.2.3 qPCR experiment

The standard guidelines for the publication of quantitative real-time PCR experiments (MIQE) were followed. The samples, their relevant controls, and inter-plate calibrators were organized in triplicates. Quant studio 1, 96 well plate detection system (Thermofisher Scientific, Massachusetts, USA) was set up to run quantitative PCR expression of BAX, Bcl_2, claudin-5, Caspase-3, INSR, IRS1, and occludin in the cDNA samples. Each 12 µl PCR well contained 1.52 µl of RNAase- free water, 6µl Power Up SYBER Green Master Mix (Applied Biosystems; A25742; Austin, Texas, USA), 0.24 Forward and Reverse Primer, and 4µl diluted cDNA samples. Thermocycler conditions were set for a reaction volume of 12µl, the hold step was set at 50°C for 2 minutes, 95°C for 2 minutes (X40 cycles), PCR step was set at 95°C for 15 seconds, 60°C for 1 minute, 72°C for 1 minute, and melt curve step was sat at 95°C for 15 seconds, 95°C for 15 seconds, 60°C for 1minute and 95°C for 15 seconds. Two housekeeping genes (β actin and GAPDH) were used to control for error and all primers were procured from Inqaba Biotechnical industries (Hatfield, Pretoria, South Africa). Samples were quantified by a standard curve and the calculation of the expression fold for each gene of interest was by the ΔΔ CT method. The primer pair sequence for each gene of interest and housekeeping gene were designed on the IDT website and verified using the Oligoanalyser tool (Table 1).

Table 3. 1. Primer sequence for the gene of interest and housekeeping genes

Gene	Primer pairs
BAX	Fwd: 5′GGTGAACTGGGGGAGGATTG3′
	Rev: 5′AGAGCGATGTTGTCCACCAG3′
Bcl_2	Fwd: 5′GGTGAACTGGGGGAGGATTG3′
	Rev: 5′AGAGCGATGTTGTCCACCAG3′
Caspase-3	Fwd: 5′GGAGCTTGGAACGCGAAGA3′
	Rev: 5′ACACAAGCCCATTTCAGGGT3′
Claudin-5	Fwd: 5′CGAGGCAAGTTAGGTTGGGT3′
	Rev: 5′GGTCGGTCAAGTCCTCACAA3′
Occludin	Fwd: 5′TTCTGTGCTCACAGGTGGTT3′
	Rev: 5′TGGGCTGGATGCCAATTTAGT3′
INSR	Fwd: 5′TGTGACTGATTATTTAGATGTCCCA3′
	Rev: 5′CATCTGGCTGCCTCTTCCTC3′
IRS1	Fwd: 5′CTGCATAATCGGGCAAAGGC′
	Rev: 5′GCCCGTGTCATAGCTCAAGT3′
GAPDH	Fwd: 5′AAGAAGGTGGTGAAGCA GG3′
Housekeeping	Rev:5′CAAAGGTGGAAGAATGG GAG3′
ACTB	Fwd: 5′AACCTTCTTGCAGCTCCTC3′
Housekeeping	Rev: 5′ACCCATACCCACCATCAC AC3′

3.5 Brain tissue preparation for histology

Each brain hemisphere per animal (in each treatment group) was placed in sucrose overnight and mounted on a freezing microtome with dry ice and sucrose and cut in the sagittal plane using a frozen cryostat at 50 µm. Repeated one in six series of free-floating sections were collected into 0.1 M PB and stored in antifreeze at -20˚C till further processing. Every first

series of sections were stained with cresyl violet, while the next two series of sections were used for immunohistochemical labelling of Ki67 and DCX, respectively.

3.6 Routine Histology using Cresyl violet for Nissl stain

Accordingly, brain sections (from each animal in each treated group) were mounted on 0.3% gelatine-coated slides and placed in 50% chloroform and 50% alcohol overnight. Six brain sections were serially collected at 300 µm apart, starting from Bregma plate 169 to plate 177 corresponding to the rat brain atlas (Paxinos and Watson, 2006), and were stained with cresyl violet. The sections (all groups in parallel to ensure uniform staining intensity) were then rehydrated in a degrading series of alcohol, placed in cresyl violet stain, and then into distilled water. Sections were then dehydrated and mounted with a coverslip.

3.7 Histomorphometry

Photomicrographs of the Nissl-stained dorsal hippocampus of each brain section were obtained using a Leica ICC50 HD video camera linked to a Leica DM 500 microscope (Leica Biosystems, USA). Six sections per animal and six animals per group (i.e., 36 sections per group) were analyzed.

3.7.1 Volume of the dentate gyrus

Within each section, the entire dorsal hippocampus was captured at X25 magnification, all 6 camera fields per group were imported in a stacked sequence, and the image j Volumest plugin was used in quantifying the volume of the granular layer and molecular layer in the dentate gyrus of each animal per group. The Volumest plugin entails a combination of the grid and Cavalieri's principle obtained by tracing out the region of interest for each of these layers in each camera field of an image sequence and the estimated volume for each layer was obtained in mm^3 (Appendix D).

3.7.2 Neuronal number and nuclei area

Within each section, nine camera fields were captured at X1000 magnification from uniformly selected areas of the hippocampal regions (Appendix E). Two camera fields each were captured within the CA1 and CA3 regions respectively while five camera fields were captured from the dentate gyrus (DG) region; two counts from each limb and one from the apex of the dentate gyrus giving a total of three hundred and twenty-four camera fields per group that was analyzed. The number of neurons and nuclei area in the upper focal plane of these camera fields were determined using the cell counter and trace plugins of ImageJ software respectively. Only neurons with a vesicular nucleus and centrally placed nucleoli were measured and counted. Representative photomicrographs were compiled using Microsoft Visio and no manipulation was made to the captured images except for brightness and contrast.

3.8 Immunohistochemistry for neurogenesis

From each brain hemisphere, six sections between plates 173 to 177 were selected using the atlas of the rat brain (Paxinos and Watson, 2006) for each histochemical labelling. Free-floating brain sections in 24 well plates first underwent endogenous peroxidase inhibition with 50% methanol, 50% PB, and 1.66% hydrogen peroxide. Sections were washed, then blocked in 3% normal goat serum, 2% (BSA), and 0.25% Triton x 100 in 0.1 M PB for 2hrs at room temperature, followed by incubation in the primary antibodies (rabbit polyclonal antibody; Abcam, Cambridge, MA, USA), Ki67 and DCX (Abcam, USA; AB15580 and AB18723 respectively) with dilution factors 1:1000 and 1:3000 respectively for 48 hours. The sections were washed with 0.1PB and incubated for 2hr with secondary antibody (goat anti-rabbit antibody IgGs; Vectastain, Burlingame, CA USA). Washed and incubated for 1hr with ABC kit (Vectastain, Burlingame, CA USA) and stained with DAB, mounted on gelatine-coated slides, dehydrated, and cleared in xylene. Control sections were incubated in 0.1MPB omitting the primary antibody. Photomicrographs of Ki67 and DCX immunolocalized dorsal

hippocampus brain sections were obtained and counts of immunolabelled cells were determined by the cell counter plugin of Image J. Only DCX immunolocalized cells in the upper focal plane with a pale centrally placed centre were counted while immunolocalized cells for Ki67 were counted in their respective clusters.

3.9 Statistical analysis

The diabetes parameters, number, and nuclei area of neurons in hippocampal regions, concentrations of cytokines and oxidative markers, expression of hippocampal Ki67 and DCX labelling as well as gene expression of insulin receptors, junctional and apoptotic genes were recorded as mean ± SEM. The data were subjected to a normality test using the Shapiro-Wilks test, parametric data were analyzed using a one-way ANOVA test and a Post hoc Bonferroni's test was conducted to determine the difference between the groups. Nonparametric data with Shapiro-wilks P value < 0.05 were analyzed by the Kruskal Wallis test and a Post hoc Bonferroni's pairwise analysis, results with $P < 0.05$ were regarded as significant. All data analysis was carried out using the IBM SPSS statistics version 28.

3.10 Ethical clearance

This study was approved by the Animal Research Ethics Committee (approval number 2018/011/58/C) of the University of the Witwatersrand. All experimental animal handling and treatments were carried out according to the standards and principles set forth by this committee.

CHAPTER 4 A Diabetic Model Suitable for Investigating Multidrug Therapy

4.0 Abstract

Due to the diabetogenic properties of many substances, there is an increasing need to investigate the concomitant presence of toxicological and therapeutic substances within a type 2 diabetic (T2D) model. This technical research aims to establish and evaluate the use of a diabetic model for investigating the co-occurrence of diabetes with other treatments or conditions. Eight-week-old male Sprague Dawley rats were randomly distributed into eleven groups. Negative control (NC), twenty percent fructose feed (2FT), sham control (SNC), alcohol alone (AL), cART alone (AV), alcohol and cART (AA), diabetic control (DB), diabetes and alcohol administration (DAL), diabetes and cART treatment (DAV), and diabetes, alcohol, and ART (DAA). The rats in the diabetic groups were fed with fructose-chow formulated pellets for two weeks while the controls received normal pellets. After two weeks, the rats in the diabetic groups received a once-off intraperitoneal injection of 40mg/kg body weight (BW) Streptozocin freshly prepared in 0.05M citrate buffer. The following week non-fasting glucose levels were recorded and levels above 14mmol/L 250mg/dl were considered diabetic. During the 12 weeks of the experiment, we observed significantly lower body weight, impaired oral glucose tolerance in addition to significantly higher fluid intake (DB and DAV), and non-fasting blood glucose in our models when compared with the non-diabetic controls. Furthermore, no significant changes were observed between the experiment vehicles and the control. These results demonstrate that a 20% fructose enriched diet followed by a 40mg/kg BW STZ injected rat can serve as a complementary T2D model for investigating diabetes in combination with other drug therapies.

4.1 Introduction

The induction of type 2 diabetes in a non-genetic animal model has been severally researched and reported. These models include single-dose streptozotocin (STZ) (Ito et al., 1999), multiple-dose STZ (Wu and Huan, 2007), high fat diet with STZ (Reed et al., 2000), nicotinamide with STZ (Masiello et al., 1998; Ghasemi et al., 2014), prolonged fructose (Lozano et al 2016), fat and fructose enriched diet (Wilson and Islam, 2012; Kumar et al., 2014). According to available literature, the most common model reported is the use of STZ (Furman, 2015) due to its ability to swiftly impair insulin secretion followed by fructose-enriched diets which is an effective dietary means of inducing obesity, insulin resistance, and hyperglycaemia in laboratory rats which mimic symptoms of type 2 diabetes mellitus in humans (Ang and Yu, 2018). While all these models can be used successfully to induce type 2 diabetes, reports are scarce or non-existent in literature where induction of diabetes on experimental animals is followed immediately with the treatment of such animals with a drug or a combination of drugs for the evaluation of the drug effects or toxicity under the diabetic condition. Furthermore, multiple drug therapy under the diabetic condition is currently uncommon due to co-morbidity and co-infection with other diseases, and documentation of such multidrug treatment effects/toxicity and with the suitable diabetic model is scarce. This study reports on a modified model of diabetic induction followed by in vivo multidrug treatment of experimental animals.

Type 2 diabetes (T2D) is one of the most common chronic health and socio-economic problems in South Africa. In contrast to type 1 diabetes, T2D shows diverse characteristics of metabolic syndrome such as hyperglycaemia, glucose intolerance, and insulin resistance. Fructose-enriched diet (FED) or fructose drinking water (FDW) is an effective way to induce hyperglycaemia and insulin resistance in laboratory rodent models (Kumar et al., 2014; Ang and Yu, 2018). A large percentage of fructose as a percentage of the total calories is referred

to as a hypercaloric diet (Rodríguez-Correa et al., 2020) and favours the development of type 2 diabetes mellitus. Fructose is absorbed and metabolized by the liver, loading the liver with excess fructose can lead to rapid stimulation of lipogenesis and triglycerides accumulations, which contributes to reduced sensitivity, hepatic insulin resistance, and glucose intolerance (Dupas et al., 2016). Initially, the state of normoglycaemia is maintained because the pancreas is still able to secrete enough insulin to overcome IR, but gradually, this compensatory response fails, and marked hyperglycaemia develops.

Several studies have successfully used FDW (10%) and FED (21%) to induce a suitable T2D model either in addition to STZ (Wilson and Islam, 2012; Kumar et al., 2014) or in a prolonged 20-25% FDW alone (Dupas et al., 2016). FED is a more effective and efficient route of administering fructose than administration through (FDW) due to the ability of FED in producing desirable symptoms of metabolic syndrome (de Moura et al., 2008; Ang and Yu, 2018). Additionally, the use of a single low dose of STZ in addition to the FED is a desirable model for T2D due to its ability to impair the pancreatic β cells but not destroy all the β cells, thereby maintaining all the hallmarks of T2D. However, 20% of FED alone may fail to induce hyperglycaemia during the two weeks of FED feeding without the injection of STZ, hence the administration of a single low dose STZ which is required to induce rapid and stable hyperglycaemia and impair β cells within 48-72hours after administration (Ito et al., 1999).

Various studies have investigated the FED and STZ mode for diabetes with different variations in dosages. However, it is essential to evaluate every model to ensure that it mimics the pathogenesis of T2D and ensure that it can be employed in further drug therapy pathological experiments.

In addition to optimizing an accurate T2D model, arises the need to evaluate the suitability of the model for investigating pathologies associated with different types of diabetes. The

American Diabetes Association classifies diabetes into the general categories of type 1, type 2, gestational and specific diabetes (Association, 2015). Specific diabetes includes monogenic diabetes syndrome, diseases of the exocrine pancreas, and recently drug or chemical-induced diabetes such as disease (such as Covid-19) associated diabetes (Accili, 2021). Studies often use established diabetic models to study the efficacy of diabetic treatments (Chatzigeorgiou et al., 2009; Fritzen et al., 2018), however, drug or chemical-induced diabetes is gradually becoming prevalent as a high proportion of individuals on chronic medications develop diabetes. Thus, co-morbidity under diabetic condition is seen to be on the increase and will require multiple drug therapy investigations. Therefore, this study aims to develop a diabetic model using 20% FED to induce insulin resistance before a single injection of STZ 40g/kg BW to facilitate the induction of T2D and also evaluate the suitability of this model for investigating the effect of multidrug treatments (cART and alcohol) within the diabetic model.

4.2 Methods and materials

4.2.1 Formulation of fructose feed

Commercially available normal rat chow pellets, obtained from LABCHEF, Nutrition hub (Pty) Ltd, Stellenbosch, South Africa, consisting of protein, oil and fats, ash, minerals, and vitamins were ground into a fine dry powder using a Nutribullet High-Speed Blender. For every 800g of this chow powder, 750ml of distilled water and 200g of fructose powder solution were added, mixed, and moulded into pellets. These pellets were then dehydrated in an incubator for three days at 35^0C and used as animals feed for the first two weeks.

4.2.2 Induction of diabetes

A diabetic model adapted from (Wilson and Islam, 2012; Kumar et al., 2014), incorporates a fructose diet (to induce peripheral insulin resistance (IR) followed by Streptozotocin (STZ)

administration. The rats (non-genetic model) in both treatment and control groups were tested for baseline fasting blood glucose levels to establish that no previous diabetic conditions existed. The rats received a 20% formulated fructose diet as a percentage of the total calories for two weeks. The rats then received a once-off intraperitoneal (I.P) injection of 40mg/kg body weight (BW) STZ prepared in 0.05M citrate buffer (pH 4.5) after 5 hours of fasting. The STZ caused the destruction or degeneration of some pancreatic Langerhans islets β-cell. Stable non-fasting hyperglycaemia confirmed diabetes.

4.2.3 Routine tests

A non-fasting blood glucose test was conducted 72hrs after the STZ administration and weekly thereafter using AccuChek Compact glucometer (Roche Diagnostics, Indianapolis, IN) via tail vein puncture. A biweekly screening of fasting blood glucose levels ≥ 250 mg/dl was conducted to establish that the diabetic condition (hyperglycaemia) was established and remained during the experiment. Monthly oral glucose tolerance tests (OGTT) were also documented to monitor the diabetic condition of the animals throughout the experiment. As described in chapter 3.

4.2.4. Experimental design

The animals were divided into eleven groups, Negative control (NC), twenty percent fructose feed (2FT), sham control (SNC), alcohol alone (AL), cART alone (AV), alcohol and cART (AA), diabetic control (DB), diabetes and alcohol administration (DAL), diabetes and cART treatment (DAV), and diabetes, alcohol, and ART (DAA) as described in chapter 3.

4.3 Results

Several parameters documented from the animal during the 90 days experiment, including mortality, mean weekly body weight, food, and fluid intake, FBG, NFBG, and OGTT were

monitored to verify or exclude the establishment and maintenance of diabetes in the animals. Therefore, diabetic parameters will be separately analyzed and discussed in the experimental vehicle's groups and the treated groups.

4.3.1 Diabetic parameters: Experimental vehicle groups

In line with recommendations of the Wits Research Animal Facility (WRAF), three experimental vehicle groups are employed in this study to verify the non-diabetic effect and otherwise of the vehicles used in the experimental model and treatment. These groups include the SNC group which received a **once-off** IP injection of citrate buffer, the 2FT which received 20% fructose enriched feed for two weeks only, and PG which received plain gelatine cubes for the 90days. The SNC and 2FT groups served as experimental vehicles for the diabetes model while the PG served as experimental vehicles for the cART administration. Diabetic parameters were documented and analyzed in these three groups and compared with the negative control to ensure that these vehicles did not induce any underlying diabetic effects.

4.3.1.1 Mortality in experimental vehicles groups

There was no mortality recorded in these groups.

4.3.1.2 Mean body weight of experimental vehicle groups

The weekly body weight revealed consistently elevated body weight in the 2FT, SNC, and PG groups for the 12 weeks of the experiment. However, no significant difference ($P>0.05$) was observed between these groups (2FT, SNC, and PG) and the NC group throughout the experimental period (Fig 4.1.1).

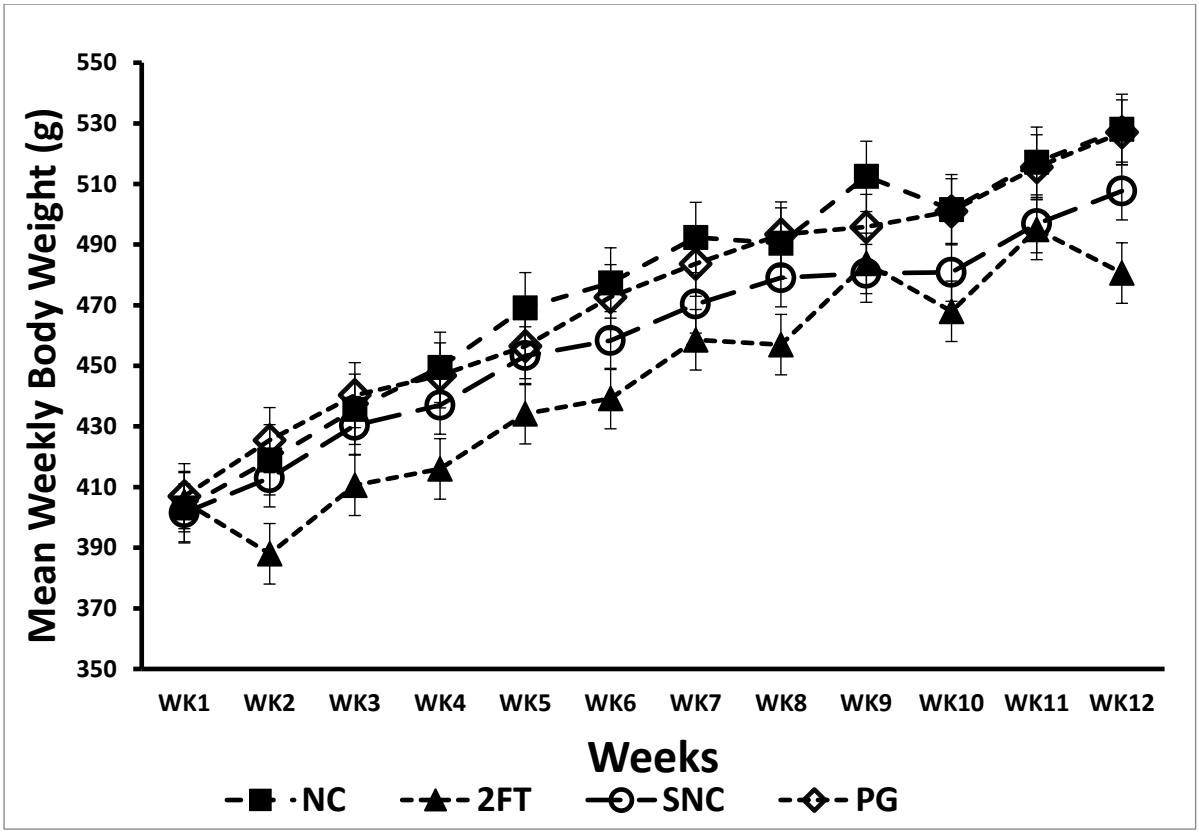

Figure 4.1. 1. Mean weekly body weight in experimental vehicle groups No significant difference observed was in mean body weight between control (NC) and other experimental vehicle groups (2FT, SNC, and PG) (One way ANOVA P>0.05). n=6

4.2.1.3 Mean fasting and non-fasting blood glucose of experimental vehicle groups

Low mean fasting glycaemic levels were uniformly observed across the experimental vehicles (2FT, SNC, and PG), and no significant differences (P>0.05) were observed between these groups compared to the control throughout the treatment period (Fig. 4.1.2A). Similarly, low random non-fasting glycaemic levels were uniformly observed across the experimental vehicle and no significant differences (P>0.05) were observed between the groups (Fig. 4.1.2B).

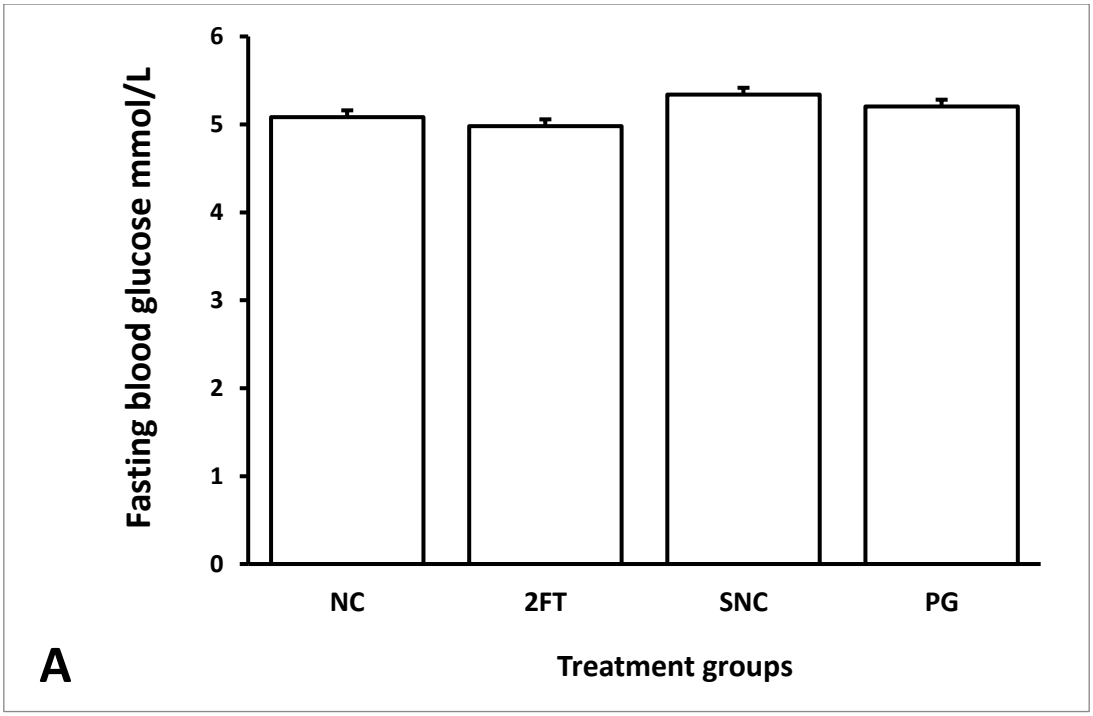

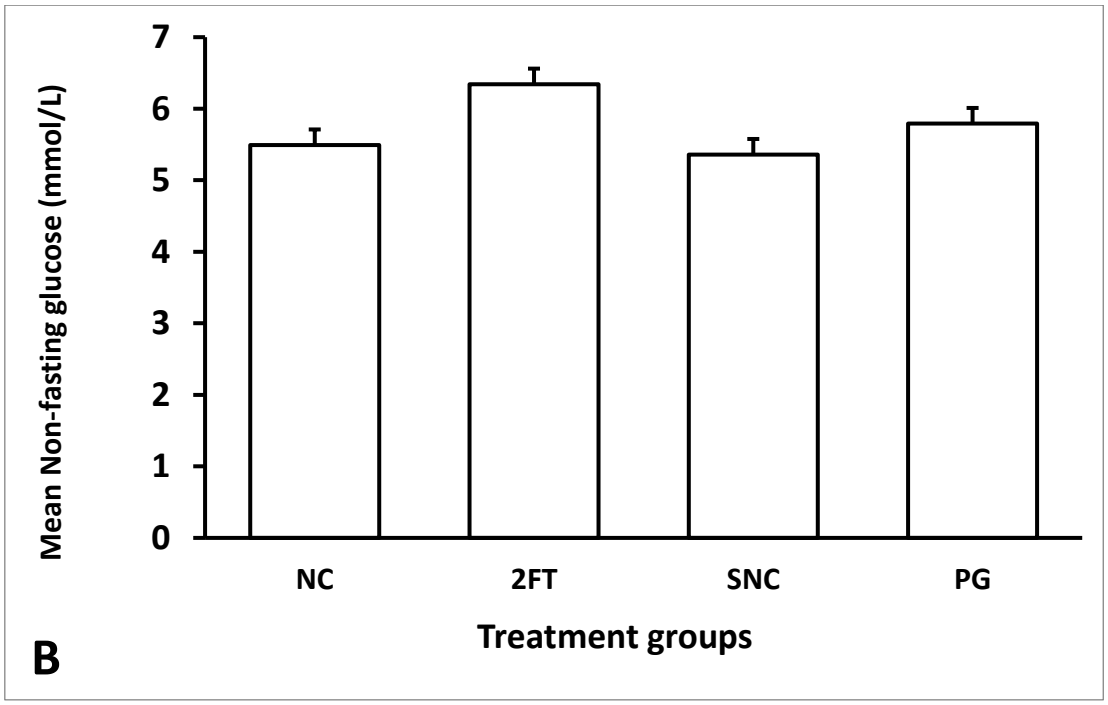

Figure 4.1. 2. Mean fasting and non-fasting blood glucose across experimental vehicle groups. A) No significant difference observed was between fasting blood glucose in experimental vehicles groups compared to the control group (One way ANOVA P>0.05). B) Mean random NFBG in experimental vehicles, no significant difference observed between groups (P>0.05). n=6

4.3.1.4 Food and fluid intake of experimental vehicles

Our results showed uniform mean weekly food intake in the NC, 2FT, SNC, and PG groups with no significant difference between these groups and the control (P>0.05, Fig 4.1.3A). Although the control consumed more water, while the SNC group consumed the least volume of water, a non-significant change in mean total water intake was observed between the experimental vehicle groups (2FT, SNC, and PG) and the control (NC) (One way ANOVA P>0.05, Fig 4.1.3B).

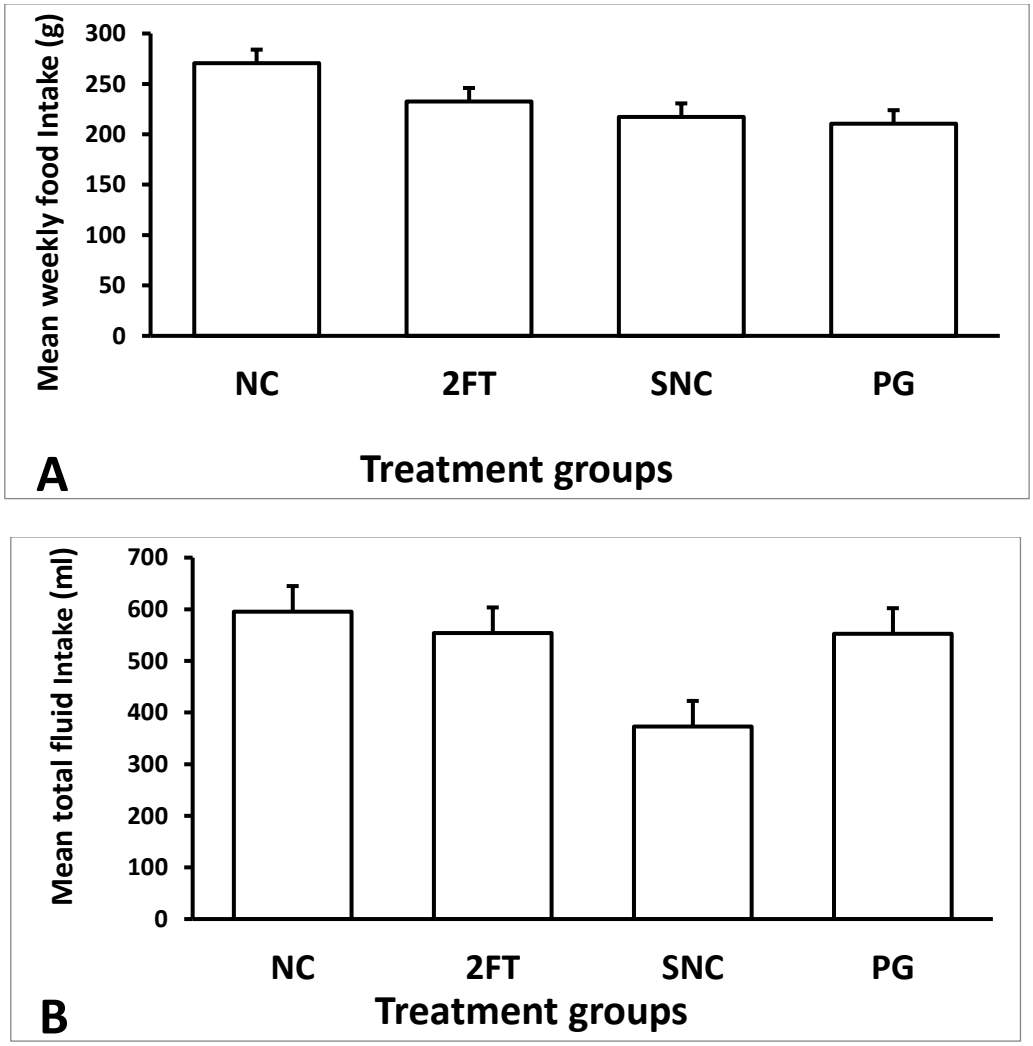

Figure 4.1. 3. Mean food and water intake across experimental vehicle groups. A**)** Mean food intake in experimental vehicle groups, no significant difference observed between groups. B) No significant difference was observed in fluid intake between NC, 2FT, SNC, and PG; One way ANOVA P=0.08). n=6

4.3.1.5 Oral glucose tolerance test of experimental vehicles groups

The initial and final OGTT were similar with uniform levels of blood glucose readings at 0 and 120 minutes in all the experimental vehicle groups. The initial OGTT highlights SNC with the highest glucose levels in the first 30 minutes but the lowest glucose level at 120 minutes. A similar pattern was observed in the PG group for terminal OGTT. However, no significant difference (P>0.05) was observed between these groups at the different time intervals, indicating suitable glucose handling at both the initial month and terminal month of the experiment (Fig 4.1.4 B).

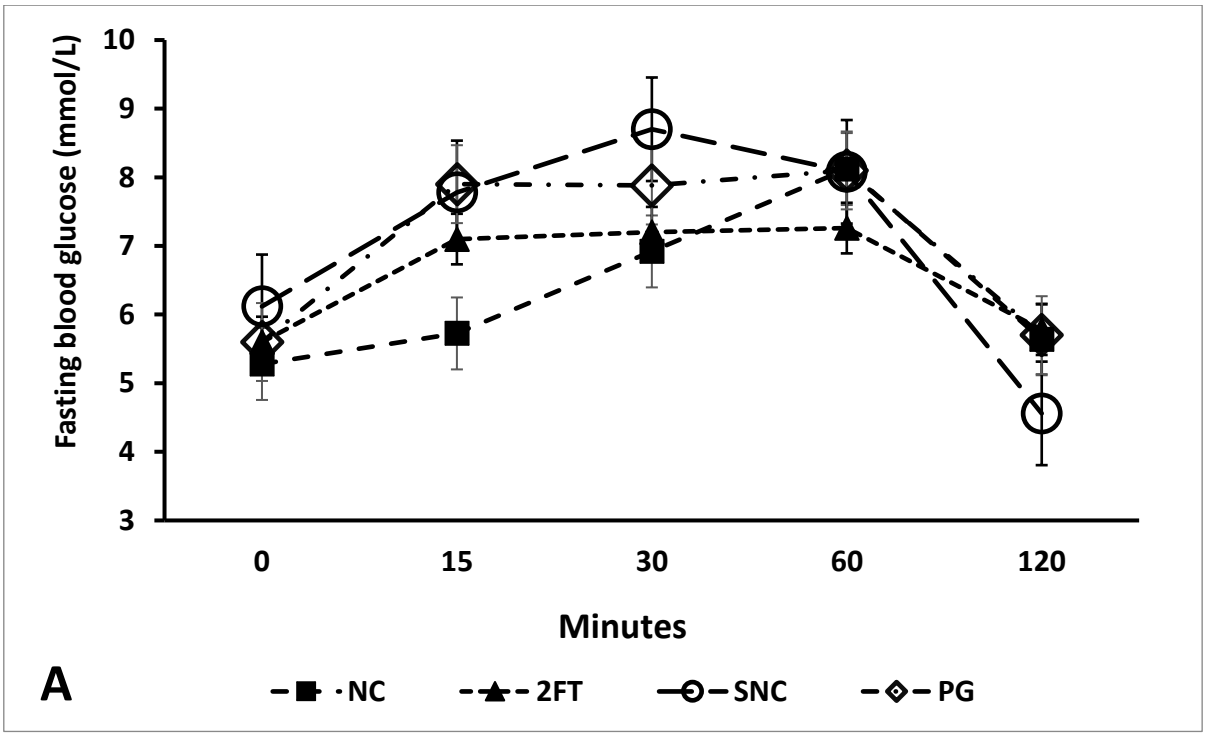

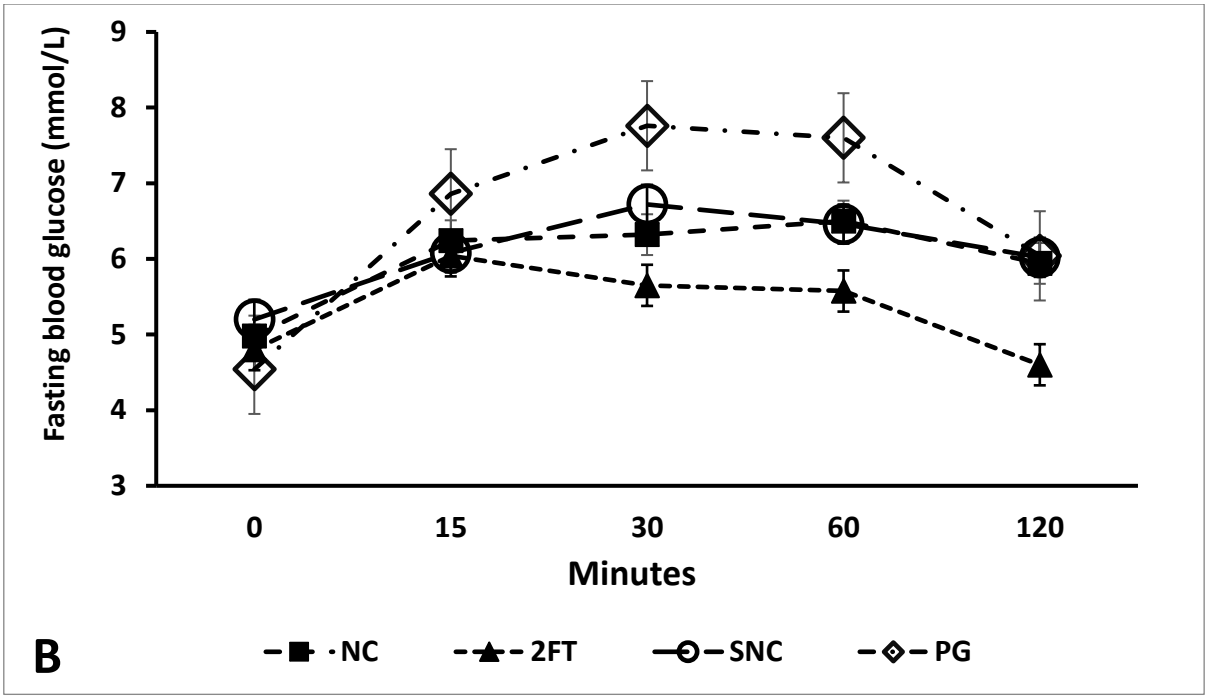

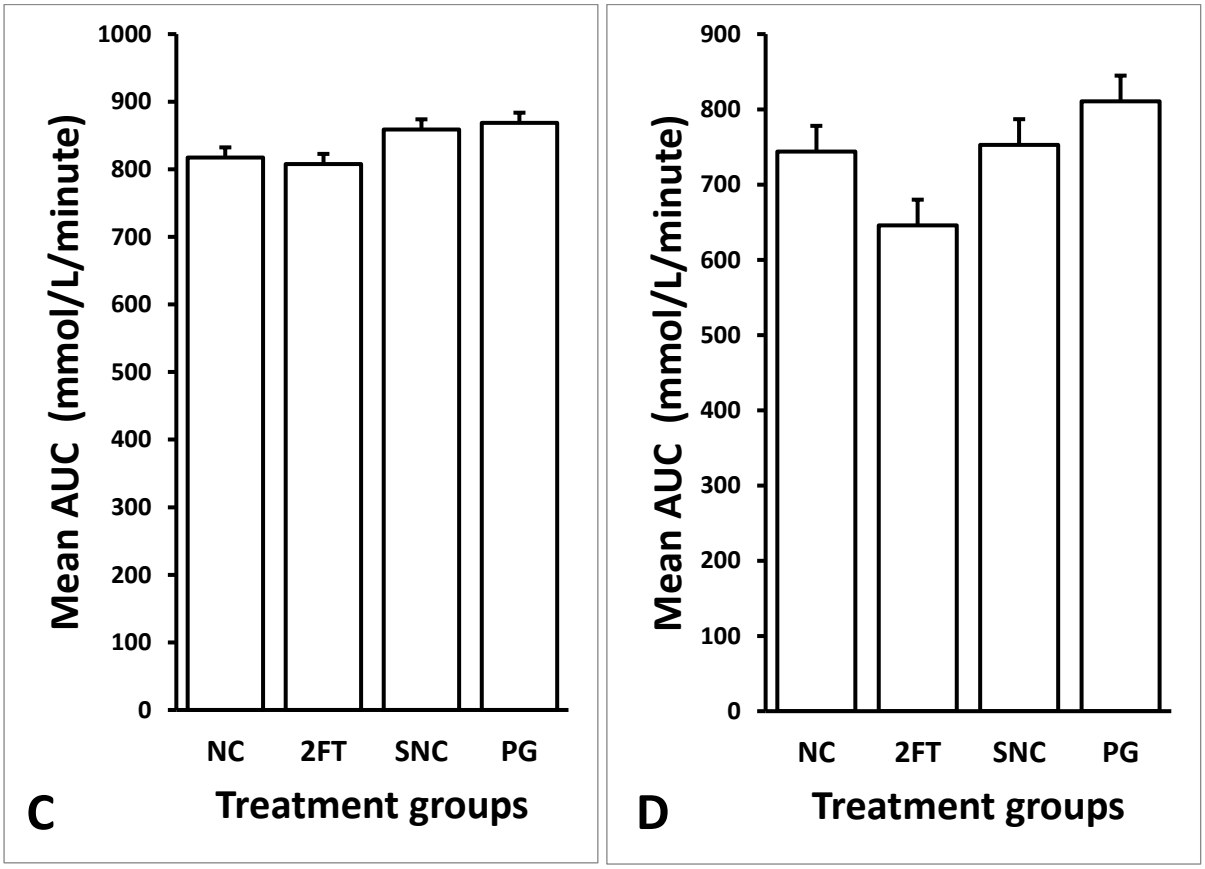

Figure 4.1.4 Mean initial and final OGTT**. A)** Mean initial OGTT B) Mean terminal OGTT C) Mean initial AUC D) Mean terminal AUC in experimental control groups maintained uniformly low levels with no significant difference between groups (One way ANOVA P> 0.05). n=6.

4.3.1.6 Discussion

These results illustrate these diabetic parameters (fluid intake, FBG, NFBG, OGTT, and body weight) were not affected in the experimental vehicle groups (2FT, SNC, and PG), and no significant differences were found in these parameters compared with the negative control (NC). This illustrates that the citric buffer, two weeks 20% fructose diet, and gelatine used as experimental vehicles for the administration of STZ and cART respectively did not induce any diabetogenic effects. Therefore, these groups (2FT, SNC, and PG) were not subsequently reported on as a nil diabetic effect has been established and the Wits ethics committee requirement was satisfied.

4.3.2 Diabetic parameters: Treatment groups

The treated group was divided into two: diabetic and non-diabetic groups. Diabetic groups consist of diabetic with no treatment (DB), diabetic and ARV treated (DAV), diabetic and alcohol-treated (DAL), and diabetic treated with both alcohol & cART (DAA) and the non-diabetic treated groups were groups treated with alcohol and cART (AA), cART only (AV), and alcohol only (AL) treated groups. The diabetic parameters in the diabetic, diabetic treated, and non-diabetic treated groups were compared with the control group (NC).

4.3.2.1 Mortality in treated groups

All the animals per group were observed daily for general wellbeing. In cases where animals were found demised in their cage during a routine check-up, a follow-up autopsy was performed and the cause(s) such as generalized organ congestion, pulmonary compromise, muscle atrophy, pulmonary congestion and cardiopulmonary compromise were determined. Mortality only occurred in the diabetic animals, with the highest mortality (3 out of 13 animals) observed in the DAV group, while the DB, DAA and DAL groups all had relatively similar mortalities (2 out of 12; & 13 animals) (Fig 4.2.1). A maximum of six animals (rats) that were

confirmed to be diabetic throughout the experiment were randomly selected from the surviving rats in each group and used for further analysis.

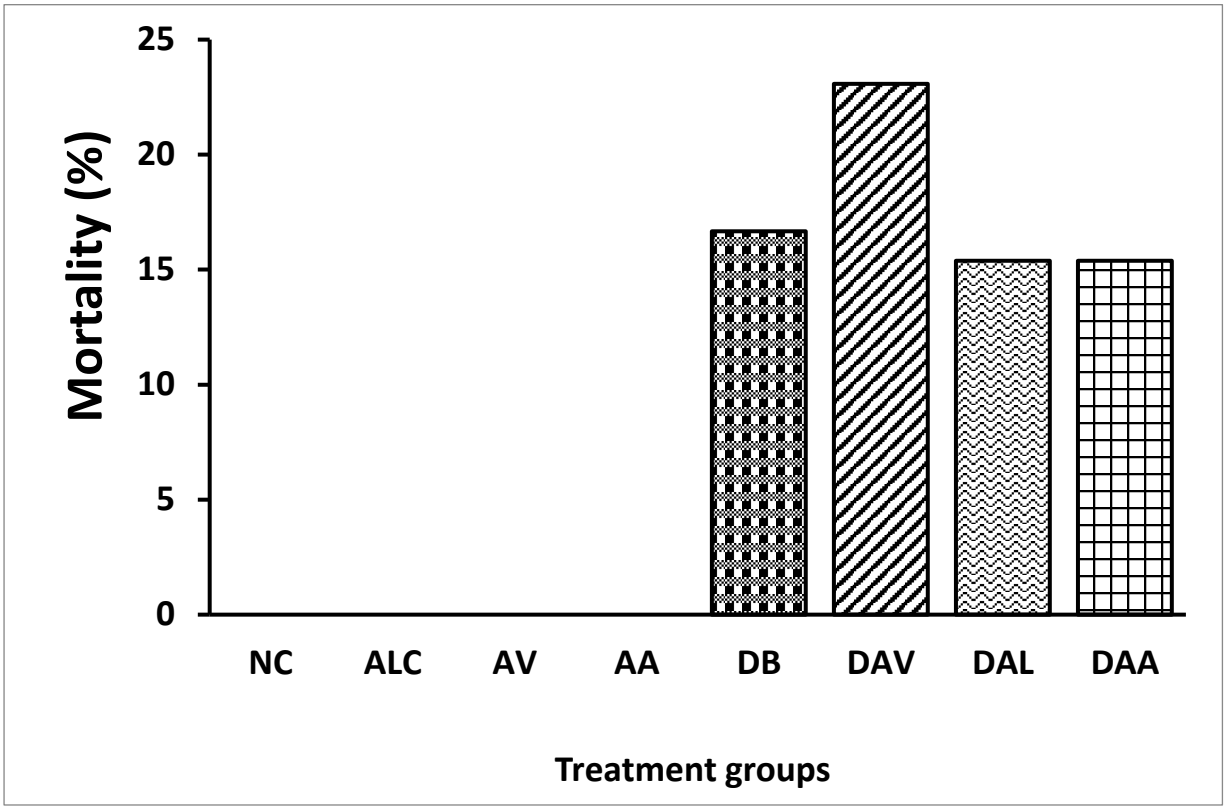

Figure 4.2. 1. Percentage mortality of animals in treated groups. No mortality occurred in the control and non-diabetic groups. In DB (16.7%; 2 out of 12 animals), DAA and DAL (15.4%; 2 out of 13 animals), and DAV (23.1 %; 3 out of 13 animals) mortalities were recorded as reported.

4.3.2.2 Mean body weight of treated groups

As shown in Figure 4.2.2, the mean body weight in DB, DAV, DAA, and DAL was significantly decreased compared to the control (NC) throughout the experiment (but in DAA and DAL from week 2 onwards to week 12) at the overall p-value per group at $P \leq 0.028$, 0.035, 0.014, 0.0018, respectively. From the third week till the end of the experiment, figure 4.2.2 further shows that the mean body weight in AL is significantly increased compared to

DB, DAV, DAA, and DAL, ($P \leq 0.018$, 0.009, 0.0016, and 0.0016 respectively; overall p-value per group). The AV group maintained the highest body weight which was significantly increased compared to the AL group (at weeks 1 and 2 only) and significantly increased ($P \leq$ 0.038, 0.0001, 0.0001, 0.0001, 0.0001, 0.0001 respectively overall p-value per group) compared to AA, DB, DAV, DAA and DAL at every week of the experiment. Additionally, AA was significantly increased compared to DAA and DAL throughout the experiment ($P \leq$ 0.035, 0.009 respectively). However, no significant difference was observed between the diabetic groups (DB, DAV, DAA, and DAL). These weekly mean body weights across all the treatment groups indicate that following weeks two and three, cART gradually and slightly induced an increase in the body weight, while diabetes had an inverse effect on body weight, and the control group maintained marginal body weight increases.

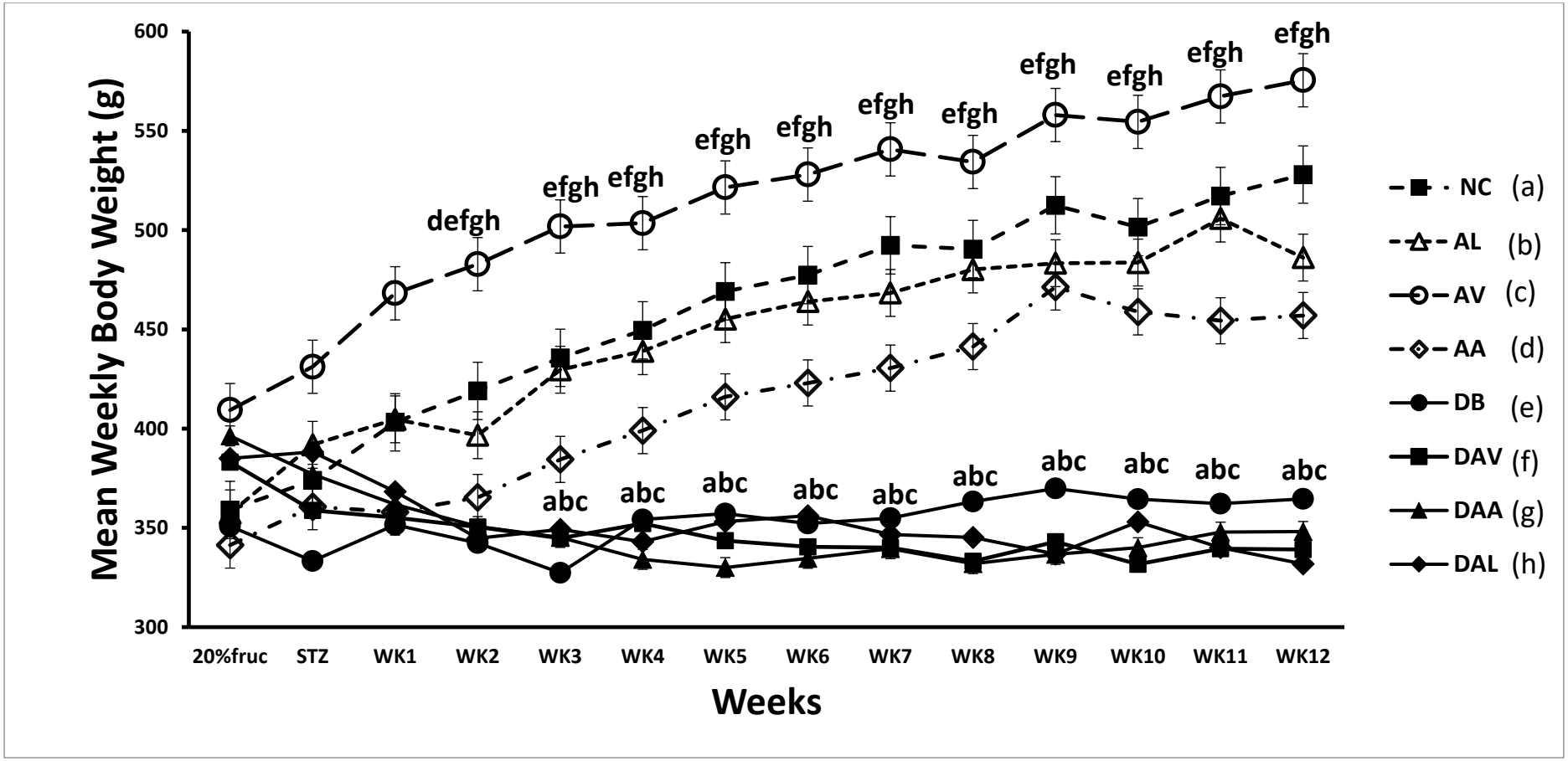

Figure 4.2. 2. Mean Weekly Body Weight in treated groups. Significant difference in body weight between groups (Kruskal Wallis p=0.0001) for the 12 weeks of treatment. DB, DAV, DAL, and DAA are significantly decreased compared to 'a'(NC), 'b' (AL), and 'c' (AV), while AV is significantly increased compared to 'd' (AA), 'e' (DB), 'f' (DAV), 'g' (DAL), 'h' (DAA) between weeks 2 to 12(Bonferroni pairwise test, P< 0.05). n=6

4.3.2.3 Random non-fasting and fasting glucose of treated groups

The mean non-fasting blood glucose of the diabetic groups was significantly increased (P< 0.05) compared to the control (NC) and non-diabetic treated groups (AL, AV, and AA). The highest mean NFBG was observed in the DB group followed by the DAV, DAA, and DAL groups respectively (Fig 4.2.3A). The mean FBG of the diabetic groups was significantly higher compared to the control and all other non-diabetic treated groups (Fig 4.2.3B).

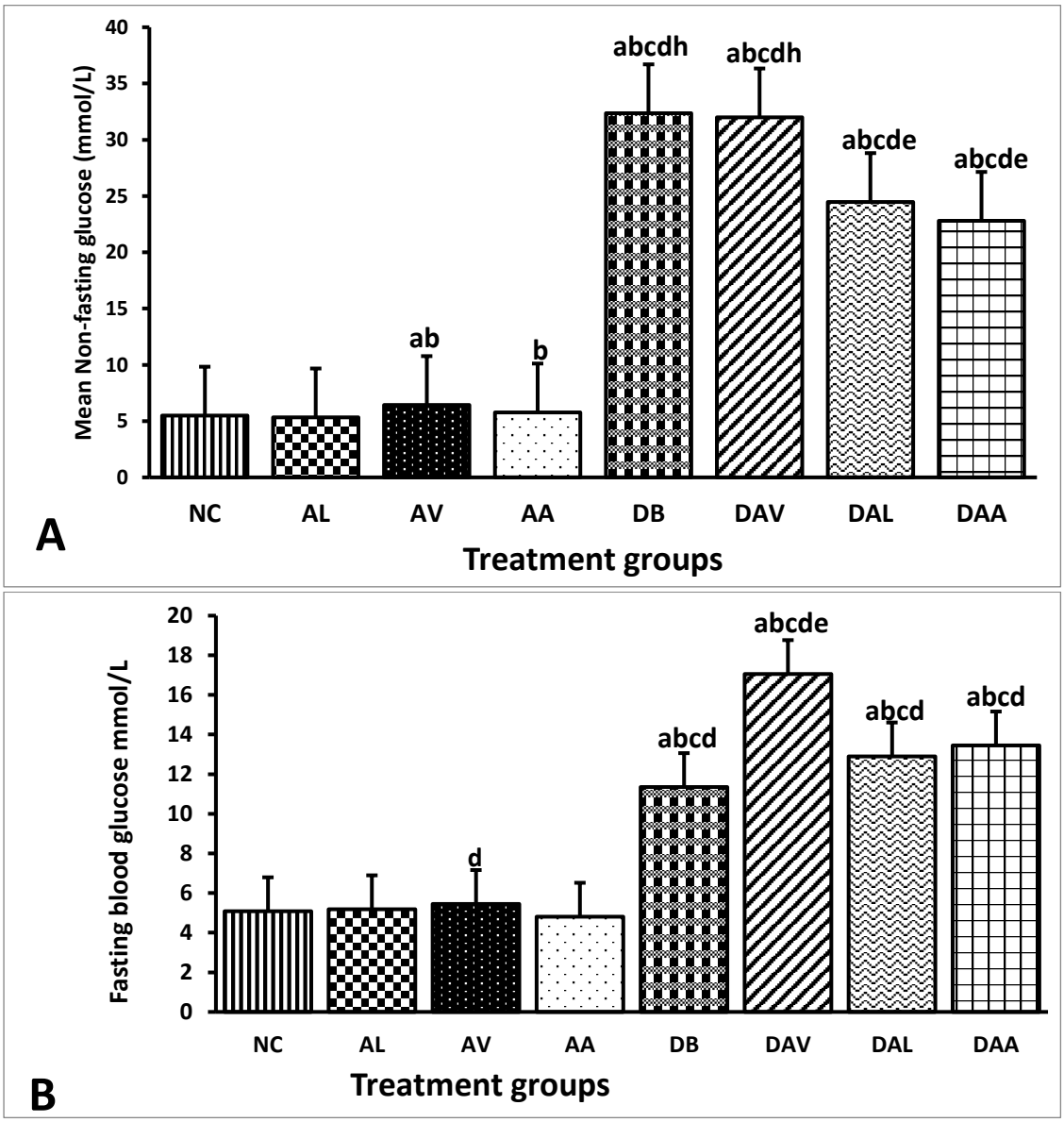

Figure 4.2. 3. Mean non-fasting and fasting blood glucose across treated groups A, B) Significant difference in mean random NFBG and FBG (One way ANOVA P< 0.001). a' (NC), 'b' (AL), 'c' (AV), 'd' (AA), 'e' (DB), 'f' (DAV), 'g' (DAL), 'h' (DAA); indicates significant increases to groups in bracket () P< 0.05. n=6. NC: Control, AV: cART, AL: alcohol, AA: cART and alcohol, DB: diabetic, DAV: diabetic and cART, DAL: diabetic and alcohol, DAA diabetic cART and alcohol.

4.3.2.4 Food and fluid intake of treated groups

A decrease in food intake across treated group was observed and was significantly reduced (P=0.05) in AL, AA, DAL, and DAA compared to the control (Fig 4.2.4A). On the other hand, the diabetic groups consumed more fluid compared to the other groups and were significantly in the DB and DAV groups. No significant difference between the AL, AV, and AA was observed (P=0.05, Fig 4.2.4B).

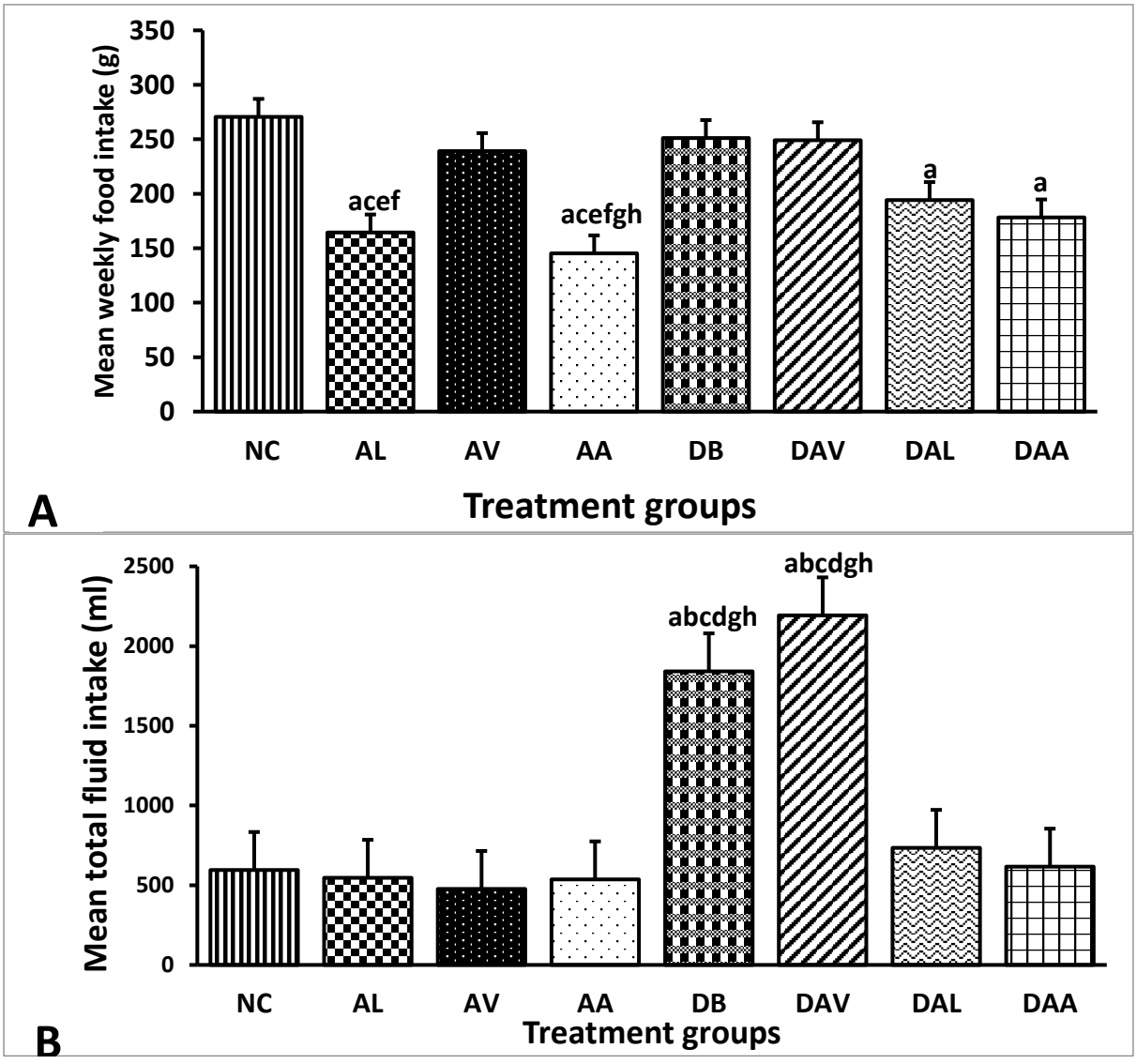

Figure 4.2. 4. Mean food and fluid intake across treated groups. A**)** Significant difference in mean food intake between groups (One way ANOVA P=0.001). B**)** Significant difference in mean fluid intake between groups (Kruskal Wallis test, P =0.001). 'a' (NC), 'b' (AL), 'c' (AV), 'd' (AA), 'e' (DB), 'f' (DAV), 'g' (DAL), 'h' (DAA); indicates significant increases to groups in bracket () P< 0.05. Bonferroni post hoc and pairwise test. n=6. NC: Control, AV: cART, AL: alcohol, AA: cART and alcohol, DB: diabetic, DAV: diabetic and cART, DAL: diabetic and alcohol, DAA diabetic cART and alcohol

4.3.2.5 Oral glucose tolerance test and AUC of treated groups

The mean area under the OGTT curve (AUC) was significantly increased in the DB, DAV, DAL, and DAA groups compared to the control, AL, AV, and AA groups (Fig 4.2.5A). The mean terminal OGTT was similar with uniform low levels of blood glucose readings for the non-diabetic treated groups at different time intervals. While the diabetic groups all had marginal erratic high glucose levels; at 2 hours post glucose load, the DAV group maintained the highest blood glucose level while the DAL dropped to the lowest level for the diabetic groups at 18,5 mmol/L (Fig 4.2.5 B).

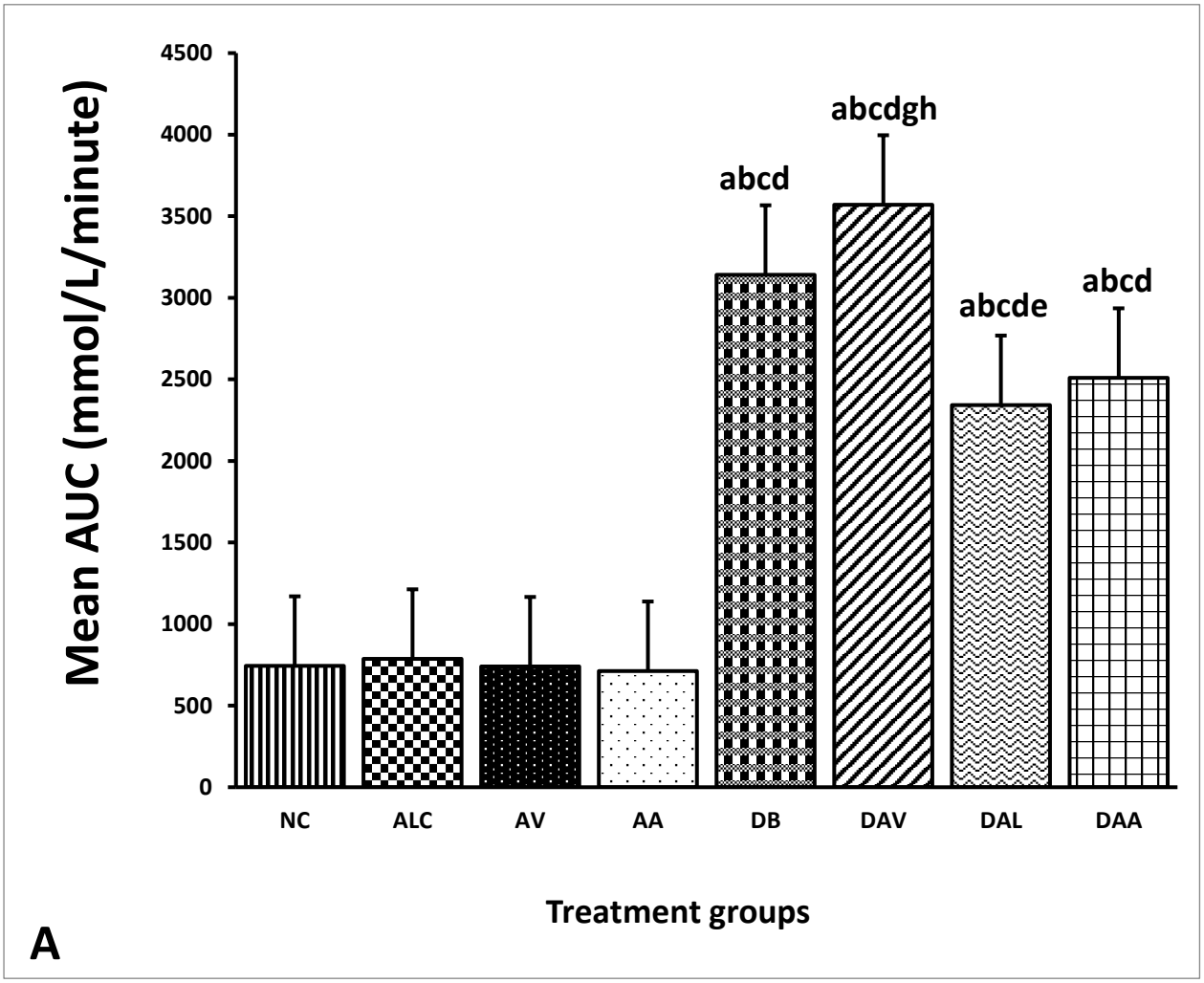

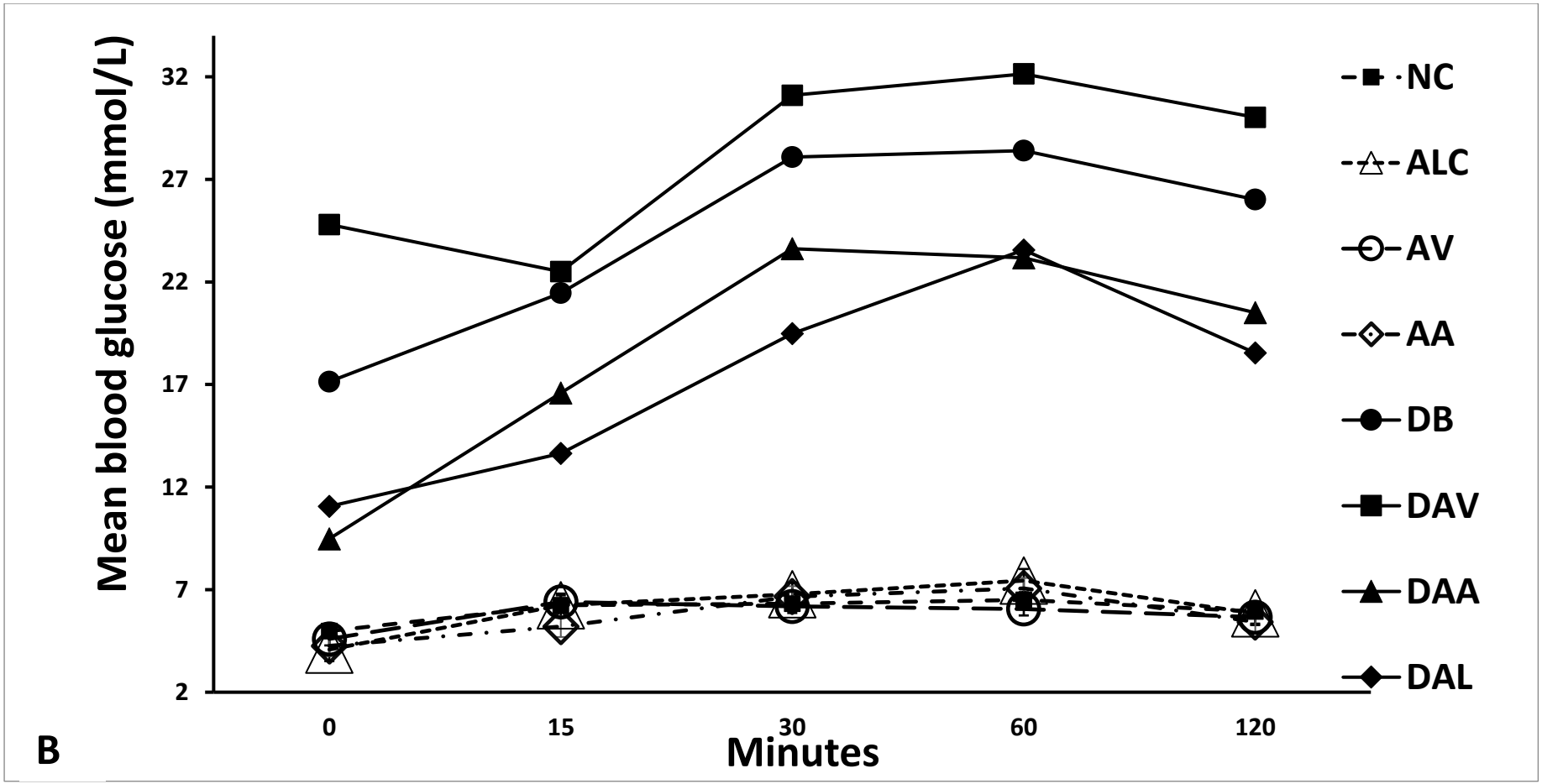

Figure 4.2. 5. Mean terminal AUC and OGTT of treated groups. A) Significant difference in mean terminal AUC (One-way ANOVA P=0.001). a' (NC), 'b' (AL), 'c' (AV), 'd' (AA), 'e' (DB), 'f' (DAV), 'g' (DAL), 'h' (DAA); indicates significant increases to groups in bracket () P< 0.05. Bonferroni post hoc test. B**)** Mean OGTT at different time intervals. n=6. NC: Control, AV: cART, AL: alcohol, AA: cART and alcohol, DB: diabetic, DAV: diabetic and cART, DAL: diabetic and alcohol, DAA diabetic cART and alcohol.

4.3.2.6 Discussion

A recent study has indicated that FBG may not always be a sufficient diagnostic tool for diabetes (Islam, 2011) while others have found significant type 2 diabetes effects with NFBG at levels of 300 mg/dl and above (Can et al., 2011; Wilson and Islam, 2012). This present study reported both FBG and NFBG levels but utilised NFBG levels as the diagnostic tool for diabetes as reported in the Wilson and Islam, 2012 diabetic model. The blood glucose levels obtained in our diabetic groups (the minimum mean level at 414 mg/dl or 23 mmol/L) validate this diabetic model adopted in our study.

In humans and clinical studies, type 2 diabetes can be diagnosed through a fasting blood glucose test above ≥7.0mmol\L, non-fasting blood glucose ≤ 11.1 mmol\L, and a 2-hour post-load glucose ≤ 11.1 mmol\L (American Diabetes Association, 2007), while in animal translational studies, establishment is confirmed with blood glucose levels ≥ 11.1 mmol/L (200mg/dL) (Pournaghi et al., 2012a; Qinna and Badwan, 2015). All our diabetic groups (DB, DAV, DAL, and DAA) were observed to maintain this FBG, NFBG, and 120 minutes glucose tolerance levels described in both clinical studies and rat models throughout the experiment confirming that their diabetic states were maintained.

The results further showed increased body weight in the cART-treated animals, though with average water and food intake, which correlates with a previous report of weight gain in mice treated with cART (Pepin et al., 2018). The alcohol-treated groups showed a non-significant reduction in body weight, though they drank more fluid and consumed less amount of food compared to the control group. This result, therefore, corroborates the report of reduced dietary intake and absence of body weight response to alcohol intake in rats (Kołota et al., 2019). However, the significantly higher FBG and NFBG in DAL and DAA groups compared to the other alcohol-treated groups (AL, AA) suggest the dominance of diabetogenic effects in DAL

and DAA groups. Furthermore, DB and DAV groups that consumed normal quantities of food and showed polydipsia (extreme thirst) had the highest level of FBG and NFBG with significantly lower body weight. All these parameters in the diabetic groups (DB, DAV, DAL, and DAA) are characteristic of well-defined type 2 diabetes. These results confirm the successful induction of diabetes in the treated animals which was also maintained in the diabetic groups throughout the experiment.

CHAPTER 5 Combination Antiretroviral Therapy (cART) in Diabetes Exacerbates Diabetogenic Effects on Hippocampal Microstructure, Neurogenesis, and Cytokine Perturbation in Male Sprague Dawley Rats

5.0 Abstract

The increasing incidence of diabetes and HIV/AIDS–diabetes comorbidity in society has led to the prevalence of combination antiretroviral therapy (cART) in diabetes, with some reported neural effects. Therefore, the effects of cART and type two diabetes (T2D) on the hippocampal levels of cytokines, lipid peroxidation; histomorphology, and neurogenesis were investigated. Adult male Sprague–Dawley rats were divided into four groups: DB (diabetic rats); DAV (diabetic rats treated with cART (efavirenz, emtricitabine, and tenofovir); AV (normal rats treated with cART) and the NC group (with no treatment). Following ninety days of treatment, the rats were terminated, and the brains excised. Immunoassay (IL-1α, IL-6, TNF-α, and MDA); immunohistochemical (Ki67 and DCX), and cresyl violet histomorphology analyses were carried out on brain homogenates and sections, respectively. In comparison to the control, the results showed that cART significantly elevated the IL-6, TNFα, and MDA levels, while DB and DAV significantly reduced the body weight, glucose tolerance, IL-1α, IL-6, and TNFα but increased MDA levels. The hippocampal neuronal number was reduced in AV (dentate gyrus; DG region), in the DB group (Cornu Ammonis subregion 1; CA1 and DG regions only), and DAV (all hippocampal regions). Additionally, the expression of neurogenic markers Ki67 and doublecortin (DCX) were reduced in the diabetic group, with a greater reduction in the cART+T2D group compared to the control. Furthermore, the neuronal number at all hippocampal regions was negatively correlated with the diabetic parameters (FBG; fasting blood glucose, NFBG; non-fasting blood glucose, AUC; area under the glucose tolerance curve) but positively correlated with body weight. Additionally, the increase in the DG

neuronal nuclei area of DB and DAV was significantly positively correlated with FBG, NFBG, and AUC and inversely correlated with the estimated number of neurons and neurogenesis. These findings indicate that cART in diabetes (DAV) has similar effects as diabetes relative to the induction of oxidative stress and impairment of the cytokine immune response, but exacerbated neurotoxicity is observed in DAV, as shown by a significantly decreased DCX expression compared to DB and reduction in the number of Cornu Ammonis subregion 3 (CA3) hippocampal neurons, unlike in cART or the diabetes-alone groups.

5.1 Introduction

Diabetes is a non-communicable disease, which is rapidly spreading throughout South Africa and globally in recent decades (Pheiffer et al., 2018). Diabetes is reported to be caused by lifestyle factors (Feng et al., 2015; Li and Sun, 2022), and recently the use of cART has also been implicated to be diabetogenic.

The introduction of combination antiretroviral therapy (cART) provided effective means of suppressing human immunodeficiency virus (HIV) replication and is clinically used in Southern African regions as a first-line drug for HIV and acquired immunodeficiency (AIDs) management (Meintjes et al., 2017). cART consists of non-nucleoside reverse transcriptase inhibitor (NNRTI); efavirenz, protases inhibitor (PI); emtricitabine, and reverse transcriptase inhibitor (RTI); tenofovir disoproxil fumarate. NNRTIs have been reported to induce oxidative stress (Fokunang et al., 2005), while PI's inhibits glucose uptake by cells and thereby stimulate inflammatory response (Zhou et al., 2007; Osuji et al., 2018). These effects of the cART component are associated with the induction of insulin resistance (Noor, 2007; Honnapurmath and Patil, 2017) and subsequent development of type 2 diabetes (Calle and Fernandez, 2012; Tsalamandris et al., 2019). The diabetogenic effects of cART contribute to the fourfold increase in the prevalence of type 2 diabetes amongst HIV patients on cART compared to untreated HIV patients (Brown et al., 2005).

Type 2 diabetes (T2D) is a metabolic disorder characterized by weight loss, hyperglycemia, insulin resistance, or lack of insulin secretion in the advanced stages of the disease. T2D induces oxidative stress and perturbation of pro-inflammatory cytokines (Muriach et al., 2014; Berbudi et al., 2020) which increases incidences of infections (Casqueiro et al., 2012) and activates a cascade of intracellular events that leads to autophagy, apoptosis and disturbances of synaptic plasticity in hippocampal neurons (Gonzalez et al., 2011; Sadeghi et al., 2016). Hippocampal neurons have numerous membrane bound glucose and insulin receptors which are dependent on the sufficient supply of glucose for the metabolic demands of cognition and memory tasks in the hippocampus (McNay et al., 2010; McNay and Recknagel, 2011). The potential for type 2 diabetes and components of cART to induce insulin resistance or insulin deficiency and inhibit glucose transport into neurons has been implicated in the impairment of hippocampus-dependent memory functions and adult neurogenesis, especially by NNRTI in cART (Stranahan et al., 2008; Ramos-Rodriguez et al., 2014; Jin et al., 2016).

T2D is associated with cognitive anomalies (Kodl and Seaquist, 2008) and dementia (McNay and Recknagel, 2011), while cART-induced oxidative stress has been linked to hippocampal atrophy, deficiencies in volume, and synaptic plasticity (Opii et al., 2007; Robertson et al., 2012) with attendant neurocognitive disorders. However, the effects of the concurrent presence of T2D and cART due to diabetes-HIV co-morbidity (T2D +cART) on hippocampal histomorphology and neurogenesis remain to be documented. Meanwhile, diabetes and HIV co-infected patients abound resulting in the prevalent use of cART amongst diabetic patients. Evidence exists on the increasing coexistence of type 2 Diabetes mellitus (T2DM) among persons living with HIV/AIDs (PLWHA) (Kousignian et al., 2021) leading to chronic cART therapy amongst them. So far, the body of evidence has focused mostly on in-vitro and MRI investigations of the independent effects of type 2 diabetes and cART on the hippocampus, and little is known about the in-vivo histopathology of coexistence of the two conditions

(cART+T2D) on the hippocampus relative to induction of inflammation, perturbation of neuronal cytoarchitecture and expression of neurogenic markers. However, in HIV-positive patients, it may be difficult to ascertain if observed oxidative stress and neuroinflammation emanate from neurotoxic interactions of cART administration in diabetes or if such effects are induced by the presence of HIV. Therefore, it is crucial to investigate and document the effects of cART administration in HIV-naïve male Sprague Dawley diabetic rats (cART+T2D) vis-à-vis the impact on pro-inflammatory cytokines and lipid peroxidation levels, and likely associated changes on neuronal histomorphology and neurogenesis relative to possible cognitive and memory adverse effects.

5.2. Materials and Methods

5.2.1 Chemical and reagents

These were obtained as follows: combination antiretroviral drug (Atripla) (Bristol-Myers Squibb and Gilead Sciences, California, USA), the primary antibodies (rabbit polyclonal antibody; Abcam, Cambridge, MA, USA), secondary antibody (goat anti-rabbit antibody IgGs; Vectastain, Burlingame, CA, USA) and ABC kit from (Vectastain, Burlingame, CA, USA).

5.2.2 Ethical clearance

This study was approved by the Wits Research Animal Facility (WRAF) (approval number 2018/011/58/C) of the University of the Witwatersrand. All experimental animal handling and treatments were carried out according to the standards and principles set forth by this committee.

5.2.3 Animal husbandry

For this study, twenty-four adult male Sprague-Dawley rats (10 weeks old) were housed under conditions highlighted in Chapter 3.

5.2.4 Experimental design

Type 2 diabetes was induced and monitored in the experimental rats accordingly as described in chapter 3, The animals were divided into four groups of six rats each (n=6). The control (NC), antiretroviral therapy group (AV), diabetic group (DB), diabetic with antiretroviral (DAV)

5.2.5 Enzyme-linked immunoassay of proinflammatory cytokines and malondialdehyde (MDA)

Dissected brain samples from each hemisphere per animal were homogenized and used to run an enzyme-linked immunosorbent assay for Rat IL-1α, Rat IL-6, Rat TNFα, and MDA Colorimetric assay kit: TBA method (Elab Science, USA; E-EL-R0011, E-EL-R0015, E-EL-R0019, and E-BC-K025-M respectively) according to the manufacturer's protocol as previously described in chapter 3.

5.2.6 Brain tissue preparation for histology

Each brain hemisphere per animal was placed in sucrose overnight and mounted on a freezing microtome with dry ice and sucrose and cut in the sagittal plane using a frozen cryostat at 50 µm. Every first series of sections were stained with cresyl violet, while the next two series of sections were used for immunohistochemical labelling of Ki67 and DCX, respectively.

5.2.7 Histology and histomorphometry

Sections were stained using routine cresyl violet stain and photomicrographs obtained for histomorphology of nuclei area and number of neurons as previously described in chapter 3.

5.2.8 Immunohistochemistry for neurogenesis

From each brain hemisphere, six sections between plates 173 to 177 were selected using the atlas of the rat brain (Paxinos and Watson, 2006) for each histochemical labelling using

polyclonal antibody raised against rabbit Ki67 and DCX (Abcam, USA; AB15580 and AB18723 respectively) as previously described in chapter 3.

5.2.9 Statistical analysis

The nuclei area and number of neurons in hippocampal regions, concentrations of cytokines, and density of immunolabelled hippocampal Ki67 and DCX were recorded as mean ± SEM and analyzed as described in chapter 3.

5.3. Results

5.3.1 Mortality

The mean percentage mortality in the DB and DAV groups was 12,5% (1 out of 8 animals) and 22,22% (2 out of 9 animals) respectively, and none in the control and AV groups. A maximum of six rats per group were randomly selected from surviving rats in each group and used for further analysis (Fig 5.1A).

5.3.2 Body weight

The mean terminal body weights in DB and DAV groups were significantly decreased compared to the AV and NC groups. The mean body weight was highest in the AV group and lowest in the DAV group. No significant change in body weight was observed between the NC and AV and between DB and DAV groups (Fig 5.1B).

5.3.3 Blood glucose levels

The mean NFBG levels in DB and DAV groups were significantly increased in comparison to levels in NC and AV groups (Fig. 5.1C). The mean FBG and NFBG levels for DAV and DB groups remained significantly high throughout the experiment compared to AV and NC groups respectively (Fig 5.1C and D). But no significant difference in mean FBG and NFBG was observed between the DB and DAV groups.

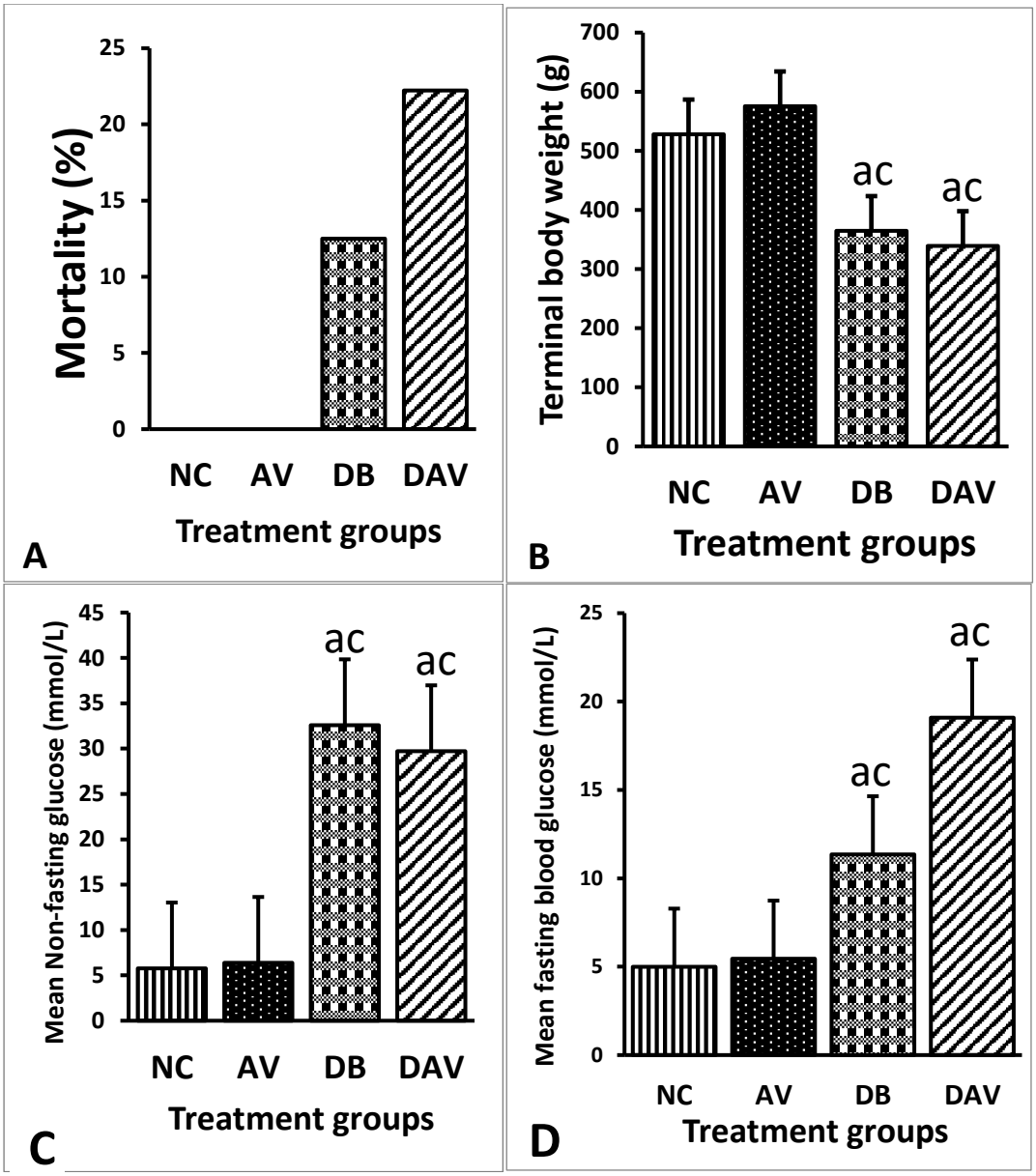

Figure 5. 1. Mean mortality, terminal body weight, and fasting and non-fasting blood glucose levels. (**A**) No mortality in the NC and AV groups, but (12.5%) 1 and (22.22%) 2 mortalities in DB and DAV, respectively. (**B**) Significant difference in mean body weight across groups (Kruskal–Walli's test, $p \leq 0.0001$). DAV and DB are significantly decreased compared to control NC ($p = 0.034$ and 0.03 respectively) and AV ($p = 0.0001$, Dunn's pairwise post hoc test). (**C**) Significant differences in the mean NFBG between groups (Kruskal–Walli's test, $p \leq 0.0001$), DAV, and DB are significantly increased compared to control ($p = 0.0001$ and 0.001, Dunn's pairwise post hoc test) and AV ($p = 0.05$ and 0.008 respectively). (**D**) Significant difference in the mean FBG between groups (Kruskal–Walli's test, $p \leq 0.001$). DAV and DB are significantly increased compared to control ($p = 0.003$ and 0.008, respectively) and AV ($p = 0.004$ and 0.05 respectively), $n = 6$. a' (NC), 'c' (AV), 'e' (DB), 'f' (DAV); indicates significant changes to groups in bracket ( ), $P< 0.05$. Key: NC, Controls; AV, cART only; DB, Diabetic; DAV, diabetic with cART.

5.3.4. Oral Glucose Tolerance Test

The mean oral glucose tolerance test showed optimal glucose handling in the NC and AV groups but poor glucose handling in the DB and DAV groups. After 2 h of glucose administration, the DAV had the highest level of blood glucose and area under the curve (AUC), followed by the DB group; however, no difference was observed between the DB and DAV groups. The AUC was significantly increased in the DB and DAV groups compared to the NC and AV groups, and the glucose levels remained high in the DB and DAV group 2 h post-glucose load (Figure 5.2A, B).

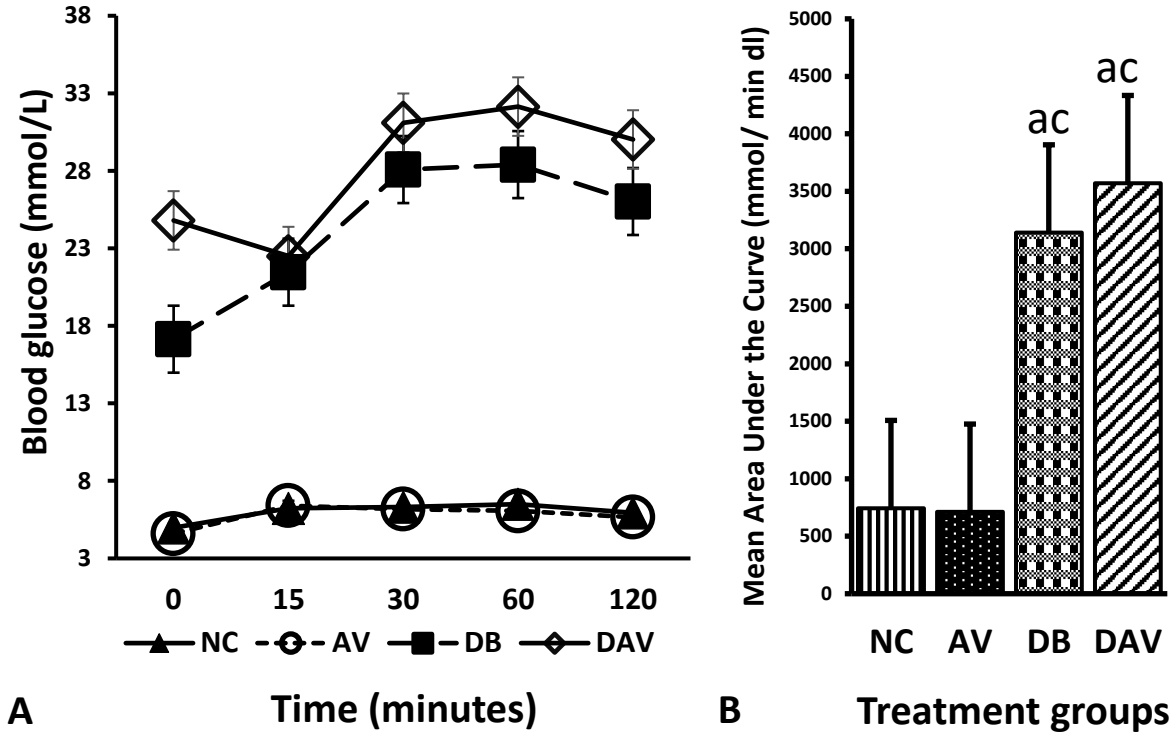

Figure 5. 2. Mean oral glucose tolerance test and area under the curve. (**A**) Mean OGTT levels. (**B**) Significant difference in the mean area under the OGTT curve across groups (Kruskal–Wallis test, $p \leq 0.0001$). DAV and DB are significantly increased compared to control ($p = 0.014$ and 0.002) and AV ($p = 0.006$ and 0.001 respectively, Dunn's pairwise post hoc test), $n = 6$. a' (NC), 'c' (AV), 'e' (DB), 'f' (DAV) ; indicates significant changes to groups in bracket () P< 0.05. Key: NC, Controls; AV, cART only; DB, Diabetic; DAV, diabetic with cART.

5.3.5. Inflammatory Cytokines and MDA

The concentrations of proinflammatory cytokines IL-1α, IL-6, and TNFα in the hippocampal tissue homogenate are shown in figure 5.3 A–C, respectively. The concentrations of all three cytokines (IL-1α, IL-6, and TNFα) in DB and DAV were significantly reduced compared to the NC (p = 0.007, 0.013, and 0.0001, respectively) and AV groups (p = 0.001). The concentrations of all three cytokines (IL-1α, IL-,6, and TNFα) in the AV groups were significantly increased compared to the control (NC) (p = 0.04, 0.001, and 0.043, respectively) (Figure 5.3A–C). Similarly, the MDA levels significantly increased in AV, DB and DAV compared to the control (NC) (p = 0.019, 0.039 and 0.001, respectively) (Figure 5.3D).

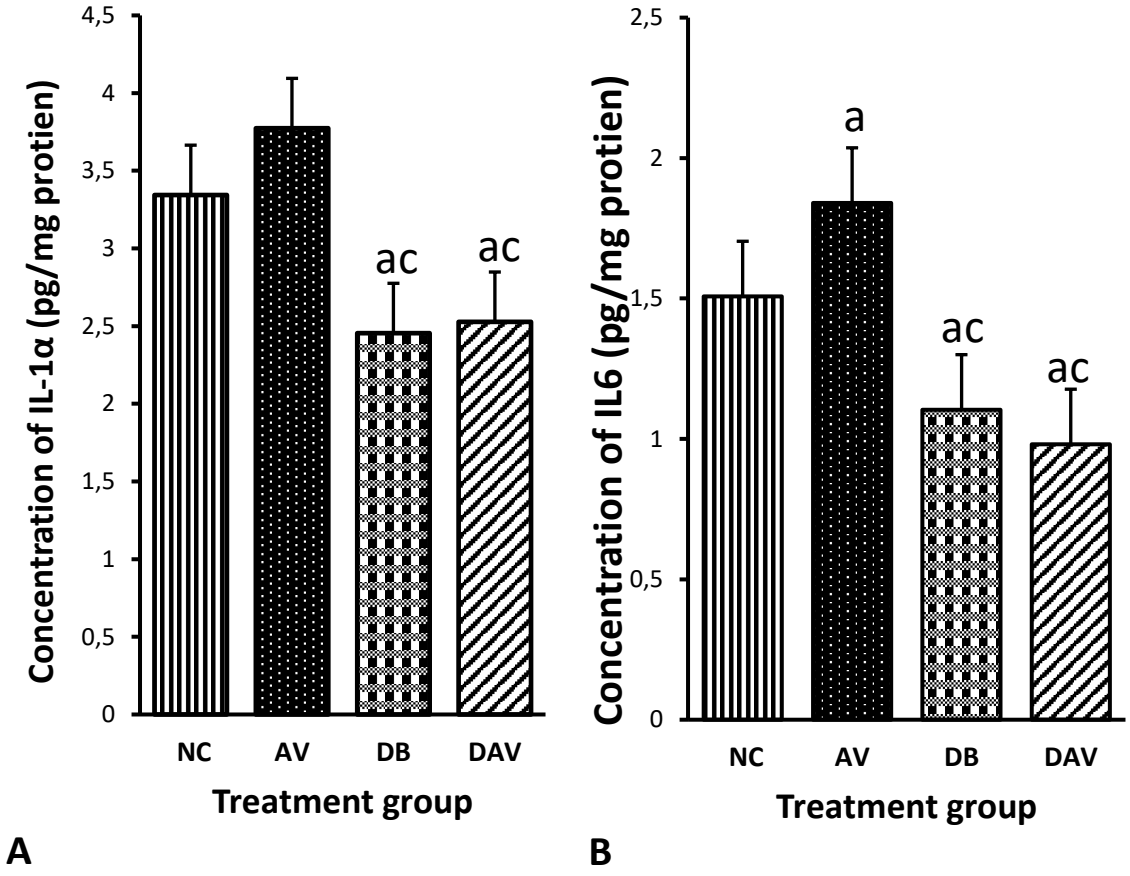

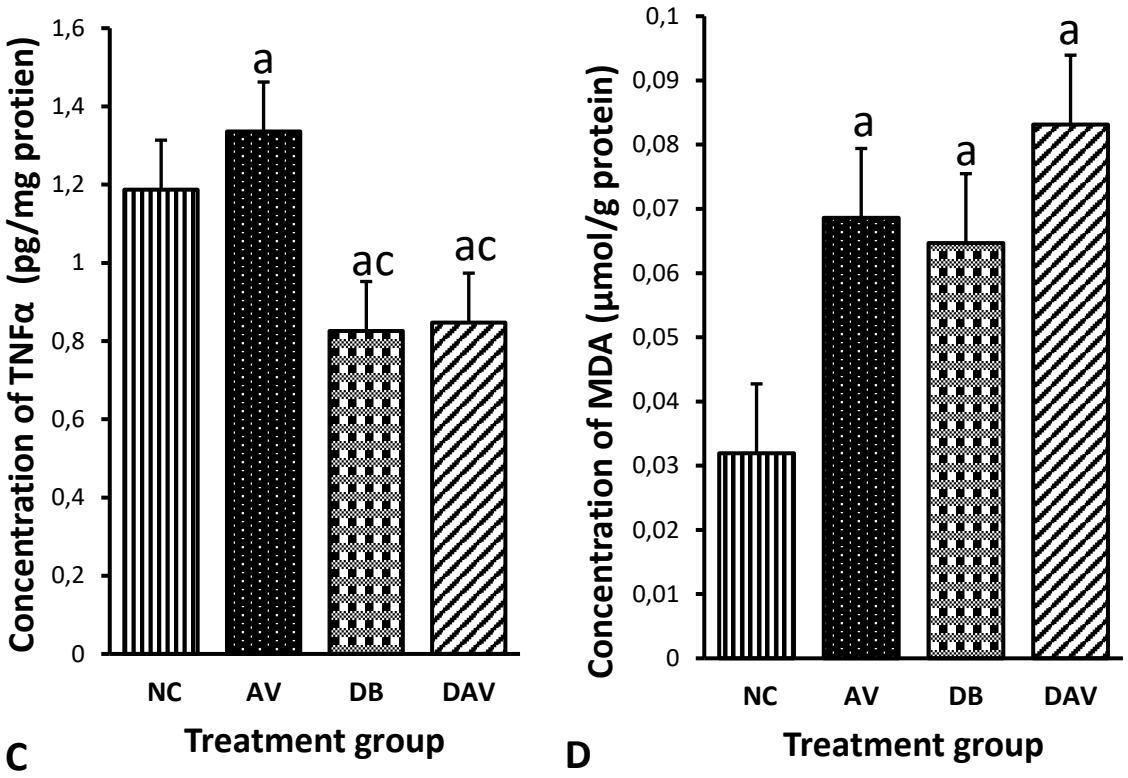

Figure 5. 3. Mean terminal concentrations of IL-1α, IL-6, TNFα, and MDA in hippocampal tissue homogenate. (**A**) Mean concentration of IL-1α. Significant changes in the concentration of cytokines between the groups (one-way ANOVA, $p < 0.0001$). DAV and DB are significantly reduced compared to AV ($p = 0.0001$), and control ($p = 0.007$ and 0.013, respectively). (**B**) Mean concentration of IL-6. Significant changes in the concentration of cytokines between the groups (one-way ANOVA, $p < 0.0001$). DAV and DB are significantly reduces compared to control and AV (p =0.001 and 0.0001, respectively, Bonferroni's post hoc test). AV is significantly increased compared to control ($p = 0.001$). (**C**) Mean concentration of TNFα. Significant changes in the concentration of cytokines between the groups (one-way ANOVA $p < 0.0001$). DAV and DB are significantly reduced compared to control and AV ($p = 0.001$ and 0.0001, respectively, Bonferroni's post hoc test). AV is significantly increased compared to control ($p = 0.043$). (**D**) Mean concentration of MDA in hippocampal tissue homogenate. Significant changes in the concentration of MDA between the groups (one-way ANOVA, $p < 0.0001$) DAV, AV and DB are significantly increased compared to the control ($p = 0.013$, 0.02,9 and 0.001, respectively, Bonferroni's post hoc test), $n = 4$. a' (NC), 'c' (AV), 'e' (DB), 'f' (DAV); indicates significant changes to groups in bracket ( ), P< 0.05. Key: NC, Controls; AV, cART only; DB, Diabetic; DAV, diabetic with cART.

5.3.6. Histopathology of the Hippocampus

5.3.6.1. Number of Neurons in Hippocampal Regions

In the control groups, a wider and densely clustered row of cells can be seen observed in all hippocampal regions (Fig 5.4 – 5.6). In the treated groups (AV, DB, and DAV), a gradual reduction in the neuronal population is observed, especially in the CA3 region of the DAV group, where the neurons appear scanty (Figure 5.5). The mean estimated number of neurons in all regions of the hippocampus of the DAV group was significantly decreased compared to the control (NC) and AV groups (Figures 5.4 – 5.6). The mean neuronal number in the CA1 region of the DB group was significantly decreased in comparison with the mean neuronal number in the NC group ($p = 0.037$). Similarly, the mean neuronal number was significantly reduced in the dentate gyrus of the DB compared to the NC and AV groups ($p = 0.0001$ and 00.034, respectively) and reduced in the AV compared to the NC group ($p = 0.001$) (Figure 5.6).

5.3.6.2. Neuronal Nuclei Area in Hippocampal Regions

The nuclei area of the DB groups is observed to be consistently increased compared to other groups in all hippocampal regions (circles; Figures 5.4 –5.6). While the mean nuclei in the DAV are slightly increased in the CA1 and DG regions but appear apoptotic in the CA3 region, incidentally, the mean neuronal number of the DAV group is also significantly reduced in this region (circles; Figure 5.5). The mean nuclei area of the neurons in all three regions of the hippocampus was significantly increased ($p \leq 0.041$, 0.016, and 0.005) in the DB group compared to the other groups (NC, AV, and DAV), except comparison with the DAV in the DG region (Figures 5.4 –5.6). However, the mean nuclei area of neurons in the DAV significantly decreased compared to the NC group in the CA3 region (Figure 5.6).

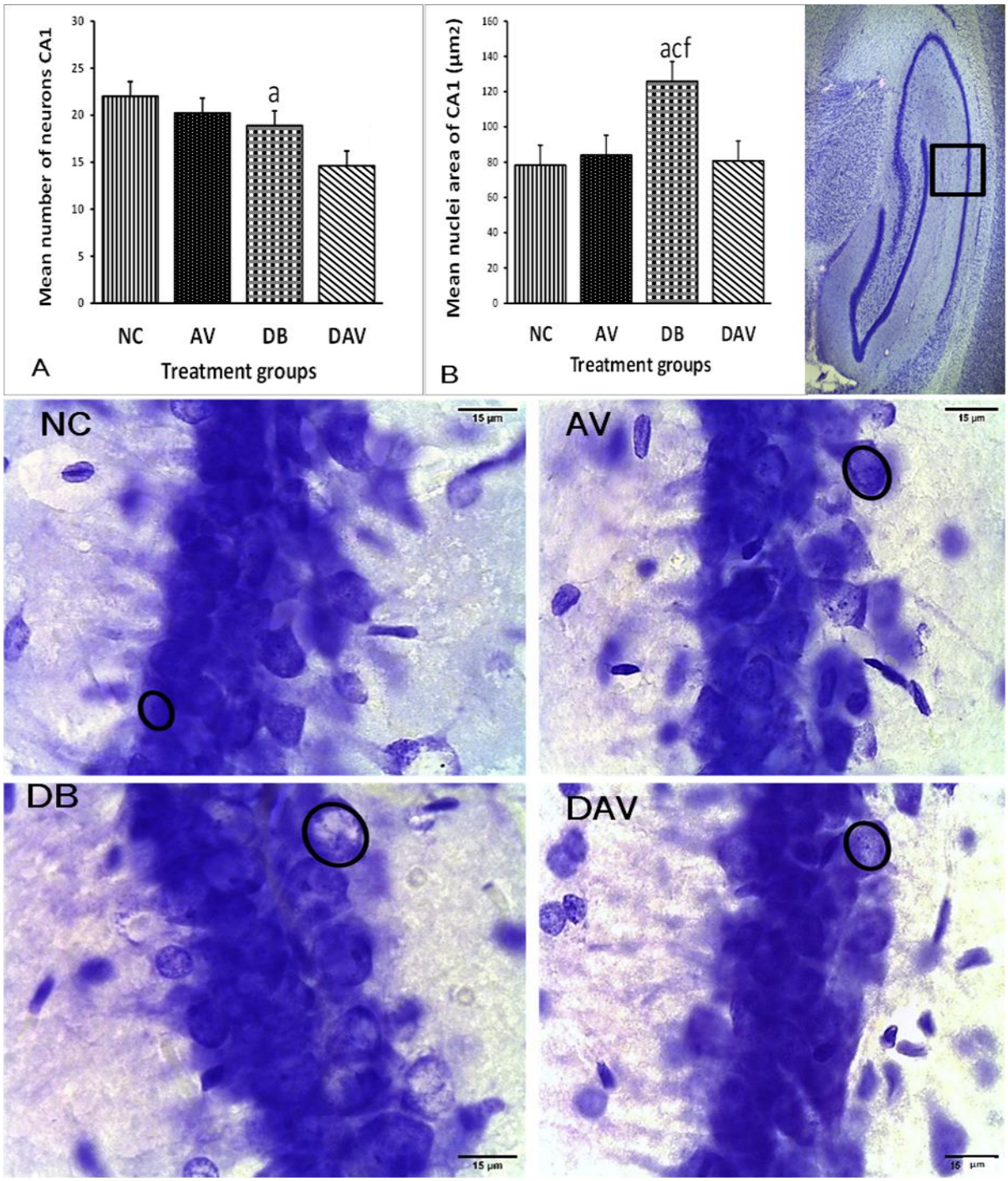

Figure 5. 4. Mean nuclei area and number of neurons in the CA1 region of the dorsal hippocampus. (**A**) Significant changes in mean number of neurons of the CA1 region (Kruskal–Walli's test, $p \leq 0.0001$) DAV is significantly decreased compared to control and AV (p = 0.037 and 0.001, respectively). DB is significantly decreased compared to control (p = 0.001). (**B**) Significant changes in the mean nuclei area between the groups (Kruskal–Walli's test, $p \leq$ 0.005). DB is significantly increased compared to NC, AV and DAV (p = 0.001,0.016 and 0.005, respectively). Circles indicate boundaries of neuronal nuclei, and squares indicate specific regions from which micrographs and measurements were made. Scale bar = 15 µm, n = 6. a' (NC), 'c' (AV), 'e' (DB), 'f' (DAV) ; indicates significant changes to groups in bracket () P< 0.05. Key: NC, Controls; AV, cART only; DB, Diabetic; DAV, diabetic with cART.

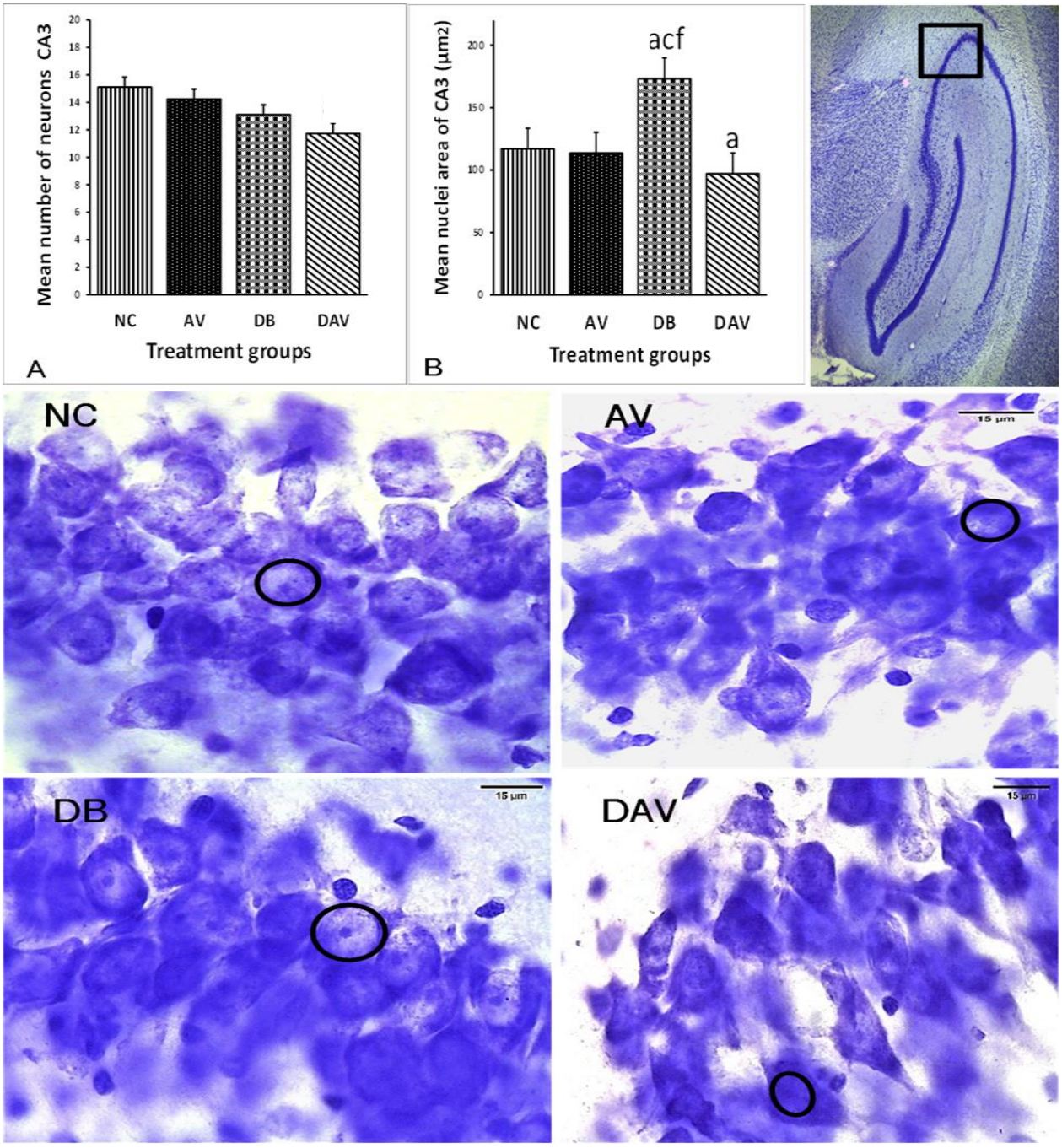

Figure 5. 5. Mean nuclei area and number of neurons in the CA3 region of the dorsal hippocampus. (**A**) Significant changes in the mean number of neurons of the CA3 region (one-way ANOVA test, $p \leq 0.001$). DAV is significantly decreased compared to control and AV ($p = 0.001$ and 0.017, respectively). (**B**) Significant changes in the mean nuclei area in the CA3 region between the groups (Kruskal–Wallis test, $p \leq 0.005$). DB is significantly increased compared to NC, AV and DAV ($p = 0.041$, 0.016 and 0.0001, respectively). DAV is significantly reduced compared to control ($p = 0.045$). Circles indicate boundaries of the neuronal nuclei, and squares indicate the specific area from which micrographs were taken and measurements made. Scale bar = 15 µm, $n = 6$. a' (NC), 'c' (AV), 'e' (DB), 'f' (DAV) ; indicates significant changes to groups in bracket ( ), P< 0.05. Key: NC, Controls; AV, cART only; DB, Diabetic; DAV, diabetic with cART.

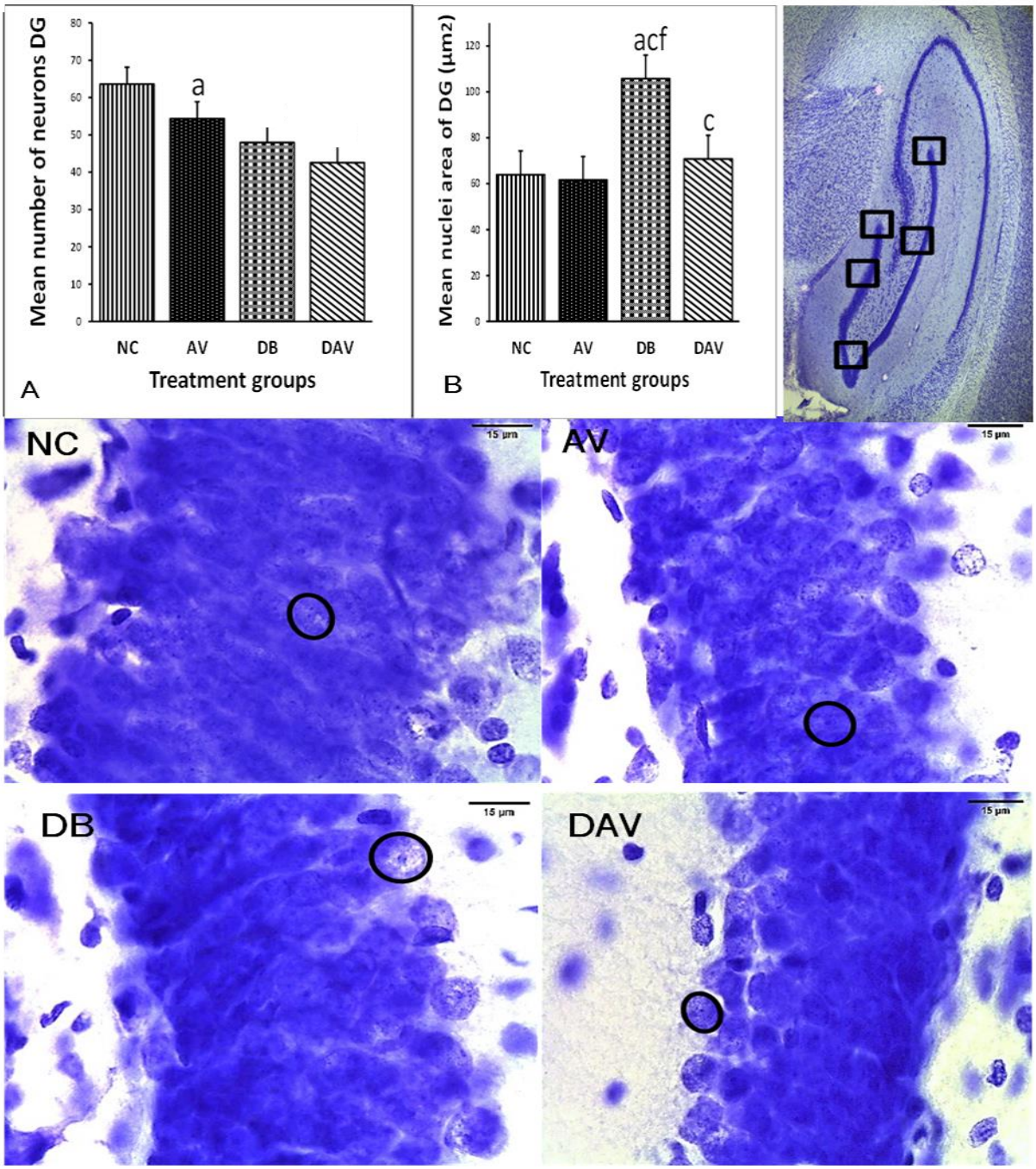

Figure 5. 6. Mean nuclei area and number of neurons in the dentate gyrus region of the dorsal hippocampus. (**A**) Significant changes in the mean number of neurons in the DG region (one-way ANOVA test, $p \leq 0.0001$). DB and DAV are significantly decreased compared to control (P=0.001) and AV (P= 0.001), while AV is reduced compared to NC ($P = 0.01$). (**B**) Significant changes in the mean nuclei area in the DG region between the groups (Kruskal–Walli's test, $p \leq 0.005$). DB is significantly increased compared to NC, AV, and DAV ($p = 0.0002$, 0.0001, and 0.0001, respectively), while DAV is significantly increased compared to AV ($p = 0.045$). Circles indicate boundaries of neuronal nuclei, and squares indicate specific regions from which micrographs were taken and measurements made $n = 6$. Scale bar = 15 µm. a' (NC), 'c' (AV), 'e' (DB), 'f' (DAV) ; indicates significant changes to groups in bracket ( ), P< 0.05. Key: NC, Controls; AV, cART only; DB, Diabetic; DAV, diabetic with cART.

5.3.7. Immunohistochemistry for Neurogenesis in the Hippocampus Double Cortin and Ki67

The number of neurons expressing DCX in the DB and DAV groups was significantly decreased compared to the NC and AV groups ($p = 0.0001$), and the expression of DCX in the DAV was also significantly decreased compared to DB ($p = 0.011$; Figure 5.7A–H, Q). Additionally, a significant reduction was observed in Ki67 expression in the DB and DAV groups compared to the NC group ($p = 0.007$ and 0.0001, respectively), and the DAV was significantly reduced compared to the AV group ($p < 0.051$; Figure 5.7I–P, R). There were no significant differences between the control and AV in both DCX and Ki67 expressions.

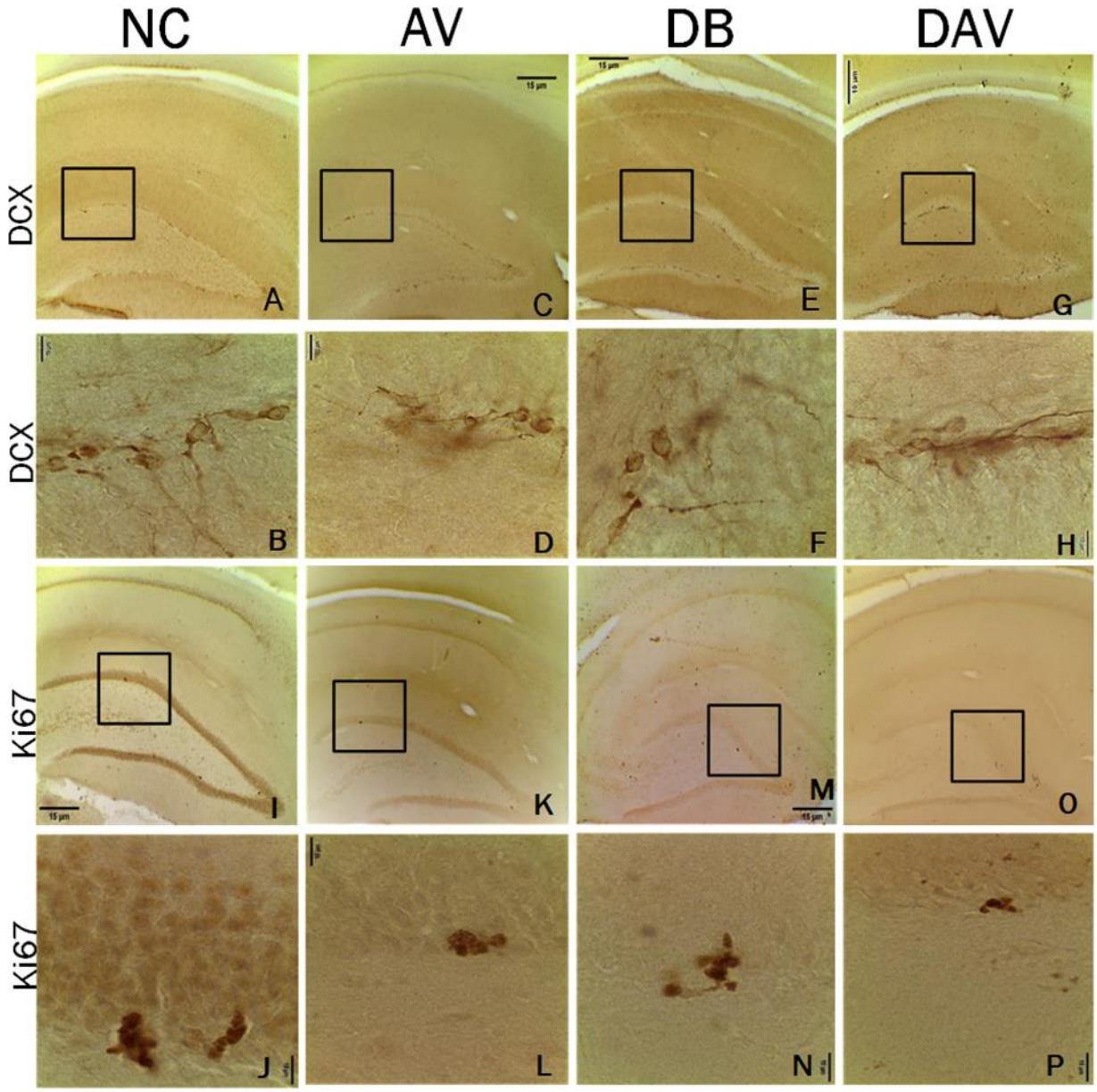
NC
AV
DB
DAV
DCX
DCX
Ki67
Ki67
A
B
C
D
E
F
G
H
I
J
K
L
M
N
O
P

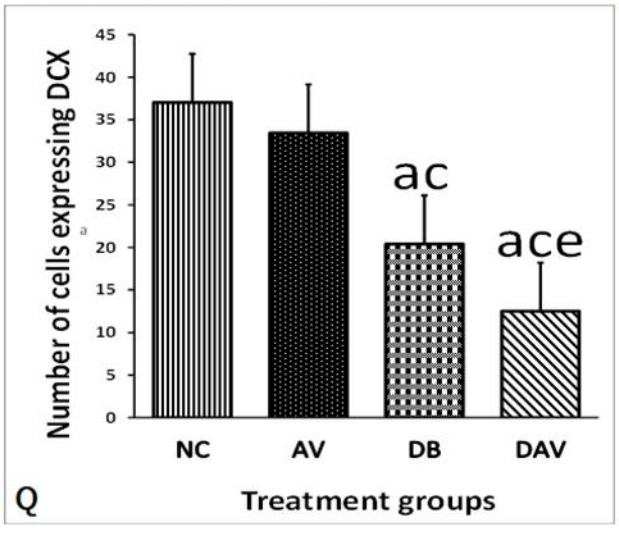
Number of cells expressing DCX
45
40
35
30
25
20
15
10
5
0
ac
ace
NC
AV
DB
DAV
Treatment groups
Q

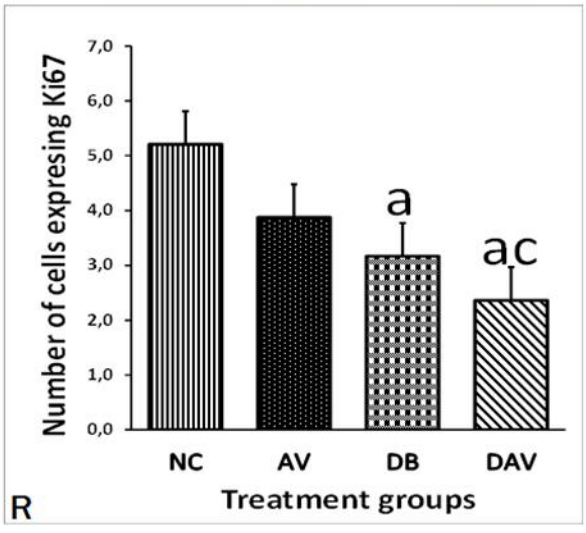
Number of cells expresing Ki67
7,0
6,0
5,0
4,0
3,0
2,0
1,0
0,0
a
ac
NC
AV
DB
DAV
Treatment groups
R

Figure 5. 7. Photomicrograph of the hippocampus showing the expression of DCX in the sub-granular zone of the dentate gyrus region. (**A**, **B**) Expression of DCX in the control, showing numerous clusters of cell bodies and projections expressing DCX. (**C**, **D**) Expression of DCX in the AV group: several small pockets of cells and projections expressing DCX. (**E**, **F**) Expression of DCX in the DB group: few cells and their projections expressing DCX. (**G**, **H**) Expression of DCX in the DAV group: minimal number of cells expressing DCX, most of the DCX expressions were observed in the projections. (**I**–**P**) Expression of Ki67 shows a gradual reduction in Ki67 expression across the groups NC, AV, DB, and DAV, respectively. (**Q**) Significant difference in the expression of DCX between groups (one-way ANOVA, P = 0.0001). DB is significantly reduced compared to control and AV (Bonferroni's post hoc, p = 0.001), while DAV is significantly decreased compared to control, AV, and DB (Bonferroni's post hoc, P = 0.001 and 0.01). (**R**) Significant difference in the expression of Ki67 between the groups (one-way ANOVA, p = 0.0001). DB is significantly decreased compared to control (Bonferroni's post hoc, P = 0.007). DAV is significantly decreased compared to control and AV (Bonferroni's post hoc, P = 0.001 and 0.05). Photomicrographs at ×100; squares indicate the area captured at ×1000 magnification, n = 6. Scale bar = 15 µm. a' (NC), 'c' (AV), 'e' (DB), 'f' (DAV) ; indicates significant changes to groups in bracket ( ), P< 0.05. Key: NC, Controls; AV, cART only; DB, Diabetic; DAV, diabetic with cART.

5.3.8. Correlation of Histomorphology and Neurogenic Parameters

Evaluation of the possible correlations between different parameters showed significant negative correlations between the mean body weight and diabetic parameters (FBG, NFBG, and AUC). Similarly, the mean estimated number of neurons (in CA1NN, CA3NN, and DG) and neurogenic markers (Ki67 and DCX) significantly positively correlated with BW and negatively with FBG, NFBG, and AUC (Table 5.1). Additionally, a significantly positive correlation was observed independently between the mean number of neurons in CA1NN, CA3NN, and DGNN (Table 5.1) and between neuronal nuclei areas in CA1NA, CA3NA, and DGNA (Table 5.2). Furthermore, the DGNA has a strong significant positive correlation with FBG, NFBG, AUC, and the nuclear area (CA1NA and CA3NA) but a significantly negative relationship with BW and neuronal numbers in CA1NN, CA3NN, and DGNN (P = 0.011, 0.032 and 0.011, R = −0.509, −0.439 and −0.510, respectively) and neurogenic markers (Table 5.2).

Table 5. 1. Spearman's rho nonparametric correlation of diabetes parameters with the neuronal number and neurogenic parameters.

	Diabetes Parameters				Neuronal Number			Neurogenic Markers
	BW	**FBG**	**NFBG**	**AUC**	**CA1NN**	**CA3NN**	**DGNN**	**Ki67**
FBG								
P value	0.0001 *							
R-value	−0.613							
NFBG								
P value	0.0001 *	0.0001 *						
R-value	−0.648	0.761						
AUC								
P value	0.0001 *	0.0001 *	0.0001 *					
R-value	−0.723	0.729	0.691					
CA1NN								
P value	0.0001 *	0.0001 *	0.0001 *	0.0001 *				
R-value	0.716	−0.808	−0.706	−0.762				
CA3NN								
P value	0.011 *	0.0001 *	0.002 *	0.004 *	0.0001 *			
R-value	0.508	−0.821	−0.593	−0.563	0.794			
DGNN								
P value	0.001 *	0.0001 *	0.0001 *	0.0001 *	0.0001 *	0.0001 *		
R-value	0.629	−0.900	−0.800	−0.692	0.824	0.794		
KI67								
P value	0.038 *	0.0001 *	0.001 *	0.006 *	0.0001 *	0.001 *	0.0001 *	
R-value	0.426	−0.735	−0.637	−0.546	0.715	0.639	0.758	
DCX								
P value	0.0001 *	0.0001 *	0.0001 *	0.0001 *	0.0001 *	0.0001 *	0.0001 *	0.0001 *
R-value	0.667	−0.882	−0.714	−0.777	0.796	0.745	0.838	0.748

Key: BW; body weight, FBG; fasting blood glucose, NFBG; non-fasting blood glucose, AUC; area under the OGTT curve. Number of neurons at CA1, CA3, and DG (CA1NN, CA3NN, and DGNN, respectively. '*' Significant correlation ($p < 0.05$), R-value; Correlation Coefficient.

Table 5. 2. Spearman's rho nonparametric correlation of diabetes parameters with neuronal nuclei area and neurogenic parameters.

	Diabetes parameters				Neuronal Nuclei Area			Neurogenic Markers
	BW	**FBG**	**NFBG**	**AUC**	**CA1NA**	**CA3NA**	**DGNA**	**Ki67**
CA1NA								
P value	0.101	0.080	0.014 *	0.245				
R-value	−0.343	0.364	0.497	0.247				
CA3NA								
P value	0.680	0.493	0.277	0.698	0.0001 *			
R-value	−0.89	−0.147	0.231	−0.083	0.719			
DGNA								
P value	0.0001 *	0.006 *	0.0001 *	0.012 *	0.0001 *	0.009 *		
R-value	−0.717	0.546	0.706	0.505	0.696	0.520		
KI67								
P value	0.038 *	0.0001 *	0.001 *	0.006 *	0.296	0.526	0.047 *	
R-value	0.426	−0.735	−0.637	−0.546	−0.222	0.136	−0.409	
DCX								
P value	0.0001 *	0.0001 *	0.0001 *	0.0001 *	0.190	0.208	0.035 *	0.0001 *
R-value	0.667	−0.882	−0.714	−0.777	−0.277	0.266	−0.433	0.748

Key: BW; body weight, FBG; fasting blood glucose, NFBG; non-fasting blood glucose, AUC; area under the OGTT curve. Neuronal nuclei area at CA1, CA3, and DG (CA1NA, CA3NA, and DGNA, respectively). '*' Significant correlation ($p < 0.05$), R-value; Correlation Coefficient.

5.4 Discussion

The diabetic brain is susceptible to oxidative damage which has been linked to neuroinflammation and autophagy (Muriach et al., 2014). Obesity, hyperglycaemia, and impaired glucose tolerance (American Diabetes Association, 2007) with an attendant elevation of MDA (Manohar et al., 2013) and proinflammatory cytokines (Alzamil, 2020) have been identified as risk factors in the pathogenesis of type 2 diabetes. Similar effects of significantly elevated body weight, cytokines (IL-1α, IL-6, and TNFα), and MDA levels were observed in the cART-treated animals. However, hyperglycemia and impaired glucose tolerance were not observed in the cART-treated groups (AV) as shown by FBG, NFBG, and AUC levels suggesting the initiation but not the establishment of metabolic perturbation in this group. Significantly elevated FBG, NFBG, AUC, lipid peroxidation levels and weight loss observed in the diabetic groups (DB and DAV) is consistent with a previous report of hyperglycemia,

oxidative stress, and lipodystrophy associated with advanced stages of T2D (Pournaghi et al., 2012b; Association, 2015; Benedé-Ubieto et al., 2020).

Cytokines in the brain may arise from circulatory invasion or are produced by support cells (microglia and astrocytes) and neurons in response to neuroinflammation and neuroprotection triggers (Muhammad, 2019; Salmeron et al., 2019). Also, diabetes is characterized as an inflammatory condition(Donath and Shoelson, 2011) with elevated levels of cytokines often reported in the serum and tissue of T2D patients and animal models (Herrero et al., 2010; Tsalamandris et al., 2019). However, inflammation, oxidative stress, and hyperglycemia together induce perturbation in immunometabolism which impairs the immune system (Daryabor et al., 2020). These immune compromise shown by decreased production of cytokines is severally reported in diabetic patients' immune cells (Martinez et al., 2016; Richard et al., 2017). Therefore, the significantly reduced cytokines (IL-1α, IL-6, and TNFα) levels in the hippocampus of the DB and DAV groups; contrary to previously reported increases (Herrero et al., 2010; Tsalamandris et al., 2019; Alzamil, 2020), may suggest compromised immune response and prolonged diabetes. Furthermore, cytokines are essential for long-term plasticity learning and memory functions (Bourgognon and Cavanagh, 2020), and as such the reduction of cytokines in the DB and DAV groups compared to the control may suggest a compromise in the cognitive and memory processes of the hippocampus. Since cytokine levels were significantly reduced in diabetes and cART treated HIV naïve rat groups, it is possible that diabetic – HIV co-infected patients on chronic cART treatment may be predisposed to greater inflammatory disturbances and therefore require more clinical attention in their diagnosis and management. Additionally, the significantly increased MDA levels in DB and DAV groups suggest that the cellular and functional integrity of the hippocampus will be more susceptible to neurotoxic effects due to cART treatment in diabetes.

Previous reports indicate that cART and diabetes are both independently implicated in hippocampal neurodegeneration (Akang et al., 2019; Madhusudhanan et al., 2020). Our results collaborate these reports with a significant decrease in the number of neurons in the AV group (in DG region), DB group (in CA1 and DG regions), and in all hippocampal regions in the DAV group (i.e., CA1, DG, and CA3). Additionally, the nuclei area of the DAV is significantly reduced compared to the control. This indicates that cART treatment in diabetes exacerbated and extended hippocampal neuronal decline into the CA3 region, which is not affected by either cART or diabetes alone. The decline in DG and CA3 neurons will adversely affect the associated functions in cognition, pattern separation, episodic memory, and pattern completion as has been previously reported (Scharfman and Myers, 2016). This is because, CA3 neurons play a crucial role in memory processes with recurrent internal and wide-ranging connectivity (Miles et al., 2014; Cherubini and Miles, 2015) to other hippocampal regions and cortices. Therefore, the reduction in CA3 neuron density and nuclei area in the DAV group may imply a reduction in the connectivity of this region within the hippocampus and may result in adverse functional defects.

The sub-granular zone of the hippocampal dentate gyrus is one of the established zones in the brain for adult hippocampal neurogenesis. The significantly decreased expression of DCX and Ki67 in diabetic (DB) and cART-treated diabetic animal (DAV) groups infer that the proliferation of hippocampal stem cells as well as migrating immature neurons was significantly impaired. Such compromised stem cell generation and migration may diminish the hippocampal potential to recover from inherent apoptotic processes. Interestingly, the number of neurons at different hippocampal regions is positively and significantly correlated with Ki67 and DCX expressions and negatively with FBG, NFBG, and AUC which is consistent with reports of persistent decline in adolescent hippocampal neurogenesis due to increased cell death of immature differentiating neurons (Broadwater et al., 2014). This also

suggests that elevated levels of diabetes parameters may exacerbate the loss of hippocampal neurons and induce a decline in neurogenesis. Additionally, the DG nuclei area positive correlation with diabetic parameters (FBG, NFBG, and AUC) and mean nuclei areas of CA1, and CA3 regions but an inverse correlation with neuronal density (in all regions of the hippocampus) and neurogenic parameters (Ki67 and DCX) may indicate a possible central functional role associated with the DG nuclei. Furthermore, the significant increase in neuronal nuclei area and a significant reduction in mean neuronal number in the DB group observed in all hippocampal regions may be due to necrosis which is morphologically characterized by cell and nuclear swelling in the initial stages of cell death (Elmore, 2007; Kwon et al., 2015).

In summary, our results indicate that cART therapy in the diabetic condition elevates lipid peroxidation but reduces body weight, pro-inflammatory cytokines, neuronal density (CA1, CA3, and DG), the proliferation of new cells, and migration of immature neurons in the dentate gyrus with likely adverse implications in hippocampal overall function. Also, cART treatment in diabetes may induce heightened oxidative stress and may worsen the previously reported CNS infections, memory, and cognitive loss involving diabetes or cART independently. The clinical implication of these findings (though in the HIV naïve rat model) hinges on the chronic cART regimen amongst diabetes patients with HIV infection and therefore calls for caution in clinical diagnosis and management of these groups of patients.

CHAPTER 6 Immunohistochemical and Molecular Evaluation of Alcohol toxicity on Diabetic Sprague Dawley Rat Hippocampus

6.0 Abstract

Diabetes affects the central nervous system through biochemical and microstructural perturbations with attendant hippocampal deficits. These diabetes-induced conditions are further burdened by the lifestyle factors such as alcohol use and abuse. Therefore, this study investigated the effects of sub-chronic alcohol consumption in type 2 diabetes on hippocampal oxidative stress, histomorphology, neurogenesis, and the expression of genes involved in insulin resistance, apoptosis, and junctional barriers in the hippocampus. Four groups of male Sprague Dawley rats of six rats each were treated as follows; NC (untreated groups), AL (normal rats treated with 10% v/v ethanol in distilled water ad libitum, DB (diabetic rats), and DAL (diabetic rats treated with 10% v/v ethanol). After ninety days of treatment, the rats were terminated, and brains were excised for immunoassay of oxidative stress (MDA and GPx), qPCR analysis of blood-brain barrier (BBB) junction proteins (claudin-5 and occludin), apoptotic gene (BAX, Bcl2, and Caspase-3) and insulin receptor (INSR and IRS) gene expression; in addition to histological and immunohistochemical (DCX and Ki67) analysis. Our results show that alcohol alone (AL), significantly elevates oxidative stress, but reduces IRS gene expression, hippocampal neurons (at CA1 and DG regions), Ki67, and DCX expression. Similarly, DB and DAL significantly increased oxidative stress, with upregulation of Caspase-3, Bcl2, and BAX; however, IRS1 is upregulated in DAL, while INSR, IRS1, claudin-5, and occludin are downregulated in DB only. Additionally, the expression of Ki67, DCX, and mean the number of hippocampal neurons was significantly decreased in DB (in CA1 and DG regions) and DAL (CA1, CA3, and DG regions). These results indicate that IRS1 and Bcl2 mediated anti-apoptosis initiated in DAL is unable to mitigate the effects of significantly elevated oxidative stress, BAX, and Caspase-3 cumulating in hippocampal

neurodegeneration. Furthermore, diabetes-induced hippocampal and neurogenic deficiencies are associated with BBB disruption, while alcohol consumption in combination with diabetes exacerbates hippocampal atrophy into the CA3 region with minimal BBB disruption, blood glucose, and glucose tolerance, and insulin resistance compared to diabetes alone.

6.1 Introduction

Reports indicate that an unhealthy diet and physical inactivity commonly lead to chronic conditions such as obesity, cardiovascular diseases, and diabetes ((Budreviciute et al., 2020; Li and Sun, 2022). The prevalence of diabetes is rapidly increasing in South Africa (3-28%) and globally (5.4 %) prevalence of type 2 diabetes (T2D) (Guariguata et al., 2014; Pheiffer et al., 2018). Similarly, South Africa is reported as the leading alcohol-consuming country in Africa and globally (Vellios and Van Walbeek, 2018). Clinically, some studies have identified that chronic and heavy alcohol use may aggravate or act as an independent risk factor for T2D (Wannamethee et al., 2002; Jung et al., 2011; Kim and Kim, 2012) suggesting a prevalent concomitant presence of alcohol use and T2D in one individual.

Independently, aldehyde metabolism in alcohol use and hyperglycaemia in T2D induce oxidative stress, with several attendant neurological conditions. Additionally, T2D factors (Salameh et al., 2016) and alcohol abuse (Haorah et al., 2007) can independently penetrate the CNS, or impair endothelial cells' tight junctions (claudins and occludin), leading to neuronal damage and consequently dysfunction. Furthermore, T2D and alcohol-induced oxidative stress activate several intracellular pathways that induce neurodegenerative processes such as neuronal apoptosis (Flora et al., 2012; Muriach et al., 2014; Sadeghi et al., 2016) and impaired neurogenesis (He et al., 2005; Bonds et al., 2020). Though reports exist on the independent adverse effects of T2D and alcohol on the CNS and hippocampus (Barcia et al., 2015; Milne et al., 2017; Zahr et al., 2019), reports on the effects of alcohol on diabetes have focused mostly

on cognitive parameters (Yen et al., 2022), pathologies of peripheral organs (Emanuele et al., 1998), and serum biochemical effects on insulin modulators in animal studies (Jung et al., 2011; Kim et al., 2013). However, the specific histopathological, molecular, and neurogenic effects in the hippocampus associated with the concomitant presence of alcohol (due to abuse) in diabetes need to be investigated and documented. Such data will be invaluable clinically.

The hippocampus is a pivotal and sensitive region in the central nervous system which is dependent on adequate insulin and glucose metabolism for its memory learning, and cognitive and executive function processes (Anand and Dhikav, 2012; Soto et al., 2019). Hippocampal neurons have abundant glucose receptors which are dependent on adequate signaling from intracellular insulin receptor substrate (IRS) and membrane-bound insulin receptors (INSR) to which insulin molecules bind for hippocampus-dependent memory, plasticity, and neurogenic function (Zhao et al., 1999; Huang et al., 2010; Spinelli et al., 2019). Additionally, T2D is severally reported to induce neuronal insulin resistance; while the amount of alcohol consumed (moderate, binge, or chronic) may improve, suppress, or inhibit insulin action respectively (Lindtner et al., 2013; Jang et al., 2019). Furthermore, the hippocampus is often profiled and studied for its involvement in neuropsychological conditions which may adversely affect the quality of life (Wicking et al., 2014; Vogel and Schwabe, 2016). Therefore, documenting the molecular and attendant structural, immunohistochemical, and histopathological implications that may arise in the hippocampus with concomitant alcohol use in diabetes will give crucial insight into the underlying neurostructural damages and the resultant hippocampal functional deficiencies and necessarily validate the neurophysiological reports.

6.2. Materials and methods

6.2.1 Chemicals

Oxidative stress markers were assessed using malondialdehyde (MDA) Colorimetric assay kit: TBA method (Elabscience, Houston, Texas USA; E-BC-K025-M), and Glutathione Peroxidase (GSH-Px) Activity Assay Kit (Elabscience, Houston, Texas USA; E-BC-K096-M WST-1 Method). For PCR, TRIzol reagent (Merck; T9424), iso-propanol (Merck; B6916), cDNA using a high-capacity cDNA RT kit (Applied Biosystems; 4368814), Power Up SYBER Green Master Mix (Applied Biosystems; A25742; Austin, Texas, USA), Forward and Reverse Primer were procured from Inquaba Biotechnical industries (Hatfield, Pretoria, South Africa), as previously described in chapter 3.

6.2.2 Animals & housing

Twenty-four adult male rats were housed separately under clean conditions in cages. For the duration of the experiment, the rats had free access to drinking water or alcohol and rat chow according to their allocated group treatment. Weekly, monthly, and total water or alcohol and normal rat chow consumed in treated and untreated animals were recorded as previously described in chapter 3.

6.2.3 Experimental design

The rats were divided into four groups of six rats each including, nontreated controls (NC), 10% alcohol in distilled water v/v *ad libitum* treated rats (AL), diabetic with no treatment (DB), and diabetic alcohol treated (DAL). Alcohol treatments continued for ninety days after which the rats were terminated, the hearts were perfused with 2ml/min 0.1M phosphate buffer (PB) in 0.9% saline, and the whole brain was immediately harvested and separated into hemispheres. One hemisphere was fixed in 0.4 paraformaldehyde for histology and the other hemisphere was stored at -80°C for immunoassay and molecular analysis.

6.2.4 Enzyme-linked immunoassay of oxidative stress markers (GPx, and MDA)

Dissected brain samples were homogenized using a handheld tissue grinder G-50 (Coyote Bioscience, Jiangsu, China) in 0.01MPBS (pH 7.4) and used to run an enzyme-linked immunosorbent assay using malondialdehyde (MDA) Colorimetric assay kit: TBA method (Elabscience, Houston, Texas USA; E-BC-K025-M), and Glutathione Peroxidase (GSH-Px) Activity Assay Kit (Elabscience, Houston, Texas USA; E-BC-K096-M WST-1 Method). All samples were diluted 1:2, all standards, and run-in duplicates. The OD was read at 620nm using an Anthos 2010, 96 well plate reader coupled to an ADAP software. OriginPro software was used to calculate the concentration of GP_X and MDA in the samples from obtained OD values according to the manufacturer's directions.

6.2.5 Quantitative qPCR for junctional proteins, insulin receptors, and apoptosis gene expression

From each brain sample, total RNA was extracted and used in a reverse transcriptase reaction to synthesize cDNA, and expression levels of BAX, BCL, CLDN5, CASP3, INSR, IRS, and OCLDN in samples were measured using a Quant studio1 96 well plate detection system as outlined in chapter 3.

6.2.6 Histology and immunohistochemistry

Each brain hemisphere per animal was sectioned in the sagittal plane using a frozen cryostat at 50 µm. One series of sections were stained with cresyl violet, and the next two series of sections were used for immunohistochemical labelling of Ki67 and DCX, respectively. From each brain, six sections were selected for histology and immunohistochemistry. As previously described in chapter 3.

6.2.7 Statistical analysis

The diabetes parameters, number of neurons in hippocampal regions, concentrations of oxidative markers, expression of hippocampal Ki67 and DCX labelling as well as gene expression levels of insulin receptors, junctional and apoptotic markers were recorded as mean ± SEM, data was analysed as described in chapter 3.

6.3 Results

6.3.1 Food and fluid consumption

All the treated groups consumed lower amounts of food compared to the control. Though the AL and DAL groups consumed the lowest amounts of food, there was no significant difference in food consumption between the groups (Fig. 6.1A; ANOVA, $P< 0.05$). The DB group consumed a significantly higher amount of fluid compared to the control, AL, and DAL groups (Fig. 6.1B).

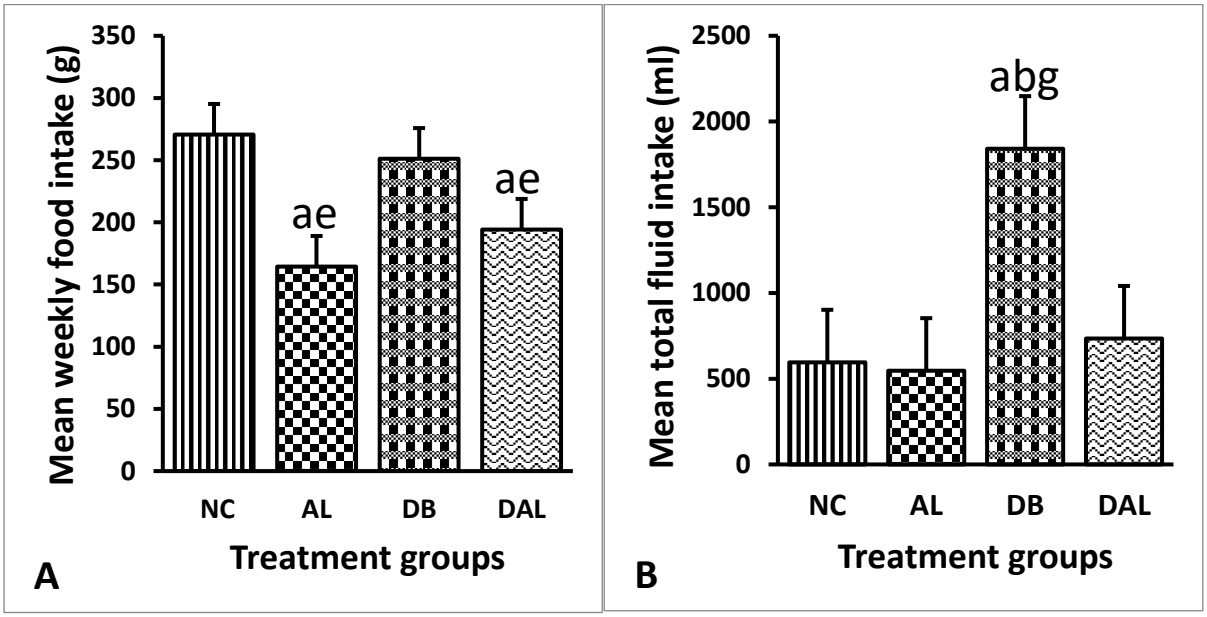

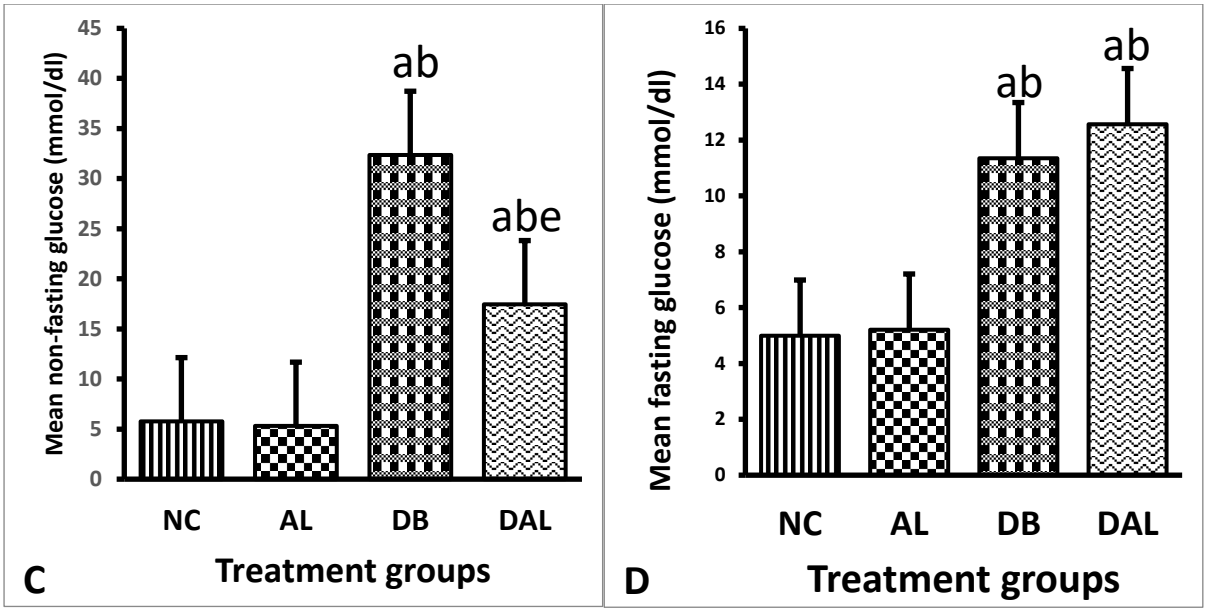

Figure 6. 1. Mean food intake, fluid consumption, fasting, and non-fasting blood glucose levels. Significant difference in mean food and water intake, NFBG, and FBG between groups (Kruskal Wallis test, P = 0.002, 0.003, 0.001, and 0.001 respectively). **A)** AL and DAL are significantly decreased respectively compared to NC (P= 0.012 and 0.001) and DB (P= 0.041 and 0.05). **B)** DB is significantly increased compared to NC, AL, and DAL (P = 0.004, 0.001, and 0.022 respectively, Dunn's pairwise test). **C)** DB is significantly increased compared to AL and control (NC) (P =0.0001 and 0.002), while DAL is significantly increased compared to control (NC) and AL (P = 0.001) and decreased compared to DB (P =0.001). **D)** DB and DAL are significantly increased compared to NC (P = 0.003 and 0.001 respectively) and AL (P =0.019 and 0.005 respectively). *n*= 6, a' (NC), 'b' (AL), 'e' (DB), 'g' (DAL); indicates significant changes to groups in bracket ( ), P< 0.05. Key: NC, Controls; AL, alcohol only; DB, Diabetic; DAL, diabetic and alcohol.

6.3.2 Mean blood glucose levels

The mean non-fasting glycaemic levels for the experimental groups are presented in figure 6.1C. The diabetic rat (DB and DAL) groups maintained consistent high mean hyperglycaemic (NFBG) levels compared to the control (NC) and AL group. The mean FBG levels in DB and DAL groups were significantly increased in comparison to AL and NC groups respectively (Fig. 6.1D).

6.3.3 Mean oral glucose tolerance levels

The mean oral glucose tolerance test showed optimal glucose handling in the NC group followed by the AL group but poor glucose handling in the DB and DAL groups (Fig. 6.2). In the first month of treatment, the DAL group showed the highest AUC but drops to the second

highest in the second month and finally with AUC level significantly lower than the DB in the third month of treatment. For all three months of the experiment, the AUC was significantly increased in the DB and DAL groups compared to NC and AL groups. No significant differences were observed between NC and AL groups (Fig. 6.2).

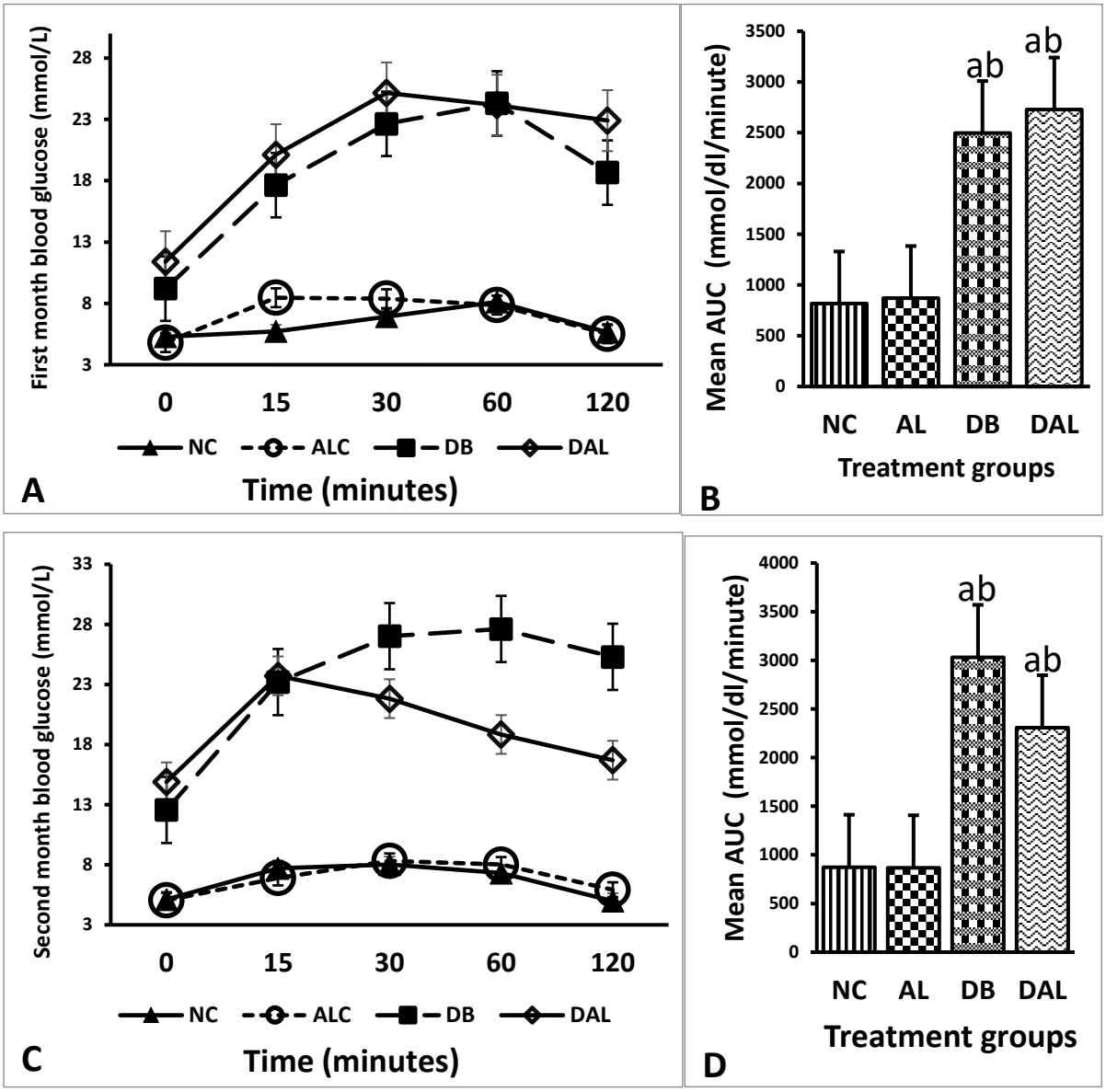

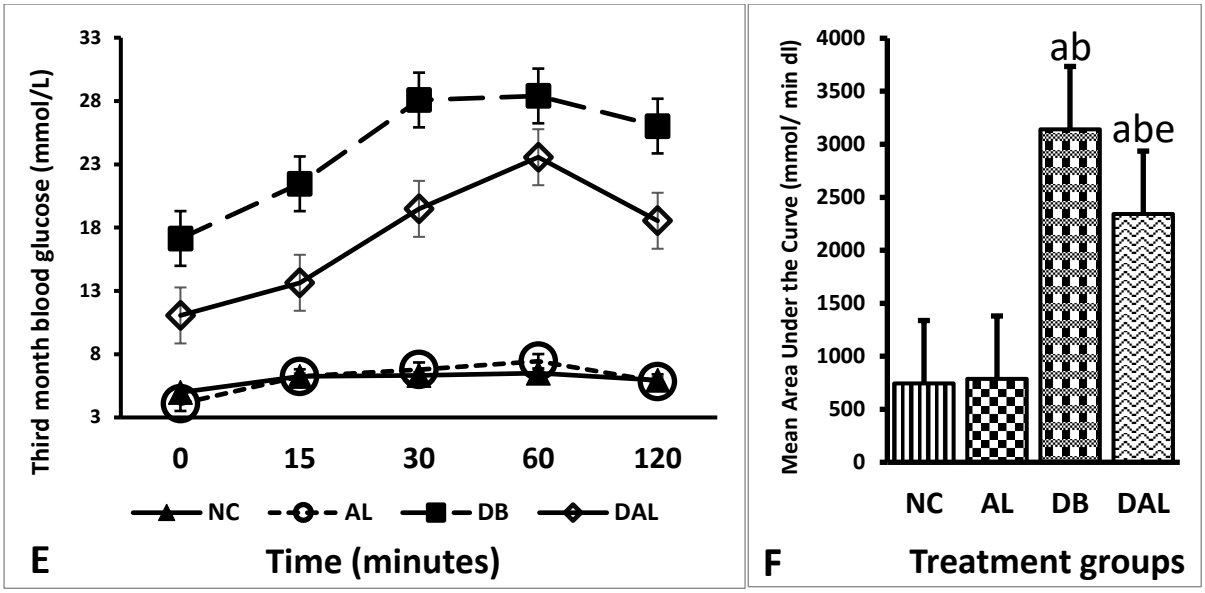

Figure 6. 2. Mean monthly oral glucose tolerance test (OGTT) and area under the curve (AUC). **A, C, E).** Mean OGTT levels in the first, second, and third months of the experiment. Significant difference in mean area under the OGTT curve across groups in the first second and third months of the experiment (Kruskal Wallis test, P =0.001). **B)** DB and DAL are significantly increased compared to AL and NC (P=0.001, Dunn's pairwise test). **D)** DB and DAL are significantly increased compared to AL (P =0.001 and 0.006) and NC (P=0.001 and 0.006) respectively (Dunn's pairwise test). **E)** DB is significantly increased compared to AL and NC (P=0.001 in all respectively, Dunn's pairwise test), but DAL significantly increased compared to AL and NC (P= 0.001) but decreased compared to DB (P= 0.022). Further analysis of repeated measures ANOVA across the AUC in three months reveal a significant increase in DB and DAL compared to control and AL (P=0.001). a' (NC), 'b' (AL), 'e' (DB), 'g' (DAL); indicates significant changes to groups in bracket ( ), P< 0.05. n= 6, Key: NC, Controls; AL, alcohol only; DB, Diabetic; DAL, diabetic and alcohol.

6.3.4 Oxidative stress markers

The malondialdehyde (MDA) levels significantly increased, while the GPx levels were significantly reduced in the AL, DB, and DAL compared to the control (NC) (P= 0.001 respectively; Fig. 6.3A and 6.3B). But no significant difference in MDA and GPX was observed between DB and DAL (Fig. 6.3A-B). Additionally, the GPX levels in the DB and DAL were significantly reduced compared to AL (P= 0.043 and 0.01 respectively).

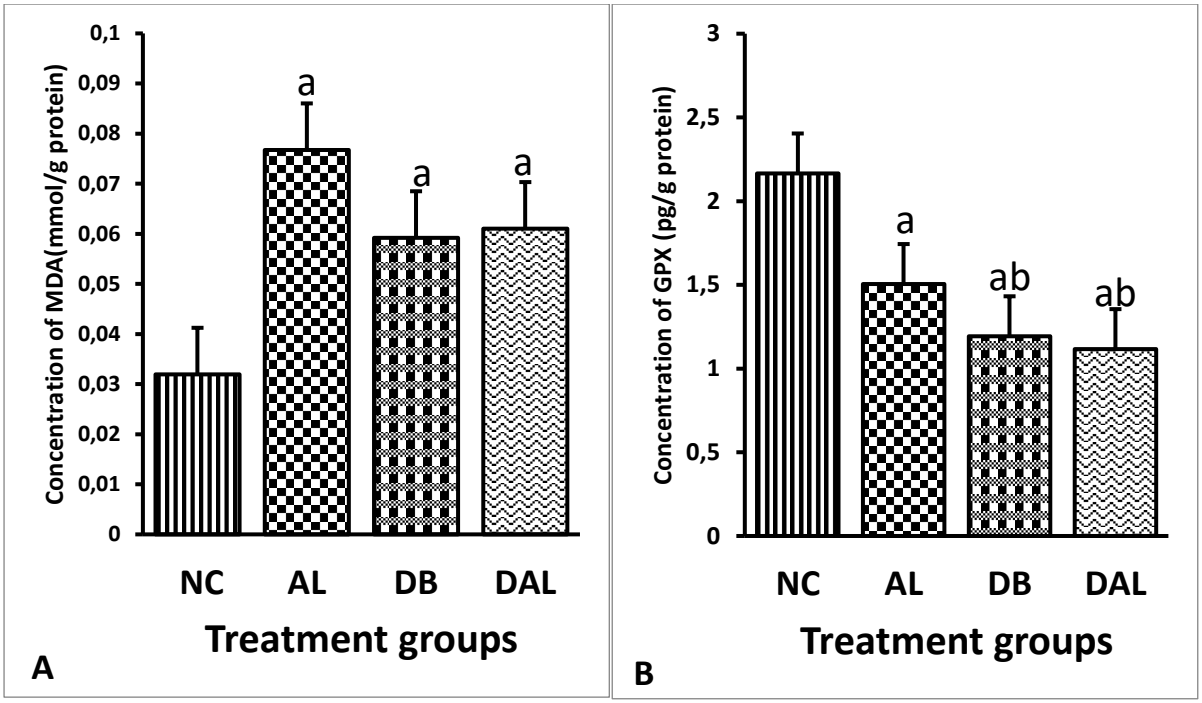

Figure 6. 3. Mean concentrations of MDA and GPX in hippocampal tissue homogenate. **A)** Significant changes in concentration of MDA between the groups (One-way ANOVA, P=0.001) AL, DB and DAL are significantly increased compared to control (NC) (P= 0.001 respectively, Bonferroni post hoc test). **B)** Significant changes in concentration of GPX between the groups (One-way ANOVA, P=0.001). AL is significantly decreased compared to control (NC) (P= 0.001 respectively, Bonferroni post hoc test). DB and DAL are significantly decreased compared to control (P= 0.001) and AL (P= 0.043 and 0.01 respectively, Bonferroni post hoc test). a' (NC), 'b' (AL), 'e' (DB), 'g' (DAL); indicates significant changes to groups in bracket ( ), P< 0.05. n= 4, Key: NC, Controls; AL, alcohol only; DB, Diabetic; DAL, diabetic and alcohol.

6.3.5 Expression of apoptotic markers RT qPCR

The results of BCL_2 BAX and Caspase-3 are shown in figure 6.4. The BCL_2 gene is upregulated in AL treatment but significantly in DB and DAL groups compared to the control group (NC). It was observed that alcohol (AL) and diabetes (DB) independently and non-significantly upregulated pro-apoptotic gene (BAX), while DAL significantly upregulated BAX expression. Furthermore, diabetes (DB) and alcohol treatment in diabetes (DAL) significantly upregulated Caspase-3 in comparison with the control group (Fig 6.4)

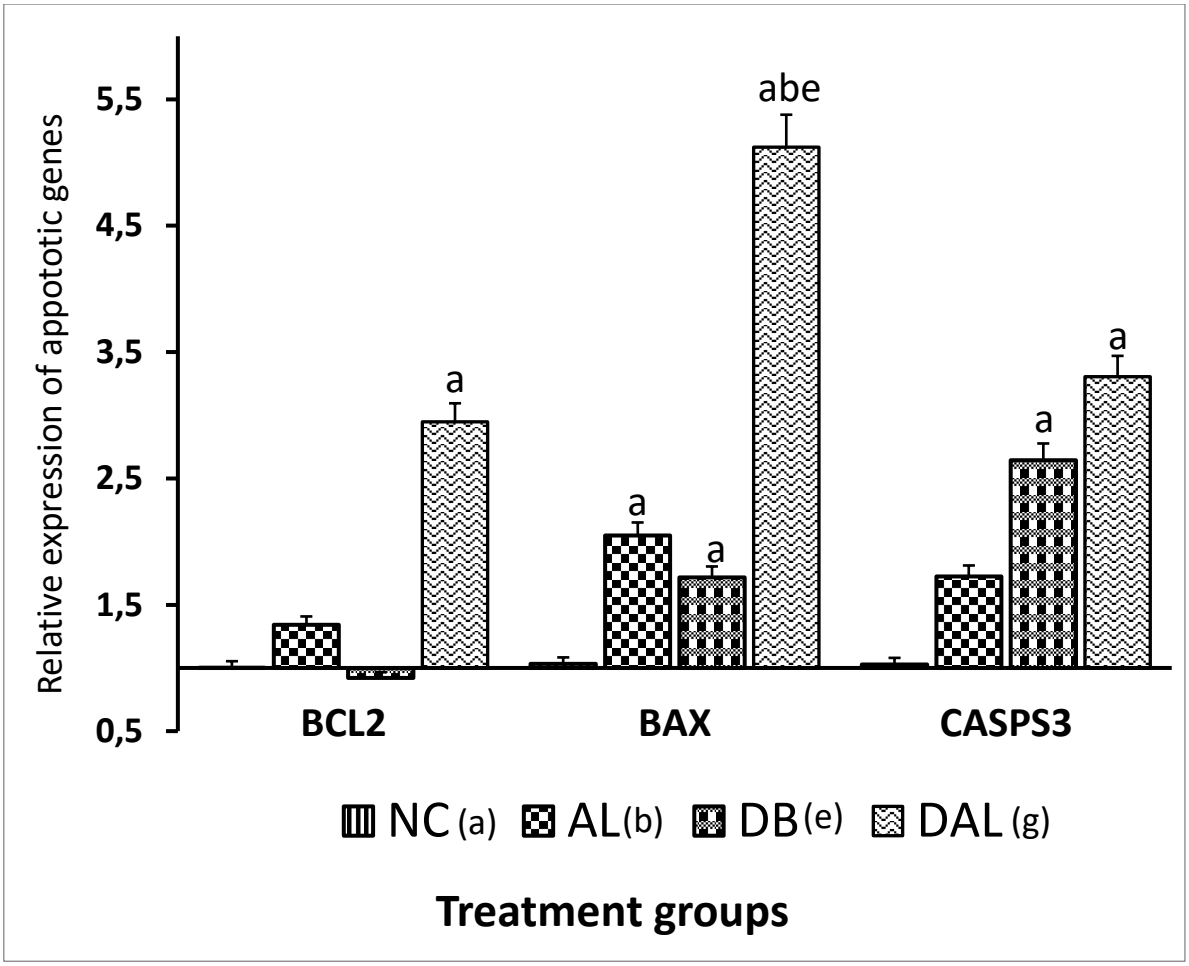

Figure 6. 4. Mean relative expression of apoptotic genes in the hippocampal homogenate. Significant changes in Bcl_2 (Kruskal Wallis, P =0.023), BAX, and Caspase-3 expression between the groups (One Way ANOVA, P= 0.05). For Bcl_2, DAL is significantly upregulated compared to control (Pairwise Post Hoc, P= 0.0024). For BAX, AL, DB and DAL are significantly upregulated compared to control, (Pairwise Post Hoc, P = 0.03, 0.05, and 0.001 respectively). For Caspase-3, DB and DAL, are significantly upregulated compared to control (Pairwise Post Hoc, Bcl_2: P =0.042 and 0.03). a' (NC), 'b' (AL), 'e' (DB), 'g' (DAL); indicates significant changes to groups in bracket ( ), P< 0.05. Columns represent the mean and standard error of biological replicates. Key: NC, Controls; AL, alcohol only; DB, Diabetic; DAL, diabetic and alcohol.

6.3.6 Expression of BBB junctional proteins (claudin-5 and occludin)

The results of the evaluation of the effects of the treatment on the BBB structural integrity through the analysis of two junctional proteins (claudin-5and occludin) are shown in figure 6.5. These BBB junctional proteins claudin-5 and occludin were downregulated in all the

experimental groups (AL, DB, and DAL) with significant down-regulation only in the DB group compared to the control (Fig. 6.5 A-B).

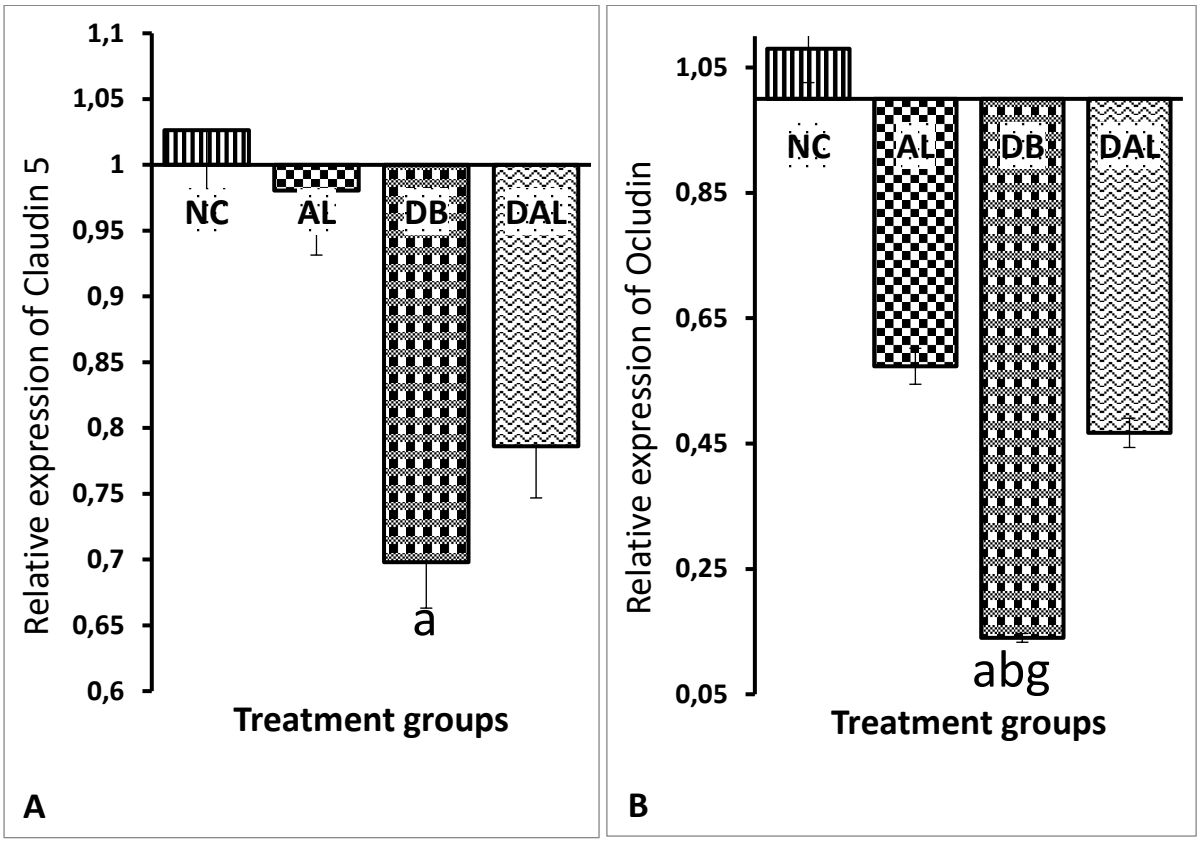

Figure 6. 5. Mean relative expression levels of membrane junctional proteins in the hippocampal homogenate. **A and B)** Significant changes in claudin-5 and occludin expressions (Kruskal Wallis, P =0.05 and 0.043 respectively). In claudin-5 and occludin, DB is significantly downregulated compared to the control (Bonferroni Pairwise test, P = 0.05 and 0.005 respectively). a' (NC), 'b' (AL), 'e' (DB), 'g' (DAL); indicates significant changes to groups in bracket ( ), P< 0.05. Columns represent the mean and standard error of biological replicates. Key: NC, Controls; AL, alcohol only; DB, Diabetic; DAL, diabetic and alcohol.

6.3.7 Expression of insulin receptors and insulin receptor substrate (INSR and IRS1)

The expression of insulin receptor genes (INSR and IRS1) differs across experimental groups as shown in figure 6.6. The gene expression of INSR was significantly downregulated in the DB compared to the control, AL, and DAL groups, while the IRS1 levels were downregulated in the AL and DB groups but upregulated in the DAL group compared to the control.

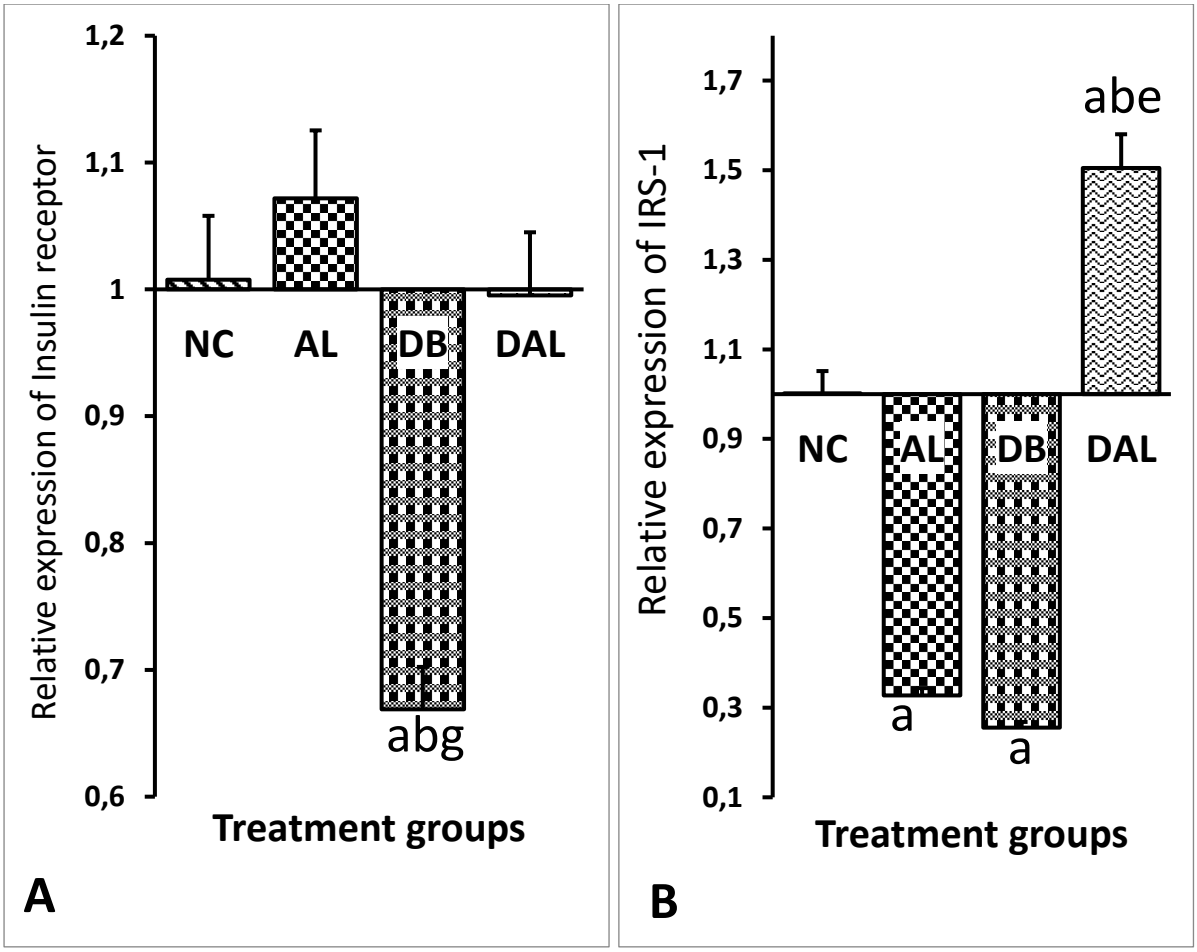

Figure 6. 6. Mean levels of insulin receptors (INSR and IRS) in the hippocampal homogenate. Significant changes in INSR and IRS mRNA levels (Kruskal Wallis, P =0.05 and 0.024 respectively). **A)** DB is significantly downregulated compared to the control AL and DAL (Dunn's Pairwise test, P = 0.020, 0.028, and 0.016 respectively). **B)** AL and DB are significantly downregulated relative to control (P= 0.008 and 0.001 respectively), while DAL is significantly upregulated compared to the control, AL, and DAL (Dunn's Pairwise test, P = 0.028, 0.028, and 0.004 respectively). a' (NC), 'b' (AL), 'e' (DB), 'g' (DAL); indicates significant changes to groups in bracket ( ), P< 0.05. Key: NC, Controls; AL, alcohol only; DB, Diabetic; DAL, diabetic and alcohol.

6.3.8 Mean number of neurons in hippocampal regions

The neuronal number count in all regions of the hippocampus was carried out and the results are shown in figure 6.7. The mean estimated number of neurons in all three regions of the hippocampus (CA1, CA3 and DG) of the DAL treated groups were significantly decreased compared to control (NC) (P<0.05). Additionally, the mean number of neurons in the CA1 and DG of the AL and DB groups was significantly decreased compared to the control group (P= 0.05, Fig 6.7). The neurons (circles; Fig 6.8) were observed as a tightly packed layer in the

control with few glial cells (arrows) but appeared dispersed in the experimental groups, especially in the DAL group which appears eroded with glial cells (arrows) in the DG region.

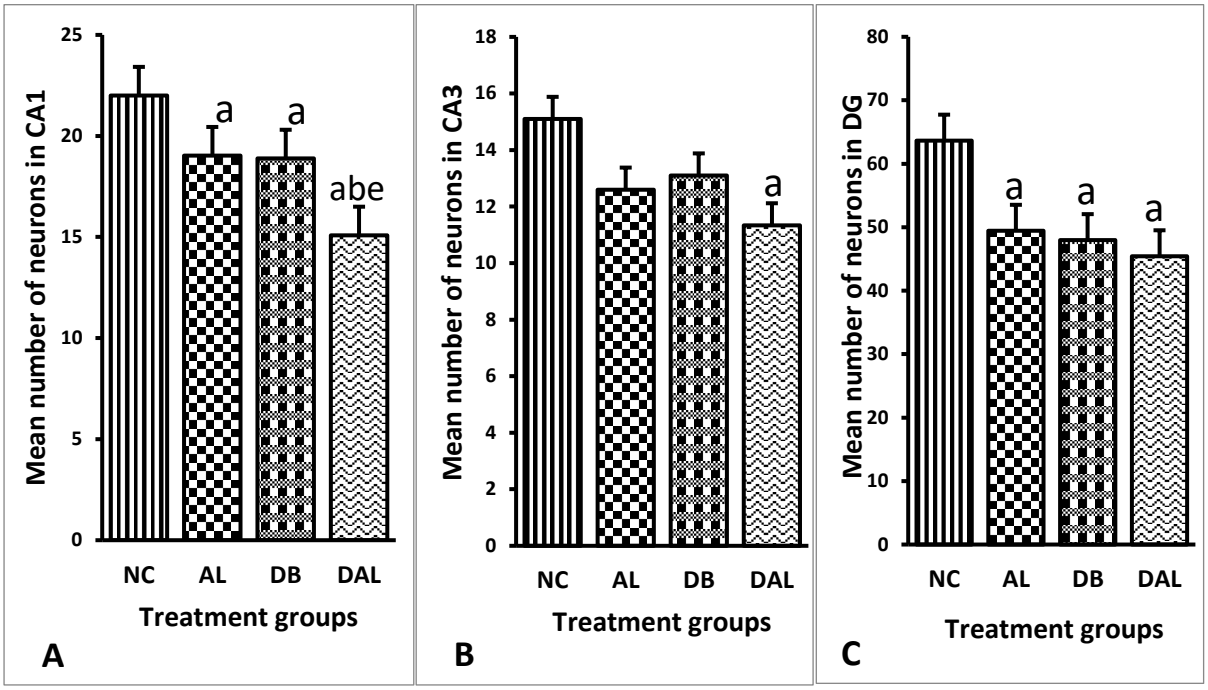

Figure 6. 7. Mean number of neurons in the CA1, CA3, and DG regions of the dorsal hippocampus. Significant changes in mean number of neurons of CA1 region (One-way ANOVA P =0.001), CA3 region (One-way ANOVA test P -=0.001), DG region (One-way ANOVA test, P =0.001). **A)** AL and DB are significantly decreased compared to control (NC) (P=0.002 and 0.001respectively). DAL is significantly decreased compared to control, AL, and DB (P=0.001 respectively). **B)** DAL is significantly decreased compared to control (P= 0.049). **C)** AL, DB and DAL significantly decreased compared to control (NC) (P=0.0001 respectively). a' (NC), 'b' (AL), 'e' (DB), 'g' (DAL); indicates significant changes to groups in bracket ( ), P< 0.05. n=6, Key: NC, Controls; AL, alcohol only; DB, Diabetic; DAL, diabetic and alcohol.

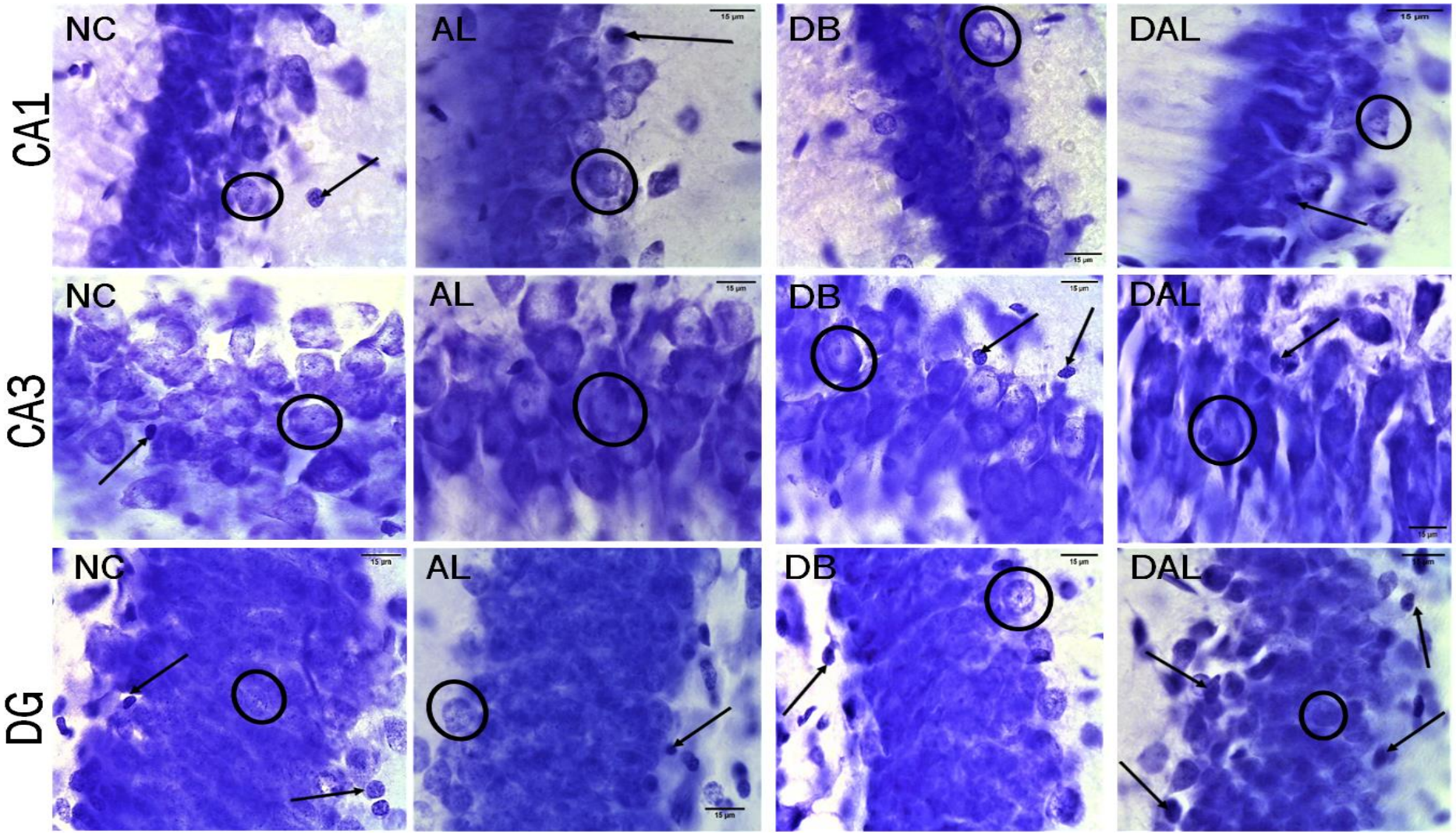

Figure 6. 8. Histomorphology in the CA1, CA3, and DG regions of the dorsal hippocampus. Arrows; glial cells nuclei, circles; an example of neurons counted, Key: NC, Controls; AL, alcohol only; DB, Diabetic; DAL, diabetic and alcohol, Scale bar=15µm**,** X1000

6.3.9 Immunohistochemistry for neurogenesis in the hippocampus Double Cortin and Ki67

The treatment impact on hippocampal neurogenesis of the different treatment groups was evaluated using Double Courtin and Ki67 neural markers. The results show that the mean number of neurons expressing DCX in the AL and DB groups was significantly decreased compared to NC (P =0.001), but DCX expression in the DAL is significantly decreased compared to NC, AL, and DB (P = 0.0001; Fig. 6.9 A-E). Also, a significant reduction was observed in Ki67 expression in the AL, DB, and DAL groups compared to the control (P= 0.002, 0.0001, and 0.0001 respectively), while the DAL group was also significantly reduced compared to the AL group (P = 0.028; Fig.6.9 F). There were no significant differences between control and AL and DB in both DCX and Ki67 expressions.

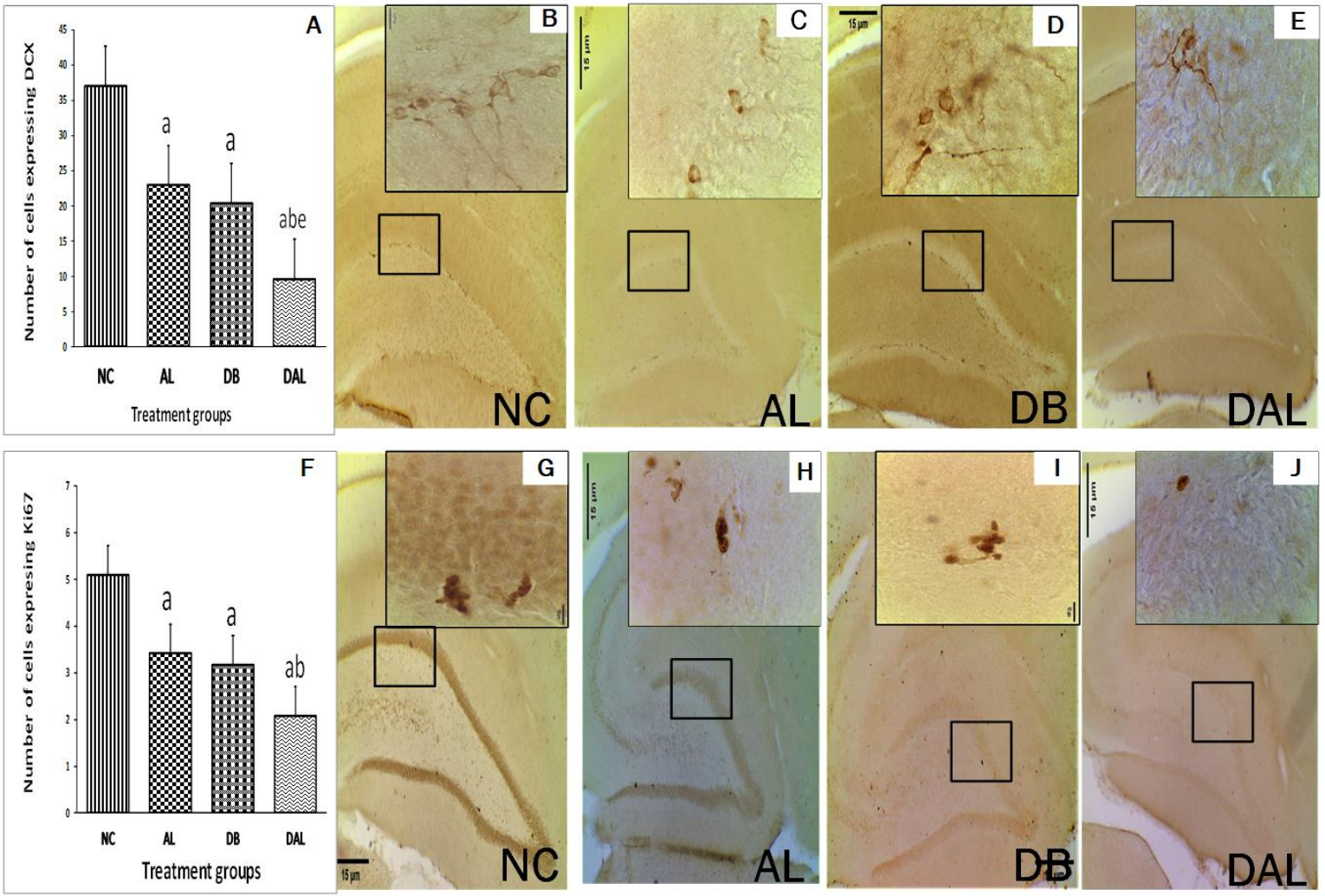

Figure 6. 9. Photomicrograph of the hippocampus showing DCX and Ki67 expression in the sub-granular zone of the dentate gyrus region.

A) Significant difference in expression of DCX between groups (One Way ANOVA, P=0.001). AL and DB significantly decreased compared to control (Bonferroni Post Hoc, P =0.001). DAL significantly decreased compared to control, AL, and DB (Bonferroni Post Hoc, P =0.001). **B)** Controls showing numerous clusters of cell bodies and projections expressing DCX. **C)** AL group: Small, isolated cell bodies and minimal projections expressing DCX. **D)** DB group: Few cells and their projections expressing DCX. **E)** DAL group: Individual cells expressing DCX were mostly observed in the projections.
F) Significant difference in expression of Ki67 between groups (One Way ANOVA, P =0.0001). AL and DB significantly decreased compared to control (NC) (Bonferroni Post Hoc, P =0.002, 0.001 and 0.0001 respectively). DAL significantly decreased compared to control and AL (Bonferroni Post Hoc, P =0.001 and 0.028 respectively) **G-J)** Images of the hippocampus showing a gradual reduction in Ki67 expression across the groups NC, AL, DB, and DAL respectively. Photomicrographs at X100, squares indicate the area captured at X1000 magnification (insert photomicrograph). a' (NC), 'b' (AL), 'e' (DB), 'g' (DAL); indicates significant changes to groups in bracket (), P< 0.05. n=6; Scale bar=15µm. Key: NC, Controls; AL, alcohol only; DB, Diabetic; DAL, diabetic and alcohol.

6.3.10 Pearson's correlation analysis: relationships between parameters

Possible correlations between the values of the different parameters evaluated (diabetic parameters (NFGT and AUC), apoptotic genes (Bcl_2 and BAX), and oxidative stress (MDA and GPX) were carried out. The correlation between these parameters and other parameters was determined as illustrated in figure 6.10. Firstly, diabetic parameters (NFGT and AUC) were significantly positively correlated with oxidative stress but negatively correlated with INSR; which in turn positively correlated with junctional proteins (occludin and claudin-5). The junctional proteins in turn were positively correlated with Ki67 expressions. Furthermore, oxidative stress markers (MDA and GPX) positively correlated with Caspase-3 and negatively correlated with Ki67 and DCX which in turn is positively correlated with neuronal number in CAI and DG (CA1N, DGN). Finally, apoptotic genes (Bcl_2 and BAX) are negatively correlated with DCX, and positively correlated with IRS, which is negatively correlated with neuronal number in CA3. The neuronal number in CA3 is further positively correlated with neuronal number in CAI and DG (CA1N, DGN), (Fig 6.10).

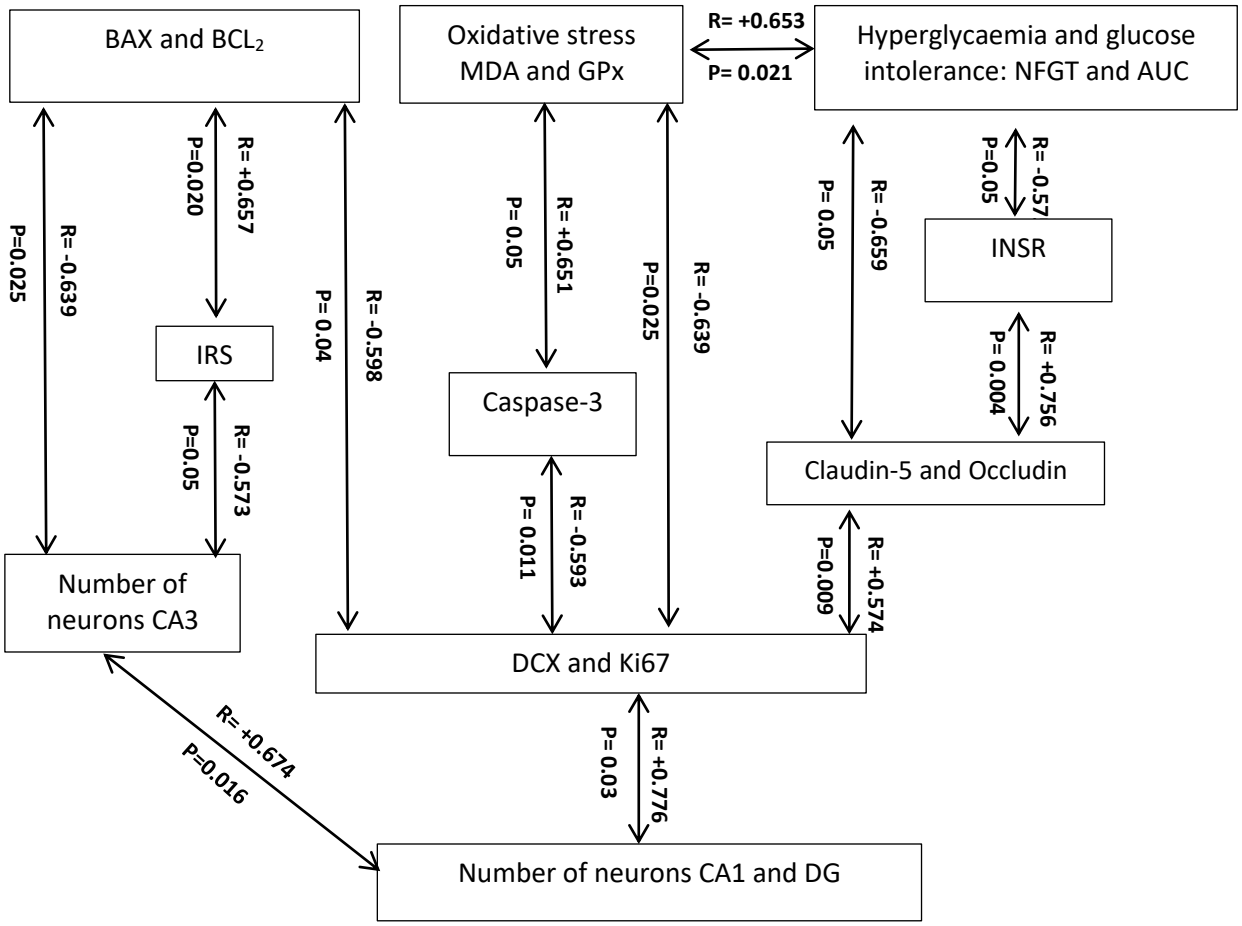

Figure 6. 10. Correlation analysis with significant Pearson correlation of hippocampal parameters affected in diabetes and alcohol experimental groups. Only statistically significant correlations are shown. Black double arrows indicate a statistically significant ($P < 0.05$) correlation between parameters. The correlation coefficient R and P values are located next to the double arrows indicating, positive (+) and negative (-) correlations between the parameters.

6.4 Discussion

The hippocampus and its functions underlie the nervous and molecular mechanism of cognition and memory (Rubin et al., 2014; Duff et al., 2020), which are fundamental aspects of learning, development, and behaviour (Cayre et al., 2009; Morgado-Bernal, 2011; Vogel and Schwabe, 2016). Although there is accumulated evidence between T2D and chronic alcohol consumption, alcohol consumption in diabetes has been controversial, and more detailed information on the hippocampal impact is necessary.

Several clinical studies have reported diminished volume and atrophy in different subfields of the hippocampus utilizing in vivo MRI scans for independent T2D and alcohol exposure studies, highlighting their implications for cognitive deficits (Biessels and Reijmer, 2014; Milne et al., 2017; Meda et al., 2018; Zahr et al., 2019). However, the present study has demonstrated histopathological structural evidence of neuronal loss across experimental groups, with significant loss of neurons in the CA1 (all experimental groups), CA3 (DAL groups), and DG (all experimental groups) regions of the hippocampus. The potential for alcohol use in diabetes to extend hippocampal apoptosis into the CA3 region is crucial because of its specific role in neurogenesis, memory processes, neurodegeneration, and vulnerability to seizures, probably because of its very rich internal connectivity to other hippocampal regions (Cherubini and Miles, 2015).

These observed neuronal losses and injury are severally reported independently in alcohol exposure and diabetes is often associated with increased oxidative stress (Das and Vasudevan, 2007; Flora et al., 2012; Zhang et al., 2020). This is consistent with our observations of oxidative stress (increased MDA, decreased GPx) in all the treated groups with heightened oxidative stress in the DB and DAL groups. The alcohol and T2D-induced oxidative stress generate an increasing amount of ROS which may initiate intrinsic apoptotic pathways cumulating in elevated apoptotic proteins (BAX, $BCL_{2,}$ and Caspase-3). Correspondingly, hippocampal apoptosis was observed in all the treated groups with significant up-regulation of Caspase-3, BCL2 and BAX relative to the control. These elevated BAX, $BCL_{2,}$ and Caspase-3 mRNA levels are consistent with previous reports of oxidative stress-induced neuronal apoptosis in T2D (Jafari Anarkooli et al., 2008; Sadeghi et al., 2016). Thus, the significant positive correlation between oxidative stress and Caspase-3, explains the presence of elevated oxidative stress markers and Caspase-3 in the diabetic groups (DB and DAL groups).

Additionally, the results showed that neuronal loss and apoptosis in the hippocampus may not always arise from direct neurotoxic effects on neurons but are often associated with a compromised state of the neurogenic niche in the hippocampus (Ho et al., 2013; Yuan et al., 2015; Dhanabalan et al., 2018). The proper proliferation and migration of neural stem cells and immature neurons in the neurogenic niche of the dentate gyrus sub-granular zone are essential for brain development, memory, and learning (Deng et al., 2010). Our findings of significantly reduced DCX and Ki67 immunolocalization in the AL and DB groups corroborates with independent reports of impaired neurogenesis with T2D and alcohol exposure (Geil et al., 2014; Ramos-Rodriguez et al., 2014). However, with alcohol in diabetes (DAL group), immunohistochemistry results reveal that neurogenesis was further impaired with significantly lower DCX expressing cells (compared to control, AL, and DB groups) and reduced Ki67 (compared to control and AL groups). This exacerbated neurogenesis deficit in DAL coupled with the CA3 neuronal loss corroborates with a report of hippocampal CA3 region regulation of neurogenesis (Liu et al., 2011). These impairments of neural progenitor and immature neurons in the hippocampal neurogenic niche may disrupt angiogenesis which is associated with the integration of new neurons and contribute to a compromised state in the blood-brain barrier (BBB) (Pozhilenkova et al., 2017). Therefore, the observed significantly reduced occludin and claudin-5 gene expression may be associated with the reduction of neural stem cells in diabetes (DB) and supports our reported positive correlation between these junctional proteins and Ki67. However, due to the ability of alcohol to easily cross the BBB, the alcohol-treated groups (AL and DAL) may induce neural stem cell loss (Phillips, 1981; He et al., 2005) in the absence of significant BBB disruption. These findings imply that alcohol use in diabetes may induce more severe neurodegeneration than is observed in either diabetes or alcohol.

Furthermore, insulin receptors (INSR and IRS1) are also found in endothelial cells of the BBB and regulate insulin availability and insulin response within the CNS (Tu et al., 2021). The

hippocampus is dependent on the activity of insulin and its receptors to meet the energy demand required for hippocampal cognitive and synaptic plasticity function (van der Heide et al., 2005; Huang et al., 2010). Thus, the down-regulation of hippocampal INSR and IRS1 in DB (increased insulin resistance), and elevated glucose tolerance and hyperglycaemia are consistent with reports of T2D-induced hippocampal glycaemic deficit associated with cognitive and memory conditions such as Alzheimer's (McNay and Recknagel, 2011; Arnold et al., 2018). Alcohol-mediated effects on appetite, glycaemic control, and insulin resistance have led to several reports of alcohol-induced T2D pathogenesis (de la Monte, 2012; Kim and Kim, 2012; Schrieks et al., 2015). This corroborates with our finding of reduced food intake, and down-regulation of IRS1 but not INSR in AL (initiation of insulin resistance), however, low AUC and NFBG (glucose tolerance and hyperglycaemia) indicate that diabetogenic effects were not established yet. On the other hand, elevated IRS1 was observed in the DAL (and no significant effects on INSR), with AUC and NFBG levels gradually reduced with terminal levels significantly lower compared to DB. The singular upregulation of both IRS1 and BCL_2 in the DAL group is consistent with previous reports of the anti-apoptotic response of BCL_2 (Ueno et al., 2000; Walker et al., 2012). However, this study has uniquely shown that despite the significant ameliorating presence of elevated Bcl_2 in alcohol use with diabetes (DAL), significant upregulation of BAX (Shinoura et al., 1999), Caspase-3, and increased oxidative stress markers were able to induce hippocampal neurodegeneration. These findings also suggest that glucose tolerance, blood glucose levels, hippocampal BBB permeability, and insulin receptors should not be used as final parameters for the diagnosis and monitoring of diabetic patients who use alcohol for possible associated neurological problems.

While some studies have reported increased diabetogenic effect, other investigations suggest beneficial or hypoglycaemic effects of alcohol in diabetes (Wannamethee et al., 2002; Carlsson et al., 2003; Ahmed et al., 2008; Jang et al., 2019). However, we show that despite slight

alleviation of insulin resistance, glycaemic control, glucose tolerance, and normal BBB, alcohol use in diabetes reduces hippocampal neurons and impairs neurogenesis. Therefore, the elevated levels of oxidative stress markers, hippocampal cellular apoptosis and impaired neurogenesis recorded in diabetes plus alcohol-treated group suggest the potential to induce neurodegenerative diseases (Chen et al., 2012; Cheyuo et al., 2019; Moujalled et al., 2021). This finding is invaluable clinically in the management of alcohol-dependent diabetic patients and warrants special clinical attention relative to the neurological management of diabetic patients who use alcohol regularly.

CHAPTER 7 Interactions of Alcohol and Combination Antiretroviral drug in diabetic Male Sprague Dawley Rats: Hippocampal Perturbations and Toxicosis

7.0 Abstract

The histopathology of alcohol and/or cART therapy in diabetes was investigated in male Sprague Dawley rat hippocampus following STZ diabetic induction and sub-chronic (90 days) treatment exposure. Forty-eight diabetic male Sprague Dawley rats were divided into eight groups (n=6): negative control (NC), alcohol (AL), cART (AV), alcohol-cART (AA), diabetic control (DB), diabetes-alcohol (DAL), diabetes-cART (DAV), and diabetes-alcohol-cART (DAA) exposure groups and profiled the levels of hippocampal pro-inflammatory cytokines and oxidative stress using immunoassay, apoptotic genes, insulin receptors, and blood-brain barrier (BBB) junctional proteins gene expression were assessed using qPCR. Histomorphology of hippocampal neuronal number, nuclei area, and volume of dentate gyrus and neurogenesis were accessed using Nissl stain, Ki67, and DCX histochemistry. The results showed DAV, DAL, and DAA treatments elevated oxidative stress markers and Caspase-3 expression but reduced neurogenesis, DG volume, and neuronal number in hippocampal CA1, CA3 and DG regions. However, differential effects underscoring the diabetes-alcohol-cART interactions were observed in levels of, proinflammatory cytokines (deficit in DAV and elevation of IL-1α and IL-6 in DAA), BAX expression (elevated in DB, DAV, DAL and DAA), Bcl_2 (elevated in DAL and DAA), claudin-5, and occludin (reduced in DAV and DAA respectively), and IRS1 (reduced in DAV and elevated in DAL) which underpin the modulating impact of diabetes either on AL, cART therapy or both. However, cART therapy in alcohol use (AA) ameliorated the independent alcohol and cART effects of elevated, MDA levels, pro-inflammatory cytokines, reduced DCX and neuronal number in CA1 and DG, but reduced expression of INSR, IRS1, claudin-5, and occludin which may impair insulin transport and

utilization (insulin-resistance) and increased BBB permeability respectively. Therefore, chronic alcohol use and cART regime in diabetes (DAA) is hugely toxic to the hippocampus, and caution is advised particularly in HIV treatment, and cART prophylaxis in diabetes.

7.1 Introduction

Type 2 diabetes (T2D) is one of the most common chronic health and socio-economic problems in South Africa and globally (Rheeder, 2006; Whiting et al., 2011). Diabetes is classified diabetes into the general categories of type 1, type 2, gestational and specific type of diabetes (Association, 2015). Specific diabetes includes monogenic diabetes syndrome, diseases of the exocrine pancreas, and recently drug or chemical-induced diabetes such as disease (for example Covid-19 and HIV) associated diabetes (Accili, 2021). Additionally, lifestyle factors such as alcohol use/abuse can exert chemotoxicity that results in diabetic condition (Carlsson et al., 2003; Englr et al., 2013). Therefore, chronic drug and chemical-induced diabetes is gradually becoming prevalent as a high proportion of individuals who are on chronic medications and regularly use alcohol may develop diabetes (Doos et al., 2014; Iglay et al., 2016). Thus, co-morbidity under diabetic condition and managed with multiple drug therapy is on the increase and will require multiple drug therapy investigations to elucidate its health impact, especially on the glucose-sensitive organs such as the brain.

The hippocampus is sensitive to insulin signalling and glucose homeostasis for the regulation of the cognitive, memory, neurogenesis, and neuroprotective functions (van der Heide et al., 2005; Huang et al., 2010; Pearson-Leary and McNay, 2016). Hippocampal neurons and endothelial cells contain several membrane-bound insulin receptors (INSR), which recruit intracellular adapter proteins; insulin receptor substrate (IRS1) in the canonical insulin signalling pathway and mediate glucose uptake into cells (Zhao et al., 1999; De Meyts, 2000; Ohtsuki et al., 2008). Additionally, junctional blood-brain barrier (BBB) proteins claudin-5 and

occludin (Daneman and Prat, 2015) are located on hippocampal endothelial cells and tightly regulate the penetration of drugs, chemicals, and inflammatory extravasation or production of cytokines by microglial cells (Harry and Kraft, 2008; Camire et al., 2015). Perturbation in the normal physiological regulation of insulin receptors, BBB proteins, and cytokines may induce a cascade of events associated with oxidative stress, apoptosis, and compromised neurogenesis which are independently reported in alcohol, cART and diabetes (Qin et al., 2008; Tovar-y-Romo et al., 2012; Volpe et al., 2018; Ferlita et al., 2019). Similarly, diabetes, alcohol, and cART are independently associated with cognitive impairment (Ma et al., 2016; Biessels and Despa, 2018; Meda et al., 2018; Reinke et al., 2022), and consequently, their comorbidity (cART+ diabetes and diabetes +alcohol) showed an exacerbated effect. However, the concomitant presence of cART and alcohol in the normal rat hippocampus (cART +alcohol) and in the diabetic hippocampus (alcohol + cART + alcohol) remains unclear. Therefore, the adverse effects of co-presence of alcohol, cART, and diabetes on some histopathological parameters that may negatively impact cognition require further elucidation for possible related neuropathological effects.

Clinical management of comorbidity patients often require multiple drug therapy which commonly is associated with several independent side effects but cumulative drug-drug interaction between therapies (Guthrie et al., 2015; Kadam et al., 2018) could together become detrimental to overall patient health. Therefore, this study is designed to investigate the dual presence of cART administration and alcohol intake in type 2 diabetic condition focused effects on investigating hippocampal pro-inflammatory cytokines, oxidative stress, apoptotic, insulin receptors, and junctional markers, neuronal histomorphology, and neurogenesis.

7.2 Materials and methods

7.2.1 Experimental groups

The adult male Sprague Dawley rats were divided into eight groups (n=6), Negative control (NC), twenty percent fructose feed (2FT), sham control (SNC), alcohol alone (AL), cART alone (AV), alcohol and cART (AA), diabetic control (DB), diabetes and alcohol administration (DAL), diabetes and cART treatment (DAV), and diabetes, alcohol, and ART (DAA) treated groups as described in chapter 3.

7.2.2 Enzyme-linked immunoassay of proinflammatory cytokines (IL-1α, IL-6, TNFα) and oxidative stress markers (GPX, and MDA)

Dissected brain samples from each hemisphere per animal were homogenized and used were used to run an enzyme-linked immunosorbent assay for proinflammatory cytokines (Rat IL-1α, Rat IL-6, Rat TNFα) according to the manufacturer's protocol (Elabscience, USA; E-EL-R0011, E-EL-R0015, E-EL-R0019 respectively). Oxidative stress markers were assessed using malondialdehyde (MDA) Colorimetric assay kit: TBA method (Elabscience, Houston, Texas USA; E-BC-K025-M), and Glutathione Peroxidase (GSH-Px) Activity Assay Kit (Elabscience, Houston, Texas USA; E-BC-K096-M WST-1 Method) as outlined in chapter 3.

7.2.3 Quantitative qPCR for junctional proteins, insulin receptors, and apoptotic markers

From each brain sample, total RNA was extracted and used in a reverse transcriptase reaction to synthesize cDNA, and expression levels of BAX, Bcl_2, claudin-5, Caspase-3, INSR, IRS1, and occludin in samples were measured using a Quant studio1 96 well plate detection system as outlined in chapter 3

7.2.4 Histomorphometry using Cresyl violet stain and Immunohistochemistry for neurogenesis

From serial 50 µm brain sections in each animal of each treated group, 36 sections per group were stained with cresyl violet, while the next two series of sections were used for immunohistochemical labelling of Ki67 and DCX, respectively. Histomorphology measurement of dentate gyrus volume, neuronal number, and neuronal nuclei areawerere obtained as previously described in chapter 3.

7.3 Results

7.3.1Oral glucose tolerance test and AUC of treated groups

The mean area under the OGTT curve (AUC) was significantly increased in the DB, DAV, DAL, and DAA groups compared to the control, AL, AV, and AA groups (Fig 7.4.1A). The mean OGTT was similar with uniform low levels of blood glucose for the non-diabetic treated groups at different time intervals, while the diabetic groups (DB, DAV, DAL, and DAA) all had marginal erratic high glucose levels; at 2 hours post glucose load, the DAV group maintained the highest blood glucose level while the DAL dropped to the lowest level for the diabetic groups at 18,5 mmol/L (Fig 7.1 B).

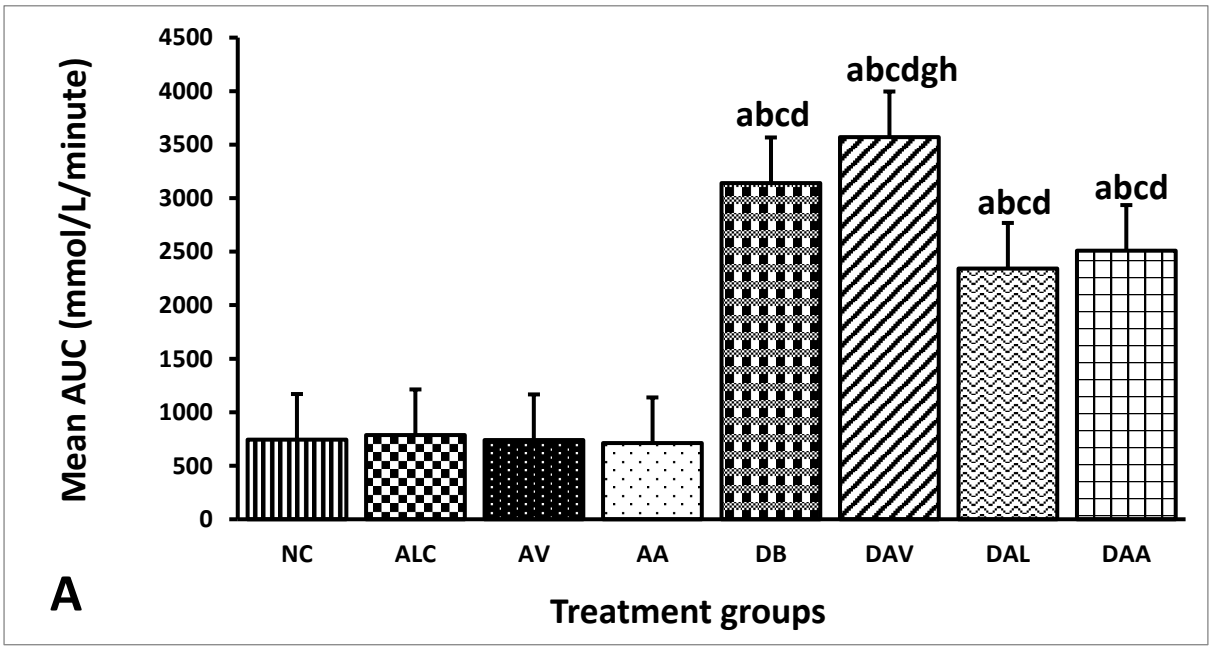

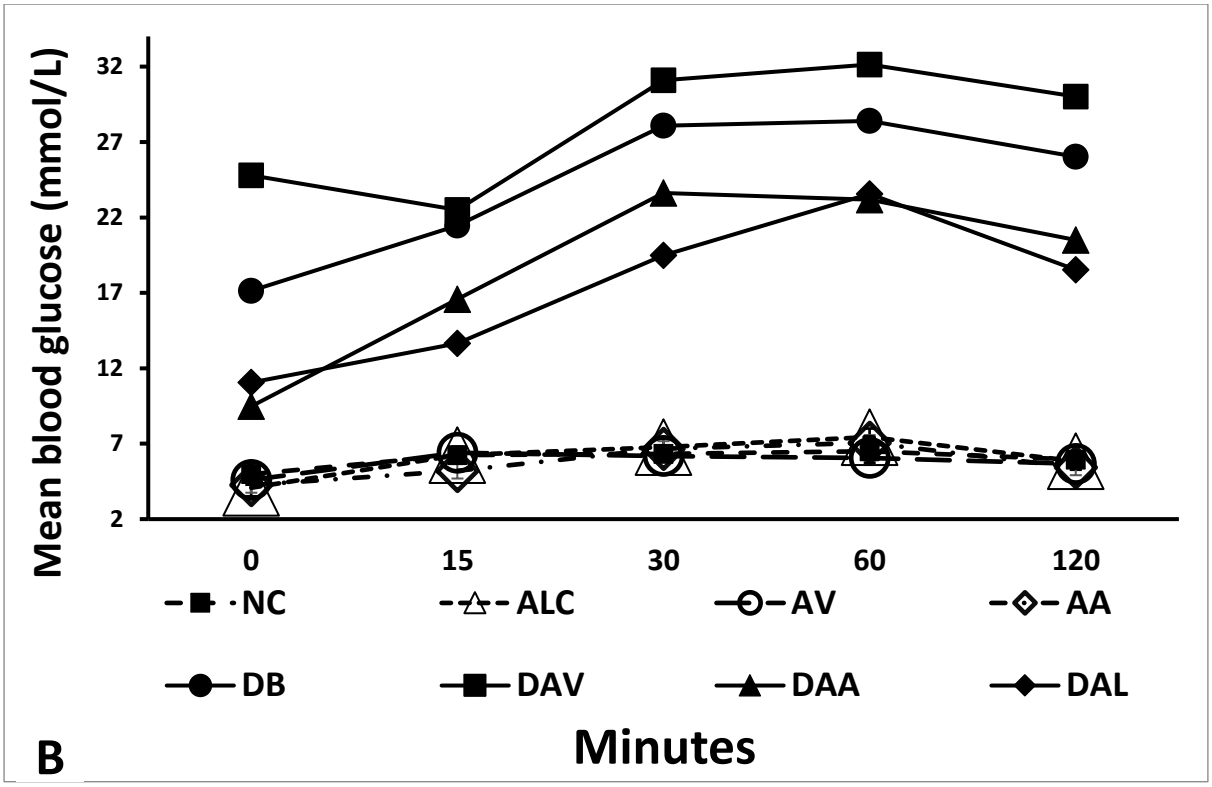

Figure 7. 1. Mean terminal AUC and OGTT of treated groups. A) Significant difference in mean terminal AUC (One way ANOVA P=0.001). DB, DAV, DAL, and DAA are elevated compared to control, AL, AV, and AA, while DAV is elevated compared to DAL and DAA (P=0.05, Bonferroni post hoc test). B**)** Mean OGTT at different time intervals, DAV with highest values. a' (NC), 'b' (AL), 'c' (AV), 'd' (AA), 'e' (DB), 'f' (DAV), 'g' (DAL), 'h' (DAA); indicates significant differences compared to groups in bracket ( ), P< 0.05. NC: Control, AV: cART, AL: alcohol, AA: cART and alcohol, DB: diabetic, DAV: diabetic and cART, DAL: diabetic and alcohol, DAA diabetic cART and alcohol.

7.3.2 Proinflammatory cytokines

The mean concentrations of proinflammatory cytokines across all the experimental groups are reported in table 7.1. It showed IL-6 in AL and AV significantly increased compared to control (P= 0.005 and 0.014), AA (P= 0.006 and 0.017), DB (P=0.001), DAV (P=0.001), while DB and DAV are significantly decreased compared to control (P=0.007,0.001), AA (P= 0.006, 0.001), DAL (P=0.001) and DAA (P=0.001). DAA is significantly increased compared to control (P=0.001) and AA (P=0.001). Secondly for TNFα, in AL and AV significantly increased compared to the control (P=0.005 and 0.043), AA (P= 0.001 and 0.006), DB (P= 0.001), and DAV (P=0.001). DB and DAV are significantly decreased compared to control

(P=0.001), AA (P= 0.002, 0.005), DAL (P= 0.001), and DAA (P= 0.001) while in DAL, it increased significantly compared to AA (P= 0.002). For IL-1α, it was significantly increased in AL compared to control, (P= 0.026), AA (P= 0.028), DB (P=0.001), DAV (P=0.001) but in DAA treated was significantly increased against control (P=0.05) and AA (P=0.014). In DB and DAV-treated, IL-1α was significantly decreased compared to control (P=0.015 and 0.034), AV (P=0.001), DAL (P=0.001), and DAA (P=0.001) treated groups.

Table 7. 1. Mean concentration of cytokines IL-1α, IL-6, and TNFα in hippocampal tissue homogenate.

	NC (a)	AL (b)	AV (c)	AA (d)	DB (e)	DAV (f)	DAL (g)	DAA (h)
IL-6 (pg/mg protein)	1.507± 0.02	1.888± 0.1[a]	1.840±0.05[a]	1.517± 0.05[bc]	1.1036±0.01[abcdgh]	0.981± 0.07[abcdgh]	1.780± 0.11	2.008± 0.09 [ad]
TNFα (pg/mg protein)	1.187± 0.05	1.429± 0.04[a]	1.333± 0.03[a]	1.098 ± 0.03[bc]	0.826±0.03[abcdgh]	0.847 ± 0.01[abcdgh]	1.260± 0.12[d]	1.272 ± 0.01
IL-1α (pg/mg protein)	3.349±0.09	3.982± 0.2[a]	3.774± 0.15	3.1321± 0.22[b]	2.455± 0.01[abcdgh]	2.527± 0.22 [abcdgh]	3.908± 0.13[d]	4.035± 0.12[ad]

Data reported as mean± SEM. Significant difference in the mean concentration of cytokines (IL-1α, IL-6, TNFα) between groups (One way ANOVA P=0.001). The concentrations of cytokines (IL-1α, IL-6, TNFα) are significantly elevated in the AL and AV (IL-6, TNFα) groups compared to the control and AA groups. In the DAA group, levels of IL-1α and TNFα are significantly elevated against control and AA groups; and elevated in the DAL group against the AA group. Also, levels of IL-1α, IL-6, TNFα in DB and DAV groups reduced significantly against the control and all other treated groups but are similar to each other.

For comparative analysis: letters in asterisk ‘ ’: ‘a’ (NC), ‘b’ (AL), ‘c’ (AV), ‘d’ (AA), ‘e’ (DB), ‘f’ (DAV), ‘g’ (DAL), ‘h’ (DAA); indicates significant differences to the treatment groups in bracket () P=0.05. n=6. Key: NC: Control, AV: cART, AL: alcohol, AA: cART and alcohol, DB: diabetic, DAV: diabetic and cART, DAL: diabetic and alcohol, DAA diabetic cART and alcohol.

7.3.3 Oxidative stress markers

The lipid peroxidation levels recorded significantly increased in all the experimental groups (AL, AV, DB, DAV, DAL and DAA) in comparison to the control except the AA group. However, MDA levels were significantly increased in the AL and DAV group compared to AA (Table 7.2). Also, the antioxidant (GP_X) level was significantly reduced in all the experimental groups (AL, AV, AA, DB, DAV, DAL and DAA) relative to the control and significantly reduced in the AA, DB, DAV, and DAL groups compared to AL and DAA groups.

Table 7. 2. Mean concentration of oxidative stress markers MDA and GPX in hippocampal tissue homogenate.

	NC (a)	**AL (b)**	**AV(c)**	**AA (d)**	**DB (e)**	**DAV (f)**	**DAL (g)**	**DAA (h)**
GPx (μmol/g protein)	2.165± 0.08	1.505± 0.09[a]	1.278±0.01[a]	1.186±0.01[abh]	1.193±0.05[abh]	1.187±0.04 [abh]	1.116±0.01[abh]	1.476± 0.10[a]
MDA (μmol/g protein)	0.032± 0.001	0.077± 0.002[a]	0.069±0.006[a]	0.044± 0.002[bf]	0.065±0.006[a]	0.083±0.011[a]	0.066±0.004[a]	0.061± 0.002[a]

Data presented as mean ± SEM. Significant difference in mean concentration of MDA and GPX between groups (One way ANOVA P=0.001).
For GPx: AL, AA, AV, DB, DAV, DAL and DAA are significantly decreased compared to control (P= 0.001). AA, DB, DAV, and DAL are significantly decreased compared to AL (P= 0.029, 0.036, 0.030, and 0.004 respectively) and DAA (P= 0.038, 0.045, 0.038, and 0.006 respectively).
For MDA: AL, AV, DB, DAV, DAL and DAA are significantly increased compared to control (P= 0.001, 0.001, 0.001, 0.004, 0.001, 0.002, and 0.015 respectively). AA is significantly decreased compared with AL (P= 0.004) and DAV (P=0.001).
For comparative analysis: letters in asterisk ' ': 'a' (NC), 'b' (AL), 'c' (AV), 'd' (AA), 'e' (DB), 'f' (DAV), 'g' (DAL), 'h' (DAA); indicates significant differences to the treatment groups in bracket () P=0.05. n=6. Key: NC: Control, AV: cART, AL: alcohol, AA: cART and alcohol, DB: diabetic, DAV: diabetic and cART, DAL: diabetic and alcohol, DAA diabetic cART and alcohol.

7.3.4 Mean apoptotic genes expression in hippocampal tissue

The expression fold of the three major apoptotic markers is shown in in figure 7.2 with significant up regulation of Bcl_2 in the DB, DAL, and DAA groups compared to the control (P=0.007, 0.045 and 0.029 respectively), and up regulation of Bcl_2 in DAL and DAA compared to DAV (P=0.018 and 0.015). Conversely, Bcl_2 in AA is downregulated compared to control, AL, AV, DB, DAL and DAA (P= 0.001, 0.039,0.023, 0.015, 0.001, 0.001 respectively). For BAX, a significant up regulation was observed in the DAL compared to the control, AL, and DB groups (P=0.002, 0.018, and 0.006) and upregulated in the DAV group compared to the control and AV groups (P=0.004 and 0.001). Similarly, BAX in AA is downregulated compared to control, AL, AV, DB, DAV, DAL and DAA (P= 0.032, 0.034, 0.001, 0.010, 0.001, 0.001, 0.048 respectively). Finally, Caspase-3 in DB, DAV, DAL and DAA was significantly upregulated against the control (P=0.037, 0.001, 0.020, and 0.036) and AA (P=0.032, 0.001, 0.017, and 0.031); but significantly upregulated in DAV compared to AL and AV treated groups (P=0.009 and 0.003).

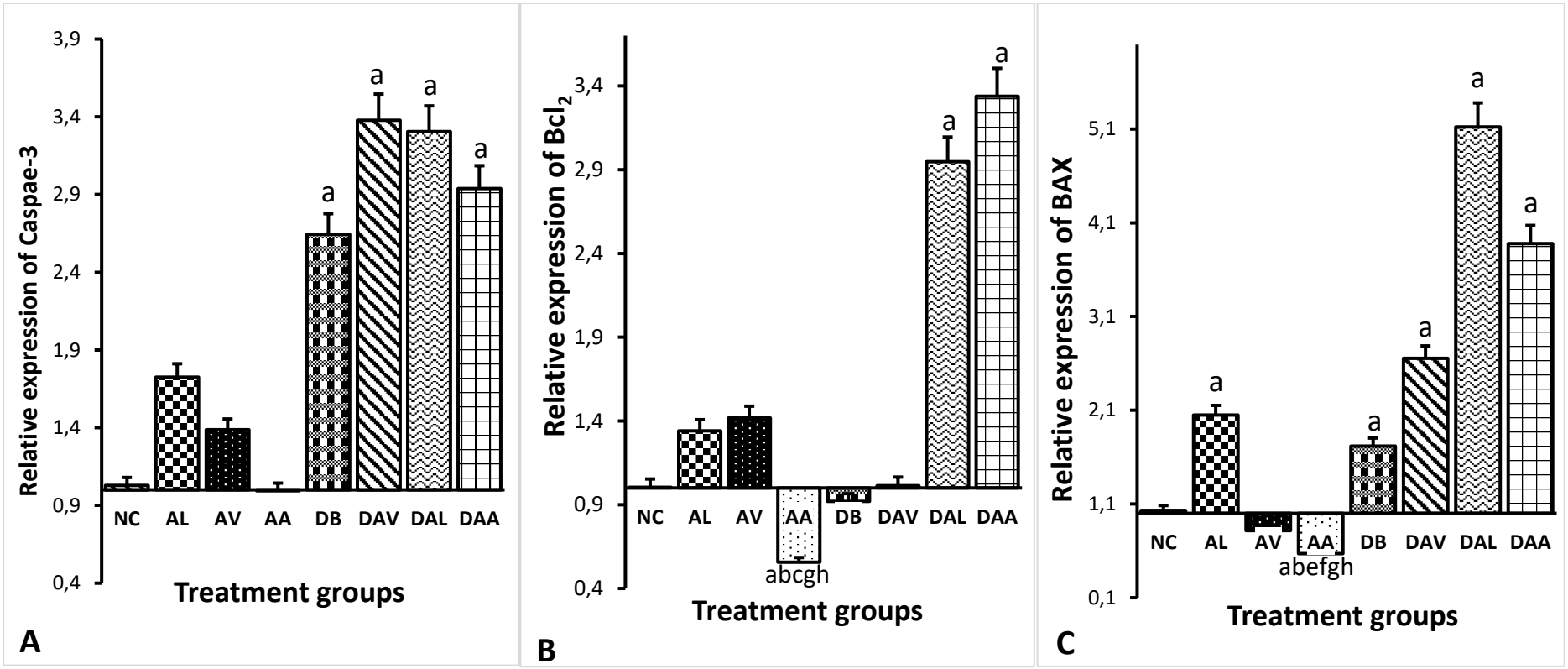

Figure 7. 2. Mean expression of apoptotic associated genes Bcl_2, BAX, and Caspase-3 in hippocampal tissue. Data presented as mean ± SEM. Significant difference in Bcl_2, BAX and Caspase-3 expressions (One-way ANOVA, P=0.007, 0.001, 0.006 respectively). **A)** For Caspase-3, DB, DAV, DAL, and DAA are significantly upregulated compared to control and AA (P=0.05). **B)** For Bcl_2, AA is significantly down regulated while DB, DAL and DAA are upregulated (P=0.05) **C)** For BAX, AA is significantly down regulated while DAV and DAL are significantly upregulated compared to the control (P= 0.05). a' (NC), 'b' (AL), 'c' (AV), 'd' (AA), 'e' (DB), 'f' (DAV), 'g' (DAL), 'h' (DAA); indicates significant differences compared to groups in bracket ( ), P< 0.05. n=3. Key: NC: Control, AV: cART, AL: alcohol, AA: cART and alcohol, DB: diabetic, DAV: diabetic and cART, DAL: diabetic and alcohol, DAA diabetic cART and alcohol.

7.3.5 Mean membrane junctional genes expression in hippocampal tissue

The analysis of claudin-5 and occludin expression levels in the hippocampus reveals mostly downregulation of these junctional proteins across the experimental groups (Fig 7.3 A-B). Claudin-5 was observed to be significantly downregulated in the AA, AV and DAV groups compared to the control (P=0.031, 0.004, and 0.034) and but downregulated in the AV treated group compared to the AL, DB, DAV, DAL, and DAA groups (P= 0.004, 0.015, 0.007, 0.001, 0.027). Occludin was significantly down regulated in the DAA group compared to the control (P=0.045) and also downregulated in the AA and DB groups compared to the control (P= 0.023, 0.017), AV (P= 0.003, 0.001) and DAL groups (P=0.025 and 0.002).

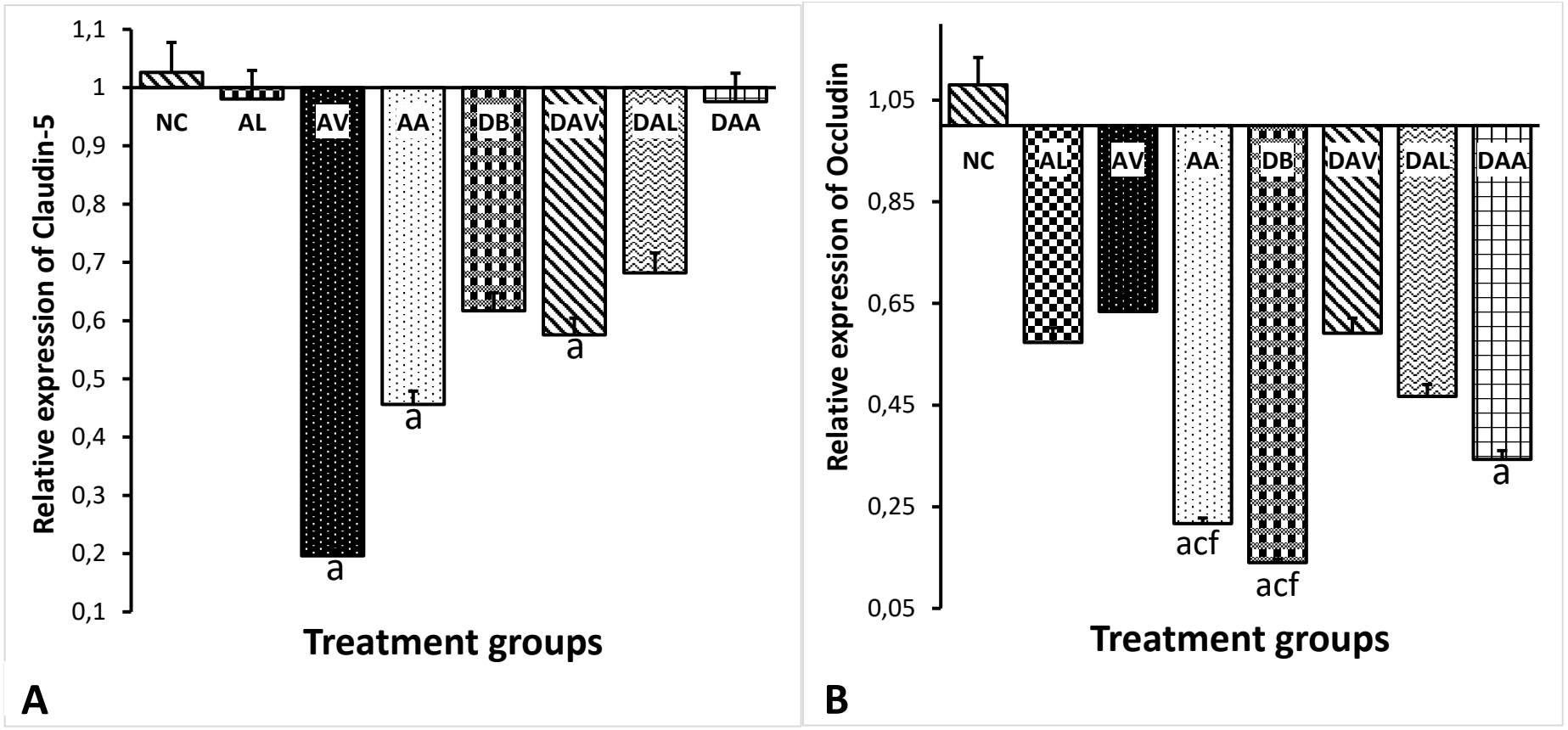

Figure 7. 3. Mean expression of junctional membrane associated genes claudin-5 and occludin in hippocampal tissue. **A)** Significant difference in claudin-5 expression (One-way ANOVA, P=0.013). AV, AA, and DAV are significantly down regulated compared to the control (P=0.05). **B)** Significant difference in occludin expression (One-way ANOVA, P=0.05). AA, DB and DAA are significantly down regulated compared to control, while AA and DB are downregulated compared to AV and DAV (P=0.05). a' (NC), 'b' (AL), 'c' (AV), 'd' (AA), 'e' (DB), 'f' (DAV), 'g' (DAL), 'h' (DAA); indicates significant differences compared to groups in bracket ( ), P< 0.05. n=3. Key: NC: Control, AV: cART, AL: alcohol, AA: cART and alcohol, DB: diabetic, DAV: diabetic and cART, DAL: diabetic and alcohol, DAA diabetic cART and alcohol.

7.3.6 Mean insulin receptor genes expression in hippocampal tissue

Figure 7.4 shows the expression levels of INSR and IRS1 genes in hippocampal homogenate across all experimental groups. The expression of INSR was significantly downregulated in the AA and DB groups compared to the control, AL, AV and DAL groups, while the DAV was down regulated compared to the DAL group only (Fig 7.4 A, $P<0.05$). Additionally, the IRS1 expression was downregulated in the AL, AV, AA, DB, and DAV groups compared to the control, DAL and DAA groups (Fig 7.4 B). Conversely, the expression of IRS1 in the DAL and DAA groups were upregulated, significantly in the DAL group compared to the control

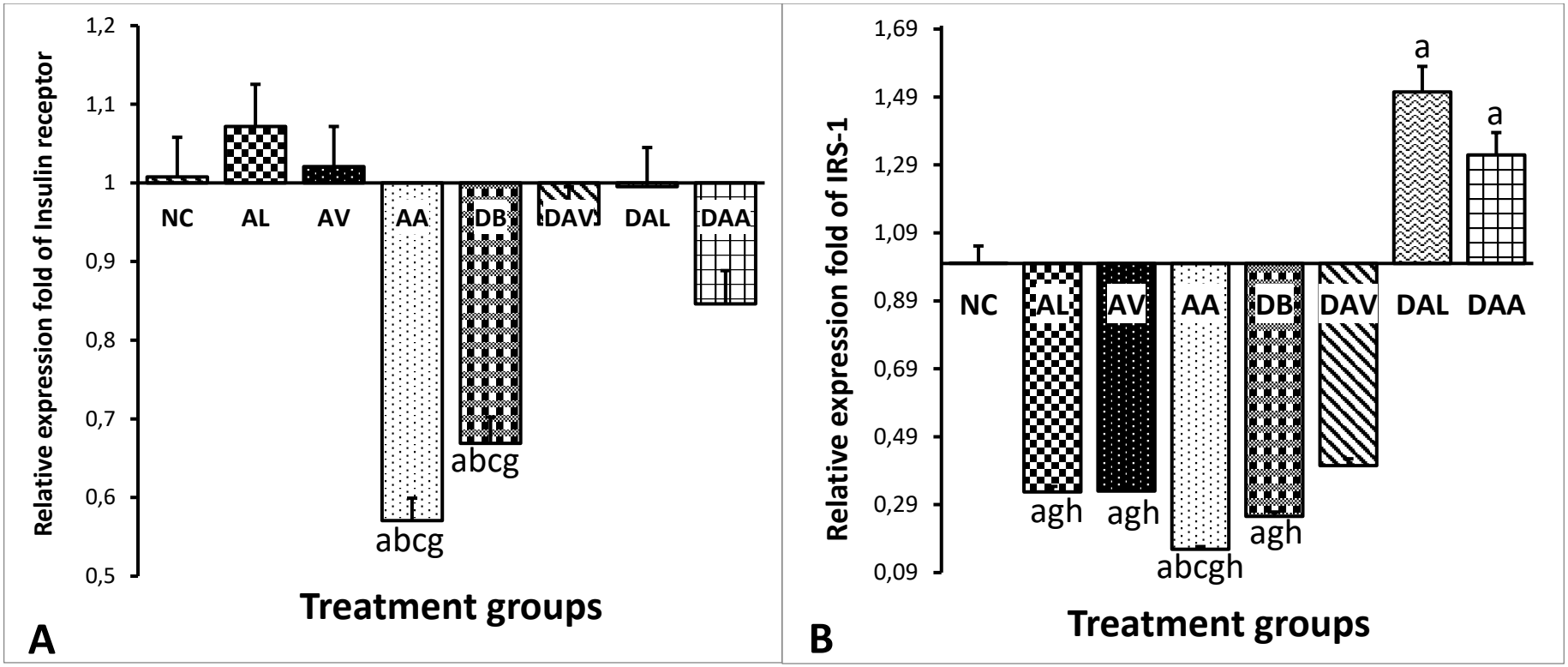

Figure 7. 4. Mean expression of insulin receptor and insulin receptor substrate in hippocampal tissue. Significant difference in insulin receptor and insulin receptor substrate mRNA level (Kruskal Wallis, P=0.05 and 0.007 respectively). **A)** AA and DB are significantly down regulated compared to the control (P=0.020 and 0.023), AL (P=0.01), AV (P=0.018 and 0.028), and DAL (P=0.016 and 0.043), while DAV and DAA are downregulated compared to DAL (P= 0.01). **B)** AL, AV, DB and DAV are significantly down regulated compared to control (P=0.001, 0.001, 0.001 and 0.008), DAL (P=0.028, 0.05, 0.004 and 0.002), and DAA (P=0.05, 0.05, 0.021 and 0.028). While, AA is downregulated compared to control, AL, AV, DAL and DAA (P=0.001, 0.05, 0.001and 0.002). a' (NC), 'b' (AL), 'c' (AV), 'd' (AA), 'e' (DB), 'f' (DAV), 'g' (DAL), 'h' (DAA); indicates significant differences compared to groups in bracket ( ), P< 0.05. n=3. Key: NC: Control, AV: cART, AL: alcohol, AA: cART and alcohol, DB: diabetic, DAV: diabetic and cART, DAL: diabetic and alcohol, DAA diabetic cART and alcohol.

7.3.7 Histomorphology of hippocampus

Histopathological photomicrographs across all experimental groups and control are shown in figures 7.5, 7.7 to 7.9. These are low power (Fig. 7.5) and high-power (Fig. 7.7 to 7.9) image illustration of histological changes that occur in neuronal population, size, and volume in response to the experimental conditions and treatment.

7.3.7.1 Mean volume of granular and molecular layer in the dentate gyrus

In the low power images, a slight reduction in the outer molecular (ML; black double arrows, Fig. 7.5) and mid granular layer (GL; red double arrows, Fig. 7.5) of the dentate gyrus in all the treated groups especially in the DAV and DAL groups were apparent (Fig.7.5). Additionally, a disruption in the layer of cells in the CA3 region (red arrows, Fig 7.5) was observed in the diabetic co-morbidity groups (DAV, DAL, and DAA; Fig. 7.5).

The quantification of the volume in the molecular and granular layers of the dentate gyrus are illustrated in figure 7.6 A and B. The volume of the dentate gyrus granular cell layer was significantly reduced in the AA, DAL, DAV and DAA compared to control (Fig. 7.6 A, P=0.05) but increased in the DB group compared to the AA and DAL groups (Fig. 7.6 A, P= 0.05). The quantification of molecular layer volume showed significant reduction in the molecular layer volume of the diabetic co-morbidity groups (DAV, DAL, and DAA) compared to the control, with further reduction in the DAL, and DAA groups compared to the AV group (Fig. 7.6 B; P= 0.05).

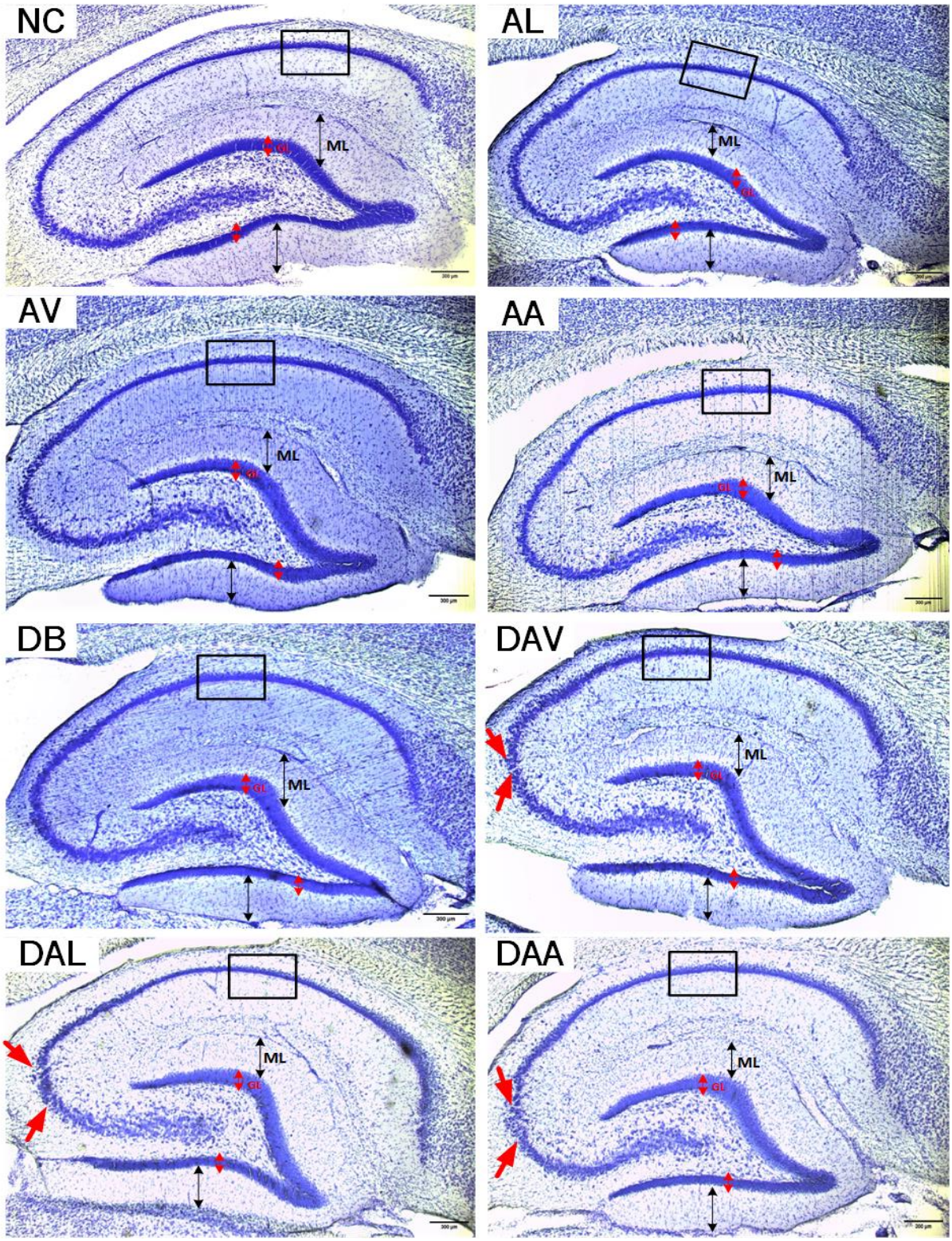

Figure 7. 5. Photomicrographs of the dorsal hippocampus across different experimental groups. Squares: region captured at higher magnification for CA1 histomorphology, disrupted CA3 region (red arrows); molecular layer (ML) of dentate gyrus (double black arrow); granular layer (GL) of dentate gyrus (double red arrow). Scale bar 300µm, X25. NC: Control, AV: cART, AL: alcohol, AA: cART and alcohol, DB: diabetic, DAV: diabetic and cART, DAL: diabetic and alcohol, DAA diabetic cART and alcohol.

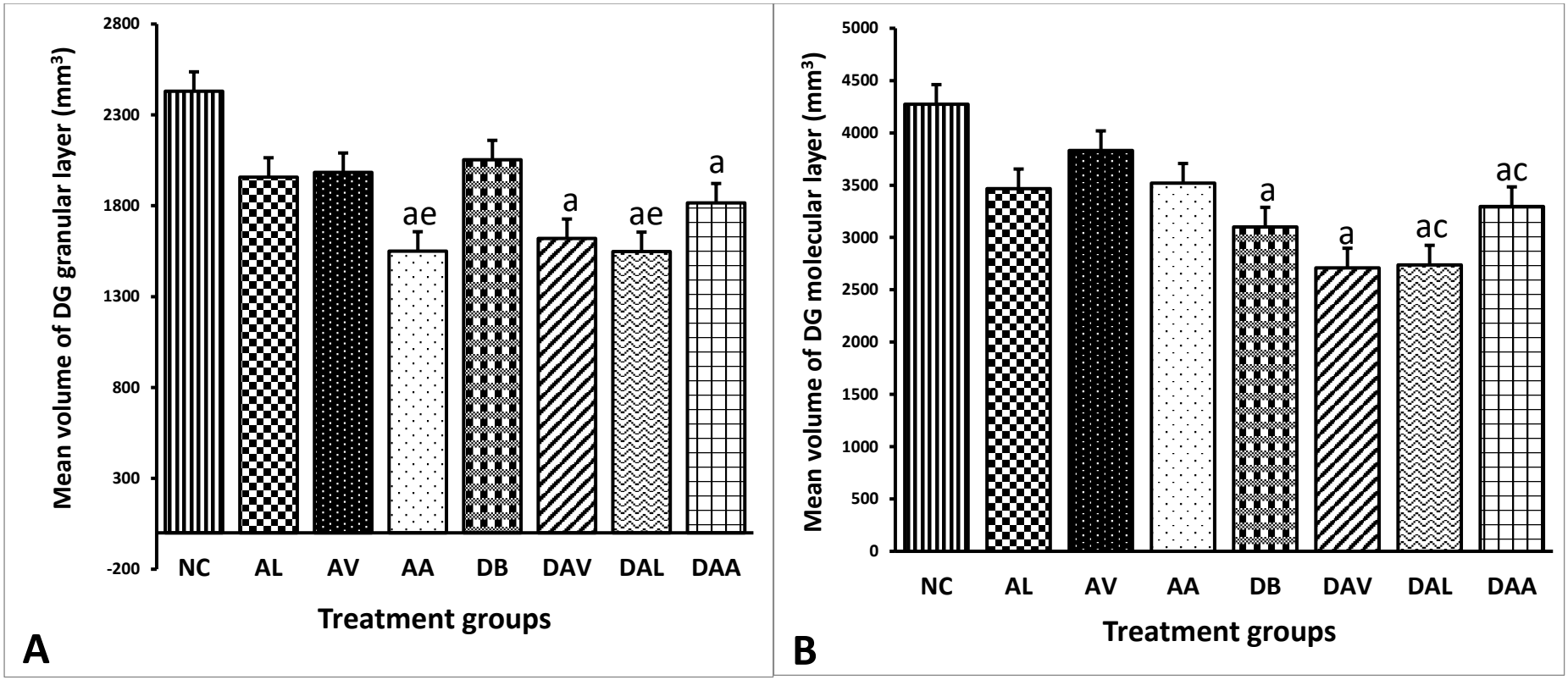

Figure 7. 6. Mean volume of granular and molecular layers in the dentate gyrus of dorsal hippocampal sections. Significant difference in VDGGL and VDGML (Kruskal Wallis test P=0.05 and 0.025 respectively). **A)** AA and DAL are significantly decreased compared to control (P=0.018 and 0.026) and DB (P=0.022 and 0.032), while DAV and DAA are significantly decreased compared to control (P= 0.05). **B)** DAL and DAA are significantly reduced compared to control (P= 0.002 and 0.007) and AV (P=0.009 and 0.022), while DB and DAV are significantly decreased compared to control (P= 0.022 and 0.05). a' (NC), 'b' (AL), 'c' (AV), 'd' (AA), 'e' (DB), 'f' (DAV), 'g' (DAL), 'h' (DAA); indicates significant differences compared to groups in bracket ( ), P< 0.05. n=6. Key: NC: Control, AV: cART, AL: alcohol, AA: cART and alcohol, DB: diabetic, DAV: diabetic and cART, DAL: diabetic and alcohol, DAA diabetic cART and alcohol.

7.3.7.2 Mean number of neurons in different hippocampal regions

Photomicrographs in figures 7.7, 7.8, and 7.9 show histomorphology of neurons at each hippocampal region in each treatment group. The estimated number of neurons in different hippocampal regions were significantly reduced, mostly in the diabetic groups (DB, DAV, DAL, and DAA) compared to other groups as shown in figure 7.10A; 7.11A and 7.12A.

In the CA1 region a uniform row of principal cells (circles, Fig. 7.7) and few peripheral glial cells (black arrows, Fig 7.7) are seen in the NC group, followed closely by the AA, and AV groups (Fig 7.7). The CA1 neuronal number in the AL and DB groups was significantly reduced compared to control. Similarly, in the diabetic co-morbidity groups (DAV, DAL, and DAA) CA1N was significantly reduced compared to the control, AL, AV, and AA groups ($P=0.05$; Fig. 7.10A) with a thin row of neurons, more glial, and some pyknotic cells (red arrows, Fig. 7.7) observed especially in the DAA group (Fig. 7.7).

In the CA3 region, a dense cluster of round neurons with few glial cell nuclei are observed in the control group, a slightly similar histology was observed in the AA, and AV groups (Fig 7.8). There number of neurons in the CA3 is significantly reduced in the DAV and DAL groups (compared to control, AV, and AA) and DAA group (compared to control, AV, AA, DB, and DAV) (Fig. 7.11A, $P<0.05$). Additionally, the neurons in the diabetic comorbidity groups (DAV, DAL, and DAA) appeared dispersed diffused with few cells pyknotic (red arrows, Fig. 7.8).

In the DG region, a wide and dense layer of granular cell neurons are observed in the control group (Fig. 7.9) with significant reduction in neuronal number in all the experimental groups compared to the control ($P<0.05$, Fig. 7.12A). The DAV group is the most severely affected with significantly reduced DG neuronal number relative the control (NC), AL, AV, AA and DAA groups (Fig. 7.12A, $P< 0.05$), followed by the DAL which showed increased glial cells

and apoptotic disruption of the sub granular region of the dentate gyrus (double edge arrows; Fig. 7.9).

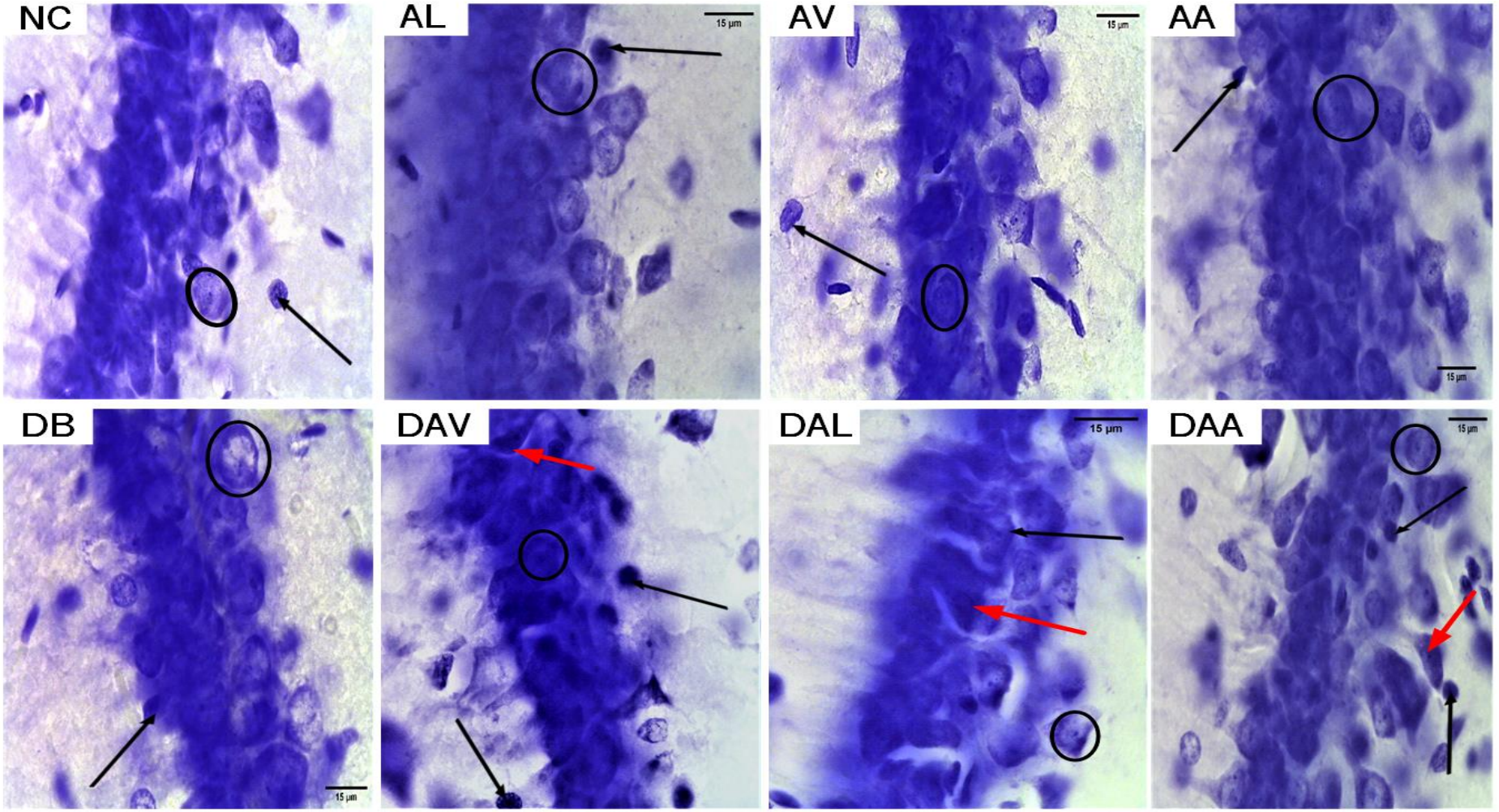

Figure 7. 7 Photomicrographs of the CA1 region in the dorsal hippocampus across different experimental groups. Circles indicate area of neuronal nuclei, black arrows indicate glial cells, red arrows indicate pyknotic nuclei of neurons Scale bar 15µm X1000. NC: Control, AV: cART, AL: alcohol, AA: cART and alcohol, DB: diabetic, DAV: diabetic and cART, DAL: diabetic and alcohol, DAA diabetic cART and alcohol.

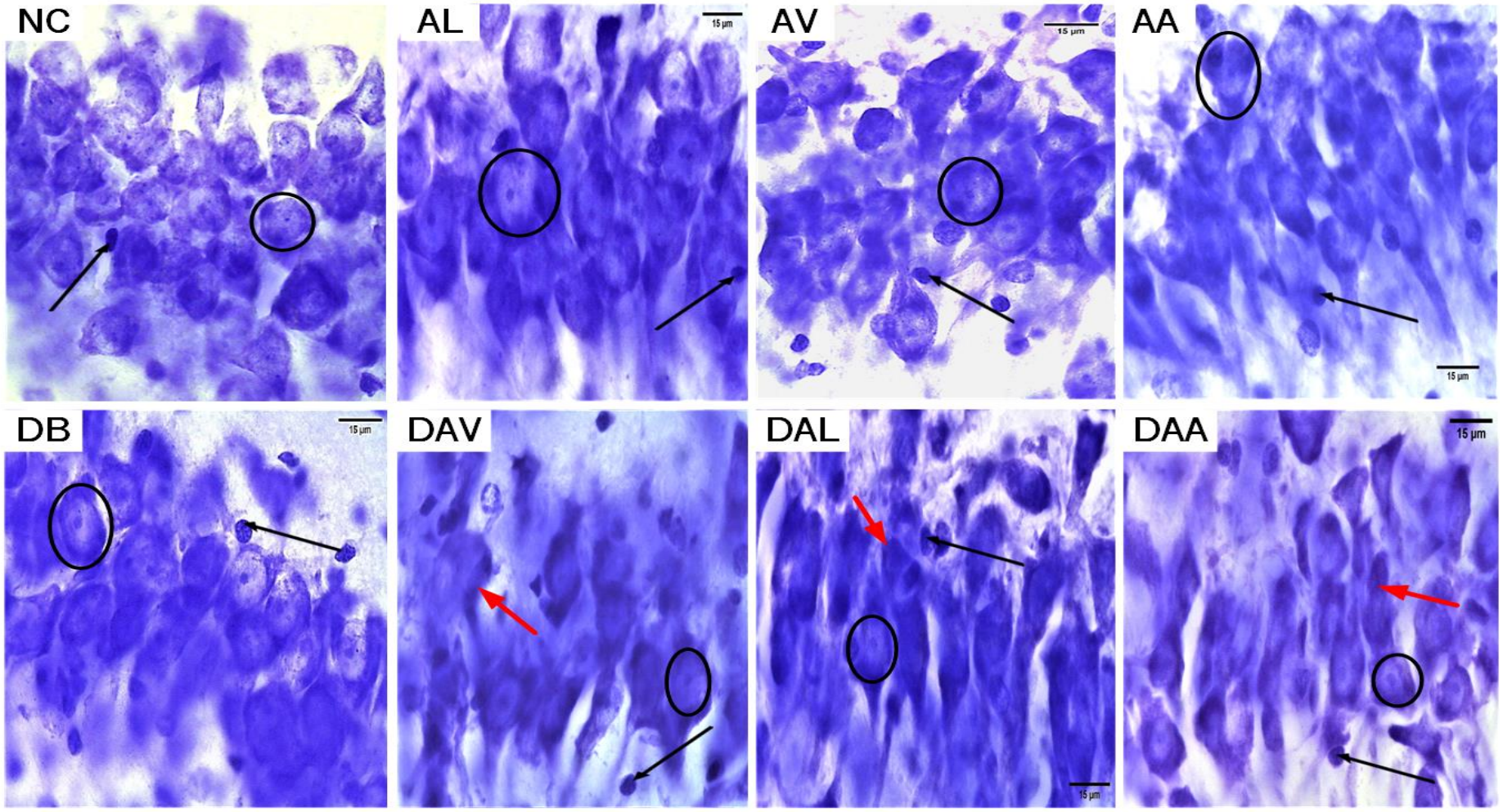

Figure 7. 8. Photomicrographs of the CA3 region in the dorsal hippocampus across different experimental groups. Circles indicate area of neuronal nuclei, black arrows indicate glial cells, red arrows indicate pyknotic nuclei of neurons Scale bar 15µm X1000. NC: Control, AV: cART, AL: alcohol, AA: cART and alcohol, DB: diabetic, DAV: diabetic and cART, DAL: diabetic and alcohol, DAA diabetic cART and alcohol.

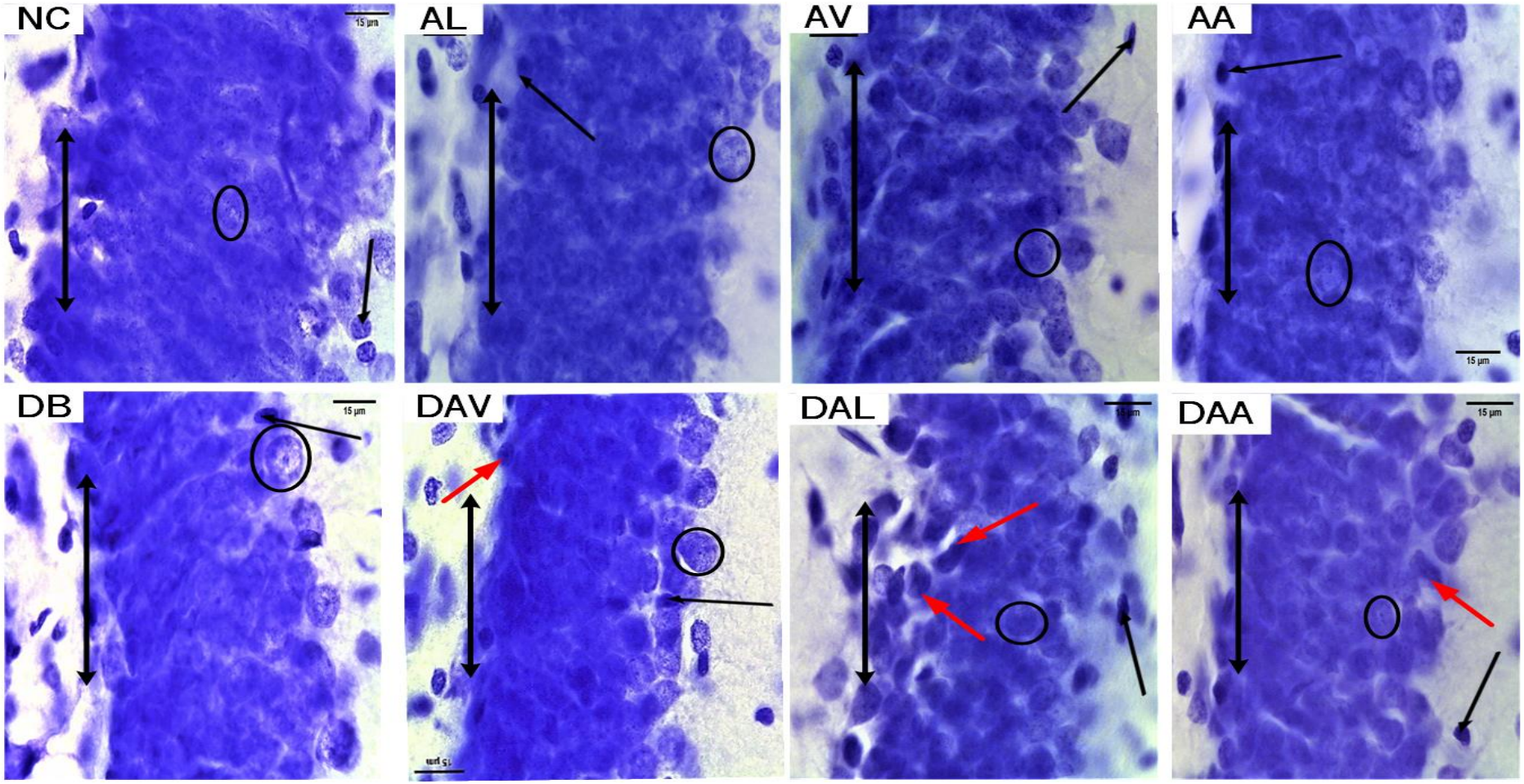

Figure 7. 9. Photomicrographs of the DG region in the dorsal hippocampus across different experimental groups. Circles indicate area of neuronal nuclei, black arrows indicate glial cells, red arrows indicate pyknotic nuclei of neurons, double sided arrow indicate sub-granular zone. Scale bar 15µm X1000. NC: Control, AV: cART, AL: alcohol, AA: cART and alcohol, DB: diabetic, DAV: diabetic and cART, DAL: diabetic and alcohol, DAA diabetic cART and alcohol.

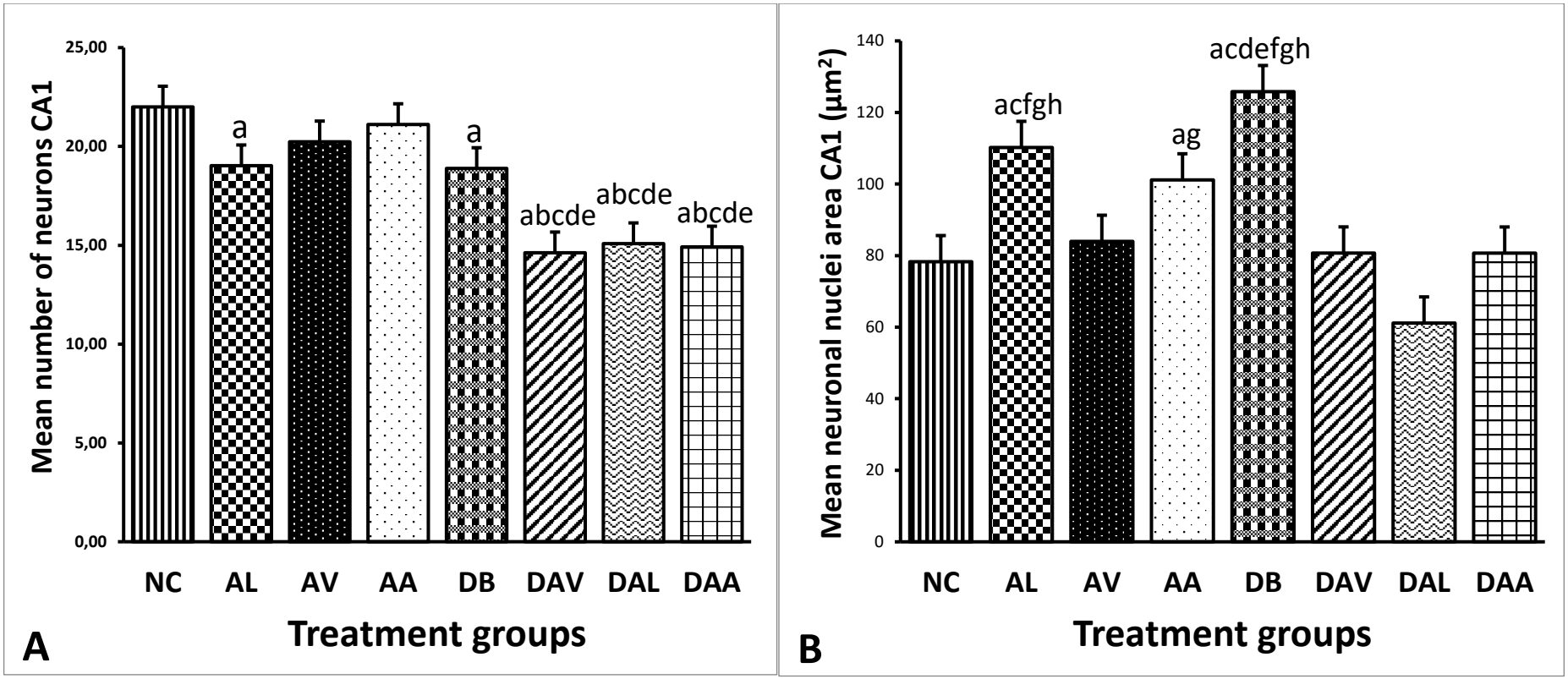

Figure 7. 10. Mean neuronal number and mean nuclei area in CA1 region of the dorsal hippocampus. Significant difference between neuronal nuclei area and neuronal number across groups (One-way ANOVA, P= 0.001). **A)** DAV, DAL and DAA are significantly reduced compared to control, AL, AV, AA and DB (P= 0.001). AL and DB are significantly decreased compared to control (P=0.007 and 0.004) **B)** AL is significantly increased compared to control, AV, DAV, DAL, and DAA (P= 0.001, 0.009, 0.003 and 0.001). AA is significantly increased compared to control and DAL (P= 0.049 and 0.001), DB is significantly increased compared to control, AV, AA, DAV, DAL, and DAA (P=0.023 and 0.001 respectively). a' (NC), 'b' (AL), 'c' (AV), 'd' (AA), 'e' (DB), 'f' (DAV), 'g' (DAL), 'h' (DAA); indicates significant differences compared to groups in bracket ( ), P< 0.05. n=6. Key: NC: Control, AV: cART, AL: alcohol, AA: cART and alcohol, DB: diabetic, DAV: diabetic and cART, DAL: diabetic and alcohol, DAA diabetic cART and alcohol.

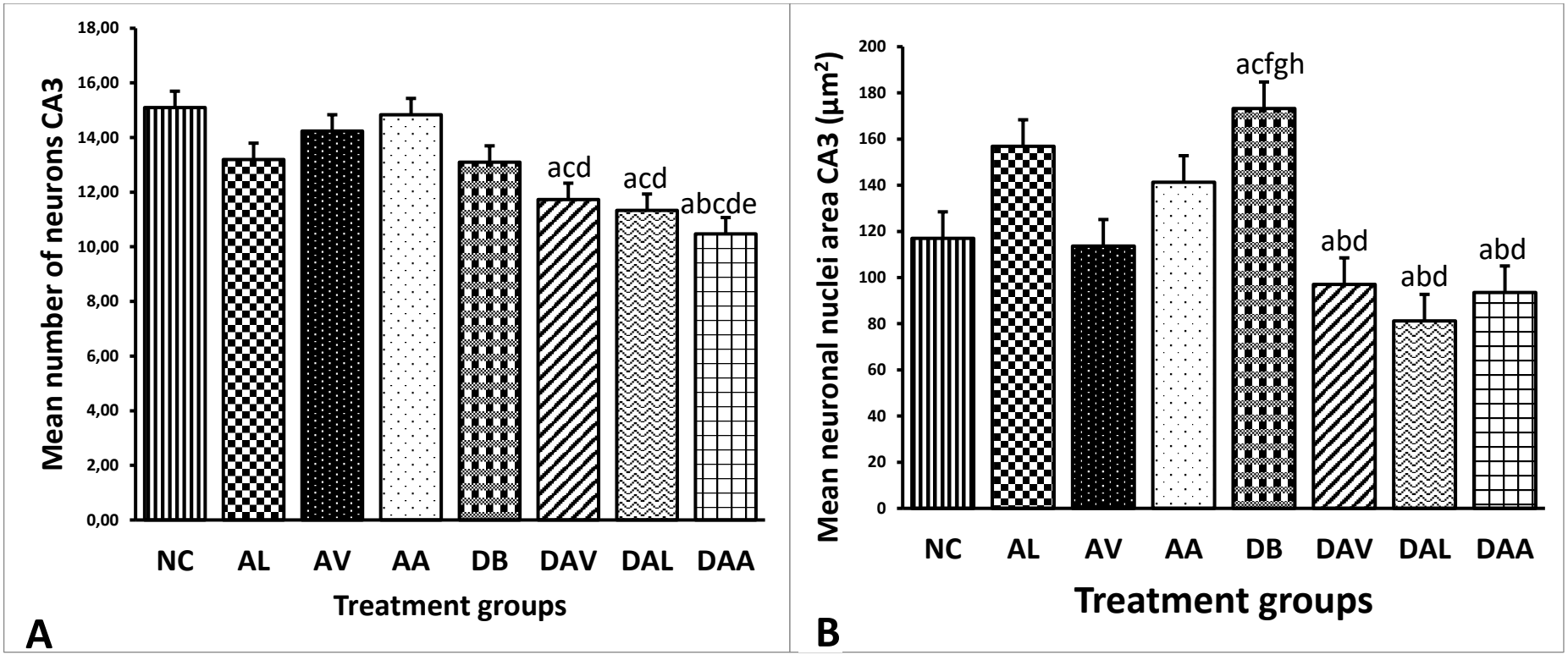

Figure 7. 11. Mean neuronal number and mean nuclei area in CA3 region of the dorsal hippocampus. Significant difference in neuronal number across groups (One-way ANOVA, P= 0.001). **A)** DAV and DAL are significantly reduced compared to control (P=0.001), AV (P= 0.016 and 0.005) and AA (P= 0.001), while DAA is significantly reduced compared to control, AL, AV, AA and DB (P= 0.001, 0.013, 0.001, 0.001 and 0.019). **B)** DB is significantly increased compared to control, AV, DAV, DAL and DAA (P=0.003, 0.001, 0.001, 0.001, and 0.001 respectively). DAV, DAL and DAA are significantly reduced compared to the control (P= 0.007, 0.003, and 0.001), AL (P= 0.001) and AA (P= 0.038, 0.001 and 0.019). a' (NC), 'b' (AL), 'c' (AV), 'd' (AA), 'e' (DB), 'f' (DAV), 'g' (DAL), 'h' (DAA); indicates significant differences compared to groups in bracket ( ), P< 0.05. n=6. Key: NC: Control, AV: cART, AL: alcohol, AA: cART and alcohol, DB: diabetic, DAV: diabetic and cART, DAL: diabetic and alcohol, DAA diabetic cART and alcohol.

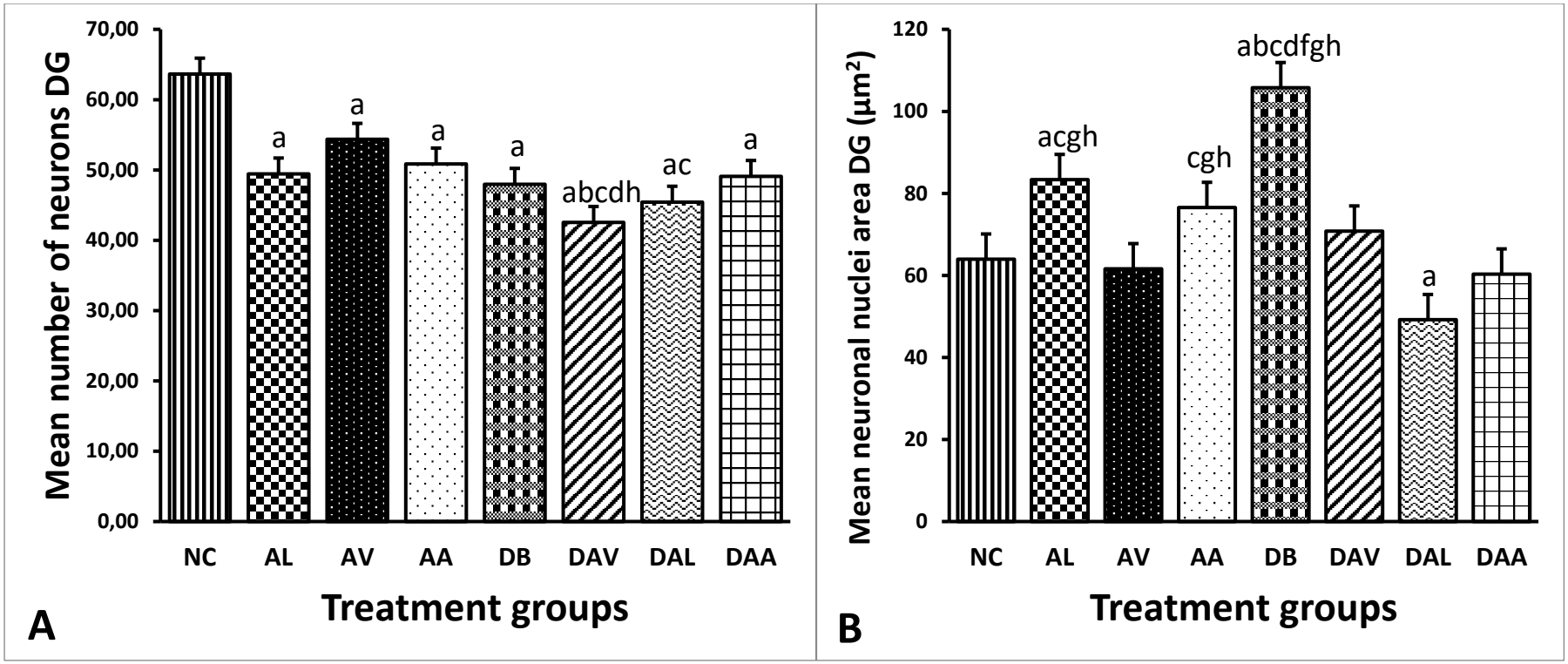

Figure 7. 12. Mean neuronal number and mean nuclei area in the dentate gyrus region of the dorsal hippocampus. Significant difference between neuronal nuclei area and neuronal number across groups (One-way ANOVA, P= 0.001). **A)** AL, AV, AA, DB and DAA are significantly reduced compared to control (P= 0.001). DAL is significantly decreased compared to control and AV (P= 0.001 and 0.003). DAV is significantly decreased compared to control, AL, AV, AA and DAA (P= 0.001, 0.033, 0.001, 0.004 and 0.044 respectively) **B)** AL is significantly increased compared to control, AV, DAL and DAA (P= 0.001). AA is significantly increased compared to AV, DAL and DAA (P=0.034, 0.001 and 0.001 respectively). DB is significantly decreased compared to AL, AV, AA, DAV, DAL and DAA (P=0.001). DAL is significantly decreased compared to the control (P= 0.035). a' (NC), 'b' (AL), 'c' (AV), 'd' (AA), 'e' (DB), 'f' (DAV), 'g' (DAL), 'h' (DAA); indicates significant differences compared to groups in bracket ( ), P< 0.05. n=6. Key: NC: Control, AV: cART, AL: alcohol, AA: cART and alcohol, DB: diabetic, DAV: diabetic and cART, DAL: diabetic and alcohol, DAA diabetic cART and alcohol.

7.3.7.3 Mean neuronal nuclei in different hippocampal regions

The neuronal nuclei area measurements in different hippocampal regions are illustrated in figures 7.7 to 7.9. The neuronal nuclei area at all hippocampal regions are significantly increased in the DB group compared to the control (NC), AV, DAV, DAL and DAA groups (P= 0.05, Fig. 7.10B to 7.12B), with observed enlarged nuclei and cell body in neurons at all the hippocampal regions of the DB groups (circles, Fig. 7.7 to 7.9). In the AL group, neuronal nuclei area significantly increased compared to the control, AV, DAV, DAL and DAA groups at the CA1 and DG regions (P= 0.05, Fig. 7.10B and 7.12B). Additionally, neuronal nuclei area in the AA groups is significantly increased in the CA1 region (compared to control and DAA groups) and in the DG region (compared to AV, DAL and DAA) (P= 0.05, Fig. 7.10B and 7.12B). These increased neuronal nuclei area in the AL and AA were observed as large round and vesicular nuclei which form a slightly wider layer of cells despite the decreased number of neurons especially in the AL group (circles, Fig. 7.7 and 7.9). Furthermore, the neurons and neuronal cell body in the diabetic co-morbidity groups (DAV, DAL, and DAA) appear diffuse and irregularly shaped especially in the DG sub granular layer (black double arrow, Fig. 7.9) of the DAL group and in the CA1 and CA3 region of the DAV group with a dark and pyknotic appearance (red arrows, Fig. 7.7 to 7.9).

7.3.8 Immunohistochemical expression of hippocampal Double Cortin

Quantification of immunolabelled cell bodies expressing DCX is presented in figure 7.13. The AL, DB, and DAA treated groups showed significantly less DCX expressing neurons compared to the control, AV and AA groups, while the DAV and DAL groups expressed significantly less DCX compared to all other groups except in comparison each other (P< 0.05, Fig. 7.13), but DCX expression levels in AV and AA was not significantly affected. The photomicrographs in figures 7.14 and 7.15 illustrate immunolabelling of DCX in the cell body and processes of dentate gyrus neurons across different treatment groups. The several areas

(black arrows, Fig 7.14) of DCX immunolabelling is observed in the control group, with similar observations in the AV and AA groups. Few DCX expressing neurons were detected in the DB and DAA groups with further minimal expression in the AL, DAV, and DAL groups (black arrows, Fig. 7.14). The apex of the dentate gurus (squares, Fig. 7.14) was captured at higher magnification (inserts, Fig 7.14) and presented in figure 7.15. In higher magnification, high amount of DCX is expressed in single neuronal processes (black arrows, Fig. 7.15) of the control and AA groups but waning DCX expression in neuronal processes was observed in the AV group followed by the DB and then DAA groups, but no expression was observed in the AL and DAL treated groups. A similar pattern of DCX expression was observed in clusters of neuronal processes in these groups (red arrows, Fig. 7.15). Additionally, numerous neuronal cells bodies expressed DCX (circles, Fig. 7.15) in the control follow by the AV, AA, AL, DB and DAA with scanty individual DCX immunolabelled cells observed in the AL and DAL groups.

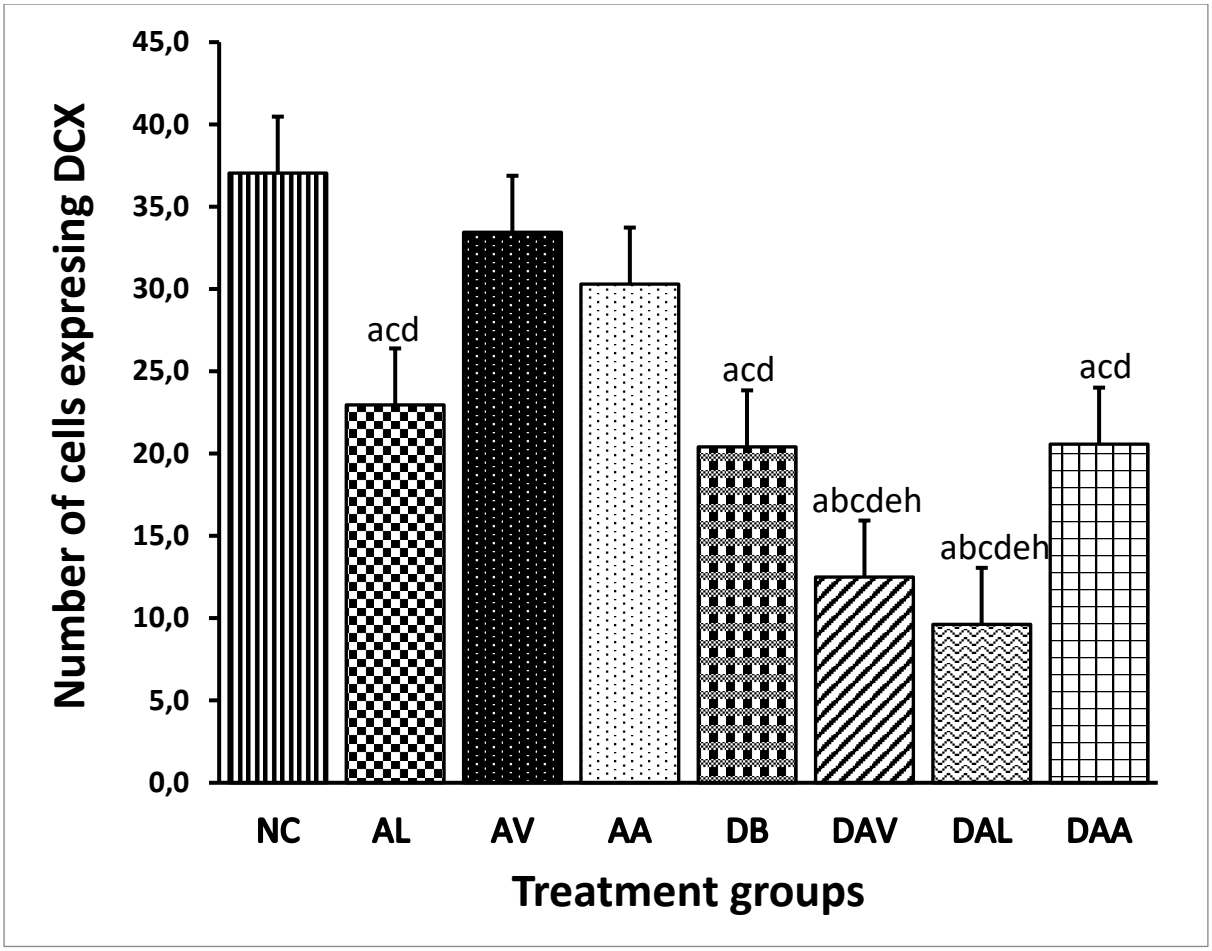

Figure 7. 13. Mean number of neurons expressing DCX in the dentate gyrus region of the dorsal hippocampus. Significant difference in expression of DCX between groups (One Way ANOVA, P=0.001). AL, DB and DAA are significantly decreased compared to control (P= 0.001), AV (P=0.001), and AA (P= 0.024, 0.001 and 0.001). DAV and DAL are significantly decreased compared to control, AL, AV, AA, DB and DAA groups (P= 0.001 and 0.11). a' (NC), 'b' (AL), 'c' (AV), 'd' (AA), 'e' (DB), 'f' (DAV), 'g' (DAL), 'h' (DAA); indicates significant differences compared to groups in bracket ( ), P< 0.05. n=6. Key: NC: Control, AV: cART, AL: alcohol, AA: cART and alcohol, DB: diabetic, DAV: diabetic and cART, DAL: diabetic and alcohol, DAA diabetic cART and alcohol.

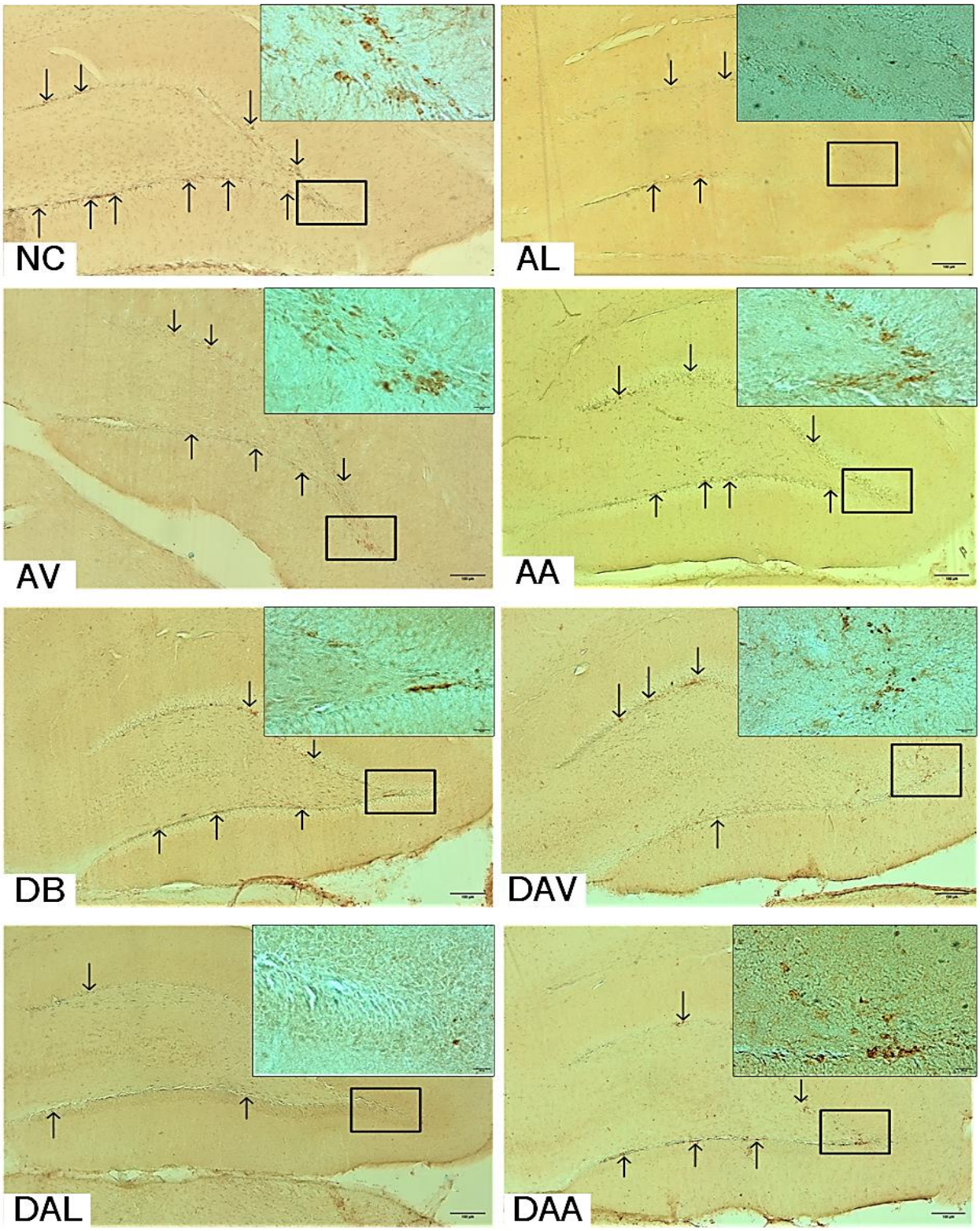

Figure 7. 14. Representative photomicrographs illustrating expression of DCX in the dentate gyrus region of the dorsal hippocampus. Arrows indicate areas of DCX expression, X50 scale bar 100µm, square indicate area captured at higher magnification X400 scale bar 100µm. Key: NC: Control, AV: cART, AL: alcohol, AA: cART and alcohol, DB: diabetic, DAV: diabetic and cART, DAL: diabetic and alcohol, DAA diabetic cART and alcohol.

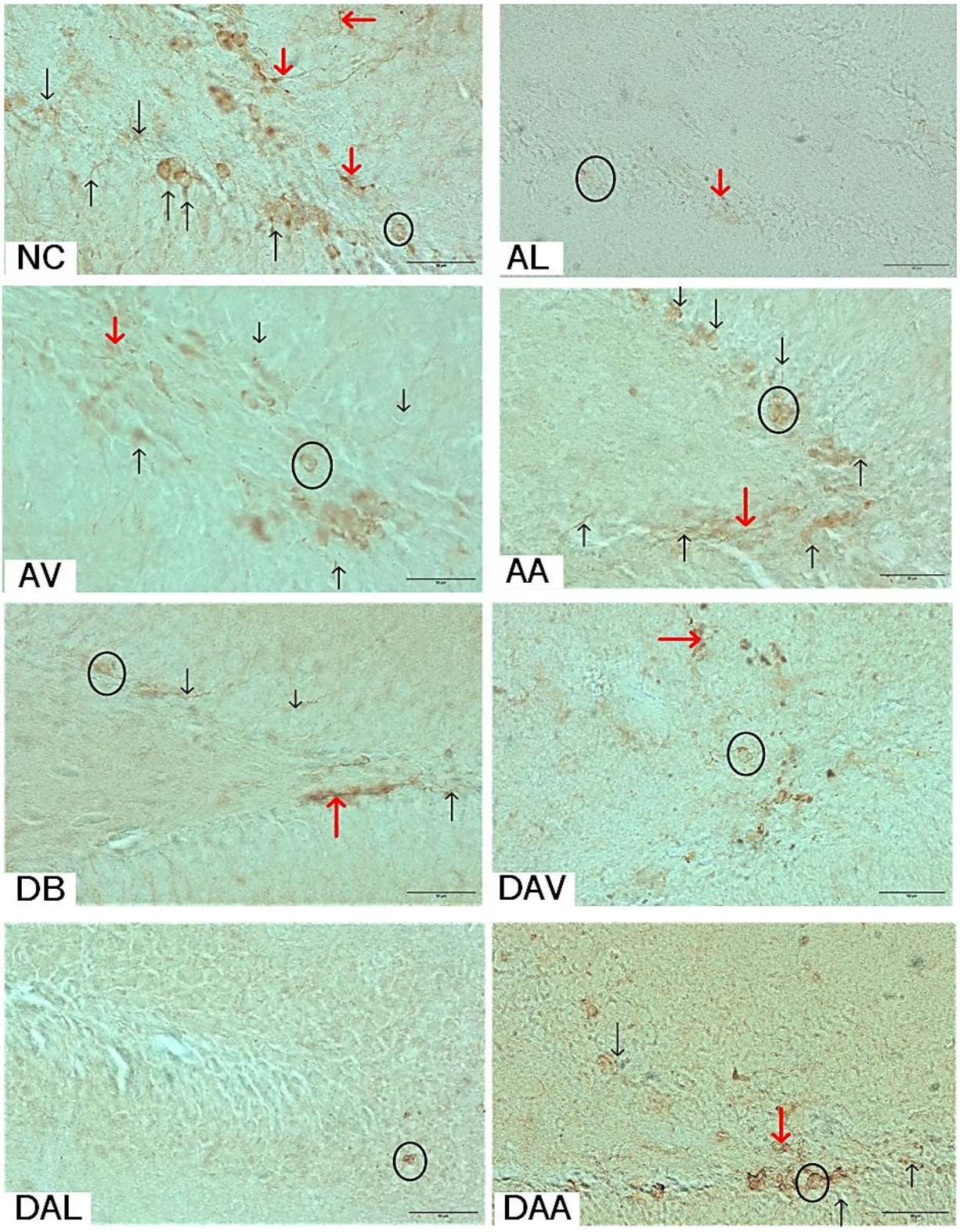

Figure 7. 15 Representative photomicrographs illustrating expression of DCX in the dentate gyrus region of the dorsal hippocampus. Circles, black arrows, and red arrows indicate cells bodies, single process and several combined processes expressing DCX respectively. Scale bar 50µm X400. Key: NC: Control, AV: cART, AL: alcohol, AA: cART and alcohol, DB: diabetic, DAV: diabetic and cART, DAL: diabetic and alcohol, DAA diabetic cART and alcohol.

7.3.9 Immunohistochemical expression of hippocampal Ki67

Figure 7.16 represents quantification of Ki67 expression across different treatment groups. All the treated animals express less Ki67 significantly in all groups except the AV group compared to the control. The DAL and DAV groups express significantly less Ki67 compared to the AV group ($P < 0.05$, Fig. 7.16). The photomicrographs in figures 7.17 and 7.18 illustrate immunolabelling of Ki67 clusters in the dentate gyrus across different treatment groups. Several areas are immunoreactive for Ki67 (black arrows, Fig. 7.17) in the control group, which is slightly similar to the AV group. Areas expressing Ki67 is reduced in other experimental groups with the most minimal Ki67 expression in the DAL and DAA groups. The apex of the dentate gurus (squares, Fig. 7.17) is captured at higher magnification (inserts, Fig. 7.17) and presented in figure 7.18. In higher magnification, a couple of Ki67 expressed clusters were observed in the control group, individual clusters in other treated groups (black arrows, Fig. 7.18) except the DAL group where no Ki67 expression was observed.

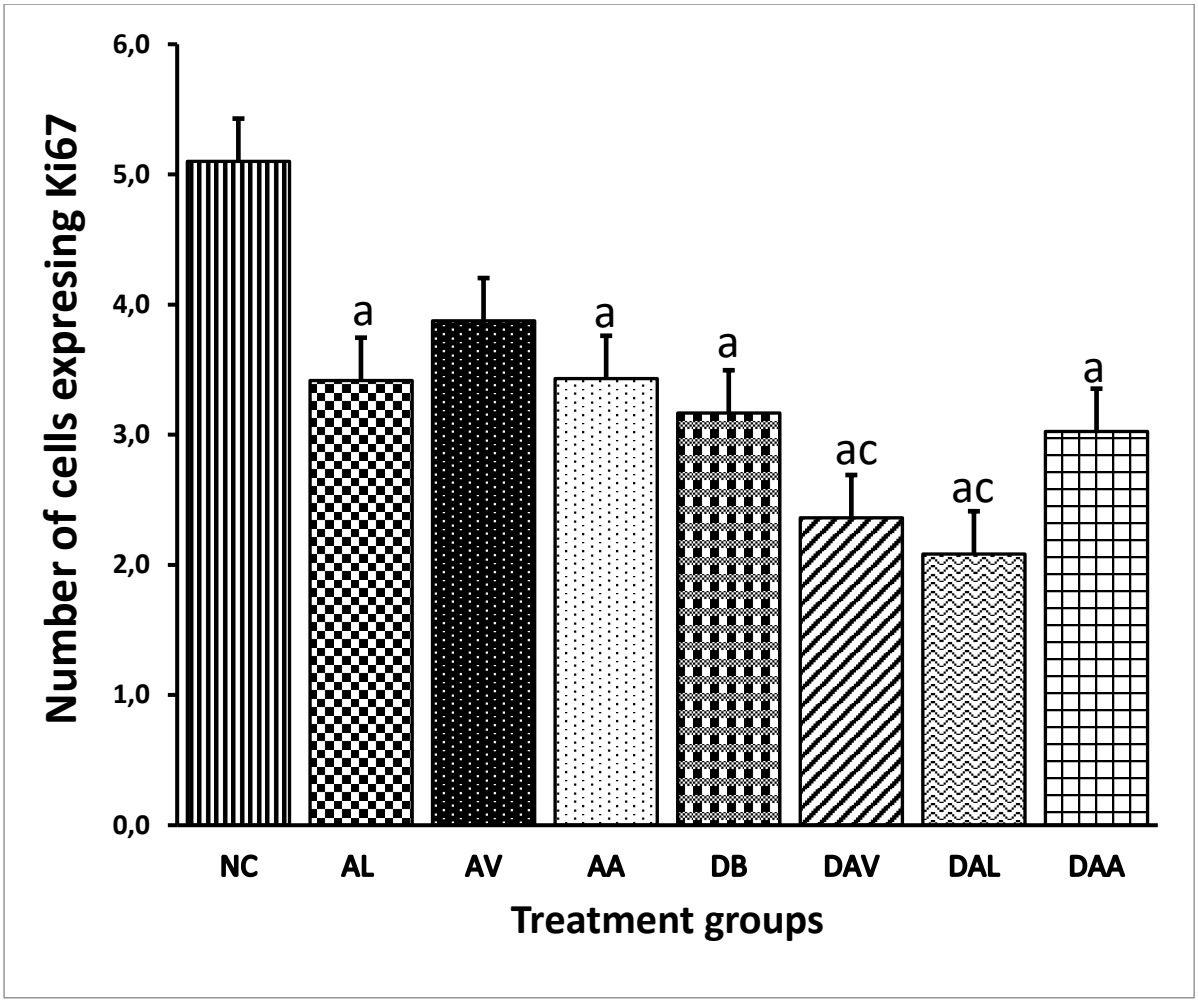

Figure 7. 16. Mean number of neurons expressing Ki67 in the dentate gyrus region of the dorsal hippocampus. Significant difference in expression of DCX between groups (One Way ANOVA, P=0.001). AL, AA, DB, and DAA are significantly decreased compared to the control (P= 0.009, 0.010, 0.002, and 0.001 respectively). DAV and DAL is significantly decreased compared to control (P= 0.001) and AV (P= 0.039 and 0.009). a' (NC), 'b' (AL), 'c' (AV), 'd' (AA), 'e' (DB), 'f' (DAV), 'g' (DAL), 'h' (DAA); indicates significant differences compared to groups in bracket ( ), P< 0.05. n=6. Key: NC: Control, AV: cART, AL: alcohol, AA: cART and alcohol, DB: diabetic, DAV: diabetic and cART, DAL: diabetic and alcohol, DAA diabetic cART and alcohol.

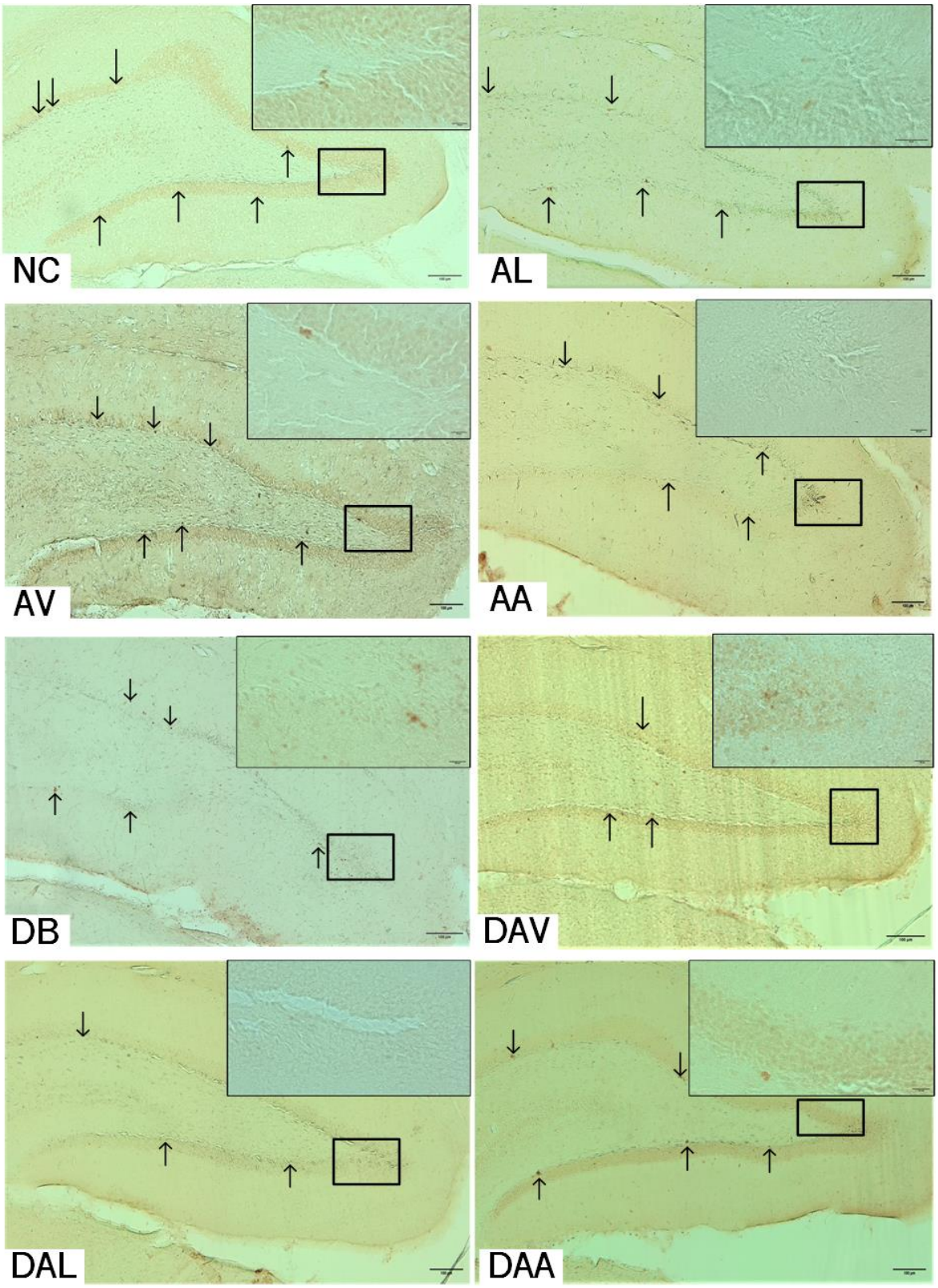

Figure 7. 17. Representative photomicrographs illustrating expression of Ki67 in the dentate gyrus region of the dorsal hippocampus. Arrows indicate areas of Ki67 expression, X50 scale bar 100µm, square indicate area captured at higher magnification X400 scale bar 100µm. Key: NC: Control, AV: cART, AA: alcohol, AA: cART and alcohol, DB: diabetic, DAV: diabetic and cART, DAL: diabetic and alcohol, DAA diabetic cART and alcohol.

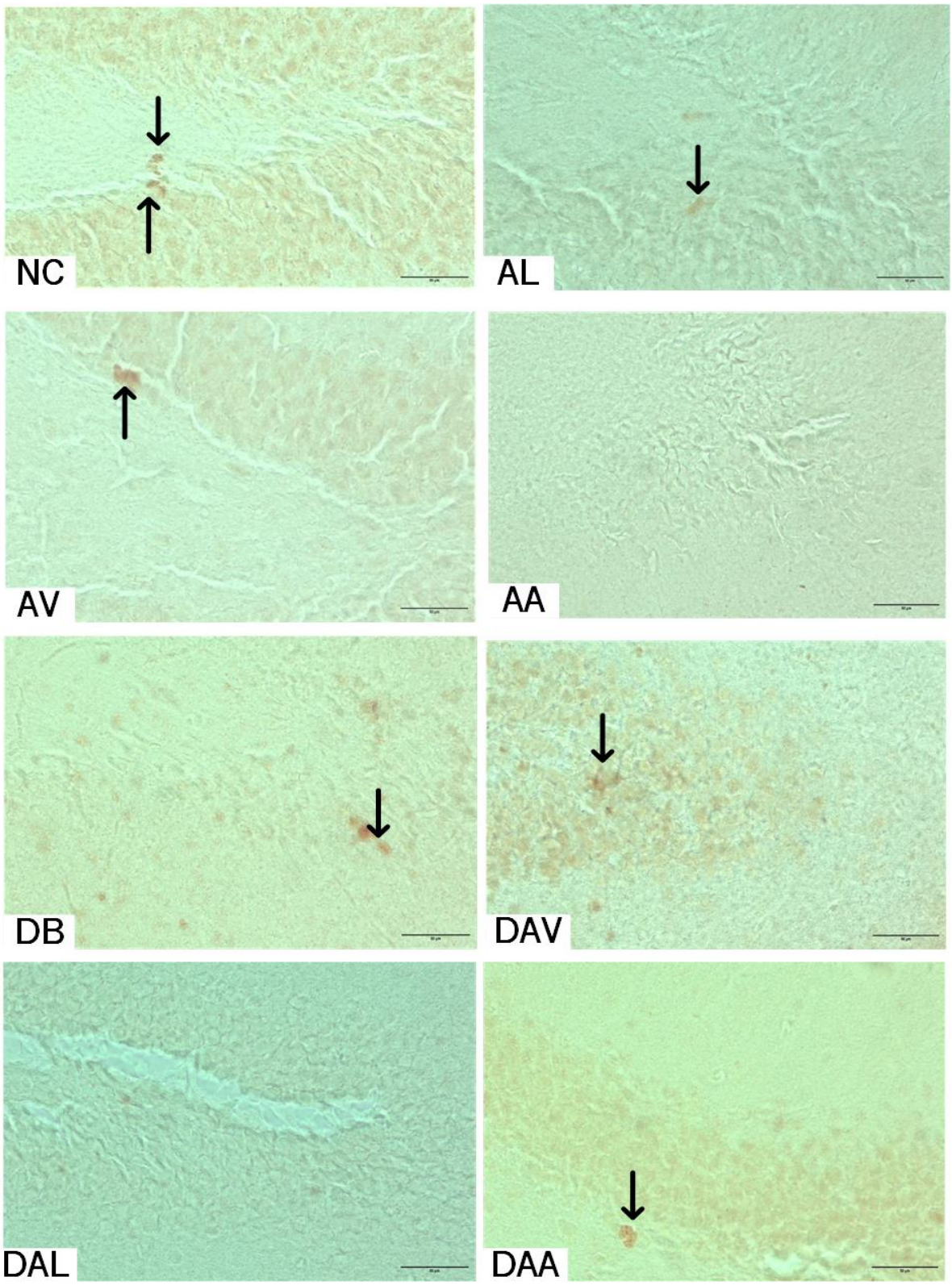

Figure 7. 18. Representative photomicrographs illustrating expression of Ki67 in the dentate gyrus region of the dorsal hippocampus. Black arrows indicate clusters of cells expressing Ki67. Scale bar 50µm X400. Key: NC: Control, AV: cART, AL: alcohol, AA: cART and alcohol, DB: diabetic, DAV: diabetic and cART, DAL: diabetic and alcohol, DAA diabetic cART and alcohol.

7.3.10 Relationship between parameters

Spearman's correlation coefficient reveals that proinflammatory cytokines (TNF-α, IL1-α, and IL6) negatively correlated with diabetic parameters (NFBG and AUC) but positively corelated with each other and with INSR, while IRS1 is positively correlated with INSR (Table 7.3). Further correlation analysis as shown in table 7.4 reveals that number of neurons (CA1N, CA3N and DGN) positively correlated with oxidative stress (MDA and GPx), neurogenesis (DCX and Ki67) and apoptotic genes (BAX and Caspase-3) at $P > 0.05$. Secondly, neurogenesis markers negatively correlated with diabetic parameters, oxidative stress, and Caspase-3 but positively correlated with neuronal nuclei area in CA3. Thirdly, IRS1 negatively correlated with number of neurons in CA1 and CA3 and neuronal nuclei area in CA1, CA3 and DG but positively correlated with apoptotic genes (Bcl_2, BAX and Caspase-3), INSR and volume of dentate gyrus molecular layer (VDGML). Fourthly, VDGML is positively correlated to oxidative stress, neurogenesis, number of neurons and neuronal nuclei area CA3A, but negatively correlated with diabetic parameters, and apoptotic genes. Finally, apoptotic genes positively correlated with oxidative stress, CA1N, CA3N, and CA3A, but negatively correlated with DCX (Table 7.4).

Table 7. 3. Spearman's rho correlation of diabetes parameters with proinflammatory cytokines, BBB genes and insulin receptor genes.

		Diabetic parameters		**Pro-inflammatory cytokines**			**BBB genes**		**Insulin receptor genes**	
		NFBG	AUC	TNF-α	IL1-α	IL6	CLDN5	OCLDN	INSR	IRS
AUC	R value	0.746**	--							
	P value	0,000								
TNF-α	R value	-0.786**	-0.601**	--						
	P value	0,000	0,002							
IL1-α	R value	-0.718**	-0.501*	0.812**	--					
	P value	0,000	0,013	0,000						
IL6	R value	-0.706**	-0.559**	0.822**	.922**	--				
	P value	0,000	0,005	0,000	0,000					
CLDN5	R value	-0,219	0,144	0,122	0,135	0,074	--			
	P value	0,304	0,501	0,569	0,528	0,731				
OCLDN	R value	-0,350	-0,270	0,245	0,324	0,325	0,285	--		
	P value	0,093	0,201	0,249	0,122	0,122	0,177			
INSR	R value	-0,305	-0,103	0.480*	0.614**	0.599**	0,287	0.667**	--	
	P value	0,147	0,632	0,017	0,001	0,002	0,174	0,000		
IRS	R value	0,159	0,277	0,058	0,160	0,062	0.535**	0,360	0.498*	--
	P value	0,457	0,190	0,788	0,456	0,773	0,007	0,084	0,013	

Key: NFBG; non-fasting blood glucose, AUC; area under the OGTT curve, CLDN5; claudin-5, OCLDN; occludin, INSR; insulin receptor, IRS1; insulin receptor substrate. '*' and '**" Significant correlation ($p < 0.05$ and 0.01 respectively), R value; Correlation Coefficient.

Table 7. 4. Spearman's rho nonparametric correlation of diabetes parameters, oxidative stress, neuronal histomorphology, neurogenesis, apoptotic genes, BBB genes and insulin receptor genes.

		Diabetic parameters		Oxidative stress		Dentate gyrus volume		Neuronal number and nuclei area						Neurogenesis		Apototic genes			Insulin receptor genes	
		NFBG	AUC	GPX	MDA	DGGL	DGML	CIN	CIA	C3N	C3A	DGN	DGA	DCX	Ki67	Bcl2	BAX	CASP3	INSR	IRS
AUC	R value	0,746**	--																	
	P value	0,000																		
GPX	R value	-0,611**	-0,637**	--																
	P value	0,002	0,001																	
MDA	R value	0,314	0,470*	-0,550**	--															
	P value	0,135	0,021	0,005																
DGGL	R value	-0,154	-0,170	0,310	-0,186	--														
	P value	0,471	0,428	0,141	0,384															
DGML	R value	-0,526**	-0,716**	,795**	-,437*	0,358	--													
	P value	0,008	0,000	0,000	0,033	0,086														
C1N	R value	-0,684**	-0,760**	,669**	-,615**	0,30862	,683**	--												
	P value	0,000	0,000	0,000	0,001	0,142	0,000													
C1A	R value	-0,081	-0,179	0,362	-0,238	,405*	0,359	,521**	--											
	P value	0,706	0,402	0,082	0,263	0,050	0,085	0,009												
C3N	R value	-0,398	-,518**	,492*	-,626**	0,391	,575**	,832**	,601**	--										
	P value	0,054	0,010	0,015	0,001	0,059	0,003	0,000	0,002											
C3A	R value	-0,324	-0,348	,492*	-,423*	0,307	,408*	,675**	,835**	,672**	--									
	P value	0,122	0,096	0,015	0,040	0,145	0,048	0,000	0,000	0,000										
DGN	R value	-,579**	-,594**	,470*	-,459*	,437*	,632**	,796**	0,275	,748**	0,289	--								
	P value	0,003	0,002	0,020	0,024	0,033	0,001	0,000	0,194	0,000	0,171									
DGA	R value	0,080	0,089	0,235	-0,242	0,329	0,127	0,292	,816**	,422*	,783**	0,037	--							
	P value	0,710	0,680	0,268	0,254	0,117	0,555	0,166	0,000	0,040	0,000	0,865								
DCX	R value	-,565**	-,787**	,649**	-,450*	0,216	,720**	,831**	0,332	,667**	,468*	,728**	0,087	--						
	P value	0,004	0,000	0,001	0,028	0,310	0,000	0,000	0,113	0,000	0,021	0,000	0,685							
Ki67	R value	-,545**	-,408*	,642**	-,523**	0,229	,488*	,591**	0,275	,477*	,443*	,599**	0,244	,599**	--					
	P value	0,006	0,048	0,001	0,009	0,281	0,016	0,002	0,194	0,018	0,030	0,002	0,251	0,002						
Bcl2	R value	0,300	,443*	-,632**	,513*	-0,047	-,579**	-,548**	-0,324	-,490*	-,447*	-0,279	-0,402	-,478*	-0,282	--				
	P value	0,155	0,030	0,001	0,010	0,829	0,003	0,006	0,122	0,015	0,029	0,187	0,052	0,018	0,181					
BAX	R value	,439*	,700**	-,548**	,487*	-0,253	-,576**	-,767**	-,463*	-,733**	-,550**	-,610**	-0,249	-,830**	-0,377	,617**	--			
	P value	0,032	0,000	0,006	0,016	0,233	0,003	0,000	0,023	0,000	0,005	0,002	0,241	0,000	0,070	0,001				
CASP3	R value	,592**	,562**	-,644**	,552**	-0,216	-,522**	-,715**	-0,245	-,610**	-,510*	-,532**	-0,063	-,722**	-,542**	,486*	,723**	--		
	P value	0,002	0,004	0,001	0,005	0,311	0,009	0,000	0,248	0,002	0,011	0,007	0,771	0,000	0,006	0,016	0,000			
INSR	R value	-0,305	-0,103	0,063	0,309	-0,147	0,034	-0,173	-0,218	-0,324	-0,272	-0,112	-0,350	-0,142	0,145	0,202	0,367	0,219	--	
	P value	0,147	0,632	0,771	0,141	0,494	0,875	0,420	0,306	0,123	0,198	0,602	0,094	0,509	0,500	0,344	0,077	0,303		
IRS	R value	0,159	0,277	-0,354	,453*	-0,353	-,437*	-,570**	-,610**	-,687**	-,649**	-0,353	-,502*	-0,332	-0,170	,582**	,587**	,468*	,498*	--
	P value	0,457	0,190	0,090	0,026	0,090	0,033	0,004	0,002	0,000	0,001	0,091	0,012	0,113	0,426	0,003	0,003	0,021	0,013	

Key: BW; NFBG; non-fasting blood glucose, AUC; area under the OGTT curve, volume of dentate gyrus granular layer and molecular layer (VDGGL and VDGML), number of neurons (CA1N, CA3N and DGN, respectively), neuronal nuclei area (CA1A, CA3A and DGA), CASP3; Caspase-3, occludin, INSR; insulin receptor, IRS; insulin receptor substrate. '*' and '**" Significant correlation ($p < 0.05$ and 0.01 respectively), R value; Correlation Coefficient

7.4 Discussion

Hippocampal cells may respond to chemo-toxicants in different ways such as through inflammatory response, oxidative stress, endothelial and membrane disruption, neurogenic and structural changes (Huang et al., 2010; Barcia et al., 2015; Salameh et al., 2019), all with attendant effects on overall hippocampal function in cognition, behavior, and memory (Rubin et al., 2014; Yang and Wang, 2017).

Several studies have reported elevated proinflammatory cytokines (IL-6, and TNFα) independently with alcohol use (AL) and cART therapy (AV) (Qin et al., 2008; Osuji et al., 2018), which corroborates our results of elevated cytokines in these groups. However, concomitant alcohol use with cART therapy (AA) ameliorated the effects on IL-6, TNFα levels, which was significantly reduced compared to AL but not control (NC). Additionally, alcohol use in cART therapy and in diabetes (DAA) exacerbated neuroinflammation (increased IL-1α and IL-6 levels) compared to levels in AA, DB, DAV. These observations of elevated IL-6 in AL AV, and DAA groups but reduced levels in DB and DAV treated groups suggests proinflammatory and anti-inflammatory role of IL-6 respectively as previously reported (Gabay, 2006; Borsini et al., 2020). Furthermore, IL-6 can act as both a stimulator or inhibitor of insulin action in the pathogenesis of T2D (Rehman et al., 2017; Shi et al., 2019) which corroborates with the positive association observed between proinflammatory cytokines, insulin receptor (INSR), and insulin receptor substrate (IRS1); but negative association between proinflammatory cytokines and diabetic parameters (NFBG and AUC). These antagonistic effects of IL-6 are observed with reduced IL-6 in DB and DAV treated groups and may be associated with INSR and IRS1 down regulation and increased NFBG and AUC levels. However, elevated IL-6 and downregulated IRS1 (in AL and AV treated groups) but non-affected IL-6 and down regulated INSR and IRS in AA groups treated group with no associated effect on NFBG and AUC suggesting pathogenesis of central insulin resistance and but not

establishment of T2D as previously reported (Rehman et al., 2017) in the non-diabetic groups (AV, AL and AA groups).

The insulin receptors (INSR and IRS1) are expressed in neurons and endothelial cells of the blood brain barrier (BBB) as required for cognitive and synaptic function (Huang et al., 2010; Tu et al., 2021) and have also been implicated in the regulation of junctional proteins (occludin and claudin-5) (Nagano et al., 2021). Thus, the significant downregulation of claudin-5 in the AV, AA, DB, and DAV groups, is positively associated with reduced expression of IRS gene in these groups, while the reduction in occludin expression in AA and DB groups is positively associated with down-regulation of INSR which agrees with insulin receptor mediated regulation of BBB protein expression as previously reported in an invitro study (Nagano et al., 2021). However, the absence of junction protein impairment in the AL and DAL groups could arise due to the ability of alcohol to readily cross the BBB.

Also, the positive association of insulin receptor substrate (IRS1) with the apoptotic genes (BAX, Bcl_2 and Caspase-3) and negative association with neuronal cell number is consistent with IRS regulated apoptosis (Ueno et al., 2000; Walker et al., 2012). This association between IRS and apoptosis was demonstrated in the DAL and DAA group with significantly elevated expression of BAX, Bcl_2, Caspase -3 and IRS1 and may explain the significant downregulation of Bcl_2, BAX and IRS1 gene in the AA group, suggesting differential role of alcohol in the hippocampus of the diabetic and in cART therapy exposure. A finding we are reporting for the first time. Therefore, elevated expressions of apoptotic genes (BAX and Caspase) observed in the DB, DAV, and DAA groups may explain the neuronal loss recorded in CA1 (in DB, DAV, DAL and DAA groups), CA3 (in DAV, DAL and DAA groups) and DG (AL, AV, AA, DB, DAV, DAL and DAA groups). Thus, hippocampal apoptosis in the diabetes (DB) and comorbidity groups (DAV, DAL, and DAA) may arise due to the central effect of Caspase-3 as previously reported in diabetic animals (Jafari Anarkooli et al., 2008; He et al., 2018).

Furthermore, the positive association of neuronal number with apoptotic genes, oxidative stress (MDA and GPx) levels and neurogenic parameters (Ki67 and DCX), suggests that the reduction of DG neurons in the non-diabetic groups (AL, AV, and AA) may involve the presence of other pathways other than apoptotic pathway.

Moreover, neuronal loss (apoptosis) is associated with oxidative stress (MDA and GPx) in alcohol use, cART, and diabetes independently (Akay et al., 2014; Han et al., 2015; Zhang et al., 2020), which corroborates our observations in the AL, AV and DB groups. However, concomitant alcohol use with cART (AA) induced significant deficiency in GPx levels but non-significantly increased MDA level, probably suggesting minimal impact on oxidative status of these treated animal group, the diabetes comorbidity groups (DAV, DAL, and DAA) maintained the high oxidative stress observed in DB group. Therefore, the elevated oxidative stress in the diabetic comorbidity groups (DAV, DAL, and DAA) may be responsible for the significant reduction in volume of the DG granular layer (VDGGL) of these groups.

Furthermore, reduced expression of Ki67 in (AL, AA, DB, DAV, DAL, and DAA) and DCX in (AL, DB, DAV, DAL, and DAA) observed in the dentate gyrus sub granular region, illustrates impaired regenerative ability of hippocampus and consequently impaired cognitive and memory activities with alcohol use and diabetes, previously reported independently (Morris et al., 2010; Ho et al., 2013). This present study illustrates that neurogenesis observed in diabetes exacerbated with ART and alcohol co-morbidity (DAV and DAL) but maintained with multiple morbidity (DAA), indicating a partial effect of alcohol and cART interaction which ameliorated alcohol induced reduction of immature neurons.

The results also reveal different forms of cell death showing certain morphological features of both necrosis and apoptosis, a condition of aponecrosis. Thus, while features of necrosis with increased neuronal nuclei size at all hippocampal regions (Fink and Cookson, 2005; Ishunina

et al., 2019) of AL and DB treated groups, and apoptosis (shrinkage of neuronal nuclei area) in DG of the DAL group and in CA3 of diabetic comorbidity groups (DAV, DAL, and DAA) as has been reported previously (Ziegler and Groscurth, 2004; Elmore, 2007). Furthermore, in the diabetes comorbidity groups (DAV, DAL, and DAA) reduction in CA3 neuronal nuclei area, where interconnectivity (Liu et al., 2011; Cherubini and Miles, 2015) with other hippocampal regions and integration of proliferating and immature neurons occur and the reduced volume of dentate gyrus is functionally crucial, especially because of synaptic plasticity required in the dentate gyrus (Kim and Diamond, 2002; Deng et al., 2010; Lodge and Bischofberger, 2019) for optimal hippocampal function, which may greatly negatively impact overall function of cognition and memory in the hippocampus.

Therefore, alcohol use in cART therapy may interactively minimally antagonize their independent hippocampal adverse effects but may cause disruption of BBB integrity as well as INSR and IRS1 and consequently may lead to induction of T2D, resulting in diabetes, alcohol and cART multiple morbidity with its attendant negative effects on oxidative stress, impaired neurogenesis, and apoptosis especially in CA3 and neuroinflammation. This finding is clinically invaluable for PLWHA who are diabetic and indulge in alcohol intake and as well as non-diabetic patients on cART prophylaxis who consume alcohol regularly, as gradual induction of diabetes will only symptomatically manifest its adverse hippocampal effects with exacerbation after prolonged intake.

Chapter 8 Concluding discussion

This study investigated possible hippocampal anatomical pathologies that may occur in patients with co-morbidities or multiple morbidity involving type 2 diabetes, alcohol use/abuse and cART administration.

In this study, diabetes was successively induced using a low dose (40mg/Kg body weight) of STZ and 20% percent fructose enriched feed which simulates the human diabetic pathogenesis of impaired insulin secretion and dietary-induced insulin resistance. Analysis of data on diabetic parameters at the end of the experimental period revealed that FBG, NFBG, OGTT, and AUC were not affected in the experimental vehicle controls groups for STZ, fructose feed, and cART administration, but were elevated in all the diabetic groups thereby confirming successful diabetes induction. Additionally, the use of the HIV naïve model in the current study excluded the possible impact (pathologies) associated with the presence of the HIV virus on tissue-drug-disease interactions and enabled the toxicity of diabetes + alcohol + cART and other treatment combinations to be studied and documented.

8.0 Independent effects of alcohol, cART, and diabetes on hippocampal histopathology

The results show that alcohol (AL) elevated pro-inflammatory cytokines (IL-1α, IL-6 and TNF-α), oxidative stress (elevated MDA, but decreased GPx), induced necrotic swelling of neuronal nuclei at CA1 and DG hippocampal regions, and reductions in neurogenesis (Ki67 and DCX), IRS1 expression and neuronal number at CA1 and DG hippocampal regions. This alcohol-induced effect suggests induction of redox imbalance in the hippocampal tissue with alcohol treatment resulting in neuro-inflammation, reduction in neurogenesis, and neuronal number in CA1 and DG hippocampal regions, and initiation of insulin resistance due to loss of IRS1 expression which is required for intracellular response to insulin for glucose uptake.

On the other hand, cART therapy (AV) elevated pro-inflammatory cytokines (IL-6 and TNF-α), and oxidative stress (elevated MDA, and decreased GPx), but reduced the expression of claudin-5, IRS1, and neuronal number in the dentate gyrus, suggesting the potential of cART components to induce oxidative stress and impair BBB permeability, which will allow the influx of circulatory cytokines into the CNS with its attendant adverse effects. Additionally, cART is known for its potential to induce metabolic perturbations, this effect is observed with cART-induced hippocampal insulin resistance.

Furthermore, diabetes (DB) induced a wide spectrum of hippocampal pathologies, including deficit in pro-inflammatory cytokines (IL-1α, IL-6, and TNF-α), neurogenesis (Ki67 and DCX), insulin receptors (INSR and IRS1), junctional proteins (claudin-5 and occludin), volume of DG molecular layer and neuronal number at CA1 and DG hippocampal regions, but elevated, oxidative stress (elevated MDA, deficit GPx), hippocampal apoptosis (Bcl_2 and Caspase-3) and necrotic swelling of neuronal nuclei at CA1 and DG hippocampal regions suggesting hippocampal atrophy and adverse effects on hippocampal cognitive and memory functions. Furthermore, the reduction of pro-inflammatory cytokines is reminiscent of compromised immune metabolism and susceptibility of diabetic patients to infection.

8.1 The hippocampal impact of diabetes and cART interaction

Diabetes and cART interaction (DAV) induced several diabetogenic effects such as decreased pro-inflammatory cytokines (IL-1α, IL-6 and TNF-α), neurogenesis (Ki67 and DCX), IRS1, claudin-5, volume of DG molecular layer and neuronal number at CA1 and DG hippocampal regions but elevated Caspase-3 expression and oxidative stress (elevated MDA, but deficit in GPx). Furthermore, the interaction between diabetes and cART (DAV) elevated the expression of proapoptotic gene (BAX), reduced the volume of DG granular layer, induced apoptotic shrinkage of neuronal nuclei, and significantly reduced neuronal number in the CA3

hippocampus region. An exacerbated diabetic condition with elevated hyperglycemia and impaired glucose intolerance (elevated NFBG and AUC levels) were also observed in diabetes and cART (DAV) treatment relative to diabetes alone suggesting that in DAV, the diabetes condition and hippocampal adverse effects were similarly heightened.

8.2 Hippocampal pathology with alcohol use in diabetes

The interaction of diabetes and alcohol treatment (DAL group) induced a reduction in, neurogenesis (Ki67 and DCX), neuronal number and neuronal nuclei area (in CA1, CA3, and DG regions), and volume of DG granular and molecular layers, elevated oxidative stress (elevated MDA, deficit in GPx), while hyperglycemia and glucose intolerance (NFBG and AUC) levels were reduced in comparison to diabetes alone. Additionally, the unique presence of elevated anti-apoptotic (Bcl_2), pro-apoptotic (BAX and Caspase-3), and improved insulin resistance (elevated IRS1) in DAL suggests that interactively diabetes and alcohol induced exacerbated hippocampal apoptosis, atrophy, and neurogenesis deficits with minimal effect on glucose homeostasis compared to diabetes alone. This novel effect necessitates caution in the management and monitoring of diabetic individuals who consume alcohol regularly.

8.3 The hippocampal impact of alcohol and cART interaction

The concomitant presence of alcohol and cART (without diabetes) induced a deficit in, antioxidant (GPx), neurogenesis (Ki67), hippocampal apoptosis (Bcl_2 and Caspase-3), insulin receptors (INSR and IRS1), BBB permeability (claudin-5 and occludin), DG neuronal number and volume of granular layer suggesting that the independent alcohol effects of reduced DCX, elevated MDA and pro-inflammatory cytokines were ameliorated by alcohol and cART interaction. However, the reduction in antioxidants and antiapoptotic gene expressions may have contributed to the loss of DG neurons and reduction in DG granular cell volume, which has potential to disrupt dentate gyrus function.

8.4 Hippocampal histopathology of diabetes, alcohol, and cART

The interactive effects of T2D, alcohol, and cART (i.e., DAA group/multiple morbidity) maintained similar diabetogenic effects of elevated hyperglycemia, oxidative stress, hippocampal apoptosis (Bcl_2 and Caspase-3), but a reduction in occluding gene expression, hippocampal neurons (in CA1 and DG regions), volume DG molecular layer ~~volume~~ and neurogenesis. Additionally, elevated pro-inflammatory cytokines (IL-1α, and IL-6), reduction of DG granular cell volume, neuronal number, and nuclei area in CA3 hippocampal region were observed in DAA treated group which were absent in diabetes (DB) or alcohol+ cART (AA) treatment groups. This interestingly suggests that patients exposed to AA treatment could progress to T2D because of the potential interactive effects of AA treatment to exacerbate insulin resistance due to downregulation of insulin receptors by the treatment, which may impair transport and cellular utilization). Thus, continued AA treatment in such patients may translate into DAA morbidity condition with resultant hippocampal effects as observed in DAA treatment. This observation is critical clinically for PLWHA and individuals on cART prophylaxis who consume alcohol regularly.

8.5 Focal hippocampal effects of diabetes, alcohol, cART, and their combinations

This study clearly highlights specific biochemical, molecular, and structural changes induced in the hippocampus due to diabetes, alcohol, cART, and their treatment combinations (Appendix F). A central hippocampal effect that underpins all treated groups is the reduction of DG neuronal number and antioxidant (GPx), highlighting the venerability of the hippocampal dentate gyrus neurons to antioxidant deficiency induced by diabetes, alcohol, cART, and their combinatorial interactions. Additionally, this study demonstrates the differential modulating effects of alcohol when combined with diabetes or with cART therapy relative to IRS1 regulated apoptosis, with elevated expression of BAX, Bcl_2, Caspase -3 and

IRS1 in the diabetes+ alcohol, but downregulation of Bcl_2, BAX and IRS gene in the cART+ alcohol. Furthermore, the diabetic comorbidity groups (DAV, DAL, and DAA) all share a central effect of reduced CA3 neuronal number and nuclei area, DG granular, and molecular layer volume, implicating the negative impact of these comorbidity treatments on the unique functional neuronal network/interconnectivity provided by hippocampal CA3 neurons and DG volume (atrophy) and with consequent hippocampal dysfunction. In the light of these findings, assessment of hippocampal wellbeing in patients with these comorbidities/treatment combinations is invaluable.

8.6 Limitations of the study

The potential of cART to independently disrupt BBB in a HIV naïve model and in combination with other factors (AV, AA, DAV, and DAA) may suggest the increased access of both cART and HIV virus in the CNS. However, it is not known how the presence of both factors (i.e., cART & HIV virus) in the hippocampus will interact in diabetes and other treatment combinations studied, and therefore hippocampal pathologies in a HIV model with these treatment combinations is recommended.

8.7 Recommendation for future studies

Additionally, diabetic-HIV patients who receive cART are often placed on anti-diabetic and anti-oxidative therapies in clinical management, therefore, the hippocampal toxicities observed in this study could be verified and authenticated in a further study by introducing treatment groups incorporating metformin and antioxidants (such as leaf or plant extracts) treated groups to clearly delineate toxicological impact of clinical treatments in the management of HIV/Aids in diabetes. In further studies it is also recommended that systemic and CNS levels of insulin (for calculation of HOMA-IR), markers of alcohol toxicity, glycated hemoglobin, proteomics

in addition to behavioral studies are employed for a multidimensional evaluation of hippocampal effects.

REFRENCE LIST

Abbott NJ, Patabendige AAK, Dolman DEM, Yusof SR, Begley DJ (2010) Structure and function of the blood-brain barrier. Neurobiol Dis 37:13–25.

Accili D (2021) Can COVID-19 cause diabetes? Nat Metab 3:123–125 Available at: https://www.nature.com/articles/s42255-020-00339-7 [Accessed July 30, 2021].

Ahmed AT, Karter AJ, Warton EM, Doan JU, Weisner CM (2008) The Relationship Between Alcohol Consumption and Glycemic Control Among Patients with Diabetes: The Kaiser Permanente Northern California Diabetes Registry. J Gen Intern Med 23:275–282 Available at: https://www.ncbi.nlm.nih.gov/pmc/articles/PMC2359478/ [Accessed April 29, 2022].

Ajibola S, Akinbami A, Elikwu C, Odesanya M, Uche E (2014) Knowledge, attitude and practices of HIV post exposure prophylaxis amongst health workers in Lagos University Teaching Hospital. Pan Afr Med J 19:172 Available at: https://www.ncbi.nlm.nih.gov/pmc/articles/PMC4366120/ [Accessed May 18, 2022].

Akang EN, Dosumu OO, Afolayan OO, Fagoroye AM, Osiagwu DD, Usman IT, Oremosu AA, Akanmu AS (2019) Combination antiretroviral therapy (cART)-induced hippocampal disorders: Highlights on therapeutic potential of Naringenin and Quercetin. IBRO Rep 6:137–146 Available at: https://www.ncbi.nlm.nih.gov/pmc/articles/PMC6488719/ [Accessed May 18, 2021].

Akay C et al. (2014) Antiretroviral drugs induce oxidative stress and neuronal damage in the central nervous system. J Neurovirol 20:39–53.

Akbarzadeh A, Norouzian D, Mehrabi MR, Jamshidi SH, Farhangi A, Verdi AA, Mofidian SMA, Rad BL (2007) Induction of diabetes by streptozotocin in rats. Indian J Clin Biochem 22:60–64.

Alaofi AL (2020) Sinapic Acid Ameliorates the Progression of Streptozotocin (STZ)-Induced Diabetic Nephropathy in Rats via NRF2/HO-1 Mediated Pathways. Front Pharmacol 11 Available at: https://www.frontiersin.org/article/10.3389/fphar.2020.01119 [Accessed May 3, 2022].

Alemany M (2021) Estrogens and the regulation of glucose metabolism. World J Diabetes 12:1622–1654 Available at: https://www.ncbi.nlm.nih.gov/pmc/articles/PMC8554369/ [Accessed October 17, 2022].

Al-Humadi H, Al-Saigh R, Sahib A (2018) The impact of low alcohol consumption on the liverand inflammatory cytokines in diabetic rats. Adv Clin Exp Med 28:331–337 Available at: http://www.advances.umed.wroc.pl/en/article/2019/28/3/331/ [Accessed February 3, 2022].

Almansa I, Barcia JM, López-Pedrajas R, Muriach M, Miranda M, Romero FJ (2013) Naltrexone Reverses Ethanol-Induced Rat Hippocampal and Serum Oxidative Damage. Oxid Med Cell

Longev 2013:e296898 Available at: https://www.hindawi.com/journals/omcl/2013/296898/ [Accessed May 12, 2022].

Alzamil H (2020) Elevated Serum TNF-α Is Related to Obesity in Type 2 Diabetes Mellitus and Is Associated with Glycemic Control and Insulin Resistance. J Obes 2020:5076858 Available at: https://www.ncbi.nlm.nih.gov/pmc/articles/PMC7013317/ [Accessed November 12, 2021].

Amaral DG, Witter MP (1989) The three-dimensional organization of the hippocampal formation: a review of anatomical data. Neuroscience 31:571–591.

American Diabetes Association (2007) Diagnosis and Classification of Diabetes Mellitus. Diabetes Care 30:S42–S47 Available at: http://care.diabetesjournals.org/cgi/doi/10.2337/dc07-S042 [Accessed June 3, 2021].

Anand KS, Dhikav V (2012) Hippocampus in health and disease: An overview. Ann Indian Acad Neurol 15:239–246 Available at: https://www.ncbi.nlm.nih.gov/pmc/articles/PMC3548359/ [Accessed May 6, 2022].

Andersen P, Andersen D of PI of BMSP, Morris R, Amaral D, Amaral PD of PD, O'Keefe J, Bliss T, O'Keefe PD of A and DBI of CNJ, Bliss D of NT (2007) The Hippocampus Book. Oxford University Press, USA.

Ang B, Yu GF (2018) The Role of Fructose in Type 2 Diabetes and Other Metabolic Diseases. J Nutr Food Sci 08 Available at: https://www.omicsonline.org/open-access/the-role-of-fructose-in-type-2-diabetes-and-other-metabolic-diseases-2155-9600-1000659-98130.html [Accessed June 2, 2021].

Apostolova N, Blas-Garcia A, Galindo MJ, Esplugues JV (2017) Efavirenz: what is known about the cellular mechanisms responsible for its adverse effects. Eur J Pharmacol 812:163–173.

Arnold SE, Arvanitakis Z, Macauley-Rambach SL, Koenig AM, Wang H-Y, Ahima RS, Craft S, Gandy S, Buettner C, Stoeckel LE, Holtzman DM, Nathan DM (2018) Brain insulin resistance in type 2 diabetes and Alzheimer disease: concepts and conundrums. Nat Rev Neurol 14:168–181.

Association AD (2015) 2. Classification and Diagnosis of Diabetes. Diabetes Care 38:S8–S16 Available at: https://care.diabetesjournals.org/content/38/Supplement_1/S8 [Accessed June 3, 2021].

Avison MJ, Nath A, Greene-Avison R, Schmitt FA, Greenberg RN, Berger JR (2004) Neuroimaging correlates of HIV-associated BBB compromise. J Neuroimmunol 157:140–146.

Ayanlaja AA, Xiong Y, Gao Y, Ji G, Tang C, Abdikani Abdullah Z, Gao D (2017) Distinct Features of Doublecortin as a Marker of Neuronal Migration and Its Implications in Cancer Cell Mobility. Front Mol Neurosci 10:199 Available at: https://www.ncbi.nlm.nih.gov/pmc/articles/PMC5487455/ [Accessed May 14, 2022].

Baizer JS (2014) Unique Features of the Human Brainstem and Cerebellum. Front Hum Neurosci 8:202 Available at: https://www.ncbi.nlm.nih.gov/pmc/articles/PMC3985031/ [Accessed May 5, 2022].

Balschun D, Wetzel W, Del Rey A, Pitossi F, Schneider H, Zuschratter W, Besedovsky HO (2004) Interleukin-6: a cytokine to forget. FASEB J Off Publ Fed Am Soc Exp Biol 18:1788–1790.

Barbiellini Amidei C, Fayosse A, Dumurgier J, Machado-Fragua MD, Tabak AG, van Sloten T, Kivimäki M, Dugravot A, Sabia S, Singh-Manoux A (2021) Association Between Age at Diabetes Onset and Subsequent Risk of Dementia. JAMA 325:1640–1649 Available at: https://doi.org/10.1001/jama.2021.4001 [Accessed May 4, 2022].

Barcia JM, Flores-Bellver M, Muriach M, Sancho-Pelluz J, Lopez-Malo D, Urdaneta AC, Martinez-Gil N, Atienzar-Aroca S, Romero FJ (2015) Matching Diabetes and Alcoholism: Oxidative Stress, Inflammation, and Neurogenesis Are Commonly Involved. Mediators Inflamm 2015:e624287 Available at: https://www.hindawi.com/journals/mi/2015/624287/ [Accessed June 11, 2022].

Barnham KJ, Masters CL, Bush AI (2004) Neurodegenerative diseases and oxidative stress. Nat Rev Drug Discov 3:205.

Bartsch T (2012) The Hippocampus in Neurological Disease. In: The Clinical Neurobiology of the Hippocampus. Oxford: Oxford University Press. Available at: https://oxford.universitypressscholarship.com/10.1093/acprof:oso/9780199592388.001.0001/acprof-9780199592388-chapter-011 [Accessed May 7, 2022].

Barve S, Chen S-Y, Kirpich I, Watson WH, McClain C (2017) Development, Prevention, and Treatment of Alcohol-Induced Organ Injury: The Role of Nutrition. Alcohol Res Curr Rev 38:289–302 Available at: https://www.ncbi.nlm.nih.gov/pmc/articles/PMC5513692/ [Accessed May 3, 2022].

Basinger H, Hogg JP (2022) Neuroanatomy, Brainstem. In: StatPearls. Treasure Island (FL): StatPearls Publishing. Available at: http://www.ncbi.nlm.nih.gov/books/NBK544297/ [Accessed May 5, 2022].

Beeri MS, Bendlin BB (2020) The link between type 2 diabetes and dementia: from biomarkers to treatment. Lancet Diabetes Endocrinol 8:736–738 Available at: https://www.thelancet.com/journals/landia/article/PIIS2213-8587(20)30267-9/fulltext [Accessed April 10, 2022].

Bell GI, Polonsky KS (2001) Diabetes mellitus and genetically programmed defects in beta-cell function. Nature 414:788–791.

Benedé-Ubieto R, Estévez-Vázquez O, Ramadori P, Cubero FJ, Nevzorova YA (2020) Guidelines and Considerations for Metabolic Tolerance Tests in Mice. Diabetes Metab Syndr Obes Targets Ther 13:439–450 Available at: https://www.dovepress.com/guidelines-and-considerations-for-metabolic-tolerance-tests-in-mice-peer-reviewed-fulltext-article-DMSO [Accessed November 24, 2021].

Benveniste EN (1992) Cytokines: influence on glial cell gene expression and function. Chem Immunol 52:106–153.

Berbudi A, Rahmadika N, Tjahjadi AI, Ruslami R (2020) Type 2 Diabetes and its Impact on the Immune System. Curr Diabetes Rev 16:442–449 Available at: https://www.ncbi.nlm.nih.gov/pmc/articles/PMC7475801/ [Accessed August 20, 2021].

Bertoli C, Skotheim JM, de Bruin RAM (2013) Control of cell cycle transcription during G1 and S phases. Nat Rev Mol Cell Biol 14:518–528 Available at: https://www.ncbi.nlm.nih.gov/pmc/articles/PMC4569015/ [Accessed May 15, 2022].

Bertrand L, Dygert L, Toborek M (2016) Antiretroviral treatment with efavirenz disrupts the blood-brain barrier integrity and increases stroke severity. Sci Rep 6:39738.

Biessels GJ, Despa F (2018) Cognitive decline and dementia in diabetes: mechanisms and clinical implications. Nat Rev Endocrinol 14:591–604 Available at: https://www.ncbi.nlm.nih.gov/pmc/articles/PMC6397437/ [Accessed May 4, 2022].

Biessels GJ, Reagan LP (2015) Hippocampal insulin resistance and cognitive dysfunction. Nat Rev Neurosci 16:660–671.

Biessels GJ, Reijmer YD (2014) Brain changes underlying cognitive dysfunction in diabetes: what can we learn from MRI? Diabetes 63:2244–2252.

Boles A, Kandimalla R, Reddy PH (2017) Dynamics of diabetes and obesity: Epidemiological perspective. Biochim Biophys Acta BBA - Mol Basis Dis 1863:1026–1036 Available at: https://www.sciencedirect.com/science/article/pii/S0925443917300297 [Accessed May 17, 2022].

Bolijn S, Lucassen P (2015) How the Body Talks to the Brain; Peripheral Mediators of Physical Activity-Induced Proliferation in the Adult Hippocampus. Brain Plast 1:5–27.

Bonds JA, Shetti A, Stephen TKL, Bonini MG, Minshall RD, Lazarov O (2020) Deficits in hippocampal neurogenesis in obesity-dependent and -independent type-2 diabetes mellitus mouse models. Sci Rep 10:16368 Available at: https://www.nature.com/articles/s41598-020-73401-9 [Accessed May 15, 2022].

Borsini A, Di Benedetto MG, Giacobbe J, Pariante CM (2020) Pro- and Anti-Inflammatory Properties of Interleukin in Vitro: Relevance for Major Depression and Human Hippocampal Neurogenesis. Int J Neuropsychopharmacol 23:738–750 Available at: https://doi.org/10.1093/ijnp/pyaa055 [Accessed May 10, 2022].

Bourgognon J-M, Cavanagh J (2020) The role of cytokines in modulating learning and memory and brain plasticity. Brain Neurosci Adv 4:2398212820979802 Available at: https://doi.org/10.1177/2398212820979802 [Accessed May 18, 2021].

Braganza D, Flores E, Crew L, Wirt R, Ortiz A, McNeela A, Kinney J, Hyman J (2021) Diabetes Mellitus Affects Working Memory. Spectra Undergrad Res J 1 Available at: https://digitalscholarship.unlv.edu/spectra/vol1/iss2/3.

Braida D, Sacerdote P, Panerai AE, Bianchi M, Aloisi AM, Iosuè S, Sala M (2004) Cognitive function in young and adult IL (interleukin)-6 deficient mice. Behav Brain Res 153:423–429.

Broadwater MA, Liu W, Crews FT, Spear LP (2014) Persistent loss of hippocampal neurogenesis and increased cell death following adolescent, but not adult, chronic ethanol exposure. Dev Neurosci 36:297–305 Available at: https://www.ncbi.nlm.nih.gov/pmc/articles/PMC4125431/ [Accessed August 24, 2021].

Brown AM, Ransom BR (2007) Astrocyte glycogen and brain energy metabolism. Glia 55:1263–1271.

Brown JP, Couillard-Després S, Cooper-Kuhn CM, Winkler J, Aigner L, Kuhn HG (2003) Transient expression of doublecortin during adult neurogenesis. J Comp Neurol 467:1–10.

Brown TT, Cole SR, Li X, Kingsley LA, Palella FJ, Riddler SA, Visscher BR, Margolick JB, Dobs AS (2005) Antiretroviral therapy and the prevalence and incidence of diabetes mellitus in the multicenter AIDS cohort study. Arch Intern Med 165:1179–1184.

Bryant NJ, Govers R, James DE (2002) Regulated transport of the glucose transporter GLUT4. Nat Rev Mol Cell Biol 3:267–277 Available at: https://www.nature.com/articles/nrm782 [Accessed May 6, 2022].

Budreviciute A, Damiati S, Sabir DK, Onder K, Schuller-Goetzburg P, Plakys G, Katileviciute A, Khoja S, Kodzius R (2020) Management and Prevention Strategies for Non-communicable Diseases (NCDs) and Their Risk Factors. Front Public Health 8 Available at: https://www.frontiersin.org/article/10.3389/fpubh.2020.574111 [Accessed May 16, 2022].

Calle MC, Fernandez ML (2012) Inflammation and type 2 diabetes. Diabetes Metab 38:183–191.

Camire RB, Beaulac HJ, Willis CL (2015) Transitory loss of glia and the subsequent modulation in inflammatory cytokines/chemokines regulate paracellular claudin-5 expression in endothelial cells. J Neuroimmunol 284:57–66.

Can ÖD, Öztürk Y, Öztürk N, Sagratini G, Ricciutelli M, Vittori S, Maggi F (2011) Effects of treatment with St. John's Wort on blood glucose levels and pain perceptions of streptozotocin-diabetic rats. Fitoterapia 82:576–584.

Cannon JR, Greenamyre JT (2011) The Role of Environmental Exposures in Neurodegeneration and Neurodegenerative Diseases. Toxicol Sci 124:225–250 Available at: https://doi.org/10.1093/toxsci/kfr239 [Accessed May 7, 2022].

Carlsson S, Hammar N, Grill V, Kaprio J (2003) Alcohol consumption and the incidence of type 2 diabetes: a 20-year follow-up of the Finnish twin cohort study. Diabetes Care 26:2785–2790.

Casqueiro J, Casqueiro J, Alves C (2012) Infections in patients with diabetes mellitus: A review of pathogenesis. Indian J Endocrinol Metab 16 Suppl 1:S27-36.

Cavallaro S (2015) Cracking the code of neuronal apoptosis and survival. Cell Death Dis 6:e1963–e1963 Available at: https://www.nature.com/articles/cddis2015309 [Accessed May 12, 2022].

Cawthorn WP, Sethi JK (2008) TNF-α and adipocyte biology. FEBS Lett 582:117–131 Available at: https://www.ncbi.nlm.nih.gov/pmc/articles/PMC4304634/ [Accessed May 10, 2022].

Cayre M, Canoll P, Goldman JE (2009) Cell migration in the normal and pathological postnatal mammalian brain. Prog Neurobiol 88:41–63.

Cejas P, Casado E, Belda-Iniesta C, De Castro J, Espinosa E, Redondo A, Sereno M, García-Cabezas MÁ, Vara JAF, Domínguez-Cáceres A, Perona R, González-Barón M (2004) Implications of Oxidative Stress and Cell Membrane Lipid Peroxidation in Human Cancer (Spain). Cancer Causes Control 15:707–719 Available at: https://www.jstor.org/stable/3554130 [Accessed May 16, 2022].

Chang L, Chiang S-H, Saltiel AR (2004) Insulin Signaling and the Regulation of Glucose Transport. Mol Med 10:65–71 Available at: https://molmed.biomedcentral.com/articles/10.2119/2005-00029.Saltiel [Accessed May 7, 2022].

Chao P-C, Li Y, Chang C-H, Shieh JP, Cheng J-T, Cheng K-C (2018) Investigation of insulin resistance in the popularly used four rat models of type-2 diabetes. Biomed Pharmacother 101:155–161 Available at: https://www.sciencedirect.com/science/article/pii/S0753332217363801 [Accessed May 15, 2022].

Chatzigeorgiou A, Halapas A, Kalafatakis K, Kamper E (2009) The Use of Animal Models in the Study of Diabetes Mellitus. In Vivo 23:245–258 Available at: https://iv.iiarjournals.org/content/23/2/245 [Accessed June 4, 2021].

Chawla A, Chawla R, Jaggi S (2016) Microvasular and macrovascular complications in diabetes mellitus: distinct or continuum? Indian J Endocrinol Metab 20:546.

Chehade JM, Haas MJ, Mooradian AD (2002) Diabetes-related changes in rat cerebral occludin and zonula occludens-1 (ZO-1) expression. Neurochem Res 27:249–252.

Chen X, Guo C, Kong J (2012) Oxidative stress in neurodegenerative diseases. Neural Regen Res 7:376–385 Available at: https://www.ncbi.nlm.nih.gov/pmc/articles/PMC4350122/ [Accessed May 16, 2022].

Chéret A, Durier C, Mélard A, Ploquin M, Heitzmann J, Lécuroux C, Avettand-Fenoël V, David L, Pialoux G, Chennebault J-M, Müller-Trutwin M, Goujard C, Rouzioux C, Meyer L (2017) Impact of early cART on HIV blood and semen compartments at the time of primary infection. PLoS ONE 12:e0180191 Available at: https://www.ncbi.nlm.nih.gov/pmc/articles/PMC5510829/ [Accessed May 4, 2022].

Cherubini E, Miles R (2015) The CA3 region of the hippocampus: how is it? What is it for? How does it do it? Front Cell Neurosci 9:19 Available at: https://www.ncbi.nlm.nih.gov/pmc/articles/PMC4318343/ [Accessed August 20, 2021].

Cheyuo C, Aziz M, Wang P (2019) Neurogenesis in Neurodegenerative Diseases: Role of MFG-E8. Front Neurosci 13 Available at: https://www.frontiersin.org/article/10.3389/fnins.2019.00569 [Accessed April 29, 2022].

Chipperfield H, Cool SM, Bedi K, Nurcombe V (2005) Adult CNS explants as a source of neural progenitors. Brain Res Brain Res Protoc 14:146–153.

Choi SS, Lee HJ, Lim I, Satoh J, Kim SU (2014) Human astrocytes: secretome profiles of cytokines and chemokines. PloS One 9:e92325.

Cholerton B, Baker LD, Montine TJ, Craft S (2016) Type 2 Diabetes, Cognition, and Dementia in Older Adults: Toward a Precision Health Approach. Diabetes Spectr 29:210–219 Available at: https://spectrum.diabetesjournals.org/content/29/4/210 [Accessed July 3, 2021].

Clifford DB, Ances BM (2013) HIV-associated neurocognitive disorder. Lancet Infect Dis 13:976–986 Available at: https://www.thelancet.com/journals/laninf/article/PIIS1473-3099(13)70269-X/fulltext [Accessed May 4, 2022].

Cohen I, Rider P, Carmi Y, Braiman A, Dotan S, White MR, Voronov E, Martin MU, Dinarello CA, Apte RN (2010) Differential release of chromatin-bound IL-1α discriminates between necrotic and apoptotic cell death by the ability to induce sterile inflammation. Proc Natl Acad Sci U S A 107:2574–2579 Available at: https://www.ncbi.nlm.nih.gov/pmc/articles/PMC2823886/ [Accessed May 10, 2022].

Cohen MS, Gay C, Kashuba ADM, Blower S, Paxton L (2007) Narrative review: antiretroviral therapy to prevent the sexual transmission of HIV-1. Ann Intern Med 146:591–601.

Cois A, Day C (2015) Obesity trends and risk factors in the South African adult population. BMC Obes 2:42.

Cooper GM (2000) The Eukaryotic Cell Cycle. Cell Mol Approach 2nd Ed Available at: https://www.ncbi.nlm.nih.gov/books/NBK9876/ [Accessed May 15, 2022].

Cu-Uvin S, Caliendo AM, Reinert S, Chang A, Juliano-Remollino C, Flanigan TP, Mayer KH, Carpenter CC (2000) Effect of highly active antiretroviral therapy on cervicovaginal HIV-1 RNA. AIDS Lond Engl 14:415–421.

Daneman R, Prat A (2015) The blood–brain barrier. Cold Spring Harb Perspect Biol 7:a020412.

Daryabor G, Atashzar MR, Kabelitz D, Meri S, Kalantar K (2020) The Effects of Type 2 Diabetes Mellitus on Organ Metabolism and the Immune System. Front Immunol 11:1582 Available at: https://www.frontiersin.org/article/10.3389/fimmu.2020.01582 [Accessed November 24, 2021].

Das SK, Vasudevan DM (2007) Alcohol-induced oxidative stress. Life Sci 81:177–187.

de la Monte SM (2012) Contributions of Brain Insulin Resistance and Deficiency in Amyloid-Related Neurodegeneration in Alzheimer's Disease. Drugs 72:49–66 Available at: https://doi.org/10.2165/11597760-000000000-00000 [Accessed November 12, 2021].

De Meyts P (2000) The Insulin Receptor and Its Signal Transduction Network. In: Endotext (Feingold KR et al., eds). South Dartmouth (MA): MDText.com, Inc. Available at: http://www.ncbi.nlm.nih.gov/books/NBK378978/ [Accessed June 30, 2022].

de Moura RF, Ribeiro C, de Oliveira JA, Stevanato E, de Mello MAR (2008) Metabolic syndrome signs in Wistar rats submitted to different high-fructose ingestion protocols. Br J Nutr 101:1178–1184.

Deeds M, Anderson J, Armstrong A, Gastineau D, Hiddinga H, Jahangir A, Eberhardt N, Kudva Y (2011) Single Dose Streptozotocin Induced Diabetes: Considerations for Study Design in Islet Transplantation Models. Lab Anim 45:131–140 Available at: https://www.ncbi.nlm.nih.gov/pmc/articles/PMC3917305/ [Accessed June 2, 2021].

Dekeyzer S, De Kock I, Nikoubashman O, Vanden Bossche S, Van Eetvelde R, De Groote J, Acou M, Wiesmann M, Deblaere K, Achten E (2017) "Unforgettable" – a pictorial essay on anatomy and pathology of the hippocampus. Insights Imaging 8:199–212 Available at: https://www.ncbi.nlm.nih.gov/pmc/articles/PMC5359145/ [Accessed May 7, 2022].

Dellamonica P, Di Perri G, Garraffo R (2012) NNRTIs: pharmacological data. Médecine Mal Infect 42:287–295.

Deng W, Aimone JB, Gage FH (2010) New neurons and new memories: how does adult hippocampal neurogenesis affect learning and memory? Nat Rev Neurosci 11:339–350 Available at: https://www.ncbi.nlm.nih.gov/pmc/articles/PMC2886712/ [Accessed May 14, 2022].

Dhaliwal J, Xi Y, Bruel-Jungerman E, Germain J, Francis F, Lagace DC (2016) Doublecortin (DCX) is not Essential for Survival and Differentiation of Newborn Neurons in the Adult Mouse Dentate

Gyrus. Front Neurosci 9:494 Available at: https://www.ncbi.nlm.nih.gov/pmc/articles/PMC4707254/ [Accessed May 14, 2022].

Dhanabalan G, Wardi Le Maitre T, Bogdanovic N, Alkass K, Druid H (2018) Hippocampal granule cell loss in human chronic alcohol abusers. Neurobiol Dis 120.

Dhikav V, Anand KS (2007) Is hippocampal atrophy a future drug target? Med Hypotheses 68:1300–1306.

Dinarello CA (2018) Overview of the IL-1 family in innate inflammation and acquired immunity. Immunol Rev 281:8 Available at: https://www.ncbi.nlm.nih.gov/pmc/articles/PMC5756628/ [Accessed May 10, 2022].

D'Mello C, Le T, Swain MG (2009) Cerebral Microglia Recruit Monocytes into the Brain in Response to Tumor Necrosis Factorα Signaling during Peripheral Organ Inflammation. J Neurosci 29:2089–2102 Available at: https://www.ncbi.nlm.nih.gov/pmc/articles/PMC6666330/ [Accessed May 10, 2022].

Doetsch F, Caillé I, Lim DA, García-Verdugo JM, Alvarez-Buylla A (1999) Subventricular zone astrocytes are neural stem cells in the adult mammalian brain. Cell 97:703–716.

Donath MY, Shoelson SE (2011) Type 2 diabetes as an inflammatory disease. Nat Rev Immunol 11:98–107 Available at: https://www.nature.com/articles/nri2925 [Accessed January 19, 2022].

Donzis EJ, Tronson NC (2014) Modulation of learning and memory by cytokines: Signaling mechanisms and long term consequences. Neurobiol Learn Mem 115:68–77 Available at: https://www.sciencedirect.com/science/article/pii/S1074742714001543 [Accessed May 18, 2021].

Doos L, Roberts EO, Corp N, Kadam UT (2014) Multi-drug therapy in chronic condition multimorbidity: a systematic review. Fam Pract 31:654–663 Available at: https://www.ncbi.nlm.nih.gov/pmc/articles/PMC5942538/ [Accessed August 4, 2021].

Du P, Crook T, Whitener C, Albright P, Greenawalt D, Zurlo J (2015) HIV transmission risk behaviors among people living with HIV/AIDS: The need to integrate HIV prevention interventions and public health strategies into HIV care. J Public Health Manag Pract JPHMP 21:E1–E10 Available at: https://www.ncbi.nlm.nih.gov/pmc/articles/PMC4051857/ [Accessed October 20, 2022].

Duff MC, Covington NV, Hilverman C, Cohen NJ (2020) Semantic Memory and the Hippocampus: Revisiting, Reaffirming, and Extending the Reach of Their Critical Relationship. Front Hum Neurosci 13 Available at: https://www.frontiersin.org/articles/10.3389/fnhum.2019.00471 [Accessed July 5, 2022].

Duko B, Ayalew M, Ayano G (2019) The prevalence of alcohol use disorders among people living with HIV/AIDS: a systematic review and meta-analysis. Subst Abuse Treat Prev Policy 14:52 Available at: https://doi.org/10.1186/s13011-019-0240-3 [Accessed May 3, 2022].

Dupas J, Goanvec C, Feray A, Guernec A, Alain C, Guerrero F, Mansourati J (2016) Progressive Induction of Type 2 Diabetes: Effects of a Reality–Like Fructose Enriched Diet in Young Wistar Rats. PLoS ONE 11 Available at: https://www.ncbi.nlm.nih.gov/pmc/articles/PMC4723014/ [Accessed June 4, 2021].

El Falougy H, Kubikova E, Benuska J (2008) The microscopical structure of the hippocampus in the rat. Bratisl Lek Listy 109:106–110.

Elmore S (2007) Apoptosis: A Review of Programmed Cell Death. Toxicol Pathol 35:495–516 Available at: https://www.ncbi.nlm.nih.gov/pmc/articles/PMC2117903/ [Accessed May 18, 2021].

Endl E, Gerdes J (2000) The Ki-67 protein: fascinating forms and an unknown function. Exp Cell Res 257:231–237.

Engler PA, Ramsey SE, Smith RJ (2013) Alcohol use of diabetes patients: The need for assessment and intervention. Acta Diabetol 50:93–99 Available at: https://www.ncbi.nlm.nih.gov/pmc/articles/PMC2954251/ [Accessed May 16, 2022].

Eriksson PS, Perfilieva E, Björk-Eriksson T, Alborn AM, Nordborg C, Peterson DA, Gage FH (1998) Neurogenesis in the adult human hippocampus. Nat Med 4:1313–1317.

Erta M, Quintana A, Hidalgo J (2012) Interleukin-6, a Major Cytokine in the Central Nervous System. Int J Biol Sci 8:1254–1266 Available at: https://www.ncbi.nlm.nih.gov/pmc/articles/PMC3491449/ [Accessed May 10, 2022].

Fang J-Y, Lin C-H, Huang T-H, Chuang S-Y (2019) In Vivo Rodent Models of Type 2 Diabetes and Their Usefulness for Evaluating Flavonoid Bioactivity. Nutrients 11:530 Available at: https://www.ncbi.nlm.nih.gov/pmc/articles/PMC6470730/ [Accessed May 15, 2022].

Feng R, Du S, Chen Y, Zheng S, Zhang W, Na G, Li Y, Sun C (2015) High carbohydrate intake from starchy foods is positively associated with metabolic disorders: a Cohort Study from a Chinese population. Sci Rep 5:16919.

Ferlita S, Yegiazaryan A, Noori N, Lal G, Nguyen T, To K, Venketaraman V (2019) Type 2 Diabetes Mellitus and Altered Immune System Leading to Susceptibility to Pathogens, Especially Mycobacterium tuberculosis. J Clin Med 8:2219 Available at: https://www.ncbi.nlm.nih.gov/pmc/articles/PMC6947370/ [Accessed November 11, 2021].

Fink SL, Cookson BT (2005) Apoptosis, Pyroptosis, and Necrosis: Mechanistic Description of Dead and Dying Eukaryotic Cells. Infect Immun 73:1907–1916 Available at: https://www.ncbi.nlm.nih.gov/pmc/articles/PMC1087413/ [Accessed May 12, 2022].

Flora SJS, Gautam P, Kushwaha P (2012) Lead and Ethanol Co-Exposure Lead to Blood Oxidative Stress and Subsequent Neuronal Apoptosis in Rats. Alcohol Alcohol 47:92–101 Available at: https://doi.org/10.1093/alcalc/agr152 [Accessed May 26, 2022].

Fogwe LA, Reddy V, Mesfin FB (2022) Neuroanatomy, Hippocampus. In: StatPearls. Treasure Island (FL): StatPearls Publishing. Available at: http://www.ncbi.nlm.nih.gov/books/NBK482171/ [Accessed April 10, 2022].

Fokunang CN, J. Hitchcock, F. Spence, E.A. Tembe-Fokunang, J. Burkhardt, L. Levy, C. George (2005) An Overview of Mitochondrial Toxicity of Nucleoside Reverse Transcriptase Inhibitors Associated with HIV Therapy. Int J Pharmacol 2:152–162 Available at: https://www.scialert.net/abstract/?doi=ijp.2006.152.162 [Accessed May 17, 2021].

Frampton JE, Croom KF (2006) Efavirenz/Emtricitabine/Tenofovir Disoproxil Fumarate. Drugs 66:1501–1512 Available at: https://doi.org/10.2165/00003495-200666110-00012 [Accessed November 18, 2021].

Fritzen K, Heinemann L, Schnell O (2018) Modeling of Diabetes and Its Clinical Impact. J Diabetes Sci Technol 12:976–984 Available at: https://www.ncbi.nlm.nih.gov/pmc/articles/PMC6134612/ [Accessed June 4, 2021].

Furman BL (2015) Streptozotocin-Induced Diabetic Models in Mice and Rats. Curr Protoc Pharmacol 70 Available at: https://onlinelibrary.wiley.com/doi/10.1002/0471141755.ph0547s70 [Accessed June 4, 2021].

Gabay C (2006) Interleukin-6 and chronic inflammation. Arthritis Res Ther 8:S3 Available at: https://doi.org/10.1186/ar1917 [Accessed May 10, 2022].

Gadient RA, Otten U (1994) Identification of interleukin-6 (IL-6)-expressing neurons in the cerebellum and hippocampus of normal adult rats. Neurosci Lett 182:243–246 Available at: https://www.sciencedirect.com/science/article/pii/0304394094908079 [Accessed November 9, 2021].

Galic MA, Riazi K, Pittman QJ (2012) Cytokines and brain excitability. Front Neuroendocrinol 33:116–125 Available at: https://www.ncbi.nlm.nih.gov/pmc/articles/PMC3547977/ [Accessed November 9, 2021].

Galicia-Garcia U, Benito-Vicente A, Jebari S, Larrea-Sebal A, Siddiqi H, Uribe KB, Ostolaza H, Martín C (2020) Pathophysiology of Type 2 Diabetes Mellitus. Int J Mol Sci 21:6275 Available at: https://www.ncbi.nlm.nih.gov/pmc/articles/PMC7503727/ [Accessed May 17, 2022].

Gaschler MM, Stockwell BR (2017) Lipid peroxidation in cell death. Biochem Biophys Res Commun 482:419–425.

Geil CR, Hayes DM, McClain JA, Liput DJ, Marshall SA, Chen KY, Nixon K (2014) Alcohol and adult hippocampal neurogenesis: promiscuous drug, wanton effects. Prog Neuropsychopharmacol Biol Psychiatry 54:103–113.

Ghasemi A, Khalifi S, Jedi S (2014) Streptozotocin-nicotinamide-induced rat model of type 2 diabetes (review). Acta Physiol Hung 101:408–420.

Ghashghaei HT, Lai C, Anton ES (2007) Neuronal migration in the adult brain: are we there yet? Nat Rev Neurosci 8:141–151 Available at: https://www.nature.com/articles/nrn2074 [Accessed May 14, 2022].

Ghavami S, Shojaei S, Yeganeh B, Ande SR, Jangamreddy JR, Mehrpour M, Christoffersson J, Chaabane W, Moghadam AR, Kashani HH, Hashemi M, Owji AA, Łos MJ (2014) Autophagy and apoptosis dysfunction in neurodegenerative disorders. Prog Neurobiol 112:24–49 Available at: https://www.sciencedirect.com/science/article/pii/S0301008213001044 [Accessed April 8, 2022].

Gispen WH, Biessels G-J (2000) Cognition and synaptic plasticity in diabetes mellitus. Trends Neurosci 23:542–549.

Gleeson JG, Lin PT, Flanagan LA, Walsh CA (1999) Doublecortin is a microtubule-associated protein and is expressed widely by migrating neurons. Neuron 23:257–271.

Gonzalez CD, Lee M-S, Marchetti P, Pietropaolo M, Towns R, Vaccaro MI, Watada H, Wiley JW (2011) The emerging role of autophagy in the pathophysiology of diabetes mellitus. Autophagy 7:2–11.

Goyal R, Jialal I (2022) Diabetes Mellitus Type 2. In: StatPearls. Treasure Island (FL): StatPearls Publishing. Available at: http://www.ncbi.nlm.nih.gov/books/NBK513253/ [Accessed May 3, 2022].

Greene C, Hanley N, Campbell M (2019) Claudin-5: gatekeeper of neurological function. Fluids Barriers CNS 16:3 Available at: https://doi.org/10.1186/s12987-019-0123-z [Accessed November 11, 2021].

Gregersen R, Lambertsen K, Finsen B (2000) Microglia and macrophages are the major source of tumor necrosis factor in permanent middle cerebral artery occlusion in mice. J Cereb Blood Flow Metab Off J Int Soc Cereb Blood Flow Metab 20:53–65.

Guariguata L, Whiting DR, Hambleton I, Beagley J, Linnenkamp U, Shaw JE (2014) Global estimates of diabetes prevalence for 2013 and projections for 2035. Diabetes Res Clin Pract 103:137–149.

Guicciardi ME, Gores GJ (2009) Life and death by death receptors. FASEB J Off Publ Fed Am Soc Exp Biol 23:1625–1637.

Guthrie B, Makubate B, Hernandez-Santiago V, Dreischulte T (2015) The rising tide of polypharmacy and drug-drug interactions: population database analysis 1995–2010. BMC Med 13:74 Available at: https://doi.org/10.1186/s12916-015-0322-7 [Accessed July 16, 2022].

Gutiérrez F, Navarro A, Padilla S, Antón R, Masiá M, Borrás J, Martín-Hidalgo A (2005) Prediction of neuropsychiatric adverse events associated with long-term efavirenz therapy, using plasma drug level monitoring. Clin Infect Dis 41:1648–1653.

Han J, Tian H, Lian Y, Yu Y, Lu C, Li X, Zhang R, Xu H (2015) Quetiapine mitigates the ethanol-induced oxidative stress in brain tissue, but not in the liver, of the rat. Neuropsychiatr Dis Treat 11:1473–1482 Available at: https://www.dovepress.com/quetiapine-mitigates-the-ethanol-induced-oxidative-stress-in-brain-tis-peer-reviewed-fulltext-article-NDT [Accessed May 12, 2022].

Haorah J, Ramirez SH, Floreani N, Gorantla S, Morsey B, Persidsky Y (2008) Mechanism of alcohol-induced oxidative stress and neuronal injury. Free Radic Biol Med 45:1542–1550 Available at: https://www.ncbi.nlm.nih.gov/pmc/articles/PMC2605399/ [Accessed April 8, 2022].

Haorah J, Ramirez SH, Schall K, Smith D, Pandya R, Persidsky Y (2007) Oxidative stress activates protein tyrosine kinase and matrix metalloproteinases leading to blood–brain barrier dysfunction. J Neurochem 101:566–576.

Hardwick JM, Soane L (2013) Multiple Functions of BCL-2 Family Proteins. Cold Spring Harb Perspect Biol 5:a008722 Available at: https://www.ncbi.nlm.nih.gov/pmc/articles/PMC3552500/ [Accessed May 13, 2022].

Harris M, Nosyk B, Harrigan R, Lima VD, Cohen C, Montaner J (2012) Cost-Effectiveness of Antiretroviral Therapy for Multidrug-Resistant HIV: Past, Present, and Future. AIDS Res Treat 2012:595762 Available at: https://www.ncbi.nlm.nih.gov/pmc/articles/PMC3502757/ [Accessed May 4, 2022].

Harry GJ, Kraft AD (2008) Neuroinflammation and Microglia: Considerations and approaches for neurotoxicity assessment. Expert Opin Drug Metab Toxicol 4:1265–1277 Available at: https://www.ncbi.nlm.nih.gov/pmc/articles/PMC2658618/ [Accessed May 9, 2022].

Hawkins BT, Lundeen TF, Norwood KM, Brooks HL, Egleton RD (2007) Increased blood–brain barrier permeability and altered tight junctions in experimental diabetes in the rat: contribution of hyperglycaemia and matrix metalloproteinases. Diabetologia 50:202–211 Available at: https://doi.org/10.1007/s00125-006-0485-z [Accessed November 12, 2021].

He J, Nixon K, Shetty AK, Crews FT (2005) Chronic alcohol exposure reduces hippocampal neurogenesis and dendritic growth of newborn neurons. Eur J Neurosci 21:2711–2720.

He X, Sun J, Huang X (2018) Expression of caspase-3, Bax and Bcl-2 in hippocampus of rats with diabetes and subarachnoid hemorrhage. Exp Ther Med 15:873–877 Available at: https://www.spandidos-publications.com/10.3892/etm.2017.5438 [Accessed May 26, 2022].

Herrero L, Shapiro H, Nayer A, Lee J, Shoelson SE (2010) Inflammation and adipose tissue macrophages in lipodystrophic mice. Proc Natl Acad Sci 107:240–245 Available at: http://www.pnas.org/cgi/doi/10.1073/pnas.0905310107 [Accessed January 20, 2022].

Hertel J, Struthers H, Horj CB, Hruz PW (2004) A structural basis for the acute effects of HIV protease inhibitors on GLUT4 intrinsic activity. J Biol Chem 279:55147–55152.

Hewett SJ, Jackman NA, Claycomb RJ (2012) Interleukin-1β in Central Nervous System Injury and Repair. Eur J Neurodegener Dis 1:195–211 Available at: https://www.ncbi.nlm.nih.gov/pmc/articles/PMC4465544/ [Accessed May 10, 2022].

Ho N, Sommers MS, Lucki I (2013) Effects of Diabetes on Hippocampal Neurogenesis: Links to Cognition and Depression. Neurosci Biobehav Rev 37:1346–1362 Available at: https://www.ncbi.nlm.nih.gov/pmc/articles/PMC3788092/ [Accessed April 29, 2022].

Honnapurmath VK, Patil VW (2017) Antiretroviral therapy-induced insulin resistance and oxidative deoxy nucleic acid damage in human immunodeficiency virus-1 patients. Indian J Endocrinol Metab 21:316.

Horberg MA, Klein DB (2010) An update on the use of Atripla® in the treatment of HIV in the United States. HIVAIDS Auckl NZ 2:135–140 Available at: https://www.ncbi.nlm.nih.gov/pmc/articles/PMC3218697/ [Accessed May 16, 2022].

Hruz PW (2006) Molecular Mechanisms for Altered Glucose Homeostasis in HIV Infection. Am J Infect Dis 2:187–192 Available at: https://www.ncbi.nlm.nih.gov/pmc/articles/PMC1716153/ [Accessed May 7, 2022].

Huang C-C, Lee C-C, Hsu K-S (2010) The role of insulin receptor signaling in synaptic plasticity and cognitive function. Chang Gung Med J 33:115–125.

Huber JD, VanGilder RL, Houser KA (2006) Streptozotocin-induced diabetes progressively increases blood-brain barrier permeability in specific brain regions in rats. Am J Physiol-Heart Circ Physiol 291:H2660–H2668.

Ighodaro OM, Akinloye OA (2018) First line defence antioxidants-superoxide dismutase (SOD), catalase (CAT) and glutathione peroxidase (GPX): Their fundamental role in the entire antioxidant defence grid. Alex J Med 54:287–293 Available at:

https://www.sciencedirect.com/science/article/pii/S2090506817301550 [Accessed May 16, 2022].

Iglay K, Hannachi H, Joseph Howie P, Xu J, Li X, Engel SS, Moore LM, Rajpathak S (2016) Prevalence and co-prevalence of comorbidities among patients with type 2 diabetes mellitus. Curr Med Res Opin 32:1243–1252.

Ishunina TA, Bogolepova IN, Swaab DF (2019) Increased Neuronal Nuclear and Perikaryal Size in the Medial Mamillary Nucleus of Vascular Dementia and Alzheimer's Disease Patients: Relation to Nuclear Estrogen Receptor α. Dement Geriatr Cogn Disord 47:274–280 Available at: https://www.karger.com/Article/FullText/500244 [Accessed July 3, 2021].

Islam MS (2011) Fasting blood glucose and diagnosis of type 2 diabetes. Diabetes Res Clin Pract 91:e26.

Ito M, Kondo Y, Nakatani A, Naruse A (1999) New model of progressive non-insulin-dependent diabetes mellitus in mice induced by streptozotocin. Biol Pharm Bull 22:988–989.

Jafari Anarkooli I, Sankian M, Ahmadpour S, Varasteh A-R, Haghir H (2008) Evaluation of Bcl-2 family gene expression and Caspase-3 activity in hippocampus STZ-induced diabetic rats. Exp Diabetes Res 2008:638467.

Jan R, Chaudhry G-S (2019) Understanding Apoptosis and Apoptotic Pathways Targeted Cancer Therapeutics. Adv Pharm Bull 9:205–218 Available at: https://www.ncbi.nlm.nih.gov/pmc/articles/PMC6664112/ [Accessed May 13, 2022].

Jang HB, Go MJ, Park SI, Lee H-J, Cho SB (2019) Chronic heavy alcohol consumption influences the association between genetic variants of GCK or INSR and the development of diabetes in men: A 12-year follow-up study. Sci Rep 9:20029 Available at: https://www.nature.com/articles/s41598-019-56011-y [Accessed April 7, 2022].

Jawabri KH, Sharma S (2022) Physiology, Cerebral Cortex Functions. In: StatPearls. Treasure Island (FL): StatPearls Publishing. Available at: http://www.ncbi.nlm.nih.gov/books/NBK538496/ [Accessed May 5, 2022].

Jeeva JS, Sunitha J, Ananthalakshmi R, Rajkumari S, Ramesh M, Krishnan R (2015) Enzymatic antioxidants and its role in oral diseases. J Pharm Bioallied Sci 7:S331–S333 Available at: https://www.ncbi.nlm.nih.gov/pmc/articles/PMC4606614/ [Accessed May 16, 2022].

Jensen T, Kiersgaard M, Sørensen D, Mikkelsen L (2013) Fasting of mice: a review. Lab Anim 47:225–240 Available at: https://doi.org/10.1177/0023677213501659 [Accessed October 20, 2022].

Jevtić P, Edens LJ, Vuković LD, Levy DL (2014) Sizing and shaping the nucleus: mechanisms and significance. Curr Opin Cell Biol 0:16–27 Available at: https://www.ncbi.nlm.nih.gov/pmc/articles/PMC4061251/ [Accessed April 10, 2022].

Jin J, Grimmig B, Izzo J, Brown LA, Hudson C, Smith AJ, Tan J, Bickford PC, Giunta B (2016) HIV non-nucleoside reverse transcriptase inhibitor efavirenz reduces neural stem cell proliferation in vitro and in vivo. Cell Transplant 25:1967–1977.

Johnson LF, Dorrington RE, Moolla H (2017) Progress towards the 2020 targets for HIV diagnosis and antiretroviral treatment in South Africa. South Afr J HIV Med 18.

Julg B, Bogner JR (2008) Atripla™–HIV therapy in one pill. Ther Clin Risk Manag 4:573.

Jung K-I, Ju A, Lee H-M, Lee S-S, Song C-H, Won W-Y, Jeong J-S, Hong O-K, Kim J-H, Kim D-J (2011) Chronic ethanol ingestion, type 2 diabetes mellitus, and brain-derived neurotrophic factor (BDNF) in rats. Neurosci Lett 487:149–152.

Kadam U, Roberts I, White S, Bednall R, Khunti K, Nilsson P, Lawson C (2018) Conceptualising multiple drug use in patients with comorbidity and multimorbidity: proposal for standard definitions beyond the term polypharmacy. J Clin Epidemiol 106.

Kalejaiye O, Getachew B, Ferguson CL, Taylor RE, Tizabi Y (2017) Alcohol-Induced Increases in Inflammatory Cytokines Are Attenuated by Nicotine in Region-Selective Manner in Male Rats. J Drug Alcohol Res 6.

Kaneko N, Kurata M, Yamamoto T, Morikawa S, Masumoto J (2019) The role of interleukin-1 in general pathology. Inflamm Regen 39:12 Available at: https://doi.org/10.1186/s41232-019-0101-5 [Accessed May 10, 2022].

Kao WL, Puddey IB, Boland LL, Watson RL, Brancati FL (2001) Alcohol consumption and the risk of type 2 diabetes mellitus: atherosclerosis risk in communities study. Am J Epidemiol 154:748–757.

Karamchand S, Leisegang R, Schomaker M, Maartens G, Walters L, Hislop M, Dave JA, Levitt NS, Cohen K (2016) Risk factors for incident diabetes in a cohort taking first-line nonnucleoside reverse transcriptase inhibitor-based antiretroviral therapy. Medicine (Baltimore) 95.

Kawamura T, Umemura T, Hotta N (2012) Cognitive impairment in diabetic patients: can diabetic control prevent cognitive decline? J Diabetes Investig 3:413–423.

Keaney J, Campbell M (2015) The dynamic blood–brain barrier. FEBS J 282:4067–4079.

Kempermann G, Gast D, Kronenberg G, Yamaguchi M, Gage FH (2003) Early determination and long-term persistence of adult-generated new neurons in the hippocampus of mice. Dev Camb Engl 130:391–399.

Kempermann G, Song H, Gage FH (2015) Neurogenesis in the Adult Hippocampus. Cold Spring Harb Perspect Biol 7:a018812 Available at: https://www.ncbi.nlm.nih.gov/pmc/articles/PMC4563705/ [Accessed May 14, 2022].

Kempuraj D, Thangavel R, Natteru PA, Selvakumar GP, Saeed D, Zahoor H, Zaheer S, Iyer SS, Zaheer A (2016) Neuroinflammation Induces Neurodegeneration. J Neurol Neurosurg Spine 1:1003.

Kilbride SM, Prehn JHM (2013) Central roles of apoptotic proteins in mitochondrial function. Oncogene 32:2703–2711 Available at: https://www.nature.com/articles/onc2012348 [Accessed May 13, 2022].

Kim B, Lee Y, Kim E, Kwak A, Ryoo S, Bae SH, Azam T, Kim S, Dinarello CA (2013) The Interleukin-1α Precursor is Biologically Active and is Likely a Key Alarmin in the IL-1 Family of Cytokines. Front Immunol 4:391.

Kim JJ, Diamond DM (2002) The stressed hippocampus, synaptic plasticity and lost memories. Nat Rev Neurosci 3:453.

Kim S-J, Kim D-J (2012) Alcoholism and diabetes mellitus. Diabetes Metab J 36:108–115.

Kirigia JM, Sambo HB, Sambo LG, Barry SP (2009) Economic burden of diabetes mellitus in the WHO African region. BMC Int Health Hum Rights 9:6 Available at: https://doi.org/10.1186/1472-698X-9-6 [Accessed May 16, 2022].

Knierim JJ (2015) The hippocampus. Curr Biol 25:R1116–R1121 Available at: https://www.cell.com/current-biology/abstract/S0960-9822(15)01312-3 [Accessed April 10, 2022].

Koch M, Fitzpatrick AL, Rapp SR, Nahin RL, Williamson JD, Lopez OL, DeKosky ST, Kuller LH, Mackey RH, Mukamal KJ, Jensen MK, Sink KM (2019) Alcohol Consumption and Risk of Dementia and Cognitive Decline Among Older Adults With or Without Mild Cognitive Impairment. JAMA Netw Open 2:e1910319 Available at: https://doi.org/10.1001/jamanetworkopen.2019.10319 [Accessed April 10, 2022].

Kodama S, Saito K, Tanaka S, Maki M, Yachi Y, Sato M, Sugawara A, Totsuka K, Shimano H, Ohashi Y (2009) Influence of fat and carbohydrate proportions on the metabolic profile in patients with type 2 diabetes: a meta-analysis. Diabetes Care 32:959–965.

Kodl CT, Seaquist ER (2008) Cognitive dysfunction and diabetes mellitus. Endocr Rev 29:494–511.

Koekkoek PS, Kappelle LJ, van den Berg E, Rutten GEHM, Biessels GJ (2015) Cognitive function in patients with diabetes mellitus: guidance for daily care. Lancet Neurol 14:329–340.

Kołota A, Głąbska D, Oczkowski M, Gromadzka-Ostrowska J (2019) Influence of Alcohol Consumption on Body Mass Gain and Liver Antioxidant Defense in Adolescent Growing Male Rats. Int J Environ Res Public Health 16 Available at: https://www.ncbi.nlm.nih.gov/pmc/articles/PMC6651161/ [Accessed June 4, 2021].

Kousignian I, Sautereau A, Vigouroux C, Cros A, Kretz S, Viard JP, Slama L (2021) Diagnosis, risk factors and management of diabetes mellitus in HIV-infected persons in France: A real-life setting study. PLOS ONE 16:e0250676 Available at: https://journals.plos.org/plosone/article?id=10.1371/journal.pone.0250676 [Accessed August 26, 2021].

Kumar C, Kumar R, Nehar S (2014) Induction of Type-II Diabetes by High Fructose Diet and Low Dose of Intraperitoneal Injection of Streptozotocin in Albino Rats. :7.

Kwon H-K, Lee J-H, Shin H-J, Kim J-H, Choi S (2015) Structural and functional analysis of cell adhesion and nuclear envelope nano-topography in cell death. Sci Rep 5 Available at: https://www.ncbi.nlm.nih.gov/pmc/articles/PMC4614995/ [Accessed May 18, 2021].

Landgren H, Curtis MA (2011) Locating and labeling neural stem cells in the brain. J Cell Physiol 226:1–7.

LaPensee CR, Hugo ER, Ben-Jonathan N (2008) Insulin Stimulates Interleukin-6 Expression and Release in LS14 Human Adipocytes through Multiple Signaling Pathways. Endocrinology 149:5415–5422 Available at: https://doi.org/10.1210/en.2008-0549 [Accessed May 10, 2022].

Lautin AL (2001) The Limbic Brain. Springer Science & Business Media.

Lepousez G, Nissant A, Lledo P-M (2015) Adult neurogenesis and the future of the rejuvenating brain circuits. Neuron 86:387–401.

Leuner B, Gould E (2010) Structural Plasticity and Hippocampal Function. Annu Rev Psychol 61:111-C3 Available at: https://www.ncbi.nlm.nih.gov/pmc/articles/PMC3012424/ [Accessed May 7, 2022].

Li C, Sun J (2022) The impact of current smoking, regular drinking, and physical inactivity on health care-seeking behavior in China. BMC Health Serv Res 22:52 Available at: https://www.ncbi.nlm.nih.gov/pmc/articles/PMC8751354/ [Accessed October 24, 2022].

Lim AK (2014) Diabetic nephropathy–complications and treatment. Int J Nephrol Renov Dis 7:361.

Lindtner C, Scherer T, Zielinski E, Filatova N, Fasshauer M, Tonks NK, Puchowicz M, Buettner C (2013) Binge Drinking Induces Whole-Body Insulin Resistance by Impairing Hypothalamic Insulin Action. Sci Transl Med 5:170ra14 Available at: https://www.ncbi.nlm.nih.gov/pmc/articles/PMC3740748/ [Accessed April 7, 2022].

Liu JX, Pinnock SB, Herbert J (2011) Novel control by the CA3 region of the hippocampus on neurogenesis in the dentate gyrus of the adult rat. PloS One 6:e17562.

Liu X, Kumar A (2015) Differential signaling mechanism for HIV-1 Nef-mediated production of IL-6 and IL-8 in human astrocytes. Sci Rep 5:9867 Available at: https://www.nature.com/articles/srep09867 [Accessed May 10, 2022].

Lodge M, Bischofberger J (2019) Synaptic properties of newly generated granule cells support sparse coding in the adult hippocampus. Behav Brain Res 372:112036 Available at: https://www.sciencedirect.com/science/article/pii/S0166432819303936 [Accessed May 14, 2022].

Lovinger DM (2008) Communication Networks in the Brain. Alcohol Res Health 31:196–214 Available at: https://www.ncbi.nlm.nih.gov/pmc/articles/PMC3860493/ [Accessed May 6, 2022].

Lozano I, Van der Werf R, Bietiger W, Seyfritz E, Peronet C, Pinget M, Jeandidier N, Maillard E, Marchioni E, Sigrist S, Dal S (2016) High-fructose and high-fat diet-induced disorders in rats: impact on diabetes risk, hepatic and vascular complications. Nutr Metab 13 Available at: https://www.ncbi.nlm.nih.gov/pmc/articles/PMC4766713/ [Accessed June 2, 2021].

Lubos E, Loscalzo J, Handy DE (2011) Glutathione Peroxidase-1 in Health and Disease: From Molecular Mechanisms to Therapeutic Opportunities. Antioxid Redox Signal 15:1957–1997 Available at: https://www.ncbi.nlm.nih.gov/pmc/articles/PMC3159114/ [Accessed April 8, 2022].

Luheshi NM, Kovács KJ, Lopez-Castejon G, Brough D, Denes A (2011) Interleukin-1α expression precedes IL-1β after ischemic brain injury and is localised to areas of focal neuronal loss and penumbral tissues. J Neuroinflammation 8:186.

Luissint A-C, Artus C, Glacial F, Ganeshamoorthy K, Couraud P-O (2012) Tight junctions at the blood brain barrier: physiological architecture and disease-associated dysregulation. Fluids Barriers CNS 9:23 Available at: https://doi.org/10.1186/2045-8118-9-23 [Accessed May 9, 2022].

Lynch SK, Abràmoff MD (2017) Diabetic retinopathy is a neurodegenerative disorder. Vision Res 139:101–107.

Ma Q, Vaida F, Wong J, Sanders CA, Kao Y, Croteau D, Clifford DB, Collier AC, Gelman BB, Marra CM, McArthur JC, Morgello S, Simpson DM, Heaton RK, Grant I, Letendre SL, CHARTER Group (2016) Long-term efavirenz use is associated with worse neurocognitive functioning in HIV-infected patients. J Neurovirol 22:170–178.

Madhusudhanan J, Suresh G, Devanathan V (2020) Neurodegeneration in type 2 diabetes: Alzheimer's as a case study. Brain Behav 10 Available at: https://www.ncbi.nlm.nih.gov/pmc/articles/PMC7218246/ [Accessed May 11, 2021].

Maldonado KA, Alsayouri K (2022) Physiology, Brain. In: StatPearls. Treasure Island (FL): StatPearls Publishing. Available at: http://www.ncbi.nlm.nih.gov/books/NBK551718/ [Accessed May 5, 2022].

Mallorquí-Bagué N et al. (2018) Type 2 diabetes and cognitive impairment in an older population with overweight or obesity and metabolic syndrome: baseline cross-sectional analysis of the PREDIMED-plus study. Sci Rep 8:16128 Available at: https://www.ncbi.nlm.nih.gov/pmc/articles/PMC6208341/ [Accessed May 17, 2022].

Manohar SM, Vaikasuvu SR, Deepthi K, Sachan A, Narasimha SRPVL (2013) An association of hyperglycemia with plasma malondialdehyde and atherogenic lipid risk factors in newly diagnosed Type 2 diabetic patients. J Res Med Sci Off J Isfahan Univ Med Sci 18:89–93 Available at: https://www.ncbi.nlm.nih.gov/pmc/articles/PMC3724384/ [Accessed May 18, 2021].

Manschot SM, Brands AM, van der Grond J, Kessels RP, Algra A, Kappelle LJ, Biessels GJ (2006) Brain magnetic resonance imaging correlates of impaired cognition in patients with type 2 diabetes. Diabetes 55:1106–1113.

Markakis EA, Gage FH (1999) Adult-generated neurons in the dentate gyrus send axonal projections to field CA3 and are surrounded by synaptic vesicles. J Comp Neurol 406:449–460.

Martinez N, Ketheesan N, Martens GW, West K, Lien E, Kornfeld H (2016) Defects in early cell recruitment contribute to the increased susceptibility to respiratory Klebsiella pneumoniae infection in diabetic mice. Microbes Infect 18:649–655 Available at: https://www.sciencedirect.com/science/article/pii/S1286457916300685 [Accessed November 12, 2021].

Martínez-Cerdeño V, Noctor SC (2018) Neural Progenitor Cell Terminology. Front Neuroanat 12 Available at: https://www.frontiersin.org/article/10.3389/fnana.2018.00104 [Accessed May 14, 2022].

Masiello P, Broca C, Gross R, Roye M, Manteghetti M, Hillaire-Buys D, Novelli M, Ribes G (1998) Experimental NIDDM: development of a new model in adult rats administered streptozotocin and nicotinamide. Diabetes 47:224–229.

Mastrototaro L, Roden M (2021) Insulin resistance and insulin sensitizing agents. Metabolism 125:154892 Available at: https://www.sciencedirect.com/science/article/pii/S002604952100192X [Accessed May 7, 2022].

Masuku (2019) HIV and antiretroviral therapy-induced metabolic syndrome in people living with HIV and its implications for care: A critical review. Available at: https://www.journalofdiabetology.org/article.asp?issn=2078-

7685;year=2019;volume=10;issue=2;spage=41;epage=47;aulast=Masuku [Accessed May 17, 2021].

Mauffrey P, Tchitchek N, Barroca V, Bemelmans A-P, Firlej V, Allory Y, Roméo P-H, Magnon C (2019) Progenitors from the central nervous system drive neurogenesis in cancer. Nature 569:672–678.

Mayer KH, Venkatesh KK (2010) Antiretroviral Therapy as HIV Prevention: Status and Prospects. Am J Public Health 100:1867–1876 Available at: https://www.ncbi.nlm.nih.gov/pmc/articles/PMC2936983/ [Accessed May 4, 2022].

McNay EC, Ong CT, McCrimmon RJ, Cresswell J, Bogan JS, Sherwin RS (2010) Hippocampal memory processes are modulated by insulin and high-fat-induced insulin resistance. Neurobiol Learn Mem 93:546–553 Available at: https://www.ncbi.nlm.nih.gov/pmc/articles/PMC2878207/ [Accessed May 17, 2021].

McNay EC, Pearson-Leary J (2020) GluT4: a central player in hippocampal memory and brain insulin resistance. Exp Neurol 323:113076 Available at: https://www.ncbi.nlm.nih.gov/pmc/articles/PMC6936336/ [Accessed May 6, 2022].

McNay EC, Recknagel AK (2011) Reprint of:'Brain insulin signaling: A key component of cognitive processes and a potential basis for cognitive impairment in type 2 diabetes.' Neurobiol Learn Mem 96:517–528.

Meagher EA, FitzGerald GA (2000) Indices of lipid peroxidation in vivo: strengths and limitations. Free Radic Biol Med 28:1745–1750.

Meda SA, Hawkins KA, Dager AD, Tennen H, Khadka S, Austad CS, Wood RM, Raskin S, Fallahi CR, Pearlson GD (2018) Longitudinal effects of alcohol consumption on the hippocampus and parahippocampus in college students. Biol Psychiatry Cogn Neurosci Neuroimaging 3:610–617 Available at: https://www.ncbi.nlm.nih.gov/pmc/articles/PMC6062479/ [Accessed April 10, 2022].

Meintjes G, Moorhouse MA, Carmona S, Davies N, Dlamini S, Van Vuuren C, Manzini T, Mathe M, Moosa Y, Nash J (2017) Adult antiretroviral therapy guidelines 2017. South Afr J HIV Med 18.

Migliore M, Ascoli GA, Jaffe DB (2010) CA3 Cells: Detailed and Simplified Pyramidal Cell Models. In: Hippocampal Microcircuits: A Computational Modeler's Resource Book (Cutsuridis V, Graham B, Cobb S, Vida I, eds), pp 353–374 Springer Series in Computational Neuroscience. New York, NY: Springer. Available at: https://doi.org/10.1007/978-1-4419-0996-1_12 [Accessed May 18, 2021].

Miles R, Le Duigou C, Simonnet J, Telenczuk M, Fricker D (2014) Recurrent synapses and circuits in the CA3 region of the hippocampus: an associative network. Front Cell Neurosci 7:262 Available at: https://www.frontiersin.org/article/10.3389/fncel.2013.00262 [Accessed August 20, 2021].

Milne NT, Bucks RS, Davis WA, Davis TME, Pierson R, Starkstein SE, Bruce DG (2017) Hippocampal atrophy, asymmetry, and cognition in type 2 diabetes mellitus. Brain Behav 8:e00741 Available at: https://www.ncbi.nlm.nih.gov/pmc/articles/PMC5853633/ [Accessed July 7, 2021].

Molina PE, Bagby GJ, Nelson S (2014) Biomedical consequences of alcohol use disorders in the HIV-infected host. Curr HIV Res 12:265–275.

Möller M, Fourie J, Harvey BH (2018) Efavirenz exposure, alone and in combination with known drugs of abuse, engenders addictive-like bio-behavioural changes in rats. Sci Rep 8.

Monroe AK, Glesby MJ, Brown TT (2014) Diagnosing and managing diabetes in HIV-infected patients: current concepts. Clin Infect Dis 60:453–462.

Moran C, Phan TG, Chen J, Blizzard L, Beare R, Venn A, Münch G, Wood AG, Forbes J, Greenaway TM (2013) Brain atrophy in type 2 diabetes: regional distribution and influence on cognition. Diabetes Care:DC_130143.

Morgado-Bernal I (2011) Learning and memory consolidation: linking molecular and behavioral data. Neuroscience 176:12–19.

Morris SA, Eaves DW, Smith AR, Nixon K (2010) Alcohol inhibition of neurogenesis: a mechanism of hippocampal neurodegeneration in an adolescent alcohol abuse model. Hippocampus 20:596–607.

Moujalled D, Strasser A, Liddell JR (2021) Molecular mechanisms of cell death in neurological diseases. Cell Death Differ 28:2029–2044 Available at: https://www.nature.com/articles/s41418-021-00814-y [Accessed April 29, 2022].

Muhammad M (2019) Tumor Necrosis Factor Alpha: A Major Cytokine of Brain Neuroinflammation. IntechOpen. Available at: https://www.intechopen.com/chapters/68123 [Accessed November 9, 2021].

Muriach M, Flores-Bellver M, Romero FJ, Barcia JM (2014) Diabetes and the Brain: Oxidative Stress, Inflammation, and Autophagy. Oxid Med Cell Longev 2014:e102158 Available at: https://www.hindawi.com/journals/omcl/2014/102158/ [Accessed October 20, 2022].

Mygind L, Bergh MS-S, Tejsi V, Vaitheeswaran R, Lambertsen KL, Finsen B, Metaxas A (2021) Tumor Necrosis Factor (TNF) Is Required for Spatial Learning and Memory in Male Mice under Physiological, but Not Immune-Challenged Conditions. Cells 10:608 Available at: https://www.ncbi.nlm.nih.gov/pmc/articles/PMC8002217/ [Accessed May 10, 2022].

Nagano H, Ito S, Masuda T, Ohtsuki S (2021) Effect of Insulin Receptor-Knockdown on the Expression Levels of Blood–Brain Barrier Functional Proteins in Human Brain Microvascular Endothelial Cells. Pharm Res Available at: https://doi.org/10.1007/s11095-021-03131-8 [Accessed June 28, 2022].

Nakazawa K, Quirk MC, Chitwood RA, Watanabe M, Yeckel MF, Sun LD, Kato A, Carr CA, Johnston D, Wilson MA, Tonegawa S (2002) Requirement for hippocampal CA3 NMDA receptors in associative memory recall. Science 297:211–218.

Nakazawa K, Sun LD, Quirk MC, Rondi-Reig L, Wilson MA, Tonegawa S (2003) Hippocampal CA3 NMDA receptors are crucial for memory acquisition of one-time experience. Neuron 38:305–315.

Nam SM, Kim JW, Yoo DY, Jung HY, Choi JH, Hwang IK, Seong JK, Yoon YS (2016) Reduction of adult hippocampal neurogenesis is amplified by aluminum exposure in a model of type 2 diabetes.

J Vet Sci 17:13–20 Available at: https://synapse.koreamed.org/articles/1041431 [Accessed May 15, 2022].

Nemeth C, Glasper E, Harrell C, Malviya S, Otis J, Neigh G (2014) Meloxicam Blocks Neuroinflammation, but Not Depressive-Like Behaviors, in HIV-1 Transgenic Female Rats. PloS One 9:e108399.

Neniskyte U, Vilalta A, Brown GC (2014) Tumour necrosis factor alpha-induced neuronal loss is mediated by microglial phagocytosis. Febs Lett 588:2952–2956 Available at: https://www.ncbi.nlm.nih.gov/pmc/articles/PMC4158418/ [Accessed May 17, 2022].

Nentwich MM, Ulbig MW (2015) Diabetic retinopathy-ocular complications of diabetes mellitus. World J Diabetes 6:489.

Neuhaus J, Jacobs DR Jr, Baker JV, Calmy A, Duprez D, La Rosa A, Kuller LH, Pett SL, Ristola M, Ross MJ, Shlipak MG, Tracy R, Neaton JD (2010) Markers of Inflammation, Coagulation, and Renal Function Are Elevated in Adults with HIV Infection. J Infect Dis 201:1788–1795 Available at: https://doi.org/10.1086/652749 [Accessed May 10, 2022].

NigatuHaregu T, Oldenburg B, Setswe G, Elliott J (2012) Magnitude of diabetes comorbidity among people living with HIV: a systematic review. Int J Diabetes Res 1:81–86.

Nixon K, Morris SA, Liput DJ, Kelso ML (2010) Roles of neural stem cells and adult neurogenesis in adolescent alcohol use disorders. Alcohol Fayettev N 44:39 Available at: https://www.ncbi.nlm.nih.gov/pmc/articles/PMC2818478/ [Accessed May 14, 2022].

Nkomozepi P, Mazengenya P, Ihunwo AO (2019) Age-related changes in Ki-67 and DCX expression in the BALB/ c mouse (Mus Musculus) brain. Int J Dev Neurosci 72:36–47 Available at: https://onlinelibrary.wiley.com/doi/abs/10.1016/j.ijdevneu.2018.11.005 [Accessed May 18, 2022].

Nolan D, Mallal S (2004) Complications associated with NRTI therapy: update on clinical features and possible pathogenic mechanisms. Antivir Ther 9:849–863.

Noor MA (2007) The role of protease inhibitors in the pathogenesis of HIV-associated insulin resistance: cellular mechanisms and clinical implications. Curr HIV/AIDS Rep 4:126–134.

Ohtsuki S, Yamaguchi H, Katsukura Y, Asashima T, Terasaki T (2008) mRNA expression levels of tight junction protein genes in mouse brain capillary endothelial cells highly purified by magnetic cell sorting. J Neurochem 104:147–154.

Oliva A, Fernández-Ruiz A, Buzsáki G, Berényi A (2016) Spatial coding and physiological properties of hippocampal neurons in the Cornu Ammonis subregions. Hippocampus 26:1593–1607 Available at: https://onlinelibrary.wiley.com/doi/abs/10.1002/hipo.22659 [Accessed May 18, 2022].

O'Mahony SM, Myint A-M, Steinbusch H, Leonard BE (2005) Efavirenz induces depressive-like behaviour, increased stress response and changes in the immune response in rats. Neuroimmunomodulation 12:293–298.

Opii WycliffeO, Sultana R, Abdul HM, Ansari M-A, Nath A, Butterfield DA (2007) Oxidative Stress and Toxicity Induced by the Nucleoside Reverse Transcriptase Inhibitor (NRTI) - 2', 3'-

dideoxycytidine (ddC): Relevance to HIV Dementia. Exp Neurol 204:29–38 Available at: https://www.ncbi.nlm.nih.gov/pmc/articles/PMC1857338/ [Accessed May 17, 2021].

Osuji FN, Onyenekwe CC, Ahaneku JE, Ukibe NR (2018) The effects of highly active antiretroviral therapy on the serum levels of pro-inflammatory and anti-inflammatory cytokines in HIV infected subjects. J Biomed Sci 25:88 Available at: https://doi.org/10.1186/s12929-018-0490-9 [Accessed August 20, 2021].

Pan H, Zhang L, Guo M, Sui H, Li H, Wu W, Qu N, Liang M, Chang D (2010) The oxidative stress status in diabetes mellitus and diabetic nephropathy. Acta Diabetol 47 Suppl 1:71–76.

Panlilio AL, Cardo DM, Grohskopf LA, Heneine W, Ross CS, U.S. Public Health Service (2005) Updated U.S. Public Health Service guidelines for the management of occupational exposures to HIV and recommendations for postexposure prophylaxis. MMWR Recomm Rep Morb Mortal Wkly Rep Recomm Rep 54:1–17.

Pastakia SD, Pekny CR, Manyara SM, Fischer L (2017) Diabetes in sub-Saharan Africa – from policy to practice to progress: targeting the existing gaps for future care for diabetes. Diabetes Metab Syndr Obes Targets Ther 10:247–263 Available at: https://www.ncbi.nlm.nih.gov/pmc/articles/PMC5489055/ [Accessed May 4, 2022].

Paula AA, Falcão MC, Pacheco AG (2013) Metabolic syndrome in HIV-infected individuals: underlying mechanisms and epidemiological aspects. AIDS Res Ther 10:32.

Paxinos G, Watson C (2006) The Rat Brain in Stereotaxic Coordinates: Hard Cover Edition. Elsevier.

Pearson-Leary J, McNay EC (2016) Novel Roles for the Insulin-Regulated Glucose Transporter-4 in Hippocampally Dependent Memory. J Neurosci Off J Soc Neurosci 36:11851–11864.

Pepin ME, Padgett LE, McDowell RE, Burg AR, Brahma MK, Holleman C, Kim T, Crossman D, Kutsch O, Tse HM, Wende AR, Habegger KM (2018) Antiretroviral therapy potentiates high-fat diet induced obesity and glucose intolerance. Mol Metab 12:48–61 Available at: https://www.ncbi.nlm.nih.gov/pmc/articles/PMC6001921/ [Accessed June 4, 2021].

Persidsky Y, Heilman D, Haorah J, Zelivyanskaya M, Persidsky R, Weber GA, Shimokawa H, Kaibuchi K, Ikezu T (2006) Rho-mediated regulation of tight junctions during monocyte migration across the blood-brain barrier in HIV-1 encephalitis (HIVE). Blood 107:4770–4780 Available at: https://www.ncbi.nlm.nih.gov/pmc/articles/PMC1895810/ [Accessed April 8, 2022].

Pheiffer C, Pillay-van Wyk V, Joubert JD, Levitt N, Nglazi MD, Bradshaw D (2018) The prevalence of type 2 diabetes in South Africa: a systematic review protocol. BMJ Open 8:e021029.

Phillips SC (1981) Does ethanol damage the blood-brain barrier? J Neurol Sci 50:81–87 Available at: https://www.sciencedirect.com/science/article/pii/0022510X81900435 [Accessed July 7, 2022].

Pizzino G, Irrera N, Cucinotta M, Pallio G, Mannino F, Arcoraci V, Squadrito F, Altavilla D, Bitto A (2017) Oxidative Stress: Harms and Benefits for Human Health. Oxid Med Cell Longev 2017:8416763 Available at: https://www.ncbi.nlm.nih.gov/pmc/articles/PMC5551541/ [Accessed May 10, 2022].

Pomytkin I, Costa-Nunes JP, Kasatkin V, Veniaminova E, Demchenko A, Lyundup A, Lesch K-P, Ponomarev ED, Strekalova T (2018) Insulin receptor in the brain: Mechanisms of activation

and the role in the CNS pathology and treatment. CNS Neurosci Ther 24:763–774 Available at: https://onlinelibrary.wiley.com/doi/abs/10.1111/cns.12866 [Accessed February 15, 2022].

Pournaghi P, Sadrkhanlou R-A, Hasanzadeh S, Foroughi A (2012a) An investigation on body weights, blood glucose levels and pituitary-gonadal axis hormones in diabetic and metformin-treated diabetic female rats. Vet Res Forum 3:79–84 Available at: https://www.ncbi.nlm.nih.gov/pmc/articles/PMC4312800/ [Accessed June 30, 2021].

Pournaghi P, Sadrkhanlou R-A, Hasanzadeh S, Foroughi A (2012b) An investigation on body weights, blood glucose levels and pituitary-gonadal axis hormones in diabetic and metformin-treated diabetic female rats. Vet Res Forum Int Q J 3:79–84.

Pozhilenkova E, Lopatina O, Komleva Y, Salmin V, Salmina A (2017) Blood-brain barrier-supported neurogenesis in healthy and diseased brain. Rev Neurosci 28.

Prasad KN (2017) Oxidative Stress, Pro-Inflammatory Cytokines, and Antioxidants Regulate Expression Levels of MicroRNAs in Parkinson's Disease. Curr Aging Sci 10:177–184.

Prieto GA, Tong L, Smith ED, Cotman CW (2019) TNFα and IL-1β but not IL-18 suppresses hippocampal long-term potentiation directly at the synapse. Neurochem Res 44:49–60 Available at: https://www.ncbi.nlm.nih.gov/pmc/articles/PMC6170724/ [Accessed May 10, 2022].

Qi C, Pekala PH (2000) Tumor necrosis factor-alpha-induced insulin resistance in adipocytes. Proc Soc Exp Biol Med Soc Exp Biol Med N Y N 223:128–135.

Qin L, He J, Hanes RN, Pluzarev O, Hong J-S, Crews FT (2008) Increased systemic and brain cytokine production and neuroinflammation by endotoxin following ethanol treatment. J Neuroinflammation 5:10.

Qinna NA, Badwan AA (2015) Impact of streptozotocin on altering normal glucose homeostasis during insulin testing in diabetic rats compared to normoglycemic rats. Drug Des Devel Ther 9:2515–2525 Available at: https://www.ncbi.nlm.nih.gov/pmc/articles/PMC4427609/ [Accessed October 24, 2022].

Rajmohan V, Mohandas E (2007) The limbic system. Indian J Psychiatry 49:132–139 Available at: https://www.ncbi.nlm.nih.gov/pmc/articles/PMC2917081/ [Accessed May 7, 2022].

Ramos-Rodriguez JJ, Molina-Gil S, Ortiz-Barajas O, Jimenez-Palomares M, Perdomo G, Cozar-Castellano I, Lechuga-Sancho AM, Garcia-Alloza M (2014) Central proliferation and neurogenesis is impaired in type 2 diabetes and prediabetes animal models. PLoS One 9:e89229.

Reed MJ, Meszaros K, Entes LJ, Claypool MD, Pinkett JG, Gadbois TM, Reaven GM (2000) A new rat model of type 2 diabetes: the fat-fed, streptozotocin-treated rat. Metab-Clin Exp 49:1390–1394.

Rehman K, Akash MSH, Liaqat A, Kamal S, Qadir MI, Rasul A (2017) Role of Interleukin-6 in Development of Insulin Resistance and Type 2 Diabetes Mellitus. Crit Rev Eukaryot Gene Expr 27:229–236.

Reinke C, Buchmann N, Fink A, Tegeler C, Demuth I, Doblhammer G (2022) Diabetes duration and the risk of dementia: a cohort study based on German health claims data. Age Ageing 51:afab231 Available at: https://doi.org/10.1093/ageing/afab231 [Accessed April 22, 2022].

Reynolds BA, Weiss S (1992) Generation of neurons and astrocytes from isolated cells of the adult mammalian central nervous system. Science 255:1707–1710.

Rheeder P (2006) Type 2 diabetes: the emerging epidemic. South Afr Fam Pract 48:20–20.

Richard C, Wadowski M, Goruk S, Cameron L, Sharma AM, Field CJ (2017) Individuals with obesity and type 2 diabetes have additional immune dysfunction compared with obese individuals who are metabolically healthy. BMJ Open Diabetes Res Care 5:e000379 Available at: https://drc.bmj.com/lookup/doi/10.1136/bmjdrc-2016-000379 [Accessed January 20, 2022].

Robertson K, Liner J, Meeker RB (2012) Antiretroviral neurotoxicity. J Neurovirol 18:388–399.

Rodríguez-Correa E, González-Pérez I, Clavel-Pérez PI, Contreras-Vargas Y, Carvajal K (2020) Biochemical and nutritional overview of diet-induced metabolic syndrome models in rats: what is the best choice? Nutr Diabetes 10:1–15 Available at: https://www.nature.com/articles/s41387-020-0127-4 [Accessed October 20, 2022].

Romao PR, Lemos JC, Moreira J, de Chaves G, Moretti M, Castro AA, Andrade VM, Boeck CR, Quevedo J, Gavioli EC (2011) Anti-HIV drugs nevirapine and efavirenz affect anxiety-related behavior and cognitive performance in mice. Neurotox Res 19:73–80.

Rothwell NJ (1999) Cytokines – killers in the brain? J Physiol 514:3–17 Available at: https://www.ncbi.nlm.nih.gov/pmc/articles/PMC2269053/ [Accessed May 9, 2022].

Rothwell NJ, Luheshi G (1994) Pharmacology of interleukin-1 actions in the brain. Adv Pharmacol San Diego Calif 25:1–20.

Rubin RD, Watson PD, Duff MC, Cohen NJ (2014) The role of the hippocampus in flexible cognition and social behavior. Front Hum Neurosci 8:742 Available at: https://www.ncbi.nlm.nih.gov/pmc/articles/PMC4179699/ [Accessed May 7, 2022].

Rubio-Araiz A, Porcu F, Pérez-Hernández M, García-Gutiérrez MS, Aracil-Fernández MA, Gutierrez-López MD, Guerri C, Manzanares J, O'shea E, Colado MI (2017) Disruption of blood–brain barrier integrity in postmortem alcoholic brain: preclinical evidence of Tlr4 involvement from a binge-like drinking model. Addict Biol 22:1103–1116.

Rushforth B, McCrorie C, Glidewell L, Midgley E, Foy R (2016) Barriers to effective management of type 2 diabetes in primary care: qualitative systematic review. Br J Gen Pract 66:e114–e127 Available at: https://www.ncbi.nlm.nih.gov/pmc/articles/PMC4723210/ [Accessed May 16, 2022].

Russo I, Barlati S, Bosetti F (2011) Effects of neuroinflammation on the regenerative capacity of brain stem cells. J Neurochem 116:947–956.

S EM, A A-I, Dh A, L P, M A (2002) Expression of insulin-responsive glucose transporter GLUT4 mRNA in the rat brain and spinal cord: an in situ hybridization study. J Chem Neuroanat 24 Available at: https://pubmed.ncbi.nlm.nih.gov/12406499/ [Accessed May 6, 2022].

Sachsenberg N, Perelson AS, Yerly S, Schockmel GA, Leduc D, Hirschel B, Perrin L (1998) Turnover of CD4+ and CD8+ T lymphocytes in HIV-1 infection as measured by Ki-67 antigen. J Exp Med 187:1295–1303.

Sadeghi A, Hami J, Razavi S, Esfandiary E, Hejazi Z (2016) The effect of diabetes mellitus on apoptosis in hippocampus: cellular and molecular aspects. Int J Prev Med 7.

Saez I, Duran J, Sinadinos C, Beltran A, Yanes O, Tevy MF, Martínez-Pons C, Milán M, Guinovart JJ (2014) Neurons have an active glycogen metabolism that contributes to tolerance to hypoxia. J Cereb Blood Flow Metab Off J Int Soc Cereb Blood Flow Metab 34:945–955.

Sajan FD, Martiniuk F, Marcus DL, Frey WH, Hite R, Bordayo EZ, Freedman ML (2007) Apoptotic gene expression in Alzheimer's disease hippocampal tissue. Am J Alzheimers Dis Other Demen 22:319–328.

Salameh TS, Mortell WG, Logsdon AF, Butterfield DA, Banks WA (2019) Disruption of the hippocampal and hypothalamic blood–brain barrier in a diet-induced obese model of type II diabetes: prevention and treatment by the mitochondrial carbonic anhydrase inhibitor, topiramate. Fluids Barriers CNS 16:1 Available at: https://doi.org/10.1186/s12987-018-0121-6 [Accessed May 9, 2022].

Salameh TS, Shah GN, Price TO, Hayden MR, Banks WA (2016) Blood–brain barrier disruption and neurovascular unit dysfunction in diabetic mice: protection with the mitochondrial carbonic anhydrase inhibitor topiramate. J Pharmacol Exp Ther 359:452–459.

Salmeron KE, Maniskas ME, Edwards DN, Wong R, Rajkovic I, Trout A, Rahman AA, Hamilton S, Fraser JF, Pinteaux E, Bix GJ (2019) Interleukin 1 alpha administration is neuroprotective and neuro-restorative following experimental ischemic stroke. J Neuroinflammation 16:222 Available at: https://doi.org/10.1186/s12974-019-1599-9 [Accessed May 18, 2021].

Sankari SL, Masthan KMK, Babu NA, Bhattacharjee T, Elumalai M (2012) Apoptosis in cancer--an update. Asian Pac J Cancer Prev APJCP 13:4873–4878.

Santello M, Volterra A (2012) TNFα in synaptic function: switching gears. Trends Neurosci 35:638–647.

Sasaki S, Inoguchi T (2012) The role of oxidative stress in the pathogenesis of diabetic vascular complications. Diabetes Metab J 36:255–261.

Saylor D, Dickens AM, Sacktor N, Haughey N, Slusher B, Pletnikov M, Mankowski JL, Brown A, Volsky DJ, McArthur JC (2016) HIV-associated neurocognitive disorder — pathogenesis and prospects for treatment. Nat Rev Neurol 12:234–248 Available at: https://www.ncbi.nlm.nih.gov/pmc/articles/PMC4937456/ [Accessed April 10, 2022].

Scatliff JH, Clark JK (1992) Special Article How the Brain Got Its Names and Numbers. :8.

Scharfman HE (2007) The CA3 "backprojection" to the dentate gyrus. Prog Brain Res 163:627–637.

Scharfman HE, Myers CE (2016) Corruption of the Dentate Gyrus by "Dominant" Granule cells: Implications for Dentate Gyrus Function in Health and Disease. Neurobiol Learn Mem 129:69–82 Available at: https://www.ncbi.nlm.nih.gov/pmc/articles/PMC4792754/ [Accessed May 18, 2021].

Schneider M, Chersich M, Temmerman M, Degomme O, Parry CD (2014) The impact of alcohol on HIV prevention and treatment for South Africans in primary healthcare. curationis 37:01–08.

Scholzen T, Gerdes J (2000) The Ki-67 protein: from the known and the unknown. J Cell Physiol 182:311–322.

Schrieks IC, Heil ALJ, Hendriks HFJ, Mukamal KJ, Beulens JWJ (2015) The effect of alcohol consumption on insulin sensitivity and glycemic status: a systematic review and meta-analysis of intervention studies. Diabetes Care 38:723–732.

Schultz S, Panzeri S, Treves A, Rolls ET (1997) Analogue resolution in a model of the Schaffer collaterals. In: Artificial Neural Networks — ICANN'97 (Gerstner W, Germond A, Hasler M, Nicoud J-D, eds), pp 61–66 Lecture Notes in Computer Science. Berlin, Heidelberg: Springer.

Schulze MB, Schulz M, Heidemann C, Schienkiewitz A, Hoffmann K, Boeing H (2008) Carbohydrate intake and incidence of type 2 diabetes in the European Prospective Investigation into Cancer and Nutrition (EPIC)-Potsdam Study. Br J Nutr 99:1107–1116.

Seguin JA, Brennan J, Mangano E, Hayley S (2009) Proinflammatory cytokines differentially influence adult hippocampal cell proliferation depending upon the route and chronicity of administration. Neuropsychiatr Dis Treat 5:5.

Shai I, Rimm EB, Schulze MB, Rifai N, Stampfer MJ, Hu FB (2004) Moderate alcohol intake and markers of inflammation and endothelial dysfunction among diabetic men. Diabetologia 47:1760–1767 Available at: https://doi.org/10.1007/s00125-004-1526-0 [Accessed February 7, 2022].

Shetty PK, Galeffi F, Turner DA (2012) Cellular Links between Neuronal Activity and Energy Homeostasis. Front Pharmacol 3:43 Available at: https://www.ncbi.nlm.nih.gov/pmc/articles/PMC3308331/ [Accessed May 6, 2022].

Shi J, Fan J, Su Q, Yang Z (2019) Cytokines and Abnormal Glucose and Lipid Metabolism. Front Endocrinol 10 Available at: https://www.frontiersin.org/articles/10.3389/fendo.2019.00703/full [Accessed May 18, 2021].

Shinoura N, Yoshida Y, Asai A, Kirino T, Hamada H (1999) Relative level of expression of Bax and Bcl-XL determines the cellular fate of apoptosis/necrosis induced by the overexpression of Bax. Oncogene 18:5703–5713 Available at: https://www.nature.com/articles/1202966 [Accessed May 27, 2022].

Shisana O, Rehle T, Simbayi LC, Zuma K, Jooste S, Zungu N, Labadarios D, Onoya D (2014) South African national HIV prevalence, incidence and behaviour survey, 2012.

Singh R (2020) Cerebellum: Its Anatomy, Functions and Diseases. IntechOpen. Available at: https://www.intechopen.com/chapters/72599 [Accessed May 5, 2022].

Sorrells SF, Paredes MF, Velmeshev D, Herranz-Pérez V, Sandoval K, Mayer S, Chang EF, Insausti R, Kriegstein AR, Rubenstein JL, Manuel Garcia-Verdugo J, Huang EJ, Alvarez-Buylla A (2019) Immature excitatory neurons develop during adolescence in the human amygdala. Nat Commun 10:2748 Available at: https://www.ncbi.nlm.nih.gov/pmc/articles/PMC6588589/ [Accessed May 14, 2022].

Sorrells SF, Paredes MF, Zhang Z, Kang G, Pastor-Alonso O, Biagiotti S, Page CE, Sandoval K, Knox A, Connolly A, Huang EJ, Garcia-Verdugo JM, Oldham MC, Yang Z, Alvarez-Buylla A (2021) Positive Controls in Adults and Children Support That Very Few, If Any, New Neurons Are Born in the Adult Human Hippocampus. J Neurosci 41:2554–2565 Available at: https://www.jneurosci.org/content/41/12/2554 [Accessed May 14, 2022].

Soto M, Cai W, Konishi M, Kahn CR (2019) Insulin signaling in the hippocampus and amygdala regulates metabolism and neurobehavior. Proc Natl Acad Sci 116:6379–6384 Available at: https://www.pnas.org/content/116/13/6379 [Accessed February 15, 2022].

Spinelli M, Fusco S, Grassi C (2019) Brain Insulin Resistance and Hippocampal Plasticity: Mechanisms and Biomarkers of Cognitive Decline. Front Neurosci 13 Available at: https://www.frontiersin.org/article/10.3389/fnins.2019.00788 [Accessed May 7, 2022].

Spruston N (2008) Pyramidal neurons: dendritic structure and synaptic integration. Nat Rev Neurosci 9:206–221.

Starr JM, Wardlaw J, Ferguson K, MacLullich A, Deary IJ, Marshall I (2003) Increased blood-brain barrier permeability in type II diabetes demonstrated by gadolinium magnetic resonance imaging. J Neurol Neurosurg Psychiatry 74:70–76.

Steiner B, Klempin F, Wang L, Kott M, Kettenmann H, Kempermann G (2006) Type-2 cells as link between glial and neuronal lineage in adult hippocampal neurogenesis. Glia 54:805–814.

Stöckli J, Fazakerley DJ, James DE (2011) GLUT4 exocytosis. J Cell Sci 124:4147–4159 Available at: https://www.ncbi.nlm.nih.gov/pmc/articles/PMC3258103/ [Accessed May 7, 2022].

Stranahan AM, Arumugam TV, Cutler RG, Lee K, Egan JM, Mattson MP (2008) Diabetes impairs hippocampal function through glucocorticoid-mediated effects on new and mature neurons. Nat Neurosci 11:309–317 Available at: https://www.nature.com/articles/nn2055 [Accessed July 6, 2021].

Strange BA, Witter MP, Lein ES, Moser EI (2014) Functional organization of the hippocampal longitudinal axis. Nat Rev Neurosci 15:655–669 Available at: https://www.nature.com/articles/nrn3785 [Accessed April 11, 2022].

Taffe MA, Kotzebue RW, Crean RD, Crawford EF, Edwards S, Mandyam CD (2010) Long-lasting reduction in hippocampal neurogenesis by alcohol consumption in adolescent nonhuman primates. Proc Natl Acad Sci:200912810.

Takahashi S, Fukushima H, Yu Z, Tomita H, Kida S (2021) Tumor necrosis factor α negatively regulates the retrieval and reconsolidation of hippocampus-dependent memory. Brain Behav Immun 94:79–88 Available at: https://www.sciencedirect.com/science/article/pii/S0889159121000982 [Accessed May 10, 2022].

Takechi R, Lam V, Brook E, Giles C, Fimognari N, Mooranian A, Al-Salami H, Coulson SH, Nesbit M, Mamo JCL (2017) Blood-Brain Barrier Dysfunction Precedes Cognitive Decline and Neurodegeneration in Diabetic Insulin Resistant Mouse Model: An Implication for Causal Link. Front Aging Neurosci 9:399.

Tovar-y-Romo LB, Bumpus NN, Pomerantz D, Avery LB, Sacktor N, McArthur JC, Haughey NJ (2012) Dendritic spine injury induced by the 8-hydroxy metabolite of efavirenz. J Pharmacol Exp Ther 343:696–703.

Trikkalinou A, Papazafiropoulou AK, Melidonis A (2017) Type 2 diabetes and quality of life. World J Diabetes 8:120–129 Available at: https://www.ncbi.nlm.nih.gov/pmc/articles/PMC5394731/ [Accessed May 4, 2022].

Tsalamandris S, Antonopoulos AS, Oikonomou E, Papamikroulis G-A, Vogiatzi G, Papaioannou S, Deftereos S, Tousoulis D (2019) The Role of Inflammation in Diabetes: Current Concepts and Future Perspectives. Eur Cardiol Rev 14:50–59 Available at: https://www.ncbi.nlm.nih.gov/pmc/articles/PMC6523054/ [Accessed May 17, 2021].

Tseng A, Seet J, Phillips EJ (2015) The evolution of three decades of antiretroviral therapy: challenges, triumphs and the promise of the future. Br J Clin Pharmacol 79:182–194 Available at: https://www.ncbi.nlm.nih.gov/pmc/articles/PMC4309625/ [Accessed May 4, 2022].

Tu Y-F, Jiang S-T, Chiang C-W, Chen L-C, Huang C-C (2021) Endothelial-specific insulin receptor substrate-1 overexpression worsens neonatal hypoxic-ischemic brain injury via mTOR-mediated tight junction disassembly. Cell Death Discov 7:1–11 Available at: https://www.nature.com/articles/s41420-021-00548-3 [Accessed June 29, 2022].

Ueno H, Kondo E, Yamamoto-Honda R, Tobe K, Nakamoto T, Sasaki K, Mitani K, Furusaka A, Tanaka T, Tsujimoto Y, Kadowaki T, Hirai H (2000) Association of Insulin Receptor Substrate Proteins with Bcl-2 and Their Effects on Its Phosphorylation and Antiapoptotic Function. Mol Biol Cell 11:735–746 Available at: https://www.ncbi.nlm.nih.gov/pmc/articles/PMC14806/ [Accessed June 14, 2022].

Uren RT, Dewson G, Bonzon C, Lithgow T, Newmeyer DD, Kluck RM (2005) Mitochondrial release of pro-apoptotic proteins: electrostatic interactions can hold cytochrome c but not Smac/DIABLO to mitochondrial membranes. J Biol Chem 280:2266–2274.

Valcour VG, Shikuma CM, Shiramizu BT, Williams AE, Watters MR, Poff PW, Grove JS, Selnes OA, Sacktor NC (2005) Diabetes, Insulin Resistance, and Dementia Among HIV-1–Infected Patients. J Acquir Immune Defic Syndr 1999 38:31–36 Available at: https://www.ncbi.nlm.nih.gov/pmc/articles/PMC1415271/ [Accessed May 4, 2022].

Valdez AN, Rubin LH, Neigh GN (2016) Untangling the Gordian knot of HIV, stress, and cognitive impairment. Neurobiol Stress 4:44–54 Available at: https://www.sciencedirect.com/science/article/pii/S2352289515300382 [Accessed May 10, 2022].

van Bussel FC, Backes WH, Hofman PA, van Oostenbrugge RJ, van Boxtel MP, Verhey FR, Steinbusch HW, Schram MT, Stehouwer CD, Wildberger JE (2017) Cerebral pathology and cognition in diabetes: the merits of multiparametric neuroimaging. Front Neurosci 11:188.

van der Heide LP, Kamal A, Artola A, Gispen WH, Ramakers GMJ (2005) Insulin modulates hippocampal activity-dependent synaptic plasticity in a N-methyl-d-aspartate receptor and phosphatidyl-inositol-3-kinase-dependent manner. J Neurochem 94:1158–1166.

van Praag H, Schinder AF, Christie BR, Toni N, Palmer TD, Gage FH (2002) Functional neurogenesis in the adult hippocampus. Nature 415:1030–1034.

Varatharaj A, Galea I (2017) The blood-brain barrier in systemic inflammation. Brain Behav Immun 60:1–12.

Vellios NG, Van Walbeek CP (2018) Self-reported alcohol use and binge drinking in South Africa: Evidence from the National Income Dynamics Study, 2014-2015. S Afr Med J 108:33–39.

Vogel S, Schwabe L (2016) Learning and memory under stress: implications for the classroom. Npj Sci Learn 1:1–10 Available at: https://www.nature.com/articles/npjscilearn201611 [Accessed May 7, 2022].

Volpe CMO, Villar-Delfino PH, dos Anjos PMF, Nogueira-Machado JA (2018) Cellular death, reactive oxygen species (ROS) and diabetic complications. Cell Death Dis 9:1–9 Available at: https://www.nature.com/articles/s41419-017-0135-z [Accessed April 29, 2022].

Walker RJ, Anderson NM, Bahouth S, Steinle JJ (2012) Silencing of insulin receptor substrate–1 increases cell death in retinal Müller cells. Mol Vis:9.

Wallet C, De Rovere M, Van Assche J, Daouad F, De Wit S, Gautier V, Mallon PWG, Marcello A, Van Lint C, Rohr O, Schwartz C (2019) Microglial Cells: The Main HIV-1 Reservoir in the Brain. Front Cell Infect Microbiol 9 Available at: https://www.frontiersin.org/article/10.3389/fcimb.2019.00362 [Accessed May 4, 2022].

Wang F, Zhang M (2021) Circ_001209 aggravates diabetic retinal vascular dysfunction through regulating miR-15b-5p/COL12A1. J Transl Med 19:294 Available at: https://doi.org/10.1186/s12967-021-02949-5 [Accessed May 3, 2022].

Wang X (2001) The expanding role of mitochondria in apoptosis. Genes Dev 15:2922–2933.

Wannamethee SG, Shaper AG, Perry IJ, Alberti KGMM (2002) Alcohol consumption and the incidence of type II diabetes. J Epidemiol Community Health 56:542–548.

Watts ME, Pocock R, Claudianos C (2018) Brain Energy and Oxygen Metabolism: Emerging Role in Normal Function and Disease. Front Mol Neurosci 11 Available at: https://www.frontiersin.org/article/10.3389/fnmol.2018.00216 [Accessed May 6, 2022].

Webster M, Witkin KL, Cohen-Fix O (2009) Sizing up the nucleus: nuclear shape, size and nuclear-envelope assembly. J Cell Sci 122:1477–1486 Available at: https://doi.org/10.1242/jcs.037333 [Accessed May 18, 2021].

Wei H, Chadman KK, McCloskey DP, Sheikh AM, Malik M, Brown WT, Li X (2012) Brain IL-6 elevation causes neuronal circuitry imbalances and mediates autism-like behaviors. Biochim Biophys Acta BBA - Mol Basis Dis 1822:831–842 Available at: https://www.sciencedirect.com/science/article/pii/S0925443912000233 [Accessed May 17, 2022].

Wei J, Dai Y, Wen W, Li J, Ye LL, Xu S, Duan DD (2021) Blood-brain barrier integrity is the primary target of alcohol abuse. Chem Biol Interact 337:109400 Available at: https://www.sciencedirect.com/science/article/pii/S0009279721000363 [Accessed May 4, 2022].

Weir GC, Bonner-Weir S (2004) Five Stages of Evolving Beta-Cell Dysfunction During Progression to Diabetes. Diabetes 53:S16–S21 Available at: https://diabetes.diabetesjournals.org/content/53/suppl_3/S16 [Accessed June 3, 2021].

Whiting DR, Guariguata L, Weil C, Shaw J (2011) IDF Diabetes Atlas: Global estimates of the prevalence of diabetes for 2011 and 2030. Diabetes Res Clin Pract 94:311–321 Available at: https://www.sciencedirect.com/science/article/pii/S0168822711005912 [Accessed May 4, 2022].

Wicking M, Nees F, Steiger F (2014) Neuropsychological measures of hippocampal function. Front Neurol Neurosci 34:60–70.

Wilcox CE, Dekonenko CJ, Mayer AR, Bogenschutz MP, Turner JA (2014) Cognitive control in alcohol use disorder: deficits and clinical relevance. Rev Neurosci 25:1–24.

Williams EC, Hahn JA, Saitz R, Bryant K, Lira MC, Samet JH (2016) Alcohol use and human immunodeficiency virus (HIV) infection: current knowledge, implications, and future directions. Alcohol Clin Exp Res 40:2056–2072.

Wilson RD, Islam MS (2012) Fructose-fed streptozotocin-injected rat: an alternative model for type 2 diabetes. Pharmacol Rep 64:129–139.

World Health Organization, World Health Organization. Management of Substance Abuse Unit (2014) Global status report on alcohol and health, 2014. World Health Organization.

Wu KK, Huan Y (2007) Diabetic atherosclerosis mouse models. Atherosclerosis 191:241–249 Available at: https://www.sciencedirect.com/science/article/pii/S0021915006004904 [Accessed June 4, 2021].

Wu M, Fatukasi O, Yang S, Alger J, Barker PB, Hetherington H, Kim T, Levine A, Martin E, Munro CA, Parrish T, Ragin A, Sacktor N, Seaberg E, Becker JT (2018) HIV disease and diabetes interact to affect brain white matter hyperintensities and cognition. AIDS 32:1803–1810 Available at: https://journals.lww.com/00002030-201808240-00008 [Accessed May 4, 2022].

Wu T, Zhang J, Geng M, Tang S-J, Zhang W, Shu J (2017) Nucleoside reverse transcriptase inhibitors (NRTIs) induce proinflammatory cytokines in the CNS via Wnt5a signaling. Sci Rep 7:4117 Available at: https://www.ncbi.nlm.nih.gov/pmc/articles/PMC5482870/ [Accessed February 4, 2022].

Xu P, Wang Y, Qin Z, Qiu L, Zhang M, Huang Y, Zheng JC (2017) Combined Medication of Antiretroviral Drugs Tenofovir Disoproxil Fumarate, Emtricitabine, and Raltegravir Reduces Neural Progenitor Cell Proliferation In Vivo and In Vitro. J Neuroimmune Pharmacol 12:682–692 Available at: https://doi.org/10.1007/s11481-017-9755-4 [Accessed May 14, 2022].

Xu S, Lu J, Shao A, Zhang JH, Zhang J (2020) Glial Cells: Role of the Immune Response in Ischemic Stroke. Front Immunol 11 Available at: https://www.frontiersin.org/article/10.3389/fimmu.2020.00294 [Accessed May 6, 2022].

Yang D, Elner SG, Bian Z-M, Till GO, Petty HR, Elner VM (2007) Pro-inflammatory Cytokines Increase Reactive Oxygen Species through Mitochondria and NADPH Oxidase in Cultured RPE Cells. Exp Eye Res 85:462–472 Available at: https://www.ncbi.nlm.nih.gov/pmc/articles/PMC2094037/ [Accessed May 10, 2022].

Yang Y, Wang J-Z (2017) From Structure to Behavior in Basolateral Amygdala-Hippocampus Circuits. Front Neural Circuits 11 Available at: https://www.frontiersin.org/article/10.3389/fncir.2017.00086 [Accessed May 7, 2022].

Yates KF, Sweat V, Yau PL, Turchiano MM, Convit A (2012) Impact of metabolic syndrome on cognition and brain: a selected review of the literature. Arterioscler Thromb Vasc Biol 32:2060–2067.

Yen F-S, Wang S-I, Lin S-Y, Chao Y-H, Wei JC-C (2022) The Impact of Alcohol Consumption on Cognitive Impairment in Patients With Diabetes, Hypertension, or Chronic Kidney Disease. Front Med 9 Available at: https://www.frontiersin.org/articles/10.3389/fmed.2022.861145 [Accessed July 5, 2022].

Yoo DY, Yim HS, Jung HY, Nam SM, Kim JW, Choi JH, Seong JK, Yoon YS, Kim DW, Hwang IK (2016) Chronic type 2 diabetes reduces the integrity of the blood-brain barrier by reducing tight junction proteins in the hippocampus. J Vet Med Sci 78:957–962.

Yu Z-Q, Jia Y, Chen G (2014) Possible involvement of cathepsin B/D and caspase-3 in deferoxamine-related neuroprotection of early brain injury after subarachnoid haemorrhage in rats. Neuropathol Appl Neurobiol 40:270–283.

Yuan S, Liu KJ, Qi Z (2020) Occludin regulation of blood–brain barrier and potential therapeutic target in ischemic stroke. Brain Circ 6:152–162 Available at: https://www.ncbi.nlm.nih.gov/pmc/articles/PMC7646391/ [Accessed May 9, 2022].

Yuan T-F, Gu S, Shan C, Marchado S, Arias-Carrión O (2015) Oxidative Stress and Adult Neurogenesis. Stem Cell Rev Rep 11:706–709 Available at: https://doi.org/10.1007/s12015-015-9603-y [Accessed July 7, 2022].

Zahr NM, Kaufman KL, Harper CG (2011) Clinical and pathological features of alcohol-related brain damage. Nat Rev Neurol 7:284–294 Available at: https://www.nature.com/articles/nrneurol.2011.42 [Accessed April 10, 2022].

Zahr NM, Pfefferbaum A (2017) Alcohol's Effects on the Brain: Neuroimaging Results in Humans and Animal Models. Alcohol Res Curr Rev 38:183–206 Available at: https://www.ncbi.nlm.nih.gov/pmc/articles/PMC5513685/ [Accessed July 24, 2022].

Zahr NM, Pohl KM, Saranathan M, Sullivan EV, Pfefferbaum A (2019) Hippocampal subfield CA2+3 exhibits accelerated aging in Alcohol Use Disorder: A preliminary study. NeuroImage Clin 22:101764 Available at: https://www.sciencedirect.com/science/article/pii/S2213158219301147 [Accessed May 4, 2022].

Zhang J-M, An J (2007) Cytokines, Inflammation and Pain. Int Anesthesiol Clin 45:27–37 Available at: https://www.ncbi.nlm.nih.gov/pmc/articles/PMC2785020/ [Accessed May 9, 2022].

Zhang L, Zhang L (2011) Voluntary oral administration of drugs in mice. Protoc Exch Available at: http://www.nature.com/protocolexchange/protocols/2099 [Accessed February 1, 2022].

Zhang P, Li T, Wu X, Nice EC, Huang C, Zhang Y (2020) Oxidative stress and diabetes: antioxidative strategies. Front Med 14:583–600 Available at: https://doi.org/10.1007/s11684-019-0729-1 [Accessed May 12, 2022].

Zhao W, Chen H, Xu H, Moore E, Meiri N, Quon MJ, Alkon DL (1999) Brain insulin receptors and spatial memory. Correlated changes in gene expression, tyrosine phosphorylation, and signaling molecules in the hippocampus of water maze trained rats. J Biol Chem 274:34893–34902.

Zhou H, Jarujaron S, Gurley EC, Chen L, Ding H, Studer E, Pandak WM, Hu W, Zou T, Wang J-Y, Hylemon PB (2007) HIV protease inhibitors increase TNF-alpha and IL-6 expression in macrophages: involvement of the RNA-binding protein HuR. Atherosclerosis 195:e134-143.

Zhou S, Zhong Z, Huang P, Xiang B, Li X, Dong H, Zhang G, Wu Y, Li P (2021) IL-6/STAT3 Induced Neuron Apoptosis in Hypoxia by Downregulating ATF6 Expression. Front Physiol 12 Available at: https://www.frontiersin.org/article/10.3389/fphys.2021.729925 [Accessed May 9, 2022].

Ziegler U, Groscurth P (2004) Morphological features of cell death. News Physiol Sci Int J Physiol Prod Jointly Int Union Physiol Sci Am Physiol Soc 19:124–128.

Zulu SS (2014) Effect of highly active antiretroviral therapy (HAART) on HIV-1 tat protein-induced neurotoxicity.

APPENDIX A: Ethical clearance

STRICTLY CONFIDENTIAL

ANIMAL RESEARCH ETHICS COMMITTEE (AREC)

CLEARANCE CERTIFICATE NO. 2018/011/58/C

APPLICANT: Dr I Eguavoen

SCHOOL: Anatomical Sciences
DEPARTMENT:
LOCATION:

PROJECT TITLE: Characterization of Streptozontocin induced diabetic male Sprague-Dawley rats with chronic alcohol intake and antiretroviral therapy

Number and Species

120X 10 weeks/270-320g male Sprague-Dawley rats

Approval was given for the use of animals for the project described above at an AREC meeting held on 2018/11/27. This approval remains valid until 2021/02/13.
Unreported changes to the application may invalidate the clearance given by the AREC
An annual progress report must be provided

The use of these animals is subject to AREC guidelines for the use and care of animals, is limited to the procedures described in the application form and is subject to any additional conditions listed below:

Signed: _____ (Chairperson, AREC) Date: 23rd April 2019

I am satisfied that the persons listed in this application are competent to perform the procedures therein, in terms of Section 23 (1) (c) of the Veterinary and Para-Veterinary Professions Act (19 of 1982)

Signed: _____ (Registered Veterinarian) Date: 23 April 2019

cc: Supervisor: Prof E Mbajirogu and Dr R Ndou
Director: CAS

Works 2000/lain0015/AESCCert.wps

APPENDIX B:

1) **High fructose diet preparation**

- Normal rodent chow was grounded into powder form
- 800grams of ground normal rodent chow was mixed with 200 grams of fructose (granulated fruit sugar, Nature's choice) to make up 1 kilogram of high fructose diet.
- Powdered high fructose diet was mixed with water to combined and placed in pellet food moulds and dehydrated in low temperature oven then fed to diabetic rat groups

2) **Citrate buffer and STZ preparation (4mg/ml of 40mg/Kg BW)**

Citrate buffer

3 parts 0.05M citrate acid

2 parts 0.05m sodium citrate

Adjust pH to 4.5

STZ

4mg STZ--1 ml citrate buffer (CB)

For a 40mg/Kg BW dose

40mg STZ in 10ml CB will be given to 1 Kg BW

10ml STZ in CB –1000g

1 ml STZ in CB - 100g

Therefore, Xml STZ in CB = X g BW x 1/100ml

Xml STZ in CB was administered to each animal according to their body weight

3) Atripla® drug dose calculations

- 45kg body weight (BW) of average adolescent receives 1 tablet of Atripla per day and 1 tablet =1045mg active ingredients (AI) per day Atripla (efavirenz 600mg+ emtricitabine 200mg+ tenofovir 245mg)

  Therefore, 1kg BW = 1045/45 = 23.22 mg AI per day

  And 1 gram BW= 0.0232 mg AI per day

- One Atripla® tablet with 1045mg AI weighs 1612mg.

  Therefore, 1mg tablet = 1X1045/1612 =0.648mg AI/mg tablet

- If 1 gram BW requires 0.0232 mg AI per day

  Then 200 g BW required = 200g x0.0232 mg AI per day/ 0.648mg AI/mg tablet

  =7.16 mg tablet per day (was administered to a rat weighing 200g)

4) Gelatine Cubes preparations

For each gelatine cube 5ml of mixture was used. The mixture consisted of 5ml distilled water, 0.25g sugar, 2g gelatine and 0.1g beefy Bovril. These quantities are adapted from (Zhang and Zhang, 2011) minimising the entire content of each gelatine cube to one calorie to ensure that the gel administration does not contribute/ influence the diabetic condition.

The required amount of water was heated in a sterile beaker, all other ingredients were added to the beaker while stirring with a stirrer. When the mixture had cooled, Atripla tablet was crushed and the required amount per cube was added, and mixture was aliquoted using a syringe into gelatine moulds (5ml each) and placed in the fringe to set. The Atripla tablet was omitted in the placebo gelatine cubes. Rats received one gelatine cube daily according to treatment.

APPENDIX C

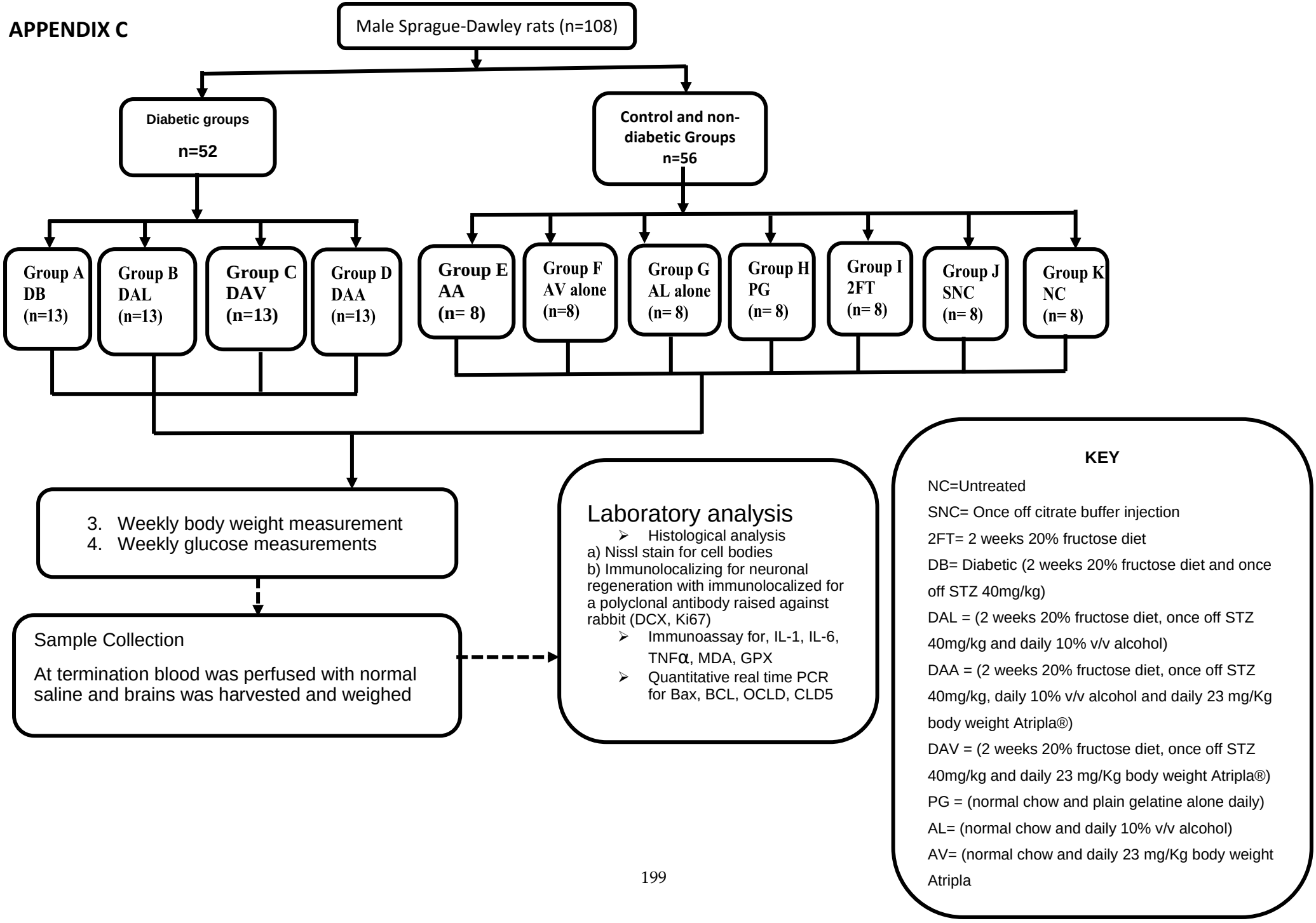
Male Sprague-Dawley rats (n=108)
Diabetic groups
n=52
Control and non-diabetic Groups
n=56
Group A
DB
(n=13)
Group B
DAL
(n=13)
Group C
DAV
(n=13)
Group D
DAA
(n=13)
Group E
AA
(n= 8)
Group F
AV alone
(n=8)
Group G
AL alone
(n= 8)
Group H
PG
(n= 8)
Group I
2FT
(n= 8)
Group J
SNC
(n= 8)
Group K
NC
(n= 8)
3. Weekly body weight measurement
4. Weekly glucose measurements
Sample Collection
At termination blood was perfused with normal saline and brains was harvested and weighed
Laboratory analysis
Histological analysis
a) Nissl stain for cell bodies
b) Immunolocalizing for neuronal regeneration with immunolocalized for a polyclonal antibody raised against rabbit (DCX, Ki67)
Immunoassay for, IL-1, IL-6, TNFα, MDA, GPX
Quantitative real time PCR for Bax, BCL, OCLD, CLD5
KEY
NC=Untreated
SNC= Once off citrate buffer injection
2FT= 2 weeks 20% fructose diet
DB= Diabetic (2 weeks 20% fructose diet and once off STZ 40mg/kg)
DAL = (2 weeks 20% fructose diet, once off STZ 40mg/kg and daily 10% v/v alcohol)
DAA = (2 weeks 20% fructose diet, once off STZ 40mg/kg, daily 10% v/v alcohol and daily 23 mg/Kg body weight Atripla®)
DAV = (2 weeks 20% fructose diet, once off STZ 40mg/kg and daily 23 mg/Kg body weight Atripla®)
PG = (normal chow and plain gelatine alone daily)
AL= (normal chow and daily 10% v/v alcohol)
AV= (normal chow and daily 23 mg/Kg body weight Atripla

APPENDIX D

Image illustrating ,volumest plugin in the image j software for the estimation of volume in the dentae gyrus. Images of the entire dorsal hippocampus was capurtured with the the X 25 objective lens.

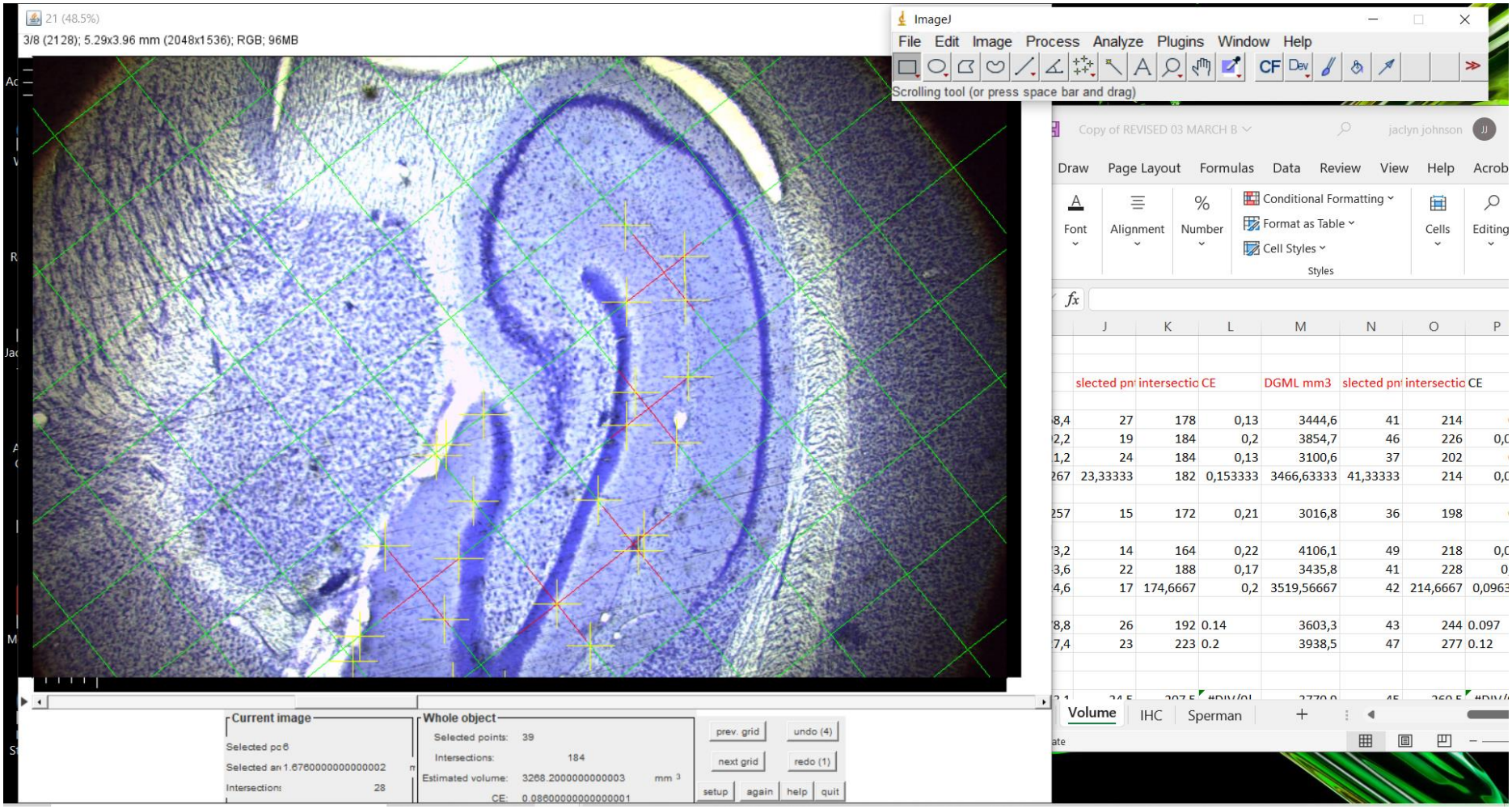

APPENDIX E

Image illustrating the different regions from which the photomicrograph were captured for the histomorphology mearsurments of neuronal number and neuronal nuclei area.

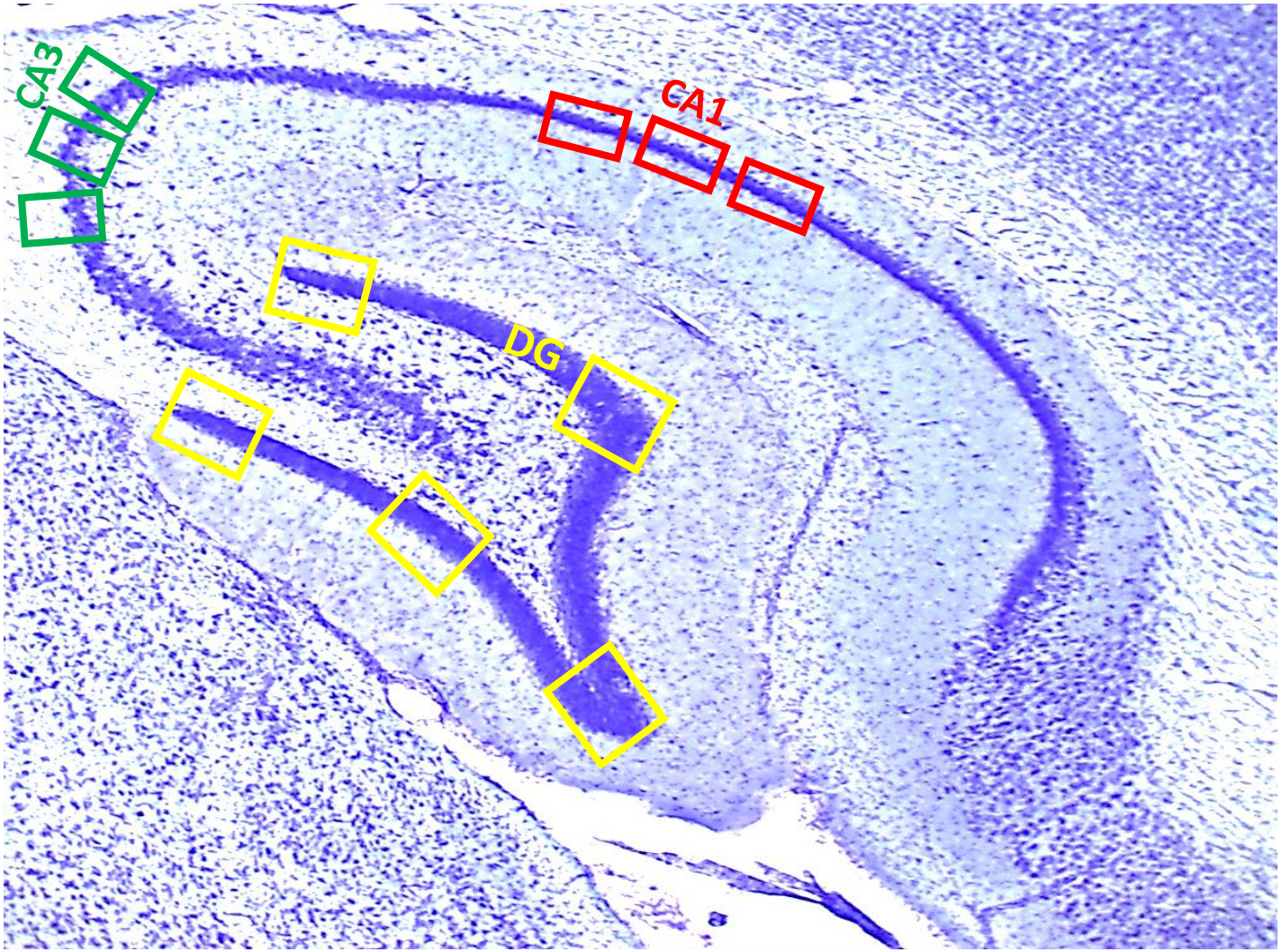

APPENDIX F: Summary of results from the study

	Alcohol	cART	Alcohol+ cART	Diabetes	Diabetes+ cART	Diabetes+ alcohol	Diabetes+ alcohol+ cART
Diabetic parameters				AUC ↑ NFBG ↑	AUC ↑ NFBG ↑	AUC ↑ NFBG ↑	AUC ↑ NFBG ↑
Proinflammatory cytokines	IL-1α, IL-6, TNFα ↑	IL-6, TNFα ↑		IL-1α, IL-6, TNFα ↓	IL-1α, IL-6, TNFα ↓		IL-1α, IL-6 ↑
Oxidative stress	MDA↑ GPx ↓	MDA↑ GPx ↓	GPx ↓	MDA↑ GPx ↓	MDA↑ GPx ↓	MDA↑ GPx ↓	MDA↑ GPx ↓
CA1 histomorphology	NA ↑ NN ↓		NA ↑	NA ↑ NN ↓	NN ↓	NN ↓	NN ↓
CA3 histomorphology				NA ↑	NA ↓ NN ↓	NA ↓ NN ↓	NA ↓ NN ↓
DG histomorphology	NA ↑ NN ↓	NN ↓	NN ↓	NA ↑ NN ↓	NN ↓	NA ↓ NN ↓	NN ↓
Dentate gyrus volume			GL ↓	ML ↓	ML ↓ GL ↓	ML ↓ GL ↓	ML ↓ GL ↓
Neurogenesis	Ki 67 ↓ DCX ↓		Ki 67 ↓	Ki 67 ↓ DCX ↓	Ki 67 ↓ DCX ↓	Ki 67 ↓ DCX ↓	Ki 67 ↓ DCX ↓
Insulin receptors	IRS1 ↓	IRS1 ↓	IRS1 ↓ INSR ↓	IRS1 ↓ INSR ↓	IRS1 ↓	IRS1 ↑	
Blood-brain barrier		CLDN5 ↓	CLDN5 ↓ OCLDN ↓	CLDN5 ↓ OCLDN ↓	CLDN5 ↓		OCLDN ↓
Apoptosis				CASPS3 ↑ BAX ↑	CASPS3 ↑ BAX ↑	CASPS3 ↑ BCL2 ↑ BAX ↑	CASPS3 ↑ BCL2 ↑ BAX ↑

AUC; area under the OGTT curve, NFBG; non-fasting blood glucose, NN; number of neurons, NA; nuclei area of neurons , ML; molecular layer, GL; granular layer, ↑ ; significantly increased relative to control , ↓ ; significantly decreased compare to control

diagnostics

MDPI

Article

Combination Antiretroviral Therapy (cART) in Diabetes Exacerbates Diabetogenic Effects on Hippocampal Microstructure, Neurogenesis and Cytokine Perturbation in Male Sprague Dawley Rats

Jaclyn Asouzu Johnson [1,*], Robert Ndou [2] and Ejikeme Felix Mbajiorgu [1]

[1] School of Anatomical Sciences, University of the Witwatersrand, Johannesburg 2193, South Africa; ejikeme.mbajiorgu@wits.ac.za

[2] Department of Anatomy and Histology, School of Medicine, Sefako Makgatho Health Sciences University, Pretoria 0204, South Africa; robert.ndou@smu.ac.za

* Correspondence: jaclyn.johnson@wits.ac.za

Abstract: The increasing incidence of diabetes and HIV/AIDS–diabetes comorbidity in society has led to the prevalence of combination antiretroviral therapy (cART) in diabetes, with some reported neural effects. Therefore, the effects of cART and type two diabetes (T2D) on the hippocampal levels of cytokines, lipid peroxidation; histomorphology and neurogenesis were investigated. Adult male Sprague–Dawley rats were divided into four groups: DB (diabetic rats); DAV (diabetic rats treated with cART (efavirenz, emtricitabine and tenofovir); AV (normal rats treated with cART) and the NC group (with no treatment). Following ninety days of treatment, the rats were terminated, and the brains excised. Immunoassay (IL-1 , IL-6, TNF and MDA); immunohistochemical (Ki67 and DCX) and cresyl violet histomorphology analyses were carried out on brain homogenates and sections, respectively. In comparison to the control, the results showed that cART significantly elevated the IL-6, TNF and MDA levels, while DB and DAV significantly reduced the body weight, glucose tolerance, IL-1 , IL-6, TNF and MDA levels. The hippocampal neuronal number was reduced in AV (dentate gyrus; DG region), in the DB group (Cornu Ammonis subregion 1; CA1 and DG regions only) and in DAV (all three hippocampal regions). Additionally, the expression of neurogenic markers Ki67 and doublecortin (DCX) were reduced in the diabetic group, with a greater reduction in the cART+T2D group compared to the control. Furthermore, the neuronal number at all hippocampal regions was negatively corelated with the diabetic parameters (FBG; fasting blood glucose, NFBG; non-fasting blood glucose, AUC; area under the glucose tolerance curve) but positively correlated with body weight. Additionally, the increase in the DG neuronal nuclei area of DB and DAV was significantly positively correlated with FBG, NFBG and AUC and inversely correlated with the estimated number of neurons and neurogenesis. These findings indicate that cART in diabetes (DAV) has similar effects as diabetes relative to the induction of oxidative stress and impairment of the cytokine immune response, but exacerbated neurotoxicity is observed in DAV, as shown by a significantly decreased DCX expression compared to DB and reduction in the number of Cornu Ammonis subregion 3 (CA3) hippocampal neurons, unlike in cART or the diabetes-alone groups.

Citation: Asouzu Johnson, J.; Ndou, R.; Mbajiorgu, E.F. Combination Antiretroviral Therapy (cART) in Diabetes Exacerbates Diabetogenic Effects on Hippocampal Microstructure, Neurogenesis and Cytokine Perturbation in Male Sprague Dawley Rats. Diagnostics **2022**, 12, 905. https://doi.org/10.3390/diagnostics12040905

Academic Editor: Benedetta Nacmias

Received: 11 February 2022
Accepted: 1 April 2022
Published: 5 April 2022

Publisher's Note: MDPI stays neutral with regard to jurisdictional claims in published maps and institutional affiliations.

Keywords: diabetes; antiretroviral; cytokines; neurogenesis; hippocampus microstructure

Copyright: © 2022 by the authors. Licensee MDPI, Basel, Switzerland. This article is an open access article distributed under the terms and conditions of the Creative Commons Attribution (CC BY) license (https://creativecommons.org/licenses/by/4.0/).

1. Introduction

Diabetes is a noncommunicable disease that has rapidly spread throughout South Africa and globally in recent decades [1]. Diabetes is reported to be caused by lifestyle factors [2,3], and recently, the use of cART has also been implicated as diabetogenic.

The introduction of combination antiretroviral therapy (cART) provided an effective means of suppressing human immunodeficiency virus (HIV) replication and is clinically

used in Southern African regions as a first line drug for HIV and acquired immunode-ficiency (AIDs) management [4]. cART consists of non-nucleoside reverse transcriptase inhibitor (NNRTI); efavirenz, a protases inhibitor (PI); emtricitabine and reverse transcrip-tase inhibitor (RTI) and tenofovir disoproxil fumarate. NNRTIs have been reported to induce oxidative stress [5], while PIs inhibits glucose uptake by cells, thereby stimulat-ing an inflammatory response [6,7]. These effects of the cART component are associated with the induction of insulin resistance [8–10] and subsequent development of type 2 diabetes [11,12]. The diabetogenic effects of cART contributes to the fourfold increase in the prevalence of type 2 diabetes amongst HIV patients on cART compared to untreated HIV patients [13].

Type 2 diabetes (T2D) as a metabolic disorder is characterized by weight loss, hyper-glycemia, insulin resistance or lack of insulin secretion in advanced stages of the disease. T2D induces oxidative stress and the perturbation of proinflammatory cytokines [14,15], which increases the incidences of infection [16] and activates a cascade of intracellular events that leads to autophagy, apoptosis and disturbances of synaptic plasticity in hip-pocampal neurons [17,18]. Hippocampal neurons have numerous membranes bound to glucose and insulin receptors, which are dependent on the sufficient supply of glucose for the metabolic demands of cognition and memory tasks in the hippocampus [19,20]. The potential for type 2 diabetes and components of cART to induce insulin resistance or insulin deficiency and inhibit glucose transport into neurons has been implicated in the impairment of hippocampus dependent memory functions and adult neurogenesis, especially by NNRTI in cART [21–23].

T2D is associated with cognitive anomalies [24] and dementia [20], while cART-induced oxidative stress has been linked to hippocampal atrophy and deficiencies in volume and synaptic plasticity [25,26], with attendant neurocognitive disorders. However, the effects of the concurrent presence of T2D and cART due to diabetes–HIV comorbidity (T2D +cART) on hippocampal histomorphology and neurogenesis remains to be documented. Meanwhile, diabetes and HIV coinfected patients abound, resulting in the prevalent use of cART amongst diabetic patients. Evidence exists for the increasing coexistence of type 2 diabetes mellitus (T2DM) among persons living with HIV/AIDs (PLWHA) [27], leading to chronic cART therapy amongst them. So far, the body of evidence has focused mostly on in vitro and MRI investigations of the independent effects of type 2 diabetes and cART on the hippocampus, and little is known about the in vivo histopathology of coexistence of the two conditions (cART+T2D) on the hippocampus relative to the induction of inflammation, perturbation of neuronal cytoarchitecture and expression of neurogenic markers. However, in HIV-positive patients, it may be difficult to ascertain if the observed oxidative stress and neuroinflammation emanates from neurotoxic interactions of cART administration in diabetes or if such effects are induced by the presence of HIV. Therefore, it is crucial to investigate and document the effects of cART administration in HIV-naïve male Sprague– Dawley diabetic rats (cART+T2D) vis-à-vis the impact on proinflammatory cytokines and lipid peroxidation levels and the likely associated changes in neuronal histomorphology and neurogenesis relative to possible cognitive and memory adverse effects.

2. Materials and Methods

2.1. Chemical and Reagents

These were obtained as follows: combination antiretroviral drug (Atripla) (Bristol-Myers Squibb and Gilead Sciences, Foster City, CA, USA), the primary antibodies (rab-bit polyclonal antibody; Abcam, Cambridge, MA, USA), secondary antibody (goat anti-rabbit antibody IgGs; Vectastain, Burlingame, CA, USA) and ABC kit from (Vectastain, Burlingame, CA, USA).

2.2. Ethical Clearance

This study was approved by the Wits Research Animal Facility (WRAF) (approval number 2018/011/58/C) of the University of the Witwatersrand. All experimental animal

handling and treatments were carried out according to the standards and principles set forth by this committee.

2.3. Animal Husbandry

For this study, twenty-four adult male Sprague–Dawley rats (10 weeks old) were housed separately under sterile conditions and a maintained temperature of 21–23 C and 12-h light–dark cycle. The rats had free access to drinking water and normal rat chow for the duration of the experiment. The rats were weighed weekly, and fasting glucose tests, non-fasting glucose tests and oral glucose tolerance tests were carried out.

2.4. Experimental Design

Type 2 diabetes was induced in the experimental rats according to Wilson and Islam's
2012 diabetic model through a high-fructose feed for two weeks and followed by a once-off 40-mg/kg body weight (BW) Streptozotocin (STZ) injection [28]. The screening results of random non-fasting blood glucose levels 250 mmol/L at the end of the third week after the onset of high-fructose feed were considered diabetic. The fasting blood glucose levels (FBG) were monitored biweekly using the Accu-Chek meter and glucose strips via tail prick after 12 h of fasting (20:00 to 08:00), while the random non-fasting blood glucose levels (NFBG) were measured and monitored biweekly using the Accu-Chek meter and glucose strips via tail prick during the evening hours without fasting to ensure that the animals remained diabetic throughout the course of the experiment. For the oral glucose tolerance test (OGTT) as an additional diagnostics of glucose tolerance for diabetes mellitus (Furman 2015), the rats were fasted for 12 h overnight (20:00 to 08:00); after which, they received an oral gavage of 2-g/kg body weight, followed by tail prick glucose monitoring using glucose strips at 0, 15, 30, 60 and 120-min intervals after glucose loading. The animals were divided into four groups of six rats each (n = 6). The rats in the first group were untreated and served as controls (NC), while the rats in the second group were treated with antiretroviral (cART) medication daily (consisting of efavirenz 600 mg + emtricitabine 200 mg + tenofovir 245 mg) at a directly extrapolated recommended dose of 23-mg cART/kg body weight of the animal [29] in gelatine cubes (AV). The rats in the third group (DB) were diabetic for ninety days (DB). In addition to the diabetic condition, the rats in the fourth group (DAV) received antiretroviral (cART) medication in gelatine cubes daily (DAV), as indicated above. Immediately following the confirmation of diabetes (end of third week), the cART treatment commenced, and daily treatments continued for ninety days; after which, the rats were terminated. At the end of the experiment, the rats were weighed and then anaesthetized with an overdose of sodium pentobarbitone. The hearts were perfused with 2 mL/min of 0.1-M phosphate buffer (PB) in 0.9% saline, the cranium was excised and the brain harvested and immediately separated into hemispheres. One hemisphere fixed in 0.4 M paraformaldehyde for histology and the other hemisphere stored at 80 C for immunoassay.

2.5. Enzyme Linked Immunoassay of Proinflammatory Cytokines and Malondialdehyde (MDA)

Dissected brain samples from each hemisphere per animal were homogenized using handheld tissue grinder G-50 (Coyote Bioscience, Jiangusu, China) in 1:9 volume of 0.01-M phosphate-buffered saline (PBS) (pH 7.4) centrifuged at 1000 g for 10 min and supernatant collected. The samples were used to run an enzyme linked immunosorbent assay for Rat IL-1 , Rat IL-6, Rat TNF and MDA. Colorimetric assay kit: TBA method (Elabscience, Houston, TX, USA; E-EL-R0011, E-EL-R0015, E-EL-R0019 and E-BC-K025-M, respectively) according to the manufacturer's protocol. All samples were diluted 1:2, and all standards and samples were run in duplicates. Diluted samples and standards were transferred to manufacturer-coated 96-well plates and incubated for 90 min. After decanting, biotinylated detection antibody was incubated in the wells for 60 min. The wells were incubated in HRP conjugate for 30 min following aspiration and washes. Thereafter, the wells were washed and incubated in substrate reagent for 15 min and, finally, in stop solution; all incubations

were at 37 C. The optical density (OD) values were read at 450 nm. The analysis for MDA was according to the TBA colorimetric method following the manufacturer's protocol; the concentration was calculated in mol/g protein. The OD was read at 620 nm using an Anthos 2010 96-well plate reader coupled to ADAP software. OriginPro software was used to calculate the concentration of cytokines in the samples from the obtained OD values according to the manufacturer's directions in pg/mL. The total protein concentration for each sample of brain homogenate was tested using Bradford reagent. The standards were made up in bovine serum albumin (BSA), and the calculated concentration of proteins in each sample was applied when calculating the final concentration of cytokines (pg/mg of protein).

2.6. Brain Tissue Preparation for Histology

Each brain hemisphere per animal was placed in sucrose overnight and mounted on a freezing microtome with dry ice and sucrose and cut in the sagittal plane using a frozen cryostat at 50 m. This was repeated in one in a series six of free-floating sections collected in 0.1-M Phosphate buffer (PB) and stored in antifreeze at 20 C until further processing. Every first series of sections was stained with cresyl violet, while the next two series of sections were used for immunohistochemical labeling of Ki67 and DCX, respectively.

2.7. Histology and Histomorphometry

For the cresyl violet stain, brain sections were mounted on 0.3% gelatine-coated slides and placed in 50% chloroform and 50% alcohol overnight. Six brain sections were stained with cresyl violet. These sections were serially collected 300 m apart, starting from Bregma plate 173 to plate 177, corresponding to the rat brain atlas [30]. The sections (all groups in parallel to ensure uniform staining intensity) were then rehydrated in a degrading series of alcohol, placed in cresyl violet stain and then into distilled water. Sections were then dehydrated and mounted with a coverslip. Photomicrographs of the dorsal hippocampus of the brain sections were obtained using a Leica ICC50 HD video camera linked to a Leica DM 500 microscope (Leica Biosystems, USA). Nine camera fields from six sections per animal, from six animals per group (i.e., 36 sections per group) were captured from uniform areas within the CA1, CA3 and dentate gyrus (DG) regions of the dorsal hippocampus per group. The nuclei area and number of the neurons in the upper focal plane of these camera fields were determined using the trace and cell counter plugins of ImageJ, respectively. Only neurons with a vesicular nucleus and a centrally placed nucleoli were measured and counted. In the dentate gyrus, five counts were taken: two counts from each limb and one from the apex of the dentate gyrus. Representative photomicrographs were compiled using Microsoft Visio, and no manipulation was made to the captured images except for brightness and contrast.

2.8. Immunohistochemistry for Neurogenesis

From each brain hemisphere, six sections between plates 173 and 177 were selected using the atlas of a rat brain [30] for each histochemical labeling. Free-floating brain sections in 24-well plates first underwent endogenous peroxidase inhibition with 50% methanol, 50% 0.1-M PB and 1.66% hydrogen peroxide. Sections were washed, then blocked in 3% normal goat serum and 2% (BSA) and 0.25% Triton X 100 in 0.1M PB for 2 h at room temperature, followed by incubation in a polyclonal antibody raised against rabbit Ki67 and DCX (Abcam, via Biocom Africa, Pretoria, South Africa; AB15580 and AB18723, respectively) at ratios 1:1000 and 1:3000, respectively, for 48 h. The sections were washed with 0.1-M PB and incubated for 2 h with goat anti-rabbit antibody IgGs washed and incubated for 1 h with ABC solution and stained with DAB, mounted on gelatine-coated slides, dehydrated and cleared in xylene. Control sections were incubated in 0.1-M PB omitting the primary antibody. Photomicrographs of Ki67 and DCX immunolocalized dorsal hippocampus brain sections were obtained, and counts of immunolabelled cells were determined by the cell counter plugin of Image J. Only DCX immunolocalized cells in the upper focal plane with

a pale centrally placed center were counted, while immunolocalized cells for Ki67 were counted in their respective clusters. Representative photomicrographs were compiled using Microsoft Visio, and no manipulation was made to the captured images except for brightness and contrast.

2.9. Statistical Analysis

The nuclei area and number of neurons in the hippocampal regions, concentrations of cytokines and density of immunolabeled hippocampal Ki67 and DCX were recorded as the mean SEM. The data were subjected to a normality test using the Shapiro–Wilks test, parametric data were analyzed using the one-way ANOVA test and a post hoc Bonferroni's test was conducted to determine the differences between the groups. Nonparametric data were analyzed by the Kruskal–Wallis test and a post hoc Bonferroni's pairwise analysis. The results with $p < 0.05$ were regarded as significant. All data were analyzed using IBM SPSS software, and graphs were prepared using the GraphPad prism.

3. Results

3.1. Mortality

The mean percentage mortality in the DB and DAV groups was 12.5% (one out of eight animals) and 22.22% (two out of nine animals), respectively, and none in the control and AV groups. A maximum of six rats per group were randomly selected from the surviving rats in each group and used for further analysis (Figure 1A).

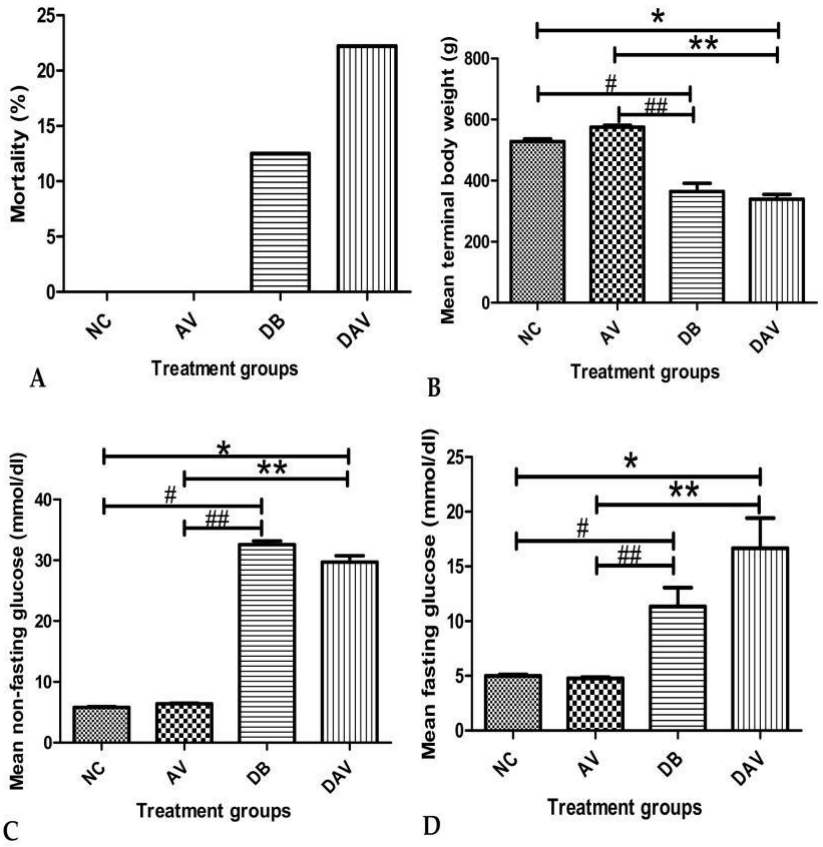

Figure 1. Mean mortality, terminal body weight and fasting and non-fasting blood glucose levels. (**A**) No mortality in the NC and AV groups, but (12.5%) 1 and (22.22%) 2 mortalities in DB and DAV, respectively. (**B**) Significant difference in mean body weight across groups (Kruskal–Wallis test, p 0.0001). '*' DAV vs. NC and '#' DB vs. NC ($p = 0.034$ and 0.03 respectively) and '**' DAV vs. AV

and '##' DB vs. AV significantly decreased (p = 0.0001, Dunn's pairwise post hoc test). (**C**) Significant difference in the mean NFBG between groups (Kruskal–Wallis test, p 0.0001), '*' DAV vs. NC and '#' DB vs. NC significantly increased (p = 0.0001 and 0.001, Dunn's pairwise post hoc test). '**' DAV vs. AV and '##' DB vs. AV significantly increased (p = 0.05 and 0.008 respectively). (**D**) Significant difference in the mean FBG between groups (Kruskal–Wallis test, p 0.001). '*' DAV vs. NC and '#' DB vs. NC significantly increased at p = 0.003 and 0.008, respectively. '**' DAV vs. AV and '##' DB vs. AV significantly increased (p = 0.004 and 0.05 respectively), n = 6. Key: NC, Controls; AV, cART only; DB, Diabetic; DAV, diabetic with cART.

3.2. Body Weight

The mean terminal body weights in the DB and DAV groups were significantly de-creased compared to the AV and NC groups. The mean body weight was highest in the AV group and lowest in the DAV group. No significant change in body weight was observed between the NC and AV and between the DB and DAV groups (Figure 1B).

3.3. Blood Glucose Levels

The mean NFBG levels in the DB and DAV groups were significantly increased in comparison to the levels in the NC and AV groups (Figure 1C). The mean FBG and NFBG levels for the DAV and DB groups remained significantly high throughout the experiment compared to the AV and NC groups respectively (Figure 1C,D). However, no significant difference in the mean FBG and NFBG was observed between the DB and DAV groups.

3.4. Oral Glucose Tolerance Test

The mean oral glucose tolerance test showed optimal glucose handling in the NC and AV groups but poor glucose handling in the DB and DAV groups. After 2 h of glucose administration, the DAV had the highest level of blood glucose and area under curve (AUC), followed by the DB group; however, no difference was observed between the DB and DAV groups. The AUC was significantly increased in the DB and DAV groups compared to the NC and AV groups, and the glucose levels remained high in the DB and DAV group 2 h post-glucose load (Figure 2A,B).

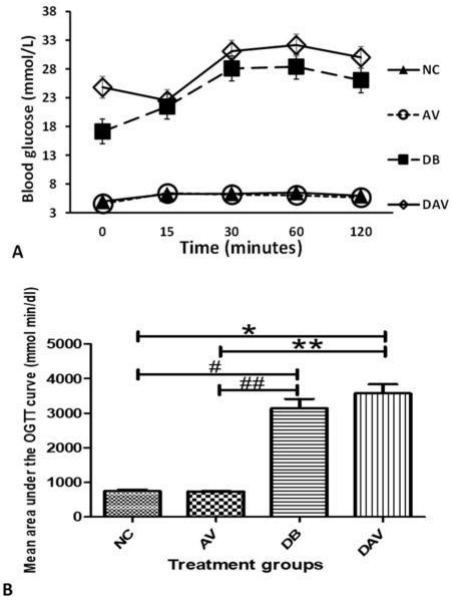

Figure 2. Mean oral glucose tolerance test and area under the curve. (**A**) Mean OGTT levels. (**B**) Significant difference in the mean area under the OGTT curve across groups (Kruskal–Wallis test, p 0.0001). '*' DAV vs. NC and '#' DB vs. NC significantly increased (p = 0.014 and 0.002) and '**' DAV vs. AV and '##' DB vs. AV significantly increased (p = 0.006 and 0.001), respectively (Dunn's pairwise post hoc test), n = 6. Key: NC, Controls; AV, cART only; DB, Diabetic; DAV, diabetic with cART.

3.5. Inflammatory Cytokines and MDA

The concentrations of proinflammatory cytokines IL-1 , IL-6 and TNF in the hip-pocampal tissue homogenate are as shown in Figure 3A–C, respectively. The concentrations of all three cytokines (IL-1 , IL-6 and TNF) in DB and DAV were significantly reduced compared to the NC (p = 0.007, 0.013 and 0.0001, respectively) and AV groups (p = 0.001). The concentrations of all three cytokines (IL-1 , IL-6 and TNF) in the AV groups were significantly increased compared to the control (NC) (p = 0.04, 0.001 and 0.043, respec-tively) (Figure 3A–C). Similarly, the MDA levels significantly increased in AV, DB and DAV compared to the control (NC) (p = 0.019, 0.039 and 0.001, respectively) (Figure 3D).

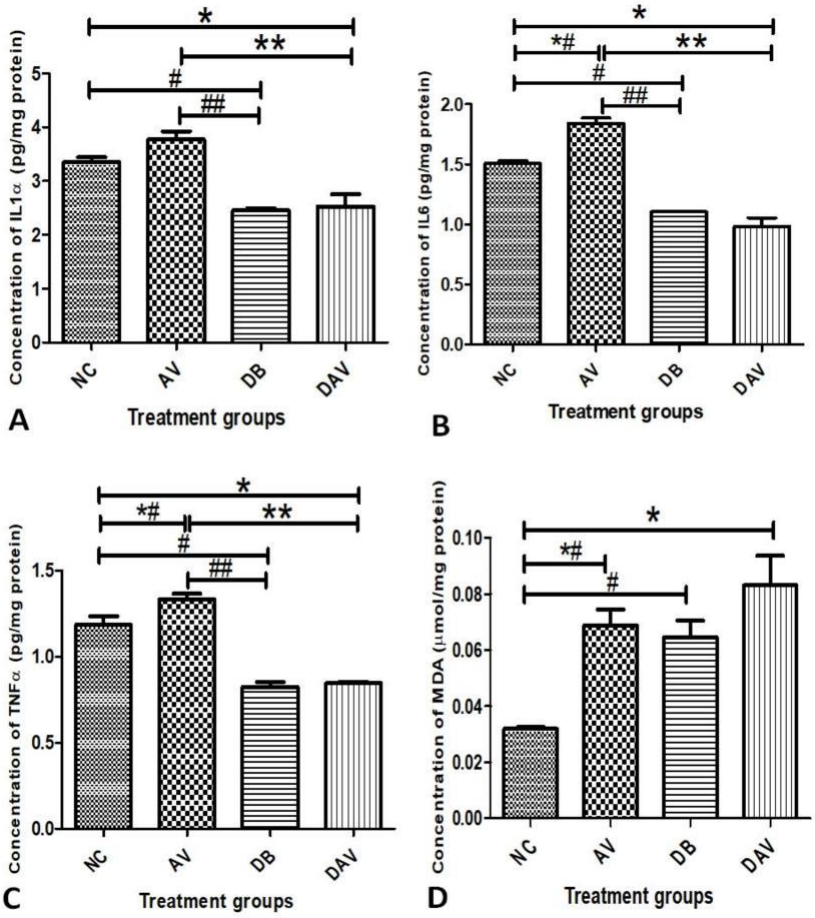

Figure 3. Mean terminal concentrations of IL-1 , IL-6, TNF and MDA in hippocampal tissue homogenate. (**A**) Mean concentration of IL-1 . Significant changes in the concentration of cytokines between the groups (one-way ANOVA, p < 0.0001). '**' DAV vs. AV and '##' DB vs. AV significantly reduced (p = 0.0001), and '*' DAV vs. NC and '#' DB vs. NC also significantly reduced (p = 0.007 and 0.013, respectively). (**B**) Mean concentration of IL-6. Significant changes in the concentration of cytokines between the groups (one-way ANOVA, p < 0.0001). '*' DAV vs. NC, '#' DB vs. NC, '##' DB vs. AV and '**' DAV vs. AV significantly reduced (p = 0.001 and 0.0001, respectively, Bonferroni's post hoc test). '*#' AV vs. NC is significantly increased (p = 0.001). (**C**) Mean concentration of TNF . Significant changes in the concentration of cytokines between the groups (one-way ANOVA p < 0.0001). '*' DAV vs. NC, '#' DB vs. NC, '##' DB vs. AV and '**' DAV vs. AV significantly reduced (p = 0.001 and 0.0001, respectively, Bonferroni's post hoc test). '*#' AV vs. NC significantly increased (p = 0.043). (**D**) Mean concentration of MDA in hippocampal tissue homogenate. Significant changes in the concentration of MDA between the groups (one-way ANOVA, p < 0.0001) '*' DAV vs. NC, '*#' AV vs. NC and '#' DB vs. NC are significantly increased compared to the control (p = 0.013, 0.029 and 0.001, respectively, Bonferroni's post hoc test), n = 4. Key: NC, Controls; AV, cART only; DB, Diabetic; DAV, diabetic with cART.

3.6. Histopathology of the Hippocampus

3.6.1. Number of Neurons in Hippocampal Regions

In the control groups, a wider and densely clustered row of cell can be seen observed in all hippocampal regions (Figures 4–6). In the treated groups (AV, DB and DAV), gradual reduction in the neuronal population is observed, especially in the CA3 region of the DAV group, where the neurons appear scanty (Figure 5). The mean estimated number of neurons in all regions of the hippocampus of the DAV group was significantly decreased compared to the control (NC) and AV groups (Figures 4–6). The mean neuronal number in the CA1 region of the DB group was significantly decreased in comparison with the mean neuronal number in the NC group ($p = 0.037$). Similarly, the mean neuronal number significantly reduced in the dentate gyrus of the DB compared to the NC and AV groups ($p = 0.0001$ and 00.034, respectively) and reduced in the AV compared to the NC group ($p = 0.001$) (Figure 6).

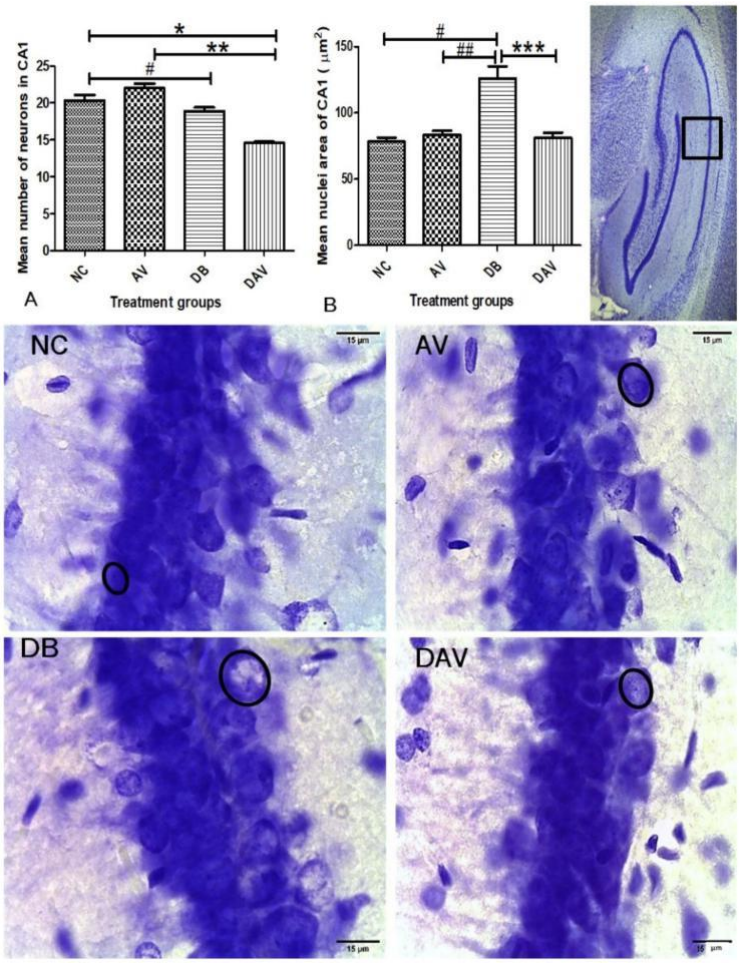

Figure 4. Mean nuclei area and number of neurons in the CA1 region of the dorsal hippocampus. (**A**) Significant changes in mean number of neurons of the CA1 region (Kruskal–Wallis test, p 0.0001) '*' DAV vs. NC and '#' DB vs. NC are significantly decreased ($p = 0.037$ and 0.0001, respectively). '**' DAV vs. AV significantly decreased ($p = 0.001$). (**B**) Significant changes in the mean nuclei area between the groups (Kruskal–Wallis test, p 0.005). '#' DB vs. NC, '##' DB vs. AV and '***' DB vs. DAV are significantly increased ($p = 0.001$,0.016 and 0.005, respectively). Circles indicate boundaries of neuronal nuclei, and squares indicate specific regions from which micrographs and measurements were made. Scale bar = 15 m, n = 6. Key: NC, Controls; AV, cART only; DB, Diabetic; DAV, diabetic with cART.

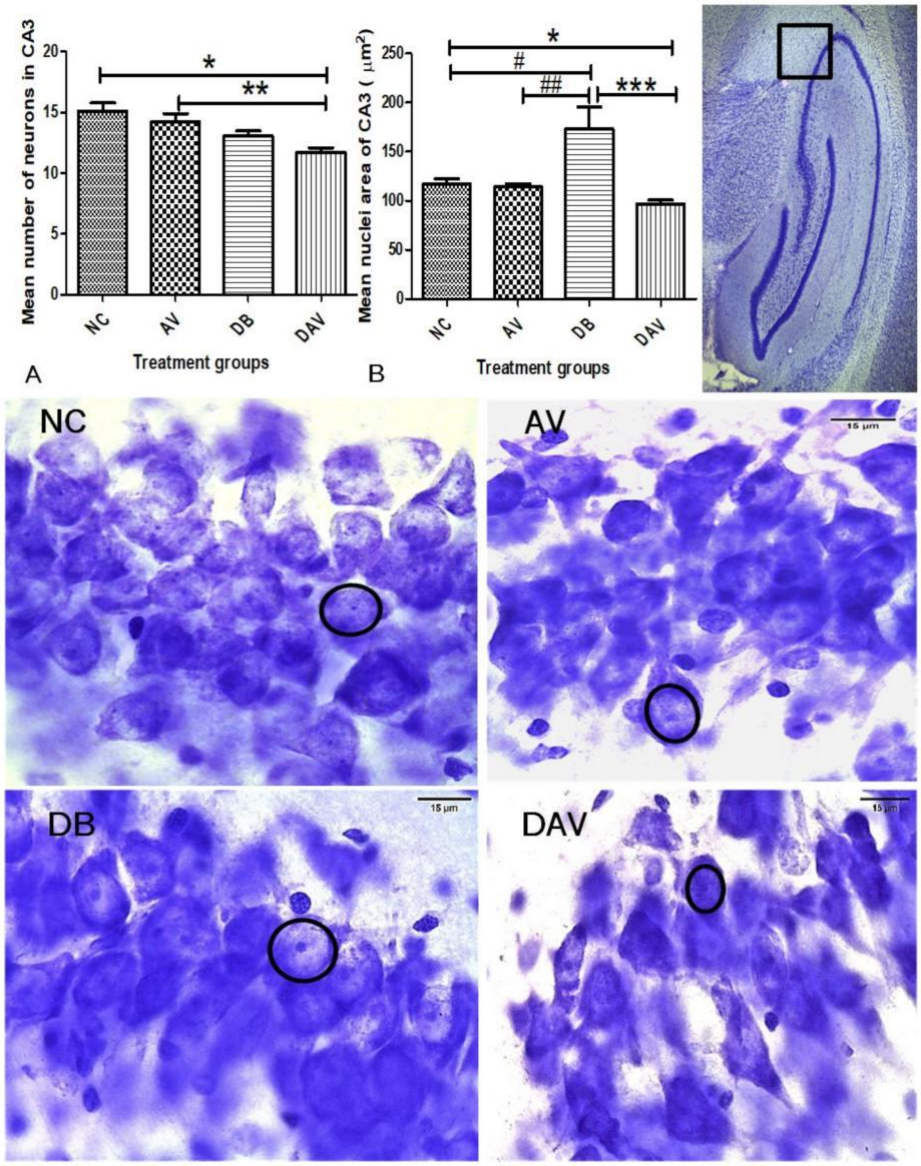

Figure 5. Mean nuclei area and number of neurons in the CA3 region of the dorsal hippocampus. (**A**) Significant changes in the mean number of neurons of the CA3 region (one-way ANOVA test, p 0.001). '*' and '**' are significantly decreased (p = 0.001 and 0.017, respectively). (**B**) Signifi-cant changes in the mean nuclei area in the CA3 region between the groups (Kruskal–Wallis test, p 0.005). '#' DB vs. NC, '##' DB vs. AV and '***' DB vs. DAV are significantly increased (p = 0.041, 0.016 and 0.0001, respectively). '*' DAV vs. NC is significantly reduced (p = 0.045). Circles indicates boundaries of the neuronal nuclei, and squares indicate the specific area from which micrographs were taken and measurements made. Scale bar = 15 m, n = 6. Key: NC, Controls; AV, cART only; DB, Diabetic; DAV, diabetic with cART.

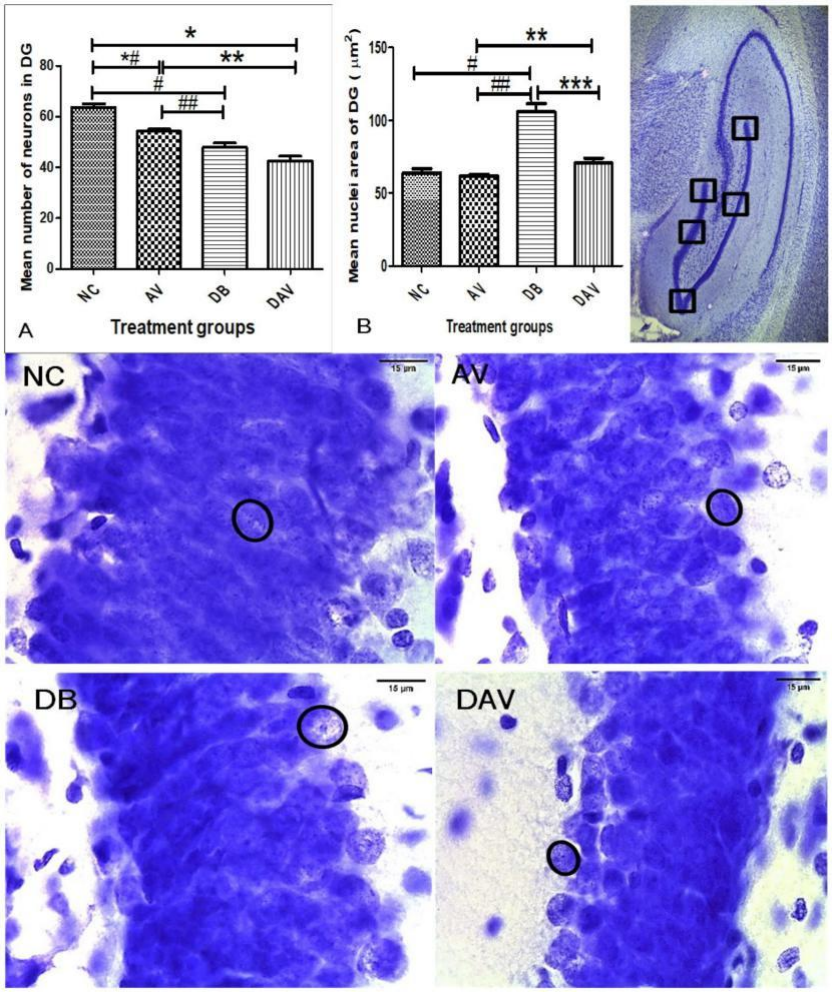

Figure 6. Mean nuclei area and number of neurons in the dentate gyrus region of the dorsal hip-pocampus. (**A**) Significant changes in the mean number of neurons in the DG region (one-way ANOVA test, p 0.0001). '*' DAV vs. AV, '*#' AV vs. NC and '#' DB vs. NC are significantly decreased (p = 0.001, 0.0001 and 0.0001, respectively). '**' DAV vs. AV and '##' DB vs. AV are significantly decreased (p = 0.0001). (**B**) Significant changes in the mean nuclei area in the DG region between the groups (Kruskal–Wallis test, p 0.005). '#' DB vs. NC, '##' DB vs. AV and '***' DB vs. DAV are significantly increased (p = 0.0002, 0.0001, and 0.0001, respectively). '**' DAV vs. AV, '#' DB vs. NC, '##' DB vs. AV and '***' DB vs. DAV are significantly increased (p = 0.045). Circles indicate boundaries of neuronal nuclei, and squares indicate specific regions from which micrographs were taken and measurements made, n = 6. Scale bar = 15 m. Key: NC, Controls; AV, cART only; DB, Diabetic; DAV, diabetic with cART.

3.6.2. Neuronal Nuclei Area in Hippocampal Regions

The nuclei area of the DB groups is observed to be consistently increased compared to other groups at all hippocampal regions (circles; Figures 4–6). While the mean nuclei in the DAV are slightly increased in the CA1 and DG regions but appear apoptotic in the CA3 region, incidentally, the mean neuronal number of the DAV group is also significantly reduced in this region (circles; Figure 5). The mean nuclei area of the neurons in all three regions of the hippocampus was significantly increased (p 0.041, 0.016 and 0.005) in the DB group compared to the other groups (NC, AV and DAV), except comparison with the DAV in the DG region (Figures 4–6). However, the mean nuclei area of neurons in the DAV significantly decreased compared to the NC group in the CA3 region (Figure 6).

3.7. Immunohistochemistry for Neurogenesis in the Hippocampus Double Cortin and Ki67

The number of neurons expressing DCX in the DB and DAV groups was significantly decreased compared to the NC and AV groups ($p = 0.0001$), and the expression of DCX in the DAV was also significantly decreased compared to DB ($p = 0.011$; Figure 7A–H,Q). Additionally, a significant reduction was observed in Ki67 expression in the DB and DAV groups compared to the NC group ($p = 0.007$ and 0.0001, respectively), and the DAV was significantly reduced compared to the AV group ($p < 0.051$; Figure 7I–P,R). There were no significant differences between the control and AV in both DCX and Ki67 expressions.

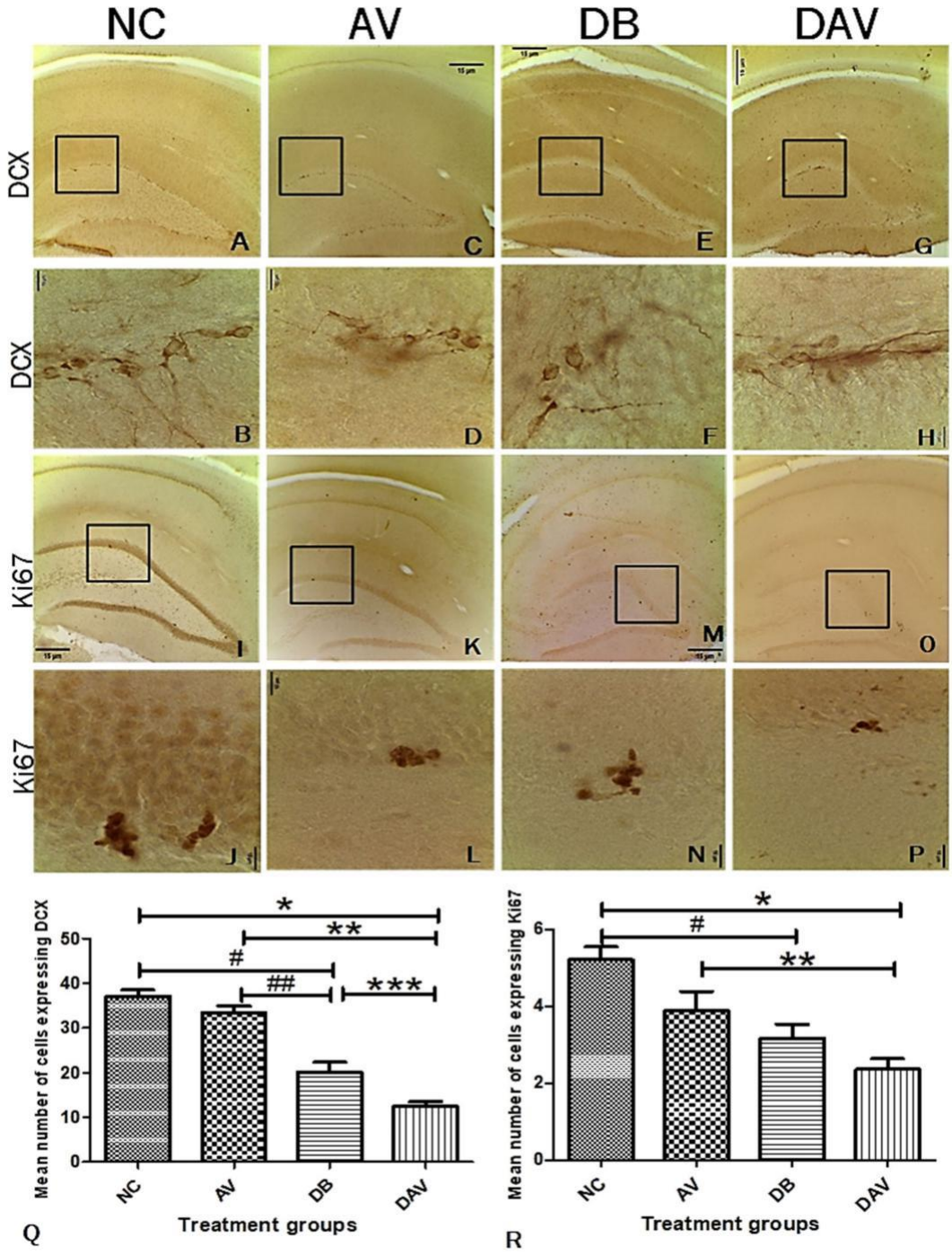

Figure 7. Photomicrograph of the hippocampus showing the expression of DCX in the subgranular zone of the dentate gyrus region. (**A**,**B**) Expression of DCX in the control, showing numerous clusters of cell bodies and projections expressing DCX. (**C**,**D**) Expression of DCX in the AV group: several

small pockets of cells and projections expressing DCX. (**E**,**F**) Expression of DCX in the DB group: few cells and their projections expressing DCX. (**G**,**H**) Expression of DCX in the DAV group: minimal number of cells expressing DCX, most of the DCX expression were observed in the projections. (**I**–**P**) Expression of Ki67 showing gradual reduction in Ki67 expression across the groups NC, AV, DB and DAV, respectively. (**Q**) Significant difference in the expression of DCX between groups (one-way ANOVA, p = 0.0001). '*' DAV vs. NC, '**' DAV vs. AV, '#' DB vs. NC and '##' DB vs. AV are significantly decreased (Bonferroni's post hoc, p = 0.0001). '***' DAV vs. DB significantly decreased (Bonferroni's post hoc, p = 0.011). (**R**) Significant difference in expression of Ki67 between the groups (one-way ANOVA, p = 0.0001). '*' DAV vs. NC and '#' DB vs. AV are significantly decreased (Bonferroni's post hoc, p = 0.007 and 0.0001, respectively). '**' DAV vs. AV is significantly decreased (Bonferroni's post hoc, p = 0.05). Photomicrographs at 100; squares indicate the area captured at 1000 magnification, n = 6. Scale bar = 15 m. Key: NC, Controls; AV, cART only; DB, Diabetic; DAV, diabetic with cART.

3.8. Correlation of Histomorphology and Neurogenic Parameters

Evaluation of the possible correlations between different parameters showed significant negative correlations between the mean body weight and diabetic parameters (FBG, NFBG and AUC). Similarly, the mean estimated number of neurons (in CA1N, CA3N and DGN) and neurogenic markers (Ki67 and DCX) significantly positively correlated with BW and negatively with FBG, NFBG and AUC (Table 1). Additionally, a significantly positive correlation was observed independently between the mean number of neurons in CA1N, CA3N and DGN (Table 1) and between neuronal nuclei area in CA1A, CA3A and DGA (Table 2). Furthermore, the DGA has a strong significant positive correlation with FBG, NFBG, AUC and the nuclear area (CA1A and CA3A) but a significantly negative relationship with BW and number of neurons in CA1N, CA3N and DGD (p = 0.011, 0.032 and 0.011, R = 0.509, 0.439 and 0.510, respectively) and neurogenic markers (Table 2).

Table 1. Spearman's rho nonparametric correlation of diabetes parameters with neuronal number and neurogenic parameters.

	Diabetes Parameters				**Neuronal Number**			**Neurogenic Markers**
	BW	**FBG**	**NFBG**	**AUC**	**CA1N**	**CA3N**	**DGN**	**Ki67**
FBG								
p value	0.0001 *							
R value	0.613							
NFBG								
p value	0.0001 *	0.0001 *						
R value	0.648	0.761						
AUC								
p value	0.0001 *	0.0001 *	0.0001 *					
R value	0.723	0.729	0.691					
CA1N								
p value	0.0001 *	0.0001 *	0.0001 *	0.0001 *				
R value	0.716	0.808	0.706	0.762				
CA3N								
p value	0.011 *	0.0001 *	0.002 *	0.004 *	0.0001 *			
R value	0.508	0.821	0.593	0.563	0.794			
DGN								
p value	0.001 *	0.0001 *	0.0001 *	0.0001 *	0.0001 *	0.0001 *		
R value	0.629	0.900	0.800	0.692	0.824	0.794		
KI67								
p value	0.038 *	0.0001 *	0.001 *	0.006 *	0.0001 *	0.001 *	0.0001 *	

Table 1. Cont.

	Diabetes Parameters				Neuronal Number			Neurogenic Markers
	BW	**FBG**	**NFBG**	**AUC**	**CA1N**	**CA3N**	**DGN**	**Ki67**
R value	0.426	0.735	0.637	0.546	0.715	0.639	0.758	
DCX								
p value	0.0001 *	0.0001 *	0.0001 *	0.0001 *	0.0001 *	0.0001 *	0.0001 *	0.0001 *
R value	0.667	0.882	0.714	0.777	0.796	0.745	0.838	0.748

Key: BW; body weight, FBG; fasting blood glucose, NFBG; non-fasting blood glucose, AUC; area under the OGTT curve. Neuronal number at CA1, CA3 and DG (CA1N, CA3N and DGN, respectively. '*' Significant correlation ($p < 0.05$), R value; Correlation Coefficient.

Table 2. Spearman's rho nonparametric correlation of diabetes parameters with neuronal nuclei area and neurogenic parameters.

	Diabetes Parameters				Neuronal Nuclei Area			Neurogenic Markers
	BW	**FBG**	**NFBG**	**AUC**	**CA1A**	**CA3A**	**DGA**	**Ki67**
CA1A								
p value	0.101	0.08	0.014 *	0.245				
R value	0.343	0.364	0.497	0.247				
CA3A								
p value	0.68	0.493	0.277	0.698	0.0001 *			
R value	0.89	0.147	0.231	0.083	0.719			
DGA								
p value	0.0001 *	0.006 *	0.0001 *	0.012 *	0.0001 *	0.009 *		
R value	0.717	0.546	0.706	0.505	0.696	0.52		
KI67								
p value	0.038 *	0.0001 *	0.001 *	0.006 *	0.296	0.526	0.047 *	
R value	0.426	0.735	0.637	0.546	0.222	0.136	0.409	
DCX								
p value	0.0001 *	0.0001 *	0.0001 *	0.0001 *	0.19	0.208	0.035 *	0.0001 *
R value	0.667	0.882	0.714	0.777	0.277	0.266	0.433	0.748

Key: BW; body weight, FBG; fasting blood glucose, NFBG; non-fasting blood glucose, AUC; area under the OGTT curve. Neuronal nuclei area at CA1, CA3 and DG (CA1A, CA3A and DGA, respectively). '*' Significant correlation ($p < 0.05$), R value; Correlation Coefficient.

4. Discussion

The diabetic brain is susceptible to oxidative damage, which has been linked to neuro-inflammation and autophagy [15]. Obesity, hyperglycemia and impaired glucose tolerance [31] with an attendant elevation of MDA [32] and proinflammatory cytokines [33] have been identified as risk factors in the pathogenesis of type 2 diabetes. Similar effects of significantly elevated body weight; cytokines (IL-1 , IL-6 and TNF) and MDA levels were observed in the cART-treated animals. However, hyperglycemia and impaired glucose tolerance were not observed in the cART-treated groups (AV), as shown by the FBG, NFBG and AUC levels, suggesting the initiation but not establishment of metabolic perturbation in this group. Significantly elevated FBG, NFBG, AUC, lipid peroxidation levels and weight loss observed in the diabetic groups (DB and DAV) are consistent with a previous report of hyperglycemia, oxidative stress and lipodystrophy associated with advanced stages of T2D [34–36].

Cytokines in the brain may arise from circulatory invasion or produced by support cells (microglial and astrocytes) and neurons in response to neuroinflammation and neu-roprotection triggers [37,38]. Additionally, diabetes is characterized as an inflammatory condition [39] with elevated levels of cytokines often reported in the serum and tissue of T2D patients and animal models [12,40]. However, inflammation, oxidative stress and hyperglycemia together induce perturbation in immunometabolism, which impairs the

immune system [41]. These immune compromises shown by the decreased production of cytokines has been reported in diabetic patient immune cells [42,43]. Therefore, the significantly reduced cytokines (IL-1 , IL-6 and TNF) levels in the hippocampus of the DB and DAV groups, contrary to previous reported increases [12,33,40], may suggest a com-promised immune response and prolonged diabetes. Furthermore, cytokines are essential for long-term plasticity learning and memory functions [44], and as such, the reduction of cytokines in the DB and DAV groups compared to the control may suggest a compromise in the cognitive and memory processes of the hippocampus. Since the cytokine levels were significantly reduced in diabetes and cART-treated HIV-naïve rat groups, it is possible that diabetic–HIV coinfected patients on chronic cART treatment may be predisposed toward greater inflammatory disturbances and, therefore, require more clinical attention in their diagnosis and management. Additionally, the significantly increased MDA levels in the DB and DAV groups suggest that the cellular and functional integrity of the hippocampus will be more susceptible to neurotoxic effects due to cART treatment in diabetes.

Previous reports have indicated that cART and diabetes are both independently implicated in hippocampal neurodegeneration [45,46]. Our results collaborate these reports with a significant decrease in the number of neurons in the AV group (in DG region); DB group (in CA1 and DG regions) and in all the hippocampal regions in the DAV group (i.e., CA1, DG and CA3). Additionally, the nuclei area of the DAV is significantly reduced compared to the control. This indicates that cART treatment in diabetes exacerbated and extended hippocampal neuronal decline into the CA3 region, which is not affected by either cART or diabetes alone. The decline in DG and CA3 neurons will adversely affect the associated functions in cognition, pattern separation, episodic memory and pattern completion, as has been previously reported [47]. This is because CA3 neurons play a crucial role in memory processes, with recurrent internal and wide-ranging connectivity [48,49] to other hippocampal regions and cortices. Therefore, the reduction in CA3 neuron density and nuclei area in the DAV group may imply a reduction in the connectivity of this region within the hippocampus and may result in adverse functional defects.

The sub-granular zone of the hippocampal dentate gyrus is one of the established zones in the brain for adult hippocampal neurogenesis. The significantly decreased expres-sion of DCX and Ki67 in the diabetic (DB) and cART-treated diabetic animal (DAV) groups infers that the proliferation of hippocampal stem cells, as well as migrating immature neu-rons, were significantly impaired. Such compromised stem cell generation and migration may diminish the hippocampal potential to recover from inherent apoptotic processes. Interestingly, the number of neurons at different hippocampal regions is positively signif-icantly correlated with Ki67 and DCX expressions and negatively with FBG, NFBG and AUC, which is consistent with reports of a persistent decline in adolescent hippocampal neurogenesis due to increased cell death of immature differentiating neurons [50]. This also suggests that elevated levels of diabetes parameters may exacerbate the loss of hippocampal neurons and induce a decline in neurogenesis. Additionally, the DG nuclei area positive correlation with the diabetic parameters (FBG, NFBG and AUC) and mean nuclei areas of the CA1 and CA3 regions but inverse correlation with neuronal density (in all regions of the hippocampus) and neurogenic parameters (Ki67 and DCX) may indicate a possible central functional role associated with the DG nuclei. Furthermore, the significant increase in neuronal nuclei area and significant reduction in mean neuronal number in the DB group observed in all hippocampal regions may be due to necrosis, which is morphologically characterized by cell and nuclear swelling in the initial stages of cell death [51,52].

In summary, our results indicate that cART therapy in the diabetic condition elevates lipid peroxidation but reduces body weight; proinflammatory cytokines; number of neu-rons (CA1, CA3 and DG); proliferation of new cells and migration of immature neurons in the dentate gyrus with likely adverse implications in hippocampal overall function. Additionally, cART treatment in diabetic conditions may induce heightened oxidative stress and may worsen the previously reported CNS infections, memory and cognitive loss involving diabetes or cART independently. The clinical implications of these findings

(though in the HIV-naïve rat model) hinges on the chronic cART regimen amongst diabetes patients with HIV infection and, therefore, calls for caution in the clinical diagnosis and management of these groups of patients.

Author Contributions: Conceptualization, J.A.J., R.N. and E.F.M.; methodology, J.A.J. and E.F.M.; software, J.A.J.; validation, J.A.J., R.N. and E.F.M.; formal analysis, J.A.J. and E.F.M.; investigation, J.A.J., R.N. and E.F.M.; resources, J.AJ. and E.F.M.; data curation, J.A.J.; writing—original draft preparation, J.A.J. and E.F.M.; writing—review and editing, J.A.J., R.N. and E.F.M.; visualization, J.A.J. and E.F.M.; supervision, R.N. and E.F.M.; project administration, J.A.J. and E.F.M. and fund-ing acquisition, J.A.J. and E.F.M. All authors have read and agreed to the published version of the manuscript.

Funding: This research was funded by the University of the Witwatersrand, Faculty of Health Sciences Faculty Research Committee Individual Grant awarded to Jaclyn Asouzu Johnson in 2019 and 2021 (grant number; 0012548421101512110500000000000000005254).

Institutional Review Board Statement: The study was conducted in accordance with the stan-dards and principles set forth by the Wits Research Animal Facility (WRAF) (approval number 2018/011/58/C) of the University of the Witwatersrand.

Data Availability Statement: The minimal dataset for the results from this study will be made available through a University of the Witwatersrand archived link.

Acknowledgments: Our appreciation goes to our coworkers Idemudia Eguavoen and Vaughan Perry for their excellent collaborative efforts, and special appreciation goes to Hasiena Ali for her technical and laboratory assistance.

Conflicts of Interest: The authors declare no conflicts of interest. The funders had no role in the design of the study; in the collection, analyses or interpretation of the data; in the writing of the manuscript or in the decision to publish the results.

References

1. Pheiffer, C.; Pillay-van Wyk, V.; Joubert, J.D.; Levitt, N.; Nglazi, M.D.; Bradshaw, D. The prevalence of type 2 diabetes in South Af-rica: A systematic review protocol. BMJ Open **2018**, 8, e021029. [CrossRef] [PubMed]
2. Al-Maskari, F. Lifestyle Diseases: An Economic Burden on the Health Services. UN Chronicle Magazine UN. 2010. Available online: https://www.un.org/en/chronicle/article/lifestyle-diseases-economic-burden-health-services (accessed on 5 November 2021).
3. Feng, R.; Du, S.; Chen, Y.; Zheng, S.; Zhang, W.; Na, G.; Li, Y.; Sun, C. High carbohydrate intake from starchy foods is positively associated with metabolic disorders: A Cohort Study from a Chinese population. Sci. Rep. **2015**, 5, 16919. [CrossRef] [PubMed]
4. Meintjes, G.; Moorhouse, M.A.; Carmona, S.; Davies, N.; Dlamini, S.; Van Vuuren, C.; Manzini, T.; Mathe, M.; Moosa, Y.; Nash, J.; et al. Adult antiretroviral therapy guidelines 2017. South. Afr. J. HIV Med. **2017**, 18, 1–24. [CrossRef]
5. Fokunang, C.N.; Hitchcock, J.; Spence, F.; Tembe-Fokunang, E.A.; Burkhardt, J.; Levy, L.; George, C. An Overview of Mitochondrial Toxicity of Nucleoside Reverse Transcriptase Inhibitors Associated with HIV Therapy. Int. J. Pharmacol. **2005**, 2, 152–162. [CrossRef]
6. Osuji, F.N.; Onyenekwe, C.C.; Ahaneku, J.E.; Ukibe, N.R. The effects of highly active antiretroviral therapy on the serum levels of pro-inflammatory and anti-inflammatory cytokines in HIV infected subjects. J. Biomed. Sci. **2018**, 25, 88. [CrossRef] [PubMed]
7. Zhou, H.; Jarujaron, S.; Gurley, E.C.; Chen, L.; Ding, H.; Studer, E.; Pandak, W.M.; Hu, W.; Zou, T.; Wang, J.-Y.; et al. HIV protease inhibitors increase TNF- and IL-6 expression in macrophages: Involvement of the RNA-binding protein HuR. Atherosclerosis **2007**, 195, e134–e143. [CrossRef] [PubMed]
8. Honnapurmath, V.K.; Patil, V.W. Antiretroviral therapy-induced insulin resistance and oxidative deoxy nucleic acid damage in human immunodeficiency virus-1 patients. Indian J. Endocrinol. Metab. **2017**, 21, 316–321. [CrossRef] [PubMed]
9. Noor, M.A. The role of protease inhibitors in the pathogenesis of HIV-associated insulin resistance: Cellular mechanisms and clinical implications. Curr. HIV/AIDS Rep. **2007**, 4, 126–134. [CrossRef] [PubMed]
10. Rehman
11. , K.; Akash, M.S.H. Mechanisms of inflammatory responses and development of insulin resistance: How are they interlinked? J. Biomed. Sci. **2016**, 23, 87. [CrossRef] [PubMed]
12. Calle, M.; Fernandez, M. Inflammation and type 2 diabetes. Diabetes Metab. **2012**, 38, 183–191. [CrossRef]
13. Tsalamandris, S.; Antonopoulos, A.S.; Oikonomou, E.; Papamikroulis, G.-A.; Vogiatzi, G.; Papaioannou, S.; Deftereos, S.; Tousoulis, D. The Role of Inflammation in Diabetes: Current Concepts and Future Perspectives. Eur. Cardiol. Rev. **2019**, 14, 50–59. [CrossRef] [PubMed]

13. Brown, T.T.; Cole, S.R.; Li, X.; Kingsley, L.A.; Palella, F.J.; Riddler, S.A.; Visscher, B.R.; Margolick, J.B.; Dobs, A.S. Antiretroviral therapy and the prevalence and incidence of diabetes mellitus in the multicenter AIDS cohort study. Arch. Intern. Med. **2005**, 165, 1179–1184. [CrossRef] [PubMed]
14. Berbudi, A.; Rahmadika, N.; Tjahjadi, A.; Ruslami, R. Type 2 Diabetes and its Impact on the Immune System. Curr. Diabetes Rev. **2020**, 16, 442–449. [CrossRef]
15. Muriach, M.; Flores-Bellver, M.; Romero, F.J.; Barcia, J.M. Diabetes and the Brain: Oxidative Stress, Inflammation, and Autophagy. Oxidative Med. Cell. Longev. **2014**, 2014, 102158. [CrossRef]
16. Alves, C.; Casqueiro, J.; Casqueiro, J. Infections in patients with diabetes mellitus: A review of pathogenesis. Indian J. Endocrinol. Metab. **2012**, 16 (Suppl. 1), S27–S36. [CrossRef] [PubMed]
17. Gonzalez, C.; Lee, M.-S.; Marchetti, P.; Pietropaolo, M.; Towns, R.; Vaccaro, M.; Watada, H.; Wiley, J.W. The emerging role of autophagy in the pathophysiology of diabetes mellitus. Autophagy **2011**, 7, 2–11. [CrossRef] [PubMed]
18. Razavi, S.; Sadeghi, A.; Hami, J.; Esfandiary, E.; Hejazi, Z. The effect of diabetes mellitus on apoptosis in hippocampus: Cellular and molecular aspects. Int. J. Prev. Med. **2016**, 7, 57. [CrossRef] [PubMed]
19. McNay, E.C.; Ong, C.; McCrimmon, R.; Cresswell, J.; Bogan, J.; Sherwin, R.S. Hippocampal memory processes are modulated by insulin and high-fat-induced insulin resistance. Neurobiol. Learn. Mem. **2010**, 93, 546–553. [CrossRef] [PubMed]
20. McNay, E.C.; Recknagel, A.K. Reprint of: 'Brain insulin signaling: A key component of cognitive processes and a potential basis for cognitive impairment in type 2 diabetes'. Neurobiol. Learn. Mem. **2011**, 96, 517–528. [CrossRef] [PubMed]
21. Jin, J.; Grimmig, B.; Izzo, J.; Brown, L.A.M.; Hudson, C.; Smith, A.J.; Tan, J.; Bickford, P.; Giunta, B. HIV Non-Nucleoside Reverse Transcriptase Inhibitor Efavirenz Reduces Neural Stem Cell Proliferation in Vitro and in Vivo. Cell Transplant. **2016**, 25, 1967–1977. [CrossRef]
22. Ramos-Rodriguez, J.J.; Molina-Gil, S.; Ortiz-Barajas, O.; Jimenez-Palomares, M.; Perdomo, G.; Cozar-Castellano, I.; Lechuga-Sancho, A.; Garcia-Alloza, M. Central Proliferation and Neurogenesis Is Impaired in Type 2 Diabetes and Prediabetes Animal Models. PLoS ONE **2014**, 9, e89229. [CrossRef]
23. Stranahan, A.M.; Arumugam, T.; Cutler, R.G.; Lee, K.; Egan, J.M.; Mattson, M.P. Diabetes impairs hippocampal function through glucocorticoid-mediated effects on new and mature neurons. Nat. Neurosci. **2008**, 11, 309–317. [CrossRef] [PubMed]
24. Kodl, C.T.; Seaquist, E.R. Cognitive Dysfunction and Diabetes Mellitus. Endocr. Rev. **2008**, 29, 494–511. [CrossRef] [PubMed]
25. Opii, W.O.; Sultana, R.; Abdul, H.M.; Ansari, M.A.; Nath, A.; Butterfield, D.A. Oxidative stress and toxicity induced by the nucleoside reverse transcriptase inhibitor (NRTI)—2^{0},3^{0}-dideoxycytidine (ddC): Relevance to HIV-dementia. Exp. Neurol. **2007**, 204, 29–38. [CrossRef] [PubMed]
26. Robertson, K.; Liner, J.; Meeker, R.B. Antiretroviral neurotoxicity. J. NeuroVirology **2012**, 18, 388–399. [CrossRef] [PubMed]
27. Kousignian, I.; Sautereau, A.; Vigouroux, C.; Cros, A.; Kretz, S.; Viard, J.P.; Slama, L. Diagnosis, risk factors and management of diabetes mellitus in HIV-infected persons in France: A real-life setting study. PLoS ONE **2021**, 16, e0250676. [CrossRef]
28. Wilson, R.D.; Islam, M.S. Fructose-fed streptozotocin-injected rat: An alternative model for type 2 diabetes. Pharmacol. Rep. **2012**, 64, 129–139. [CrossRef]
29. Frampton, J.E.; Croom, K.F. Efavirenz/Emtricitabine/Tenofovir Disoproxil Fumarate. Drugs **2006**, 66, 1501–1512. [CrossRef]
30. Paxinos, G.; Watson, C. The Rat Brain in Stereotaxic Coordinates: Hard Cover Edition; Elsevier: Amsterdam, The Netherlands, 2006.
31. American Diabetes Association Diagnosis and Classification of Diabetes Mellitus. Diabetes Care **2007**, 30, S42–S47. [CrossRef]
32. Manohar, S.M.; Vaikasuvu, S.R.; Deepthi, K.; Sachan, A.; Narasimha, S.R.P.V.L. An association of hyperglycemia with plasma malondialdehyde and atherogenic lipid risk factors in newly diagnosed Type 2 diabetic patients. J. Res. Med. Sci. Off. J. Isfahan Univ. Med. Sci. **2013**, 18, 89–93.
33. AlZamil, H. Elevated Serum TNF- Is Related to Obesity in Type 2 Diabetes Mellitus and Is Associated with Glycemic Control and Insulin Resistance. J. Obes. **2020**, 2020, 5076858. [CrossRef] [PubMed]
34. American Diabetes Association 2. Classification and Diagnosis of Diabetes. Diabetes Care **2015**, 38, S8–S16. [CrossRef] [PubMed]
35. Benedé-Ubieto, R.; Estévez-Vázquez, O.; Ramadori, P.; Cubero, F.J.; Nevzorova, Y.A. Guidelines and Considerations for Metabolic Tolerance Tests in Mice. Diabetes Metab. Syndr. Obes. Targets Ther. **2020**, 13, 439–450. [CrossRef] [PubMed]
36. Pournaghi, P.; Sadrkhanlou, R.-A.; Hasanzadeh, S.; Foroughi, A. An investigation on body weights, blood glucose levels and pituitary-gonadal axis hormones in diabetic and metformin-treated diabetic female rats. Vet. Res. Forum **2012**, 3, 79–84.
37. Muhammad, M. Tumor Necrosis Factor Alpha: A Major Cytokine of Brain Neuroinflammation. In Cytokines; IntechOpen: London, UK, 2020. [CrossRef]
38. Salmeron, K.E.; Maniskas, M.E.; Edwards, D.N.; Wong, R.; Rajkovic, I.; Trout, A.; Rahman, A.A.; Hamilton, S.; Fraser, J.F.; Pinteaux, E.; et al. Interleukin 1 alpha administration is neuroprotective and neuro-restorative following experimental ischemic stroke. J. Neuroinflamm. **2019**, 16, 222. [CrossRef]
39. Donath, M.Y.; Shoelson, S.E. Type 2 diabetes as an inflammatory disease. Nat. Rev. Immunol. **2011**, 11, 98–107. [CrossRef]
40. Herrero, L.; Shapiro, H.; Nayer, A.; Lee, J.; Shoelson, S.E. Inflammation and adipose tissue macrophages in lipodystrophic mice. Proc. Natl. Acad. Sci. USA **2010**, 107, 240–245. [CrossRef]
41. Daryabor, G.; Atashzar, M.R.; Kabelitz, D.; Meri, S.; Kalantar, K. The Effects of Type 2 Diabetes Mellitus on Organ Metabolism and the Immune System. Front. Immunol. **2020**, 11, 1582. [CrossRef]

42. Martinez, N.; Ketheesan, N.; Martens, G.W.; West, K.; Lien, E.; Kornfeld, H. Defects in early cell recruitment contribute to the increased susceptibility to respiratory Klebsiella pneumoniae infection in diabetic mice. Microbes Infect. **2016**, 18, 649–655. [CrossRef]
43. Richard, C.; Wadowski, M.; Goruk, S.; Cameron, L.; Sharma, A.M.; Field, C. Individuals with obesity and type 2 diabetes have additional immune dysfunction compared with obese individuals who are metabolically healthy. BMJ Open Diabetes Res. Care **2017**, 5, e000379. [CrossRef] [PubMed]
44. Bourgognon, J.-M.; Cavanagh, J. The role of cytokines in modulating learning and memory and brain plasticity. Brain Neurosci. Adv. **2020**, 4, 1–13. [CrossRef]
45. Akang, E.N.; Dosumu, O.O.; Afolayan, O.O.; Fagoroye, A.M.; Osiagwu, D.D.; Usman, I.T.; Oremosu, A.A.; Akanmu, A.S. Combination antiretroviral therapy (cART)-induced hippocampal disorders: Highlights on therapeutic potential of Naringenin and Quercetin. IBRO Rep. **2019**, 6, 137–146. [CrossRef] [PubMed]
46. Madhusudhanan, J.; Suresh, G.; Devanathan, V. Neurodegeneration in type 2 diabetes: Alzheimer's as a case study. Brain Behav. **2020**, 10, e01577. [CrossRef] [PubMed]
47. Scharfman, H.E.; Myers, C.E. Corruption of the dentate gyrus by "dominant" granule cells: Implications for dentate gyrus function in health and disease. Neurobiol. Learn. Mem. **2016**, 129, 69–82. [CrossRef]
48. Cherubini, E.; Miles, R.M. The CA3 region of the hippocampus: How is it? What is it for? How does it do it? Front. Cell. Neurosci. **2015**, 9, 19. [CrossRef]
49. Le Duigou, C.; Simonnet, J.; Teleñczuk, M.T.; Fricker, D.; Miles, R.M. Recurrent synapses and circuits in the CA3 region of the hippocampus: An associative network. Front. Cell. Neurosci. **2014**, 7, 262. [CrossRef]
50. Broadwater, M.A.; Liu, W.; Crews, F.T.; Spear, L.P. Persistent Loss of Hippocampal Neurogenesis and Increased Cell Death following Adolescent, but Not Adult, Chronic Ethanol Exposure. Dev. Neurosci. **2014**, 36, 297–305. [CrossRef]
51. Elmore, S. Apoptosis: A review of programmed cell death. Toxicol. Pathol. **2007**, 35, 495–516. [CrossRef]
52. Kwon, H.-K.; Lee, J.-H.; Shin, H.-J.; Kim, J.-H.; Choi, S. Structural and functional analysis of cell adhesion and nuclear envelope nano-topography in cell death. Sci. Rep. **2015**, 5, 15623. [CrossRef]